Miller, Angela (2015) Peptide based hydrogels in the study of mesenchymal stem cells for the purposes of regenerative medicine. PhD thesis.

http://theses.gla.ac.uk/6880/

Copyright and moral rights for this thesis are retained by the author

A copy can be downloaded for personal non-commercial research or study, without prior permission or charge

This thesis cannot be reproduced or quoted extensively from without first obtaining permission in writing from the Author

The content must not be changed in any way or sold commercially in any format or medium without the formal permission of the Author

When referring to this work, full bibliographic details including the author, title, awarding institution and date of the thesis must be given

Glasgow Theses Service
http://theses.gla.ac.uk/
theses@gla.ac.uk

Peptide based Hydrogels in the study of Mesenchymal stem cells for the purposes of regenerative medicine

Angela Miller

(BSc (Hons), MRes)

Submitted in fulfilment of the requirements for the Degree of Doctor of Philosophy (PhD)

Centre for Cell Engineering

College of Medical, Veterinary and Life Sciences,

Institute of Molecular, Cell and Systems Biology,

University of Glasgow,

October 2015

Abstract

Regenerative medicine is a vastly expanding subject area, with a number of different strategies and substrates being studied to ultimately create a model for repairing diseased and injured tissue. Stem cells are a promising cell type in this field as they are known to differentiate into a number of cell types and contribute to normal cell repair. However, despite their potential as a useful cell choice in the field of regenerative medicine, stem cell based therapies have limited potential due to their ability to form tumours when implanted in the human body, problems arising with immunogenicity and the difficulty in obtaining adequate cell numbers for transplantation.

To overcome these problems, many research groups are interested in using biomimetic substrates and scaffolds to mimic the architecture, chemical composition and stiffness properties of the *in vivo* cell niche and various human tissues, but in an *in vitro* setting. By doing so, the MSC behaviour can be studied and the differential lineages examined allowing the desired substrate to be tuned to obtain the desired cellular outcome.

In this work, hydrogels composed of Fmoc diphenylalanine and Fmoc Serine have been characterised and used to study changes in Mesenchymal stem cell (MSC) responses in a two and three dimensional state. The results obtained from this work demonstrate that such hydrogels support MSC growth and produce a mixed phenotype population which differentiates over time. A further hydrogel paired with collagen has shown promise in promoting MSC differentiation down the osteogenic lineage and has potential for the future study in maxillofacial reconstruction models.

Table of Contents

List of Tables

List of Figures

Presentations

Oral Presentations made by the candidate relating to research in this thesis

(2014) Glasgow Orthopaedic Research Inititaive (GLORI) meeting, University of Glasgow, UK. Macintyre,A, Ulijn RU, Meek, DM and Dalby, M.J. Peptide based biomaterials for studying MSC behaviour.

(2014) Institute of Molecular, Cell and Systems Biology Symposium, University of Glasgow, UK. MacintyreA; Ulijn RU and Dalby MJ. Isolating stem cells for controlling cellular behaviour in peptide based biomaterials

(2013) Doctoral Training Centre (DTC) Symposium, University of Glasgow, UK. Macintyre A; Ulijn RV and Dalby MJ. Substrate driven differentiation, 2D versus 3D.

(2013) Centre for Doctoral Training (CDT) Conference. Imperial College, London, UK. Macintyre A; Ulijn RV and Dalby MJ. Designing peptide based biomaterials for influencing mesenchymal stem cell behaviour

(2013) Scottish Federation of University Women Research Presentations. Glasgow, UK. Macintyre A, Ulijn RV and Dalby MJ. MSC's to be or not to be? Understanding stem cell behavior.

(2013) Invited speaker at Queens University Belfast, Belfast, UK Centre for Experimental Medicine (formally Centre for Vision & Vascular Science).Macintyre A; Reynold P;Ulijn RV and Dalby MJ. Isolating stem cells for controlling cellular behaviour in peptide based biomaterials.

(2012) Doctoral Training Centre (DTC) Symposium, University of Glasgow, UK. Macintyre A; Ulijn RV and Dalby MJ. Controlling Mesenchymal Stem Cell Behaviour using Peptide Based Biomaterials

Poster Presentations

(2014) Tissue Engineering & Regenerative Medicine International Society (TERMIS), Genoa, Italy. Macintyre A; Ulijn RV and Dalby MJ. Peptide Based Hydrogels for influencing Mesenchymal Stem Cell Behaviour

(2013) Tissue and Cell Engineering Society (TCES), Cardiff, UK. Macintyre A; Ulijn RV; Burgess KV and Dalby MJ. Designing peptide based biomaterials for influencing Mesenchymal stem cell behaviour.

(2011) Radical Solutions for Researching the Proteome (RASOR), Glasgow, UK; Macintyre A; Burgess KV; Ulijn RV and Dalby MJ.

Publications

Dalby MJ, Macintyre A, Roberts JN, Yang J, Lee LC, Tsimbouri, PM and McNamara LE (2012) 3D patterned agarose hydrogels for investigation of precurser cells in differentiation and chemoattraction. Nanomedicine 7 (1),

Dalby MJ, Lee LC, Yang J, Macintyre A and McCully M (2013) Hydrogel nanoparticles for drug delivery. Nanomedicine 8 (11), 1744-5

Acknowledgements

To start, I would like to thank my supervisors Prof. Matthew Dalby and Prof. Rein Ulijn for their help and encouragement over the past three years.

To Vineetha Jayawarna, Monica Tsimbouri and Carol-Anne Smith, you have helped me so much throughout the years and I can't thank you enough. You have taught me the skills I know to complete this PhD and I value our friendship tremendously. To Dr Roberts, you have been a gem the past 2 years and given me valuable advice throughout. I'm going to miss not seeing your cheery wee face every morning.

I'd like to thank my friends outside of university, especially Ishbel and Anne. I thank you for listening to my gripes, taking me out and making sure I forget my woes by drinking copious amount of sparkling wine and cocktails! These were the good days and I'll treasure our friendship forever. We've gone through a lot the past 8 years, but I'm glad we've shared it together. If anything, our friendship has made me realise that nothing else matters in life as long as you're happy, have your health and family. Let's look back and laugh when we're rocking the retirement years!

To my mum and dad, I would not be here without you both. You have made me the person I am today and I thank you for giving me the independence and support when I needed it the most.

Last but not least, I thank my best friend Gary. I can't thank you enough for everything you've done for me, especially these last 4 years. We've made sacrifices, learnt lessons and shared the ups with the downs. Who'd have thought in 2010 when I began this PhD that we would be moving in together, engaged, married and have a baby all before the end? You have been my support all the way through and you don't know how that much means to me. I can't wait to spend the rest of my life with you making new memories.

"Nothing lasts forever, so live it up, drink it up, laugh it off, avoid the bullshit, take chances and never have regrets, because at one point everything you did was exactly what you wanted"

Marilyn Monroe

Author's Declaration

I hereby declare that the research presented within this thesis is my own work unless otherwise stated, and has not been submitted for any other academic degree.

Angela Miller
October 2015

Abbreviations

2D	Two Dimension
3D	Three Dimension
10^4	10,000
%	Percent
°C	Degree Celsius
µl	Microlitre
µM	Micro molar
AFM	Atomic force microscope
ALCAM	Activated leukocyte cell adhesion molecule
ANOVA	Analysis of variance
ASCs	Adult stem cells
ATP	Adenosine Triphosphate
BMP	Bone morphogenic protein
BSA	Bovine serum Albumin
cDNA	Complementary deoxyribose nucleic acid
CO_2	Carbon Dioxide
DAPI	4'6-diamidino-2-phenylindole
dH_20	Distilled water
DMEM	Dulbecco's modified eagles media
DMSO	Dimethyl Sulfoxide
DNA	Deoxyribonucleic acid
EBL	Electron Beam Lithography
ECM	Extracellular matrix
ERK	Extracellular signal regulated kinase
ESCs	Embryonic stem cells
FA	Focal adhesion
FACS	Fluorescence activated cell sorting
FAK	Focal adhesion kinase
FBS	Foetal Bovine serum
Fmoc	9-Fluorenylmethloxycarbonyl
Fmoc F_2	9-Fluorenylmethloxycarbonyl di-phenylanine
Fmos-S	9-Fluorenylmethloxycarbonyl Serine
FN	Fibronectin
x g	G Force
G'	Elastic modulus
G"	Viscous modulus
GapDH	Glyceraldehyde-3-phosphate dehydrogenase
Glut-4	Glucose transporter Type 4
GPa	Giga Paskals
HEPES	2-hydroxylethyl-1-piperazine-ethanesulphonic acid
HSC	Haematopoietic stem cell
Hz	Hertz

IBMX	Isobutylmethylxanthine
iPSCs	Induced pluripotent stem cells
HEPES	4-(2-hydroxyethyl)-1-piperazineethanesulfonic acid
HCl	Hydrochloric acid
HSC	Hematropoietic stem cell
kPa	kilo Pascal
LC-MS	Liquid chromatography –mass spectrometry
LVE	Linear viscoelastic
M	Molar
MAPK	Mitogen activated protein kinase
ml	millitlitre
mm	millimetre
mM	milli Molar
mRNA	messenger Ribonucleic acid
MSCs	Mesenchymal Stem Cells
MTT	(3-(4,5-Dimethylthiazol-2-yl)-2,5-Diphenyltetrazolium Bromide)
MuMSCs	Muscle MSCs
NaOH	Sodium Hydroxide
nm	nano metre (10^{-9})
OCN	Osteocalcin
OD	Optical density
OMF	Oral and maxillofacial
OPG	Osteoprogenitor
OPN	Osteopontin
OSX	Osterix
Pa	Pascals
PBS	Phosphate buffer solution
PBST	PBS and Tween
PCL	Polycaprolactone
PD	Parkinson's Disease
PCR	Polymerase chain reaction
PEG	Polyethylene glycol
PPAR-γ	Peroxisome proliferator activating receptor gamma
p-value	Probability value
qRT-PCR	Quantitative real time polymerase chain reaction
RGD	Arg-Gly-Asp; peptide sequence
RNA	Ribonucleic acid
Rpm	Revolutions per minute
RUNX2	Runt-related transcription factor 2
SAMS	Self-assembled monolayer
SCs	Stem Cells
STRO-1	Stromal cell surface protein
SEM	Scanning electron Microscope
SOX-9	Sex determining region Y-box 9
TEM	Transmission electron Microscope

UV	Ultraviolet
v/v	Volume per volume
w/v	Weight per volume
ZIC-HILIC	Zwitterionic hydrophilic interaction liquid Chromatography

Chapter 1

General Introduction

1.1 Regenerative medicine & tissue engineering

The term tissue engineering was first coined in 1993 by Robert Langer and Joseph Vacanti and described as being "an interdisciplinary field of research that applies the principles of engineering and the life sciences towards the development of biological substitutes that restore, maintain or improve tissue function" (Langer & Vacanti., 1993). The concept of tissue engineering itself is illustrated in Figure 1.1. The process typically begins by isolating specific cells from a patient and expanding their numbers *in vitro*. These cells are then added to a scaffold designed for the specific therapeutic application, perhaps alongside growth factors and mechanical stimuli and cultured *in vitro* under defined conditions for cell incorporation and tissue formation. The optimal measure of success is the implantation of the scaffold into the donor to replace damaged or diseased tissue. The use of the patients' own cells replaces the need for immunosuppressive drugs, as theoretically the cells transplanted are originally derived from that of the patient (Fauza *et al.*, 1998; Koh & Atala., 2004). There are many bottle necks in this concept, as there is currently not a standard culture substrate that is able to maintain cells, such as stem cells, in their original, undifferentiated state. For this concept to be successful in tissue engineering, cells need to be expanded in order to have the adequate numbers to implant back into the patients own body and to initiate the tissue remodelling process. To overcome this, nanopatterns and culture substrates such as hydrogels are being researched in order to expand stem cell populations *in vitro*. When a suitable material is designed to expand cells in culture, the next obstacle to overcome is designing alternative materials that will promote these cells to become or "differentiate" specific cell types so that they can be tailored for their application.

In 1995 Nerem and Sambanis further defined tissue engineering as an emerging multidisciplinary field involving the development of bioartificial implants and/or the fostering of tissue remodelling with the purpose of repairing or enhancing tissue or organ function (Nerem & Sambanis., 1995). Current tissue engineering strategies can utilise autogeneic (patient's own) or allogeneic (derived from donor) cell types for transplantation (Griffith and Naughton., 2002). Tissue

engineering scaffolds have been exploited for the reconstruction and growth of bone (Nandi *et al.*, 2015), cartilage (Grande *et al.*, 1995; Ando *et al.*, 2007) and nerve (Chen & Tong., 2012) due to injury or disease. However, early engineered devices such as hip or knee replacements presented a problem in that they could promote aseptic loosening leading to periprosthetic osteolysis (Purdue *et al.*, 2006).

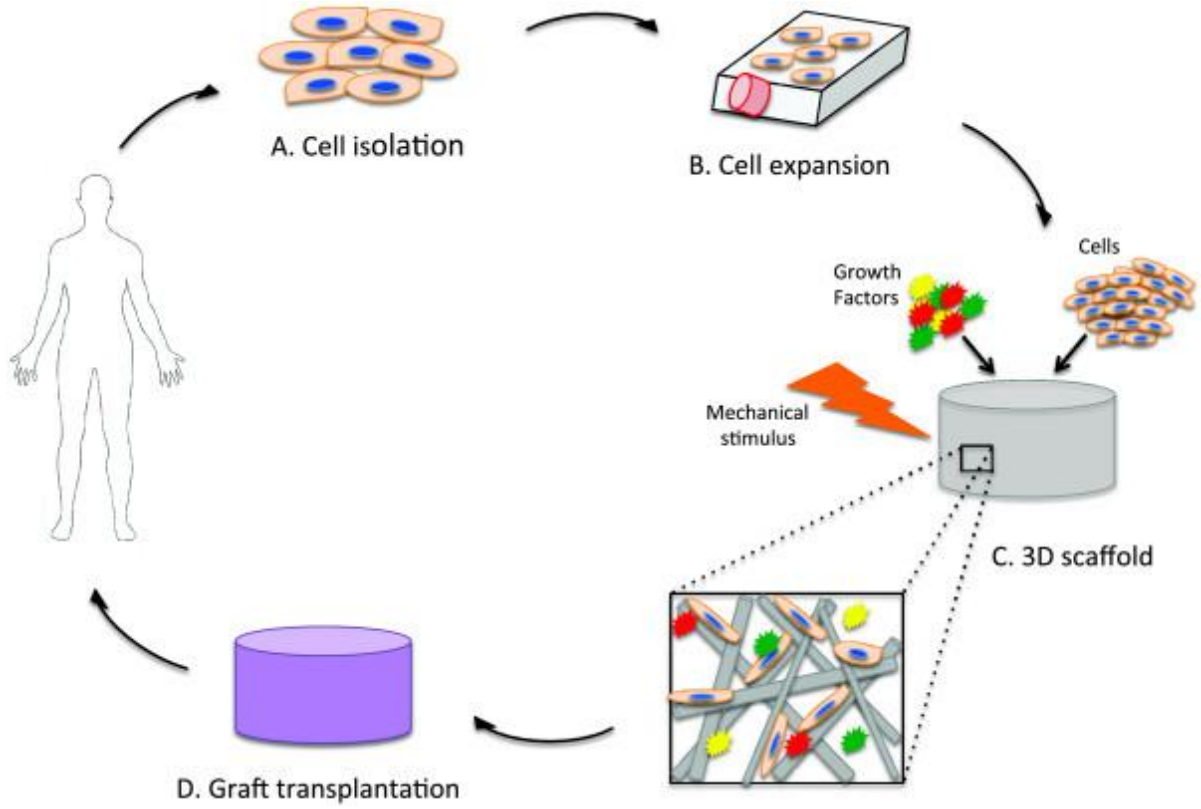

Figure 1.1 General overview of the process behind tissue engineering.
Figure represents the process of isolating homogenous cells from a patient starting with the isolation of these cells from the patient (A), and their expansion in culture (B). The cells are then incorporated into a suitable scaffold and stimulated with appropriate cues (C) before being placed back into the patient (D). By using autologous cells, the patient does not require the use of immune suppressive drugs. Figure adapted from Serbo & Gerecht, 2013. .

As well as the tissue-engineered scaffold providing the correct biochemical cues and stimulus, the implant itself needs to have a degree of biocompatibility. Biocompatibility was first described by Williams whereby a scaffold would elicit a desirable biological response without resulting in toxicity (Williams, D., 2003 and Williams, DP., 2008). It is essential that cell scaffolds should be nontoxic to the host and must not interfere with the regeneration process (Athanasiou *et*

al., 1995). The biodegradability of the material must be assessed as degradation can have detrimental effects on cell survival for the incorporated cells and the tissue surrounding the wound site with the degradation rate required to match that of new tissue growth (Barrera *et al.*, 1993 and Martins *et al.*, 2008). *In vivo*, the scaffold functions to aid in wound healing and the regeneration process and ideally should contain a reservoir of cells plus effector molecules to promote cell viability, differentiation and integration wit the surrounding tissue (Griffith and Swartz, 2006). Incorporation of cytokine growth factors with controlled release to the cells, such as fibroblast growth factor (FGF), transforming growth factor (TGF) and bone morphogeneic protein (BMP) to name a few examples, has been investigated to enhance cell activity and differentiation of the incorporated cells and those around the implanted device (Nathan and Sporn, 1991). For example, BMP-2 has been shown to induce osteoblast differentiation, cell proliferation and the synthesis of osteocalcin at the site of implantation (Yamaguchi *et al.*, 1991) while TGF-ß1 regulates cell growth, differentiation and migration (Grimaud *et al.*, 2002 and Massagué & Wolten., 2002). There are however, problems with incorporating growth factors with scaffolds. For example, the use of BMPs has been linked to cancer (Thawani et al., 2010) leading researchers looking for alternative means of inducing a specific cellular response without the use of chemical induction and supplements.

1.1.1 Functional Tissue Engineering

Over a decade ago, a new term was coined which placed emphasis on the role of biomechanics and mechanobiology in the tissue engineering field. This term, “functional tissue engineering”, places focus on understanding more about the biomechanical properties of the native tissue, developing scaffolds with specific biomechanical properties and how mechanical forces affect tissue repair *in vivo* (Guilak and Baaijens, 2014). Previously, scaffolds have been developed which result in adequate cell incorporation, but once mechanical forces are applied the construct can fail over time resulting in subsequent operations to replace the device. Surgeons have faced challenges, such as the promotion of function between the implant and the host tissue, in repairing or replacing tissues that have a predominantly mechanical function such as the articular cartilage of the knee joint. This tissue has limited capacity for intrinsic repair and even slight injury can progress to joint degeneration (Guilak *et al.*, 2001). For successful

scaffolds, first the *in vivo* stress and strain must be measured for a variety of activities, with this providing the necessary mechanical threshold that the replaced tissue will experience after surgery (Butler, *et al* 2000). Therefore, the field of tissue engineering is becoming one of increasing complexity with more attention emphasised on achieving a long lasting mechanically sound scaffold to replace the diseased or damage tissues (Stella *et al.*, 2010).

1.1.2 Bone Tissue Engineering

Bone tissue engineering is a field which has grown rapidly in the past ten years, in particular with the introduction of hip replacements, and more recently, the development of materials with nanotopographic signals to promote stem cell differentiation. These materials have been designed to successfully promote bone formation at the implant site and titanium has consistently demonstrated its suitability as a scaffold material for orthopeadic implants such as in knee and hip replacement surgeries (Goodman *et al.*, 2013). However, in bone tissue engineering (repair not replacement), it is a mistake to assume a one scaffold fits all approach. In bone tissue engineering, the scaffold is required to be specific to the location of damage (Sanz-Herera *et al.*, 2009) such as in maxillofacial reconstruction. In this field, the geometry of the bone, which must be replaced and regenerated, is highly specific and depends on the extent of damaged tissue. A material or scaffold is required which matches the exact shape of the defect site (Healy and Guldberg., 1995). In recent years, researchers and clinicians have begun to work together with the purpose of developing a suitable biomaterial restoring function where disease tissue was removed.

Willert and Semlitsch were the first to describe aseptic loosening and osteolysis due to periprosthetic tissue reacting to prosthetic wear microparticles (Willert & Semlitsch., 1977). This is caused by introducing a device that alters the load transmitted to the surrounding tissue, initiating the bone remodelling process that then results in reduced bone mass density because of progressive bone resorption (Muratone *et al.*, 2012). The device used in these replacement surgeries also initiated a local inflammatory response and recruitment of inflammatory cells such as macrophages, neutrophils, fibroblasts and lymphocytes. These cells interacted with implant wear particles leading to the

secretion of pro-inflammatory factors, causing increased survival and proliferation of bone absorbing cells. This prevented bone forming cell activity, promoting proteolysis resulting in implant failure (Shanbag *et al.*, 1994; Harris., 2001 and Purdue *et al.*, 2007). As a result of bone destruction around the device, aseptic loosening, loss of implant functions and pathological fractures (Clohisy *et al.*, 2004) occurred. These factors have led to the urgent need for better modes of surgery to prevent device failure occurring due to the wrong cell type forming around the device preventing integration with the host tissue.

Implant failure results in the patient requiring revision surgery, which can have an increased risk of complications, such as postoperative dislocation, infection and intraoperative diaphyseal fractures to name a few examples (Pekkarinen *et al.*, 2000). To look at circumventing this problem, McNamara *et al*, 2011 have investigated different nanotopographies on titanium implants to influence cell behaviour. It has been shown that certain nanopatterns induce stem cells to differentiate (specialise) into osteogenic lineages (Dalby *et al.*, 2005; Biggs *et al.*, 2009; McNamara *et al.*, 2011; McMurray *et al.*, 2011 and Wilkinson *et al.*, 2011). It is predicted that this would prevent implant failure as in time, the specific nanopatterns on the implant will promote the stem cells to correctly integrate with the native bone tissue therefore reducing the risk of implant failure. Overall, a suitable scaffold is required for numerous tissue applications to ensure that such devices will promote the correct cell population arising by guiding their growth and providing the correct biochemical and topographical cues (Yang, 2001 and Reichert & Hutmacher, 2011).

In maxillofacial reconstruction, there is increasing research into alternative methods in aiding repair and reconstruction. In this case, the properties of scaffolds as well as hydrogels may be beneficial in promoting cell viability and differentiation, and they can be moulded to fit a particular defect site. Oral and maxillofacial (OMF) surgery is performed to treat many conditions affecting the mouth, jaws, face and neck and may be caused by tumours, infections and facial disproportion due to fractures (Sutton *et al.*, 2003; Caccamese & Coletti., 2008 and Kim & Huoh., 2010). The research regarding alternative approaches for OMF surgery has developed considerably in recent years. Traditional approaches to OMF surgeries involved using methods such as the free fibula flap where a piece

of the patients' fibula bone is removed and used to repair a defect in the jaw (Hidalgo., 1989). However, newer approaches are utilising stem cells and biomaterials to promote osteogenic differentiation to occur in the area that has been removed (Alfotawi *et al*., 2013).

1.2 Bone and bone marrow

Bone is a highly complex tissue which is made up of cancellous and cortical bone (Rho *et al*., 1999). This tissue provides a number of essential functions in the human body such as structural support, the protection of vital internal organs, mobility (as muscle can attach via tendons), and also homes tissue where stem cells reside (Clarke., 2008). In the past, bone and bone marrow were considered two different systems (even though they are anatomically contiguous), because the bone provided support whereas the bone marrow homed stem cells involved in hematopoiesis giving rise to all cells of the blood (Taichman., 2005). However, it is now known that the bone marrow is a complex tissue in itself, and also is the location where bone precursor cells reside. This is beneficial as cortical bone undergoes constant remodelling due to mechanical load, commonly referred to as Wolff's Law (Pearson & Lieberman., 2004). The majority of the bone mass is taken up by the bone extracellular matrix, consisting mainly of type I collagen and hydroxyapetite (Reichart & Hutmaker, 2011).

The bone marrow is described as soft tissue present and confined to the cavities of bones, and is home to hematopoietic stem cells (HSCs) and mesenchymal stem cells (MSCs) as shown in Figure 1.2, which will be discussed in section 1.4. Other cell types are also present such as red blood cells, osteoblasts and osteoclasts. Decreased bone formation and mass, as well as an increase in the volume of adipose tissue is associated with osteoporosis and an increased susceptibility to fractures as discussed by Riggs & Melton., 1983. Within the bone marrow niche there are regions where stem cells can be obtained, these are referred to as the sinusoidal niche, which is highly vascularised and in the centre of the bone marrow, and the endosteal niche which is located next to osteoblast cells. These will be discussed further in section 1.6.

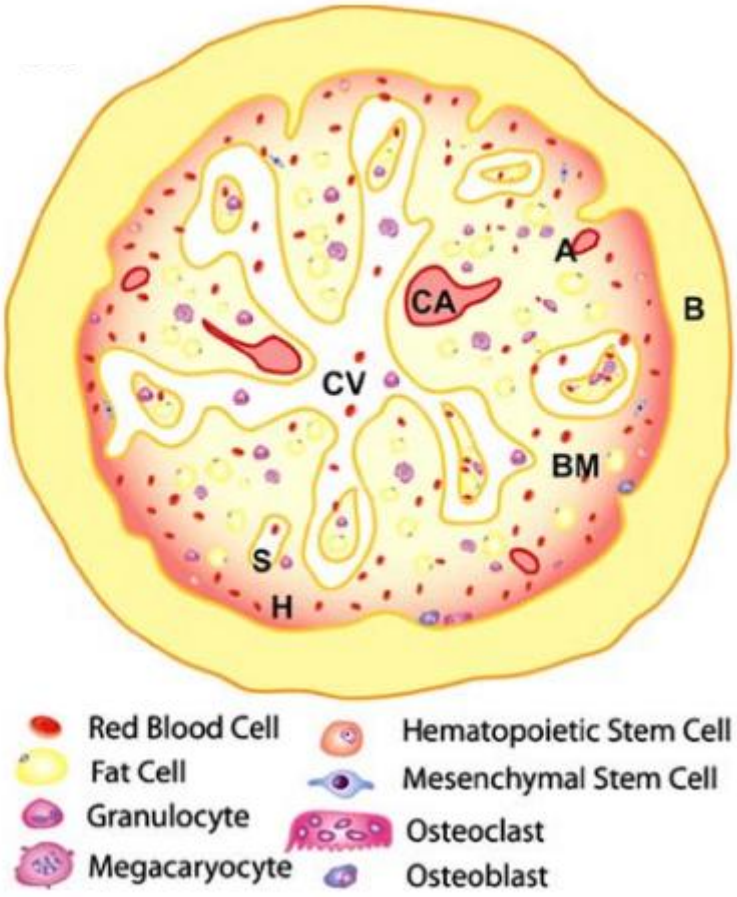

Figure 1.2 Bone marrow layout in a cross sectional view of tubular bone.
Bone (B) contains the bone marrow (BM). Within the BM are the central vein (CV) and the central artery (CA), which branch towards the periphery to form arterioles (A) and sinusoids (S). (H) refers to the hematopoietic space of the bone marrow, and the key below illustrates the cell types present within this tissue. Figure adapted from Gurkan & Akkas., 2008.

1.2.1 Process of bone remodelling

Bone remodelling occurs through the process of bone resorption and formation, a specialised function performed by osteogenic cells. This is an important process in the maintenance of healthy bone during growth (Sims & Martin, 2014). There are three main cell types involved in the process of bone formation, these being osteoblasts, osteoclasts and osteocytes (as reviewed by Lerner., 2012). Osteoblasts are derived from MSCs, and function to make organic matrix whereas osteocytes are formed when osteoblasts are trapped in the mineralized matrix of bone (Franz-Odendaal *et al.*, 2006). Thirdly, osteoclasts originate from HSCs and are bone resorbing cells (Parrika *et al.*, 2005). Bone resorption occurs in pits known as Howship's lacunae, which are associated with the process of bone

formation (Little *et al.*, 2011). Figure 1.3 illustrates the process of bone formation and resorption. The process has three steps starting with resorption whereby osteoclasts digest old bone, a reversal stage whereby mononuclear cells appear on the surface of the bone and finally new bone is formed by osteoblast cells (Hadjidakis & Androulakis, 2006).

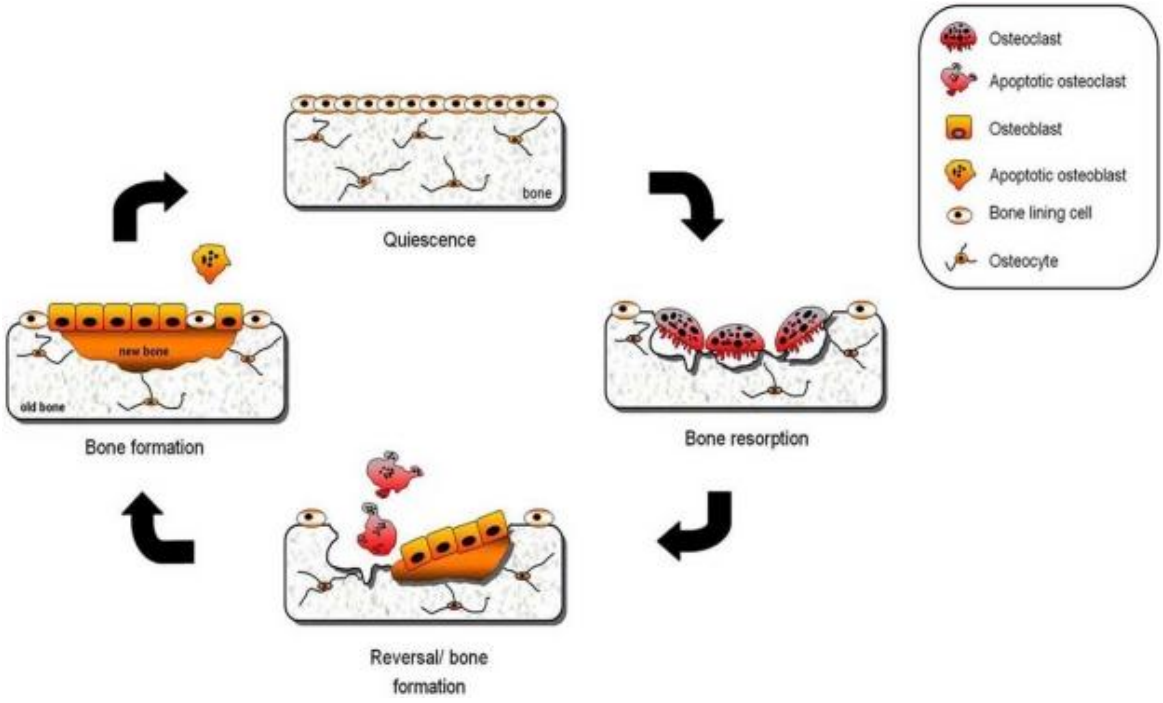

Figure 1.3 Process of bone remodelling.
This presents the cycle that occurs during the process of bone resorption by osteoclasts and bone remodelling by osteoblasts. Osteocytes within the bone tissue attract osteoclasts to the site of remodelling. These cells attach, resorb the bone matrix and detach as apoptotic osteoclasts when the process is complete. Following on from this, osteoblasts are attracted, proliferate and deposit osteoid which initiates new bone formation. To complete the cycle, this newly formed osteoid becomes mineralized and a layer of bone lining cells populates the lining of the bone tissue. Figure adapted from Idris *et al.*, 2010.

1.3 Stem cells

Stem cells are a specialized progenitor population that can undergo self-renewal and differentiate into a number of tissue types within the human body (reviewed in Kolf *et al.*, 2007; He *et al.*, 2009; Sieta & Weissman., 2010 and Fuchs *et al.*, 2012). There are generally three broad categories of stem cells, embryonic stem cells (ESCs); induced pluripotent stem cells (iPSCs) and adult stem cells (ASCs). ESCs can be derived from a developing foetus and possess the ability to differentiate into cell types from all three germ layers; endoderm, mesoderm and ectoderm, as shown by Figure 1.4 (Thomson *et al.*, 1998). The use of ESCs in research is of ethical concern due to the process of obtaining these cells from a foetus. Their capacity to form teratomas by spontaneously and unregulated

differentiation is also of concern (Wakatani *et al.*, 2002 and Nussbaum *et al.*, 2007). Teratomas are non-malignant tumours composed of multiple cell types from all three germ layers (Wesselschmidt, 2011).

iPSCs are normally fibroblast cells that have been reprogrammed, resulting in the capacity to differentiate into any cell type. Reprogramming of such cells is possible by delivery of viral plasmid vectors containing transcription factors such as Oct 3/4, Sox2, c-Myc and Kl4f which are used to induce pluripotency (Merkl *et al.*, 2013). After such processes, the transformed cells have similar properties to ESCs such as gene expression profile, proliferative ability and cell surface markers (Yu *et al.,* 2007). These iPSCs have gained interest as they do not possess the same ethical restrictions as ESCs and have been shown to differentiate into a number of cell types such as β cells to be used as a model of human diabetes treatment (Shaer *et al.*, 2014).

The third types of stem cells, ASCs, are derived from an adult tissue. This stem cell is restricted to form the specialized cells of the tissue that it is derived from (Lutolf & Blau., 2009). These cells are responsible for tissue regeneration throughout life. ASCs are present at specific anatomical positions and their main role is to facilitate tissue repair and wound healing (Chen *et al.*, 2009). There are a number of locations where ASCs reside, and each has specific differentiation ability as shown in Table 1.1. These stem cells have become key players in tissue engineering as they are known to have a pivotal role in normal tissue repair and remodelling due to their differentiation abilities (discussed in section 1.4.1). There are, however, implications with this cell source, as the vast number of cells required for implantation into potential scaffolds is generally greater than what can be achieved in standard cell culture, and the cells often lose their multipotent ability due to excess passaging (Zhang & Kilian., 2013). Standard cell culture methods fail to promote rapid cell division as well as promote stem cell “stemness” as the conventional culture conditions lack the complex and nurturing microenvironment found in the *in vivo* niche (McMurray *et al.*, 2012).

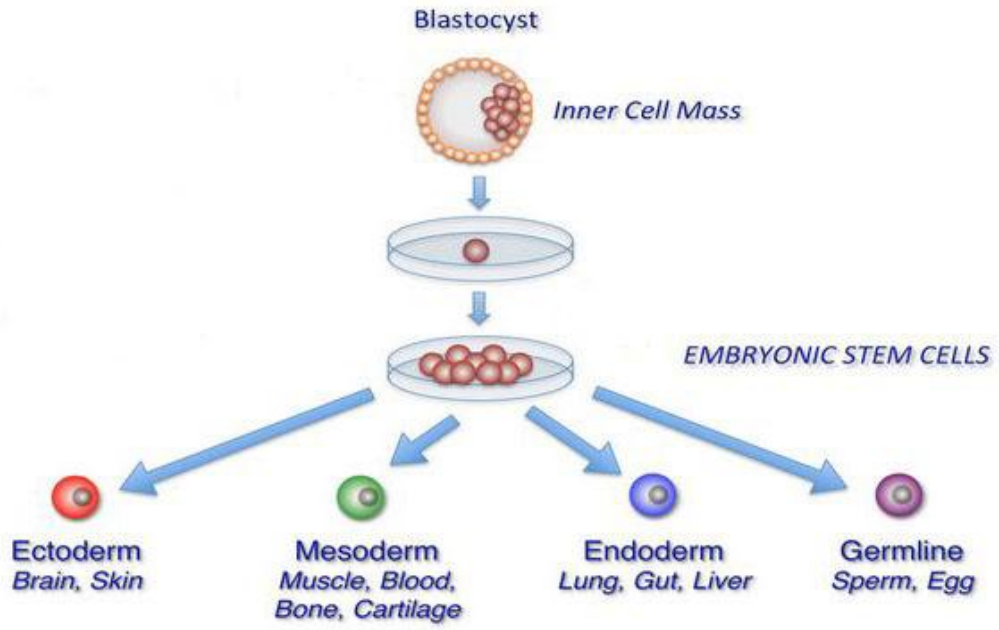

Figure 1.4 Embryonic stem cell differentiation *in vivo*.
ESCs can be obtained from the inner cell mass of a blastocyst after fertilisation has occurred. The cells can be cultured *in vivo* and can be differentiated to form the three human germ layers, the ectoderm, mesoderm and endoderm, as well as form germ line cells such as the egg and sperm. Figure adapted from Yabut and Bernstein, 2007).

1.3.1 Stem cell self-renewal and differentiation

Creating reservoirs of undifferentiated stem cells as well as understanding their ability to differentiate *in vitro* is critical for creating a large pool of cells to be used in cellular therapies (Dawson *et al.*, 2008). Stem cell self-renewal is defined as the process by which a stem cell divides, that results in new cells that have similar development potential to that of the original mother cell, and can otherwise be described as maintenance of stemness (He *et al.*, 2009). This process can also be described as symmetric division (Morrison *et al.*, 1997). In the stem cell niche, self-renewal is critical as it allows the size of the stem cell pool to be regulated and maintained within adult tissues as well as helping to replenish stem cell numbers due to tissue damage or disease (Potten & Loeffler., 1990). Self-renewal is not to be confused with cell proliferation, which is a general term used to describe all cell divisions and not those specifically associated with the maintenance of developmental potential (He *et al.*, 2009). Stem cell differentiation is defined as the switch from self-renewal to lineage commitment, a process whereby the original stem cells have lost their ability to

self-renewal. This process is believed to involve Wingless-type (Wnt), Notch and mitogen-activate protein kinase (MAPK) pathways (Oeztuerk-Winder & Ventora., 2012).

Name	Tissue of Origin	Differentiation Potential
Mesenchymal stem cells	Bone Marrow Adipose Tissue Umbilical Cord	Bone, Fat, Cartilage, Fibroblast Muscle, Nerve
Hematopoetic stem cells	Bone Marrow Peripheral Blood Placenta	Erythrocytes, Neutrophils, Lymphocytes, Macrophages, Platelets
Neural stem cells	Brain	Neurons Oligodendrocytes Astrocytes
Endothelial stem cells	Peripheral Blood Bone Marrow	Blood Vessels
Epithelial Stem Cells	Digestive tract	Goblet Cells Absorption Cells Enteroendocrine Cells

Table 1.1 Stem cells residing in adult tissues.
A number of adult stem cells are present within a variety of anatomical niches in the human body. The cells within each niche can differentiate into specialised subset of cells depending on their location (Pittenger., 1999; Sieweke & Allen., 2013; Merkle *et al*., 2007; Yoder., 2007; Blanpain *et al*., 2007).

1.3.2 Mesenchymal Stem Cells

Mesenchymal stem cells (MSCs) belong under the family of stem cells referred to as adult stem cells. Mesenchymal stem cells can be extracted from the bone marrow, which is derived from the embryonic mesenchyme, and such cells are defined as a multipotent, self-replicating population, which upon stimulation can differentiate toward osteogenic, adipogenic, reticular and chondrogenic cell lineages (Figure 1.5) (Zuk *et al*., 2001 and Hass *et al*., 2011). Due to their limited ability to differentiate, MSCs are referred to as being multipotent which separates them from the pluripotent ESCs (Zuk *et al*., 2002). In the bone marrow niche where these cells reside, there is a fine balance between self-renewal and

differentiation to allow proper development and to avoid uncontrolled growth, which is characteristic of cancer (Koch *et al.*, 2013).

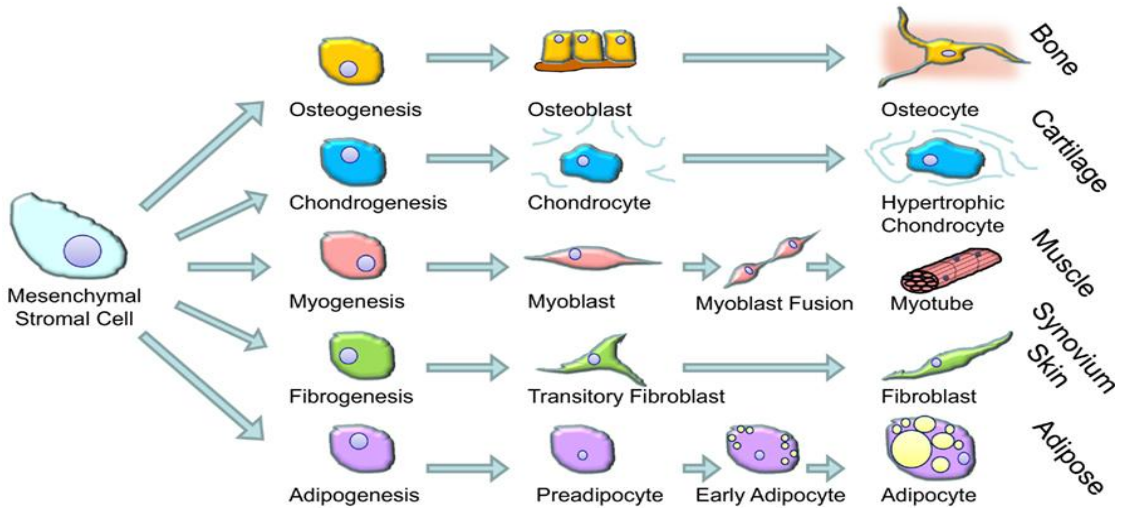

Figure 1.5 Mesenchymal stem cell differentiation.
Mesenchymal stem cells derived from bone marrow tissue have the differentiation capacity to become a number of cell types as illustrated. The process of differentiation is not a straight forward action; it involves a number of stages for full commitment to be achieved, as can be shown with adipogenic differentiation. Figure adapted from Hardy & Cooper, 2011.

1.4 Pericytes

Pericyte is the term used to describe mural cells which are embedded within the vascular basement membrane of blood vessels and are therefore associated with endothelial cells, micro-vessels, capillary walls and vascularisation (Armulik *et al.*, 2005). This property makes them highly abundant in comparison to other stem cells such as MSCs. Association with the vascular system may allow them to relocate and supply various niches around the human body with a multipotent population (da Silva Meirelles *et al.*, 2006). It is thought that MSCs originate from perivascular cells, which also include adventitial cells. Pericyte cells can be separated by means of Fluorescence activated cell sorting (FACS), which is a method utilising light to separate a cell population based on fluorescent characteristics of each cell by using a fluorophore attached to an antibody. As the adventitial cells presenting the surface markers $CD146^{+}$ and $CD34^{-}$ this method of FACS can be applied (Zimmerlin *et al.*, 2010 and Levesque., 2013). In the literature pericytes are referred to as mural, vascular smooth muscle cells or Rouget cells, after the Charles Rouget who first identified these cells (Bergers & Song., 2005). A number of studies have presented the multipotent capacity of

pericytes (Cai *et al.*, 2009; Farrington-Rock *et al.*, 2004; Brighton *et al.*, 1992 and Diefenderfer & Brighton., 2000), a property associated with MSCs. Pericytes are hypothesised to be required for microvascular function and stability (Lindahl *et al.*, 1997). Pericytes have shown osteogeneic differentiation in culture and this, alongside their vascular location, may make them a promising cell source in the field of bone regeneration (Caplan & Correa., 2011).

1.5 Stem cell niche

The concept of the stem niche was initiated by Schofield (Schofield., 1978) and is defined as a complex and dynamic microenvironment believed to comprise not only of stem cells, but also a diverse gathering of neighbouring differentiated cell types. These secrete and organise a rich milieu of extracellular matrix (ECM) and other factors that allow stem cells to manifest their unique intrinsic properties, shown by Figure 1.6 (Fuchs *et al.*, 2004). Neural signalling, metabolic changes in response to cellular processes, extrinsic signals from outwith the niche as well as physical interactions with the niche basement membrane, ECM and other cell types, all promote regulation of the stem cell niche (Li & Xie., 2005). The niche functions to control cell quiescence, self-renewal and differentiation to ensure population homeostasis by balancing the proportion of cells undergoing division (Simons & Clevers., 2011). Stem cells divide by two means in the niche, symmetrically and asymmetrically. The former method relies on one stem cell dividing to create two identical daughter stem cells while the latter describes stem cell division whereby a committed cell and one stem cell are produced from the original stem cell (Yamashita *et al.*, 2010).

Most mammalian niches remain ill defined because of their potential locations in the body (Lutolf and Blau, 2009), however, the best understood niche is the hematopoietic stem cell (HSC) niche (Ehninger & Trumpp., 2011). Niche locations are not fully identifiable and niches in the bone marrow and epithelial gut have been proposed due to the architecture, cell types present and their location for cells to be maintained as well as exit in response to extracellular signals (Isern & Mendez-Ferrer., 2011). HSCs are found as single cells in the trabecular cavities of long bones, which contain two regions where HSCs may reside, the endosteal or sinusoidal niches. The endosteal location is situated in the immediate proximity of the bone-lining osteoblast cells, (Nakamura et al.,

2010) and the sinusoidal niche which is a highly vascularised area near the centre of the marrow (Di Maggio *et al.*, 2011).

Nestin^{+} MSCs reside within the HSC niche and express CXCL12, which is a HSC maintenance factor transcript, and have multipotent differentiation potential. These MSCs are closely associated with HSCs at the endosteal lining and sinusoids however they are generally found at more central locations in the niche as they are vascular. Another cell population present is a CXCL12 abundant reticular cell (CAR cells) which are bipotent progenitors able to differentiate down the adipo- and osteogenic lineages. CAR cells are also found in the central locations of the bone marrow niche, are tightly associated with the sinusoidal endothelium and have morphology similar to pericyte cells (Ehninger & Trumpp., 2011). This data suggests MSC activity occurs within the larger pericyte population that associates closely with the vascular system in the human body (Crisan *et al.*, 2008).

The architecture of the bone marrow niche is said to be composed of hydrated crosslinked networks of ECM proteins and sugars in a three-dimensional state, whereas in epithelial tissues such as the gut, the stem cells have been found to adhere to a two dimensional sheet-like basement membrane (Lutolf et al., 2009). This suggests the anatomical location and complexity of the microenvironment niches can diverse and may well depend on the unique requirements of the residing stem cell population. The rigidity of the niche is determined by the structure of the surrounding ECM but the function to maintain stem cell population is uniform throughout. Overall, the niche is believed to function as a regulatory system to maintain the MSC population, preventing depletion and over production of this vital cell source (Scadden, 2006).

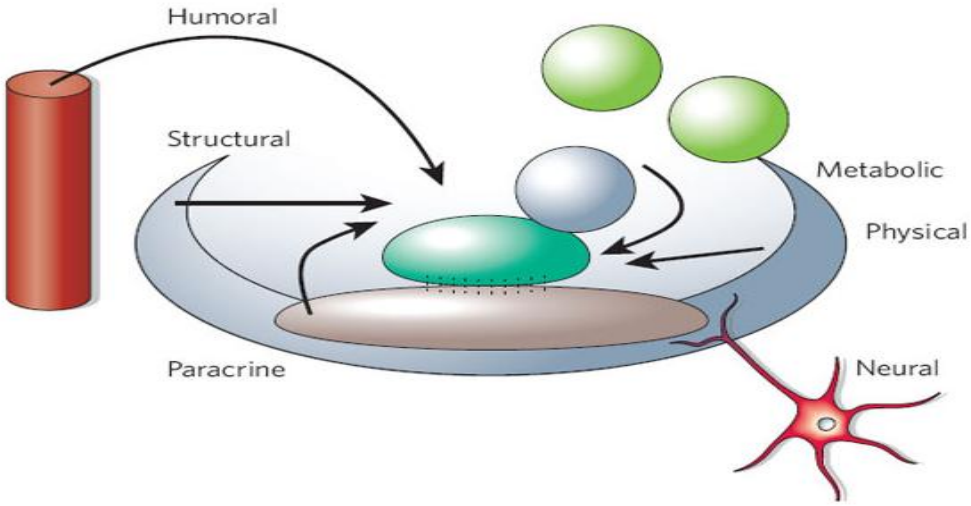

Figure 1.6 Elements of the stem cell niche that contribute to stem cell maintenance. Dark green cell in centre depicts stem cell. The niche architecture, cell-cell contact with neighbouring cells, signalling molecules such as those from paracrine and endocrine origin, neural cell input as well as metabolic and humoral products are believed to be important players in the maintenance of MSCs within the niche. (Figure from Scadden, 2006).

1.6 Cell and ECM interactions

Living cells in their natural environment are tightly associated with their ECM, with focal adhesion (FA) structures forming at the contact point between a cell and its substrate. Transmembrane receptors, known as integrins, are critical to the focal adhesion assembly (Petit & Thiery., 2000). They are a family of heterodimeric cell surface receptors consisting of α and ß subunits (Plow *et al.*, 2000), which bind to specific ligands within many ECM proteins e.g. collagen, Laminin and fibronectin (Stupack & Cheresh., 2002), and also associate with the actin cytoskeleton through a large multimolecular protein complex termed the focal adhesion plaque (Bershadsky *et al.*, 2003). Adhesion to the ECM in this manner, allows a cell to anchor and spread while the tractional forces generated at these focal points facilitates cell mobility (Rape *et al.*, 2011).

Adhesions formed from integrins binding to ECM ligand are differentiated by their size and location, as shown in Table 1.2. Focal complexes are small adhesions, which are present at the leading edge of a migrating cell, and are the precursor to FAs (Cukierman *et al.*, 2002). FAs are larger in size and located at the cell periphery. Strong adhesion occurs when integrins cluster together and bundle multiple actin filaments into large stress fibres. Once these are stable

and mature, the anchor points to the ECM may drive the formation of fibrillar adhesions (Geiger *et al.*, 2001 and Wozniak *et al.*, 2004). The adhesions described here are interrelated, as the focal complexes cannot mature to FAs if Rho or cell contractility is prevented (Geiger & Bershadsky., 2001).

	Size (μm)	Location
Focal complexes	~1	Leading edge of the cell
Focal adhesion	2-5	Cell periphery
Fibrillar adhesions	1-10	Central area of the cell

Table 1.2 Focal adhesion classifications
Table presents the three classifications of interactions that occur with integrin receptions. (Alexandrova *et al.*, 2008; Ciobanasu *et al.*, 2012, Friedland *et al.*, 2009)

As previously indicated, when a cell binds to an ECM ligand, integrin activation occurs and triggers clustering and the formation of focal adhesion plaques. While this enables a cell to anchor itself to a surface, it also enables the transmission of important regulatory signals between the cell and the ECM (Wehrle-Haller *et al.*, 2012). Proteins and kinases associated with the focal adhesion plaque are believed to assemble as per Figure 1.7, however the actual order these proteins assemble in is still largely unknown (Kanchanawong *et al.*, 2010). As most of the focal adhesion components contain multiple binding sites for other components, this model can, in theory, assemble in a number of alternate ways (Zamir & Geiger, 2001). Cell adhesion initially results in changes in integrin affinity and conformation promoting integrin clustering (Paszek *et al.*, 2009). Within the complex, talin alongside vinculin, function to link the actin cytoskeleton to the integrin receptors. Actin linked FAs remain stable in response to tension until adhesion disassembly in triggered (Grashoff *et al.*, 2010). Focal adhesion kinase (FAK) is an enzyme present within this complex and plays an important role in integrin signalling after cell adhesion to ECM has occurred. When localised to the adhesion plaque, it initiates signal transduction pathways within the cell (Parsons *et al.*, 2008) such as ERK signalling.

Focal complex progression into FAs is believed to be due to changes in intracellular tension or due to the elasticity of the substrate material. Cellular tension has been shown to direct stem cell differentiation, a substrate with low tensile state promoting cells to differentiate to the adipogenic lineage, whereas high tension induces ostegenesis (McBeath *et al.*, 2004). For MSC self-renewal to occur, it is hypothesised that an intermediate tension may be required (Gilbert *et al.*, 2010 and Tsimbouri *et al.*, 2012).

Thus, in addition to providing adhesion contacts to a surface, the focal adhesion assembly also plays a role in recognising the rigidity, spatial organisation and biochemical characteristics of the cell microenvironment. Since the focal adhesion complex is connected to the cell cytoskeleton and, by extension, the nucleus, this information can be transduced across the cell membrane and through the cytoskeleton eliciting a molecular response within the cell itself (Hu *et al.*, 2003). This is known as mechanotransdution.

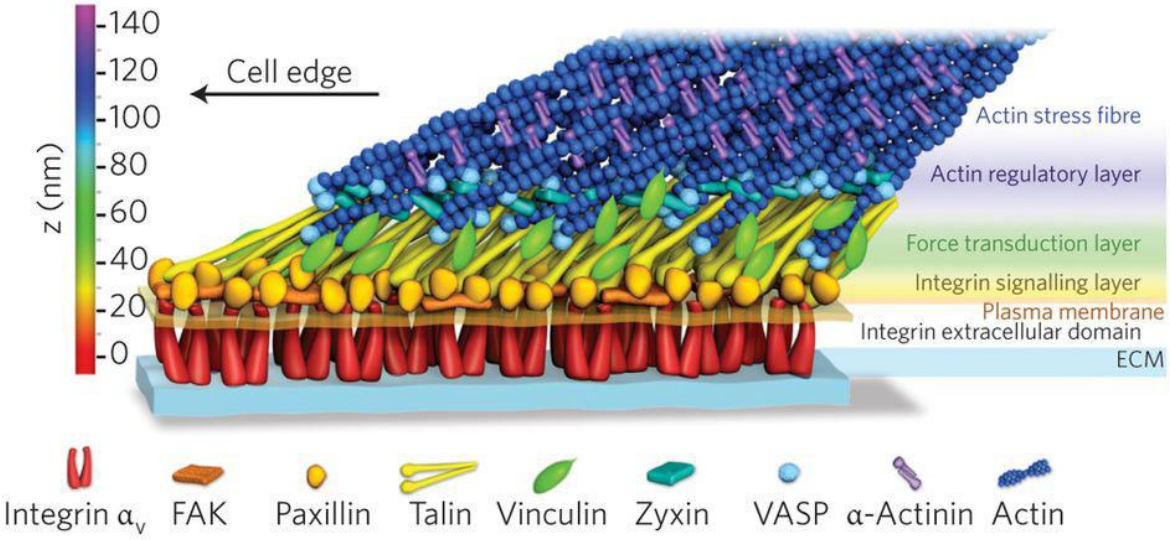

Figure 1.7 Focal adhesion complex.
This schematic diagram illustrates the position of proteins that are present in the adhesion assembly structure. Integrins initiate the attachment to the ECM, with FAK and Paxillin proteins forming an integrin signalling layer involved in signal transduction. Vinculin and Talin connect from this layer and play a role in force transduction between the integrins and actin filaments. Adapted from Kanchanawong *et al.*, 2010.

1.6.1 Catch Bonds

As previously discussed, integrins are adhesions formed between the cell and their ECM environment. The rigidity of the material substrate to which the cell is attached to is believed to tune the binding strength of the cell to its environment, and that a stiff substrate wound increase the lifetime of the integrin-receptor bond (Vogel & Sheetz., 2006). Catch bonds are so called because they can undergo tension strengthening and force can deform the molecules present within integrins allowing them to lock tighter with their corresponding ligands (Marshall *et al.*, 2003 and Friedland *et al.*, 2009). As integrins have been described as being mechanotransducers, a process which will be discussed in the following section, catch bonds have been discussed as playing a physical role in sensing forces as different force lifetimes correspond to different activation states that transduce direct signals into the cell (Kong *et al.*, 2009).

1.7 Mechanotransduction

Mechanotransduction is the process of converting physical forces into biochemical reactions, which affect cell behaviour and phenotype (Huang *et al.*, 2004; Vogel., 2006 & Wolf & Mofrad, 2009,). This process can be divided into two forms: direct and indirect mechanotransduction. The former relies on the cytoskeleton to relay messages about the local microenvironment to the cell nucleus as mechanical signals, while the latter relies on biochemical signalling through chemical cascades to send information to the nucleus (reviewed in Dalby, 2005). Numerous chemical, cellular and ECM components have been shown to play a role in mechanochemical transduction and these are shown in Figure 1.8. Mechanical forces directly effect integrin binding sites and changes to the ECM can alter the properties of integrin structure activating secondary messenger pathways (Silver & Siperko., 2003). Cells cultured on any given substrate, exert tensional forces against this surface as the cell adheres, migrates and spreads. In doing so, the cell can ascertain information about the physical properties of its environment. A surface that is pliable and easy to deform, will result in low tension feedback while one which is stiff and not easy to deform, will result in a much higher tensional feedback (Provenzano & Keely,

2011). As a result, the tensional forces exerted back onto the cell alter the tension experienced across the cell cytoskeleton and leads to changes in cell output (Discher *et al.*, 2005).

The intracellular pathways initiated by mechanical forces and transmitted by focal adhesion assemblies are shown in Figure 1.9. Cytoskeletal contractibility involves Ras homologue guanasine triphosphatases (Rho GTPases), which are involved in the transmittance of force through intracellular force-generating proteins (Provenzano & Keely, 2011). The GTPase Rho is essential in controlling contractility resulting in the ability of cells to respond to the stiffness of their culture substrate. This function of sensing matrix stiffness is controlled by the Rho effector protein Rho-associated protein kinase (ROCK) (Wozniak *et al.*, 2011). Mechanical stress can also be applied from the outside, with the stress referred to as "outside-in" stimuli (Figure 1.10a). This system is common in cells present in load bearing tissues. An "Inside-out" stimulus (Figure 1.10b) is caused by cells pulling on their ECM environment (Provenzano & Keely., 2011).

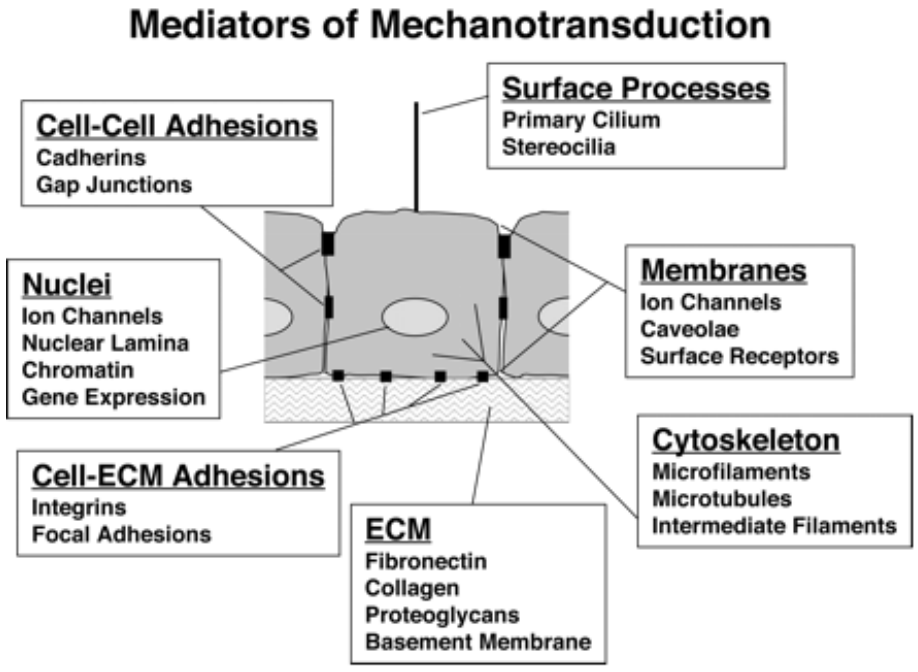

Figure 1.8 Mediators of Mechanotransduction.
Many molecules and processes play a role in mechanotransduction events. Cell – Cell contact, cell-ECM adhesions, membrane components cytoskeletal elements and nuclear structures can all play a role in this process. Adapted from Ingber, 2006.

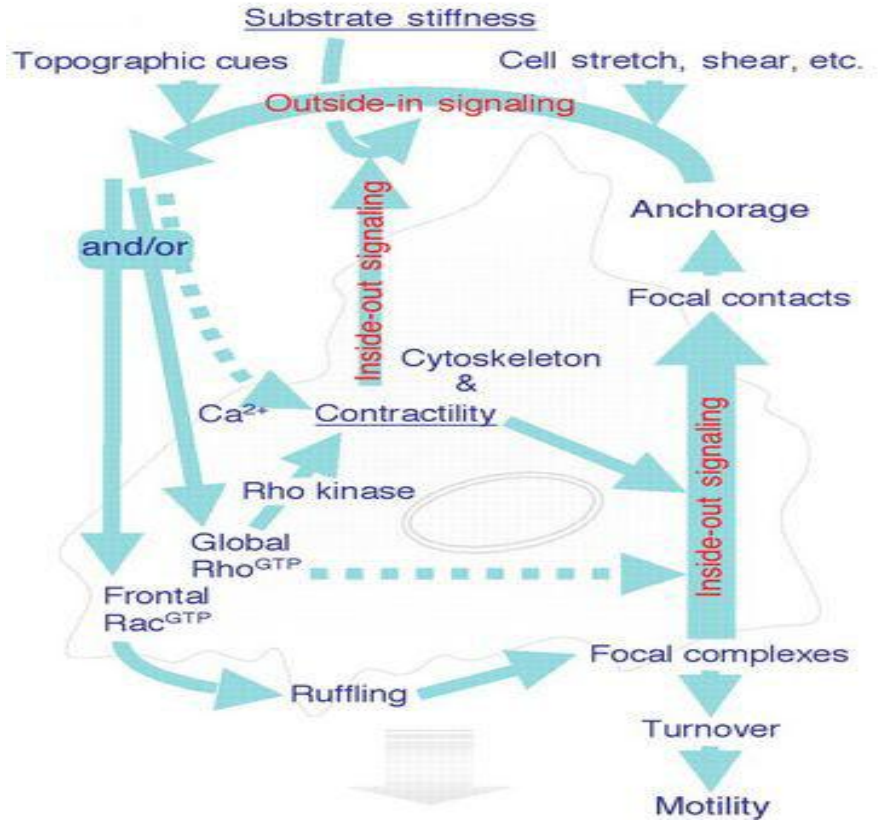

Figure 1.9 Feedback mechanisms of substrate elasticity.
Many molecules and processes play a role in mechanotransduction including cell–cell contact, cell-ECM adhesions, membrane components, cytoskeletal elements and nuclear structures. Adapted from Ingber, 2006.

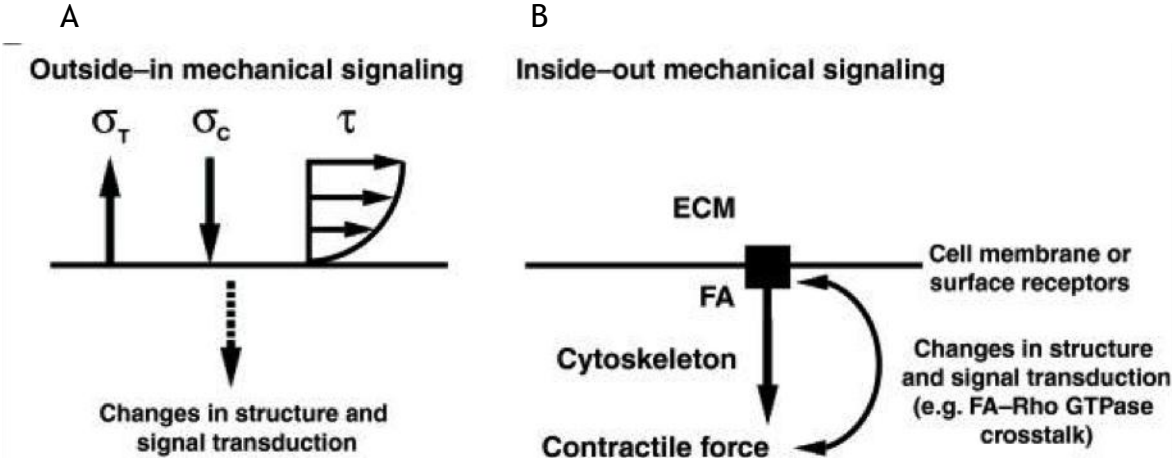

Figure 1.10 Outside in and Inside out Mechanical Signalling.
In section A, "outside-in" mechanical signalling is presented with σ_T illustrating tensile strength, σ_C compressive strength and τ shear stress as fluid flows over the cell. Cells in their physiological environment experience external forces producing stress within the cell such as those mentioned above. In section B, for "inside-out" mechanical signalling, the cell is generating mechanical energy from chemical energy in order to create a force used to deform the matrix substrate. Adapted from Provenzano and Keely, 2011.

1.8 Materials for MSC self-renewal and differentiation

Chemical induction is defined as the use of small molecules to promote a specific cellular response such as differentiation (Xie *et al.*, 2006). It has shown that MSCs can differentiate towards the adipogenic, osteogenic, myogenic and chondrogenic lineages in response to chemical cues, (Scott *et al.*, 2011; Jaiswal *et al.*, 1997; Wakitani *et al.*, 1995; Hagmann *et al.*, 2013) however materials are now being investigated to direct stem cell fate in the absence of chemical supplements (McMurray *et al.*, 2012). In this field, chemistry, elasticity and nanotopography have been investigated and demonstrate how materials with specific properties can direct MSC phenotype, as well as induce lineage commitment. The ECM is a highly complex microenvironment and to mimic all aspects of the niche for a suitable biomaterial is challenging. It has been suggested that, nanotopography, rigidity cues as well as ligand presentation all play a crucial role in maintaining MSCs in their undifferentiated state (McMurray *et al.*, 2011; Gilbert *et al.*, 2010 and Curran *et al.*, 2005). As a result, researchers have aimed to incorporate single aspects of this tissue to study the cell/material interface *in vivo* to understand the role they play in the maintenance of the MSC phenotype.

Maintaining the MSC phenotype *in vitro* is difficult; as there is a tendency for the cells to spontaneously differentiate reducing the proportion of true stem cells in a culture population (Tsimbouri *et al.*, 2012). This section will discuss how nanotopography, elasticity and chemistry have been applied to maintain the MSC phenotype and also promote differentiation in a different application.

1.8.1 Nanotopography

Nanotopography-induced stem cell maintenance has been shown by McMurray (McMurray *et al.*, 2010). In this work, it was shown that polycaprolactone (PCL) could be patterned with 120 nm diameter pits in a square arrangement with a centre-to-centre spacing of 300 nm. When STRO 1^+ MSCs were cultured on this substrate over eight weeks, they were found to retain their multipotency as evidenced by their continued expression of the stem cell surface markers STRO-1, activated leukocyte cell adhesion molecule (ALCAM) and CD63. These markers are typically used to identify undifferentiated stem cells (Lv *et al.*, 2014). To

confirm retention of the MSC multipotency, these cells were removed from the substrate and cultured on glass coverslips in osteogenic and adipogenic induction media. After a further 14 days, these cells were seen to express the peroxisome proliferator-activated receptor gamma (PPARG) indicative of adipogenesis, and osteopontin (OPN) indicative of an osteogenic commitment. Interestingly, when induction media was added to MSCs cultured on the square topography, which retained the stem cell phenotype, there was low expression of lineage markers suggesting a competition between the topographical cues embossed on the PCL, and the soluble factors within the induction media.

With regards to studies presented on nanotopography and MSCs, it is suggested that cellular response largely relies on the tension within the MSC cytoskeleton, and that a surface promoting high intracellular tension promotes osteogenesis, while one that induces low intracellular tension promotes adipogenesis (Engler *et al*, 2006; Kilian *et al*, 2010; McBeath *et al*, 2004). It is also suggested that, in order to maintain MSC multipotency, a surface neither promoting high or low intracellular tension is essential (Tsmibouri *et al*., 2012 and Gilbert *et al.,* 2010).

The evidence for topography induced differentiation is well documented, and is the process by which the specific patterning on the culture substrate has an effect on the stem cell phenotype (Gallagher *et al*., 2002, Gadegaard *et al*., 2009; Huang *et al*., 2009, Kruss *et al*., 2010 , McMurray et al., 2012 and Salvi *et al*., 2010). The material cells are cultured on can influence cell behaviour, such as influencing intracellular signalling (Hamilton *et al*, 2007), cytoskeletal organization (Yim *et al*, 2010), cell morphology (Andersson *et al*, 2003) and alignment (Andersson, 2003) to name a few examples. Nanotopography is important as cells encounter specific topographies depending on their anatomical location with bone for example presenting macro-sized pores and proteins in the nanoscale (Dalby, 2005).

Developments in electron beam lithography have allowed the advancement of polymethylmethacrylate (PMMA) substrates patterned with 120 nm diameter by 100 nm deep nanopits, in various patterns for studying MSC behaviour. By culturing cells on these substrates, cell adhesion and cytoskeletal tension within the cells have been investigated with the specific nanopatterns being shown to have a downstream effect on cell morphology. It was found that disordered

topographies favoured osteogenic differentiation and early mineralization was apparent after 28 days in culture (Dalby *et al.*, 2007). Further improvements in the nanotopography field have led to patterning on titanium substrates with 15 nm, 55 nm and 90 nm high nanopillars with controlled disorder hence moving towards orthopaedic applications. By culturing MSCs on these substrates, the aim was to induce osteogenic differentiation in these cells with the intention of improving orthopeadic devices as knee and hip replacement implants fail if an unsuitable tissue type forms around the implant. In this work it was found that MSCs grown on the 15 nm pillars displayed increased levels of RUNX-2, larger focal adhesions and deposition of osteocalcin (OCN) (markers for bone cell development) than any other of the other sized pillars, suggesting osteogenesis is induced on this substrate (McNamara *et al.*, 2011).

It is thought that this drive toward osteogenesis was brought about by increased intracellular tension within the cells, and that this increased tension resulted from the formation of super-mature focal adhesions greater than 5 μm in size. It is known that increased cytoskeletal tension induces differentiation toward the osteo lineages (Engler *et al*, 2006; Kilian *et al*, 2010; McBeath *et al*, 2004). Together, these findings indicate nanotopography can be used to influence MSCs toward osteogenic differentiation by promoting a high-tensional state within the within the MSC cytoskeleton, and that the optimal features for doing so, are 15 nm high with a disordered arrangement. Additionally, as well as maintaining MSC multipotency, these works demonstrate a potential use for nanotopography in a clinical role where it could be used to induce osteogenic differentiation in MSCs surrounding an orthopaedic device.

1.8.2 Substrate elasticity

The stiffness of a particular niche depends largely on the architecture, which is determined by protein constituents, as it is believed that stem cell differentiation is directed by the cell sensing changes in its environment from its native niche where stemness is maintained (Schofield., 1978). The bone marrow niche is reported to be approximately 250-750 Pa (Winer *et al.*, 2009), however when MSCs exit this niche and are targeted to new tissue due to inflammatory cytokines, the elasticity of the new tissue and environment promotes lineage commitment to occur. In a study by Gilbert (Gilbert *et al.*, 2010), laminin was

crosslinked to a polyethylene glycol (PEG) gel to produce a hydrogel substrate of 12 kPa in stiffness, mimicking the rigidity of the muscle microenvironmnt where muscle stem cells (MuSCs) reside. MuSCs cultured upon this substrate retained their multipotent properties and this was shown *in vivo* when these MuSCs were transplanted into the tibialis anterior muscles of immunodeficient mice and successful engraftment was confirmed by the expression of green flurescent protein (GFP) and firefly luciferase (Fluc) as MuSCs were originally isolated from mice constitutively expressing these markers. Stem cell integration was assessed by non-invasive *in vivo* bioluminescence imaging, which provided information regarding cell number, engraftment as well as validation of stemness of the transplanted MuSCs due to detection of these fluorescent proteins (Gilbert *et al.*, 2010).

Naive MSCs have been shown to specify lineage and phenotype due to tissue-like elasticity in culture, where is was discussed that gels 0.1-1 kPa are neurogenic, 8-17 kPa are myogenic and 25-40 kPa are osteogenic (Engler et al., 2006). Other research groups have studied elasticity in relation to differentiation and have discovered that cells cultured with substrates of low elasticity have resulted in poor focal adhesion formation and cell attachment due to the substrates inability to resist tractional forces (Grinnell & Ho., 2013). If the substrate surface is soft and easily deformed then the adhesions remain small and the natural tension within the cell that induces it to round when not adhered is the over riding force. In 2008, Rowlands and colleagues (Rowlands *et al.*, 2008) described how polyacrylamide gel stiffness could be modified by increasing the acrylamide monomer or bis acrylamide crosslinker, and incorporated this culture substrate with ECM proteins such as collagen I, collagen IV, laminin and fibronectin. It was found that the stiffest gel of 80 kPa, which contained collagen I, resulted in osteogenic differentiation as identified by the expression of Runx2, a transcription factor associated with osteogenic differentiation. Myogenic differentiation was also observed on hydrogels with a stiffness greater than 9 kPa, however highest MyoD expression, a regulatory factor in skeletal muscle development (Berkes & Tapscott, 2005), was found with a 25 kPa hydrogel. In this study, cell proliferation was also observed to increase in trend with increasing hydrogel stiffness due to integrin signalling through focal adhesion complexes. A model was hypothesised, as cells cultured on a stiff

matrix will promote a high contractility therefore resulting in the assembly of focal adhesions and highly clustered integrins. As a result, phosphorylation of FAK will be higher, resulting in activation of Extracellular signal regulated kinase (ERK) and hence proliferation to occur. In response to low substrate stiffness, the inverse relationship occurs with a low contractility cell state and low FAK phosphorylation and activity with differentiation occurring over cell proliferation (Schwartz & Ginsberg, 2002).

1.8.3 Surface chemistry

MSCs cultured upon glass and polymer surfaces patterned with a $-CH_3$ (methyl) group by use of dip pen nanolithography (DPN) has illustrated maintenance and enhanced expression of stem cell markers over a period of 28 days in culture, in the absence of media chemical supplements. In this study by Curran (Curran *et al.*, 2010) $-CH_3$ groups were deposited in a nano-structured self- assembled monolayer with a centre-to-centre spacing of 280 nm and dot diameter of 65-70 nm of this chosen functional group. By use of FACS analysis, MSC markers were quantified and presented expression of CD29, CD73, CD90, CD105 and ALCAM at a higher level than that of unmodified substrates and in comparison to cells cultured with standard tissue culture polystyrene. It was also interesting to note that expression of CD34 which is a marker not associated with MSCs, and instead HSCs, was lower on the $-CH_3$ surfaces than on tissue culture substrates suggesting that this functionally patterned substrate can maintain as well as purify the MSC phenotype. Overall, this substrate demonstrates a potential use in the field of regenerative medicine, as it would be beneficial to maintain and expand a multipotent MSC population *in vitro*, which could be used at a later stage with a different functional group such as $-NH_2$ to promote differentiation down the osteogenic lineage (Curran *et al.*, 2010).

Studies have revealed MSC differentiation can be achieved by confining cell shape by patterning substrates with adhesive ligands such as fibronectin (Kilian *et al.,* 2009) as shown in Figure 1.11 a. By patterning specific areas with ligands to which integrins bind (Figure 1.11 b and c) and making the area between the pattern non-conducive to cell adhesion, cell shape is confined to that of the pattern and results in alteration of phenotype. This effect is generally limited to adipogenic and osteogenic lineages as an inverse relationship occurs between

these two cell phenotypes where up-regulation of genes associated with one phenotype occurs at the expense of the other (James, 2013). It was found that when cells were maintained to a small area, MSC differentiation was driven down the adipogenic lineage due to low level tension within the cell, whereas with larger islands, where MSCs were able to spread, osteogenic differentiation resulted due to this specific patterned area promoting intracellular tension which is osteoinductive. Thus, by controlling ligand density, the MSC shape is altered and phenotype is affected. Confinement of cell shape also affects cell apoptosis and cell viability, as cells were more likely to undergo apoptosis on small fibronectin adhesive ligands as shown in Figure 1.11 d. Those cells cultured upon islands of larger size underwent DNA synthesis rather than apoptosis, which confirms the results of Rowlands *et al* in section 1.9.2.2 where cell proliferation was greater on stiffer substrates due to FAK phosphorylation. Ligand density was also described by Cavalcanti-Adam *et al.*, 2007 where integrin lateral clustering was investigated and showed that variations in spacing between tethered RGD peptides (a known integrin binding sequence), had an effect on cell spreading, migration and focal adhesion dynamics.

Silane modification of glass coverslips with $–NH_2$, -SH, -OH or –COOH functional groups have illustrated MSC differentiation *in vitro* in the absence of biological stimuli such as induction media. These functional groups were chosen as they can all be found in biological systems, and utilising the silane modification method, enables well-defined and organized substrates with different surface chemistries (Curran *et al.*, 2006). Through use of real time PCR (RT-PCR) and immunocytochemistry, MSC differentiation was confirmed to be driven towards the osteogenic and chondrogenic lineages when cultured on $–NH_2$ and –SH groups respectively. The amino ($-NH_2$) and silane (-SH) groups promoted and maintained osteogenic differentiation and confirmed the osteogenic capacity of the NH_2 functional group as described by Keselowsky (Keselowsky *et al.*, 2004, 2005). When cultured on these surfaces, cells stained positive for Osteocalcin (OCN) and core binding factor alpha-1 (CBFA1), which are both indicators of osteogenic differentiation and phenotype. When such cells were subjected to chondrogenic induction media, detection of collagen II was detected through staining, however cells presented reduced adhesion that suggests that even though

chondrogenesis can be promoted on this surface, it cannot be maintained and that osteogenic differentiation is preferred by MSCs.

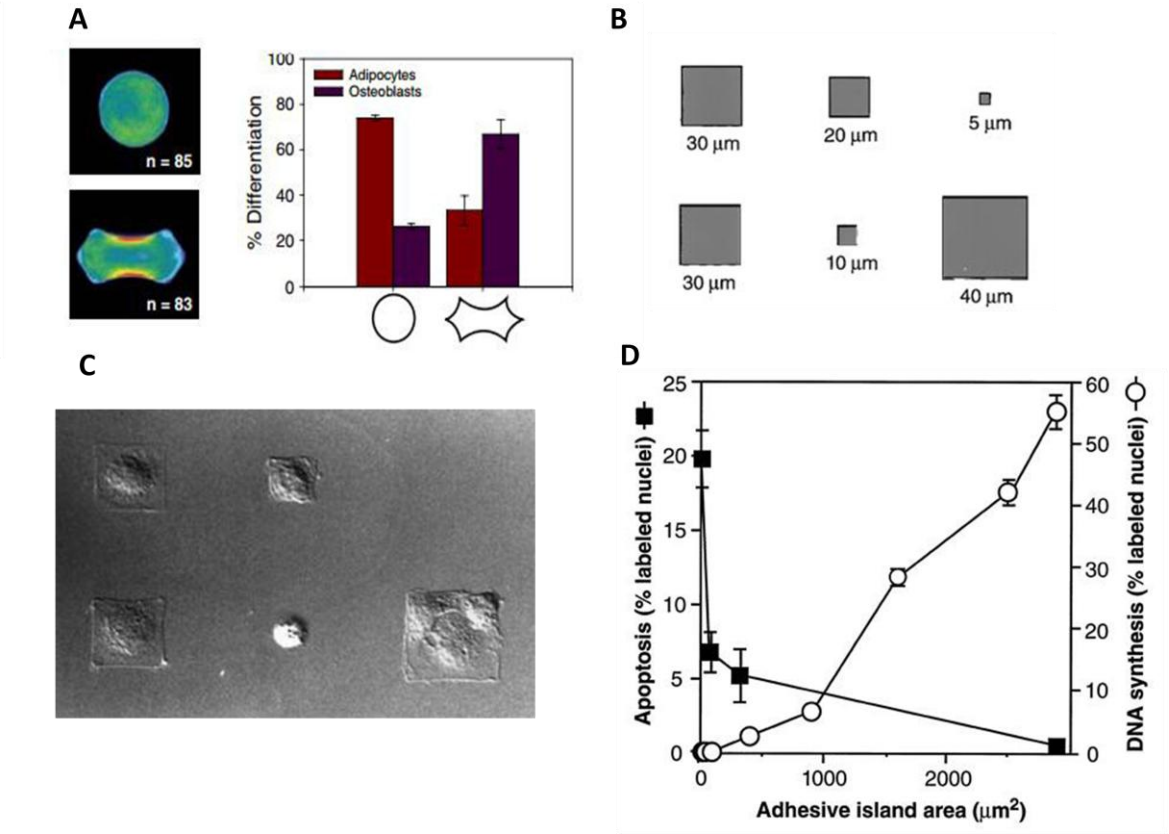

Figure 1.11 Geometric shape and MSC differentiation
(A) Specific adhesive shapes were created with octadecanethiolate on a glass cover slip covered with gold. The region was then modified with a monolayer and the hydrophobic island region was immersed in a solution of the ECM protein fibronectin, this allowed MSCs to adhere to the desired region and take on the shape of the island. When single cells were cultured upon the rounded island, it was found that they preferred to differentiate down the adipogenic lineage, whereas if MSCs were allowed to spread out and achieve higher cytoskeletal tension, osteogenic differentiation occurred. Adapted from Kilian *et al.*, 2009. Images (B) and (C) refer to schematic diagram of patterns containing different sized fibronectin adhesive ligands and the shape endothelial cells take when cultured upon these. It was found that the cells closely matched the size and shape of the fibronectin adhesive islands, and overall as the island area size increased from 75 μm^2 the rate of apoptosis decreased. DNA synthesis was also affected by island area, as area sized increased so did that of cell spreading and switch on of DNA synthesis rather than epithelial cells undergoing apoptosis (D). Adapted from Chen *et al.*, 1997.

MSCs seeded on glass functionalised with –OH and –COOH groups, demonstrated chondrogenic differentiation as identified by the presence of collagen II using immunocytochemistry after 7 and 21 days in culture. However, osteogenic markers OCN and CBFA1 were also expressed by cells cultured upon this modified substrate, but only up to 7 days in culture, after which expression was

diminished. These finding illustrate an example of how glass coverslips can be modified to incorporate functional groups such as those described above. By doing so, MSCs have shown to differentiate in culture, and express markers associated with that defined lineage. The use of these functional groups present in biological systems presents that by changing the surface chemistry alone, can be sufficient in controlling differentiation pathways of MSCs in the absence of chemical and supplement agents (Curran *et al.*, 2005 and Curran *et al.*, 2006).

Overall, material science has demonstrated the use of chemical, elasticity and nanotopographical means as a way to retain the MSC phenotype, as well as promote differentiation. With regards to the nanotopography described in this section by McMurray *et al*, 2011, the surfaces have similar chemistry and stiffness values as they are embossed on the same material and have identical contact angles. This illustrates one example of how substrate patterning can be used to modify the MSC response, allowing the other surface properties to remain uniform. For materials to be successful and used in the tissue engineering field, the response elucidated by the cells must be homogeneous, with all cells presenting a uniform phenotype in response to the stimulus presented, with the aim of creating a tissue which is structurally correct. The examples mentioned in section 1.9 present the use of materials-induced multipotency as well as material-induced differentiation, which will have an enormous effect in future tissue engineering constructs as the efficiency will be greater than current scaffolds and devices due to homogeneous cell populations arising and the redundancy of chemical inducers.

1.9 Hydrogels

Hydrogels are an emerging group of biomaterials that are providing researchers with new culture substrates for the growth and study of many cell types *in vitro*. They can be composed of synthetic or natural compounds such as PEG and collagen, respectively (Bryant & Anseth., 2002 and Helary *et al.*, 2012). Hydrogels are made up of a network of polymers that are extensively swollen with water due to the hydrophilic functional groups on the backbone of the polymeric components (Mathur *et al.*, 2006 and Ahmed *et al.*, 2013). These hydrogels can be used for the purpose of regenerative medicine as the water content of these gels can closely mimic that of natural tissues in the human body

(Jatav *et al.*, 2011). Their use is not restricted to this field, however, and they also have applications in wound healing and drug delivery systems (Kokabi *et al.*, 2007 and Qui & Park., 2002).

Such materials can be synthesized by various means such as cross-linking, copolymerization and self–assembly processes, or designed to form a hydrogel from solution in the presence of pH, light, temperature or magnetic stimuli (Na *et al.*, 2003; Haines *et al.*, 2005; Collier *et al.*, 2001 and Li *et al.*, 2012). Nanoparticles have also been incorporated within hydrogels in the development of antimicrobial delivery systems against gram positive and negative bacteria (Marsich *et al.*, 2011). Hydrogels are becoming increasingly popular due to their inexpensive and relatively easily production in comparison to manufacturing and patterning surfaces such as ceramics and titanium. Depending on the desired application, hydrogels can be patterned with ligands or growth factors to promote a desired cellular response such as cell survival, proliferation and differentiation (Lanniel *et al*, 2011). By utilising tunable peptide hydrogels and incorporating cell adhesion receptors such as the integrin receptor and tripeptide motif RGD, (arginine-glycine-aspartate), it is possible to control cellular behaviour such as cell migration as they mediate in interactions between the actin cytoskeleton and the ECM (Barczyk *et al.*, 2010 and Chan *et al.*, 2007). This RGD sequence plays a role in cell attachment as it can be found on proteins such as laminin and fibronectin within the ECM and integrin receptors on the cell surface bind to these.

1.10 Aims & Objectives

The aim of this thesis is to examine the effect that Fmoc peptide hydrogels have on MSC renewal and differentiation as a culture substrate in the field of regenerative medicine. This will be determined by:

- Creating a number of potential hydrogels with varying stiffnesses and characterising their properties by using methods such as scanning electron microscopy (SEM), high performance liquid chromatography (HPLC) and rheology.

- Studying MSC behaviour by in a 2D and 3D hydrogel environment and detecting markers associated with multipotency and commitment.
- Creating a collagen-Fmoc hydrogel model, and testing the biologically active compound cholesterol sulphate, a glucorticoid metabolite to examine whether or not this substance induces osteogenic differentiation in this model.

Chapter 2

General materials & methods

2.1 General Introduction

Mesenchymal stem cells have illustrated the ability to differentiate down a number of cellular lineages and this factor has made them a suitable candidate cell source for use in regenerative medicine. These cells are found in a number of anatomical locations but overall, they are found at low frequencies, approximately 1 in 10,000 cells from the bone marrow is defined as a MSC (Friedenstein *et al.*, 1970). Long-term culture of this valuable cell source has shown loss of the multipotency phenotype (Zhang & Kilian., 2013) so MSCs and osteoprogenitors (OPGs) described in this thesis were used at low passage number throughout.

In vitro, MSCs have shown to differentiate due to culture upon nanotopography, and differentiate in response to specific cues such as matrix elasticity (Engler *et al.*, 2006; Lavenus *et al.*, 2011; Hamilton & Brunett, 2007; Dalby *et al.*, 2007 and Park *et al.*, 2011). Biomaterials such as hydrogels are becoming increasingly popular for the study of MSCs as they can be patterned with ligands and growth factors to enhance cell growth and promote a particular cellular response (Comisar *et al.*, 2007).

In this thesis, peptide based hydrogels were the general culture substrate under investigation. In order to establish the effect substrate elasticity had on the MSCs, cell morphology, immunocytochemistry as well as gene expression studies were performed. Immunofluorescent labelling of markers was used to detect proteins associated with MSC multipotency as well as differentiation. Gene expression analysis of the MSC population was possible through the use of quantitative real time polymerase chain reaction (qRT-PCR). FACS is a method which can be used to detect the phenotype of each cell residing in a population. However when cells are cultured with a complex two and three dimensional (2D and 3D) substrate system such as the Fmoc based biomaterials which are used throughout this thesis, this method of cell sorting cannot be used as it is difficult to recover cells from the gel intact.

This section will provide understanding as to the methodologies used to examine the effect of hydrogel stiffness on MSC behaviour in 2D and 3D studies.

2.2 Materials

Materials / Reagents	Supplier
Human bone marrow mesenchymal stem cells-osteoprogenitors and CD271 selected cells	Southern General Hospital, Glasgow, UK
Adipose derived Mesenchymal stem cells	University of Edinburgh, UK
Dulbeccos modified eagle medium (DMEM)	Sigma Aldrich, UK
Foetal bovine serum (FBS)	Sigma Aldrich, UK
Antibiotic Mix	In house*
L-Glutamine (200mM)	Sigma
Trypsin	Sigma Aldrich, UK
Versene	In-house*
HEPES	In-house*
CD271 Positive Selection Kit	STEMCELL© Technologies
2% FBS in 1x PBS Solution	In- house*
TRIzol	Life technologies, UK
Chloroform	Ambion, UK
Isopropanol	Sigma Aldrich, UK
Glycoblue	Life technologies, UK
Ethanol	VWR Chemicals, France
Guanidine hydrochloride	Sigma Alrich, UK
Sodium citrate	Sigma Aldrich, UK
RNAse free water	Qiagen UK
Quantitect Reverse Transcription	Qiagen, UK
Quantifast Sybr Green PCR Kit	Qiagen, UK
Ficoll Paque	GE Healthcare Life Sciences
Bone Marrow Transfer media	In-house*

***Recipes detailed in Appendix**

2.3 Methodology

This chapter describes the common methodology and materials used throughout this research project. It focuses primarily on cell culture techniques and common extraction protocols which are used, and each section will be referred to in proceeding experimental chapters.

2.3.1 Bone Marrow Processing

Bone marrow was provided from patients who had given consent of use of their tissue for scientific research. Samples were obtained from hip and knee transplants, where healthy bone marrow was removed as part of the procedure in removing diseased and damaged joints and connective tissue. Only tissue that would have been otherwise discarded was used in this thesis. After extraction,

bone marrow tissue was transported from the Southern General hospital (Glasgow) to the University in transfer media in order to maintain cell survival.

The protocol of bone marrow processing was optimised previously. Bone marrow was processed by initially washing in complete DMEM cell culture media (supplemented with 100 µM sodium pyruvate, non essential amino acids, 0.8 mM L-glutamate, 10% foetal bovine serum and antibiotics mix) cell culture media and centrifuged at 1400 rpm for 10 minutes to pellet the cells within. The supernatant was removed and the pellet was washed again as described above. The remaining pellet was resuspended in 10 ml DMEM and slowly overlaid onto 7ml Ficoll paque centrifugation gradient to separate cells within the sample while being centrifuged at 1513 rpm for 45 minutes. The interphase layer containing the cells of interest was removed, and washed in DMEM media twice as descried previously. The cell pellet was resuspended in 2 ml cell culture media and spotted onto the bottom of a T25 cell culture flask and placed in 37°C incubator for approximately 60 minutes to allow cell attachment. Following this, media was added to flasks to a volume of 10 ml and returned to cell culture incubator. Cells were left to attach to flask for 1 week, and all culture media containing non-adherent cells was removed and discarded. Fresh media was replaced every 2-3 days. This was optimised by previous member of lab group.

2.3.2 CD271+ Selection

Bone marrow adherent cells were cultured for approximately 3 weeks until T25 flasks were 70 – 80% confluent. Cells were trypsonised with 3 ml volume of trypsin/versine and returned to cell culture incubator for 5 minutes. Cells were observed for detachment by use of microscope and once all cells had detached, 3 ml volume of DMEM with FCS was added to stop action of trypsin/versene. Cells were centrifuged at 1400 rpm for 10 minutes and all media was removed. Cells were re-suspended in a 500 µl volume of 1 x PBS with 2% FBS and transferred to plastic tube for use with a cell sorting magnet.

A volume of 12.5 µl human FcR receptor blocker was added to the solution and mixed several times, before addition of 25 µl positive selection cocktail and mixed again by pipetting. Solutions were incubated at room temperature for 15

minutes before addition of 25 µl of magnetic nanoparticles. Again, the sample was mixed by pipetting and incubated for 15 minutes at room temperature. Solutions were made up to 2.5 ml by addition of PBS/FBS solution and placed inside the selection magnet without the plastic cap. The solutions were incubated in the magnetic field for 5 minutes and then inverted in a continuous motion for 2- 3 seconds to remove unselected cells, then returned to upright position. The tube was removed and 2.5 ml PBS/FBS medium added and mixed again, and plastic tube returned to magnet for a further 5 minutes. This process was repeated a further 3 times to ensure unselected cells were removed from the suspension.

The cells remaining within the plastic tube were $CD271^+$ MSCs as they had been positively selected by the magnetic sorting protocol. These cells were resuspended in 2 ml DMEM cell culture media and spotted onto T25 cell culture flasks and incubated for 60 minute to allow cells to attach before the flask was flooded with media. Unselected bone marrow cells, referred to throughout as OPGs were kept and placed into T75 cell culture flask with DMEM cell culture media.

The CD271 selection method was utilised as commercially available MSCs are selected based on a number of MSC cell surface markers such as CD166 and STRO-1. A flask of such cells is not cost-effective and the use of this tetrameric antibody nanoparticle kit enabled us to obtain bone marrow sample from patient, select the mononuclear layer and select for one such MSC marker reported in the literature. By doing so, it allowed a relatively inexpensive method of MSC supply that could be used in the following experiments, allowing the research group to become self-sufficient in the supply of MSCs.

2.3.3 Pericytes

Unselected adipose derived MSCs were obtained from Dr Chris West at the University of Edinburgh, UK. Cells had been selected for the Pericyte markers $CD146^+$ and $CD34^-$ and were maintained in tissue culture flasks until tissue culture flasks with complete DMEM cell culture media.

2.3.4 Cell Culture with OPG's, CD271+ MSCs and Pericytes

OPGs and $CD271^+$ MSCs were maintained in a cell culture incubator, with complete DMEM media changed every 2-3 days. If tissue culture flasks became confluent, MSCs were split into two new flasks, with passage number noted.

For experimental use, cells were removed from tissue culture flasks by trypsin/versene as described previously, and resuspended in complete media to ensure cell concentration was approximately 1-2 x 10^5 per ml following cell count using a haemocytometer. This cell concentration was used throughout, for culture on hydrogels and glass controls unless otherwise stated.

2.3.5 RNA Extraction

Ribonucleic Acid (RNA) was extracted from MSCs by TRIzol reagent according to manufacturer's guidelines. In summary, 1 ml of TRIzol was used per sample and incubated at room temperature in an Eppindorf tube for 10 minutes to allow cells to lyse. Samples were centrifuged at 12,000 x g for 15 minutes at 4°C and supernatant removed and placed into a new Eppindorf tube before addition of 200 μl chloroform. The tubes were shaken vigorously for 20 seconds to ensure samples were evenly mixed and left to incubate at room temperature for 3 minutes. Samples were then centrifuged at 12,000 x g for 15 minutes at 4°C and the upper aqueous layer was removed and placed into new tube in order to isolate the RNA. A 0.5 μl volume of Glycoblue was added to the aqueous phase which aids in the visualization of RNA, as well as 500 μl isopropanol and the tube inverted 10 times to ensure samples were thoroughly mixed before incubating for 10 minutes at room temperature. Samples were centrifuged at 12,000 x g for 20 minutes at 4°C and the supernatant removed leaving a small blue pellet at the bottom of the tube. To this, 1 ml of 75% ethanol solution was added and tubes vortex briefly to wash the pellet and then centrifuged at 7,500 x g for 5 minutes at 4°C. All ethanol supernatant was removed and the pellet was left to air dry before a 20 μl volume of RNAse free water was used to resuspend the pellets and the samples incubated at 55°C for 10 minutes to aid this process. RNA concentration was then determined using NanoDrop® ND-1000UV-Vis Spectrophotometer at ratios of 230/260 nm and 260/280 nm.

2.3.6 DNA Extraction

DNA isolation from samples was obtained from the TRIzol separation method, after the upper aqueous layer containing the RNA was removed. A volume of 300 µl of 100% ethanol was added to homogenize the samples which were then incubated for 2-3 minutes at room temperature prior to centrifugation at 2000 x g for 5 minutes at 4°C. The phenol-ethanol supernatant layer was removed and placed in a new eppendorf tube for protein extraction as described in section 2.1.7. The remaining DNA pellet underwent a series of 30 minute washes starting with 0.1 M sodium citrate in 10% ethanol at a pH of 8.5. After this time, the solution was centrifuged at 2000 x g for 4 minutes at 4 °C and the supernatant removed. This was step was repeated. A 1500 µl volume of 75% ethanol was added to the DNA pellet and incubated for 20 minutes at room temperature while the tube was inverted occasionally. Again, centrifugation was performed at 2000 x g for 5 minutes at 4 °C the supernatant removed and the pellet was left to air dry for 10 minutes. The pellet was resuspended in a 300 µl volume of 8 mM solution sodium hydroxide and incubated at room temperature for 15 minutes. The samples were then centrifuged at 12,000 x g for 10 minutes at 4 °C to remove any insoluble material, and the supernatant containing the DNA was removed and placed into a new tube prior to measurement of DNA concentration using nanodrop.

2.3.7. Protein Extraction

The process of isolating protein from samples begins with the phenol-ethanol layer left over from DNA isolation described in section 2.3.6. To this, a 1500 µl volume of isopropanol was added to the supernatant samples and they were incubated at room temperature for 10 minutes prior to centrifugation at 12,000 x g for 10 minutes and the supernatant was discarded. The protein pellet was washed in a 2 ml volume of 0.3 M guanidine hydrochloride in 95% ethanol and incubated for 20 minutes. Samples were subjected to centrifugation at 7500 x g for 5 minutes at 4 °C. This wash step was repeated a further two times. After the third wash, 2ml of 100% ethanol was added to the pellet which was subject to vortexing prior to incubation for 20 minutes at room temperature. Samples were centrifuged again at 7500 x g for 5 minutes at 4 °C and the ethanol wash was removed allowing the protein pellet to air dry for 10 minutes. A 200 µl

volume of 1% Sodium dodecyl sulphate (SDS) solution was added to resuspend the protein pellet and samples were then incubated at 50°C for 15 minutes before centrifugation at 10,000 x g for 10 minutes at 4°C to sediment any insoluble material. The supernatant containing the protein was transferred to a new eppendorf tube and measured using nanodrop.

2.3.8 RNA Reverse Transcription

Reverse transcription was carried out on sample RNA using QuantiTect Reverse Transcription Kit to enable synthesis of complementary DNA (cDNA) for qRT-PCR analysis. RNA was thawed on ice and 2 μl gDNA Wipeout Buffer 7x and volume of RNase-freewater was added to small Eppindorf tubes to a total volume of 14 μl. Samples were incubated at 42 °C for 2 minutes to remove any contaminating genomic DNA and then samples placed immediately on ice. To reverse transcribe the RNA, a 1 μl volume of Quantiscript Reverse-transcriptase, 4 μl Quantitiscript RT Buffer 5x and 1μl volume of RT Primer Mix was added to each tube containing RNA from the previous step. Samples then underwent incubation at 42°C for 15 minutes, 3 minutes at 95°C to inactivate the reverse transcriptase and held at 4°C. Sples were stored at -20°C for performing qRT-PCR.

2.3.9 qRT-PCR

qRT-PCR was carried out using a 7500 Real Time PCR system and corresponding software (Applied Biosystems, UK). Each sample had a total volume of 20 μl which was made up of 2 μl of cDNA, forward and reverse primers at a final concentration of 100 μM, 10 μl SYBR Green Mastermix and RNAse free water to make up the total volume. The PCR cycle was as follows:

- Samples held at 50°C for 2 minutes
- 95°C for 10 minutes
- Amplification occurred at 95°C for 15 seconds
- And then 60°C for 1 minute.

The last two steps were repeated for a total of 40 cycles. The specificity of the PCR amplification was checked with a heat dissociation curve which was performed following the final PCR cycle. Glyceraldehyde- 3-Phosphate

dehydrogenase (GapDH) was the gene used for standardisation and acted as an internal control. Quantification of genes was performed using ΔΔCT method as described by Schefe *et al.*, 2006, and gene expression was calculated as fold change relative to control, which was maintained throughout as cells cultured on glass cover slips. A number of primers were used throughout this thesis and are presented in Table 2.1.

Gene		Primer Sequence	Transcription associated with
GapDH	Forward	5'-ACC CAG AAG ACT GTG GAT GG-3'	n/a acts as an internal control
	Reverse	5'-TTC TAG ACG GCA GGT CAG GT-3'	
CD63	Forward	5'-GCC CTT GGA ATT GCT TTT GTCG-3'	MSC marker
	Reverse	3'-CAT CAC CTC GTA GCC ACT TCTG-3'	
ALCAM	Forward	5'-ACG ATG AGG CAG ACG AGA TAA GT-3'	MSC marker
	Reverse	3'-CAG CAA GGA GGA ACC AAC AAC-3'	
CD271	Forward	5'- CCC GAG GCA CCA CCG ACA AC-3'	MSC marker
	Reverse	5'- TGG TGG GGG CGT CTG GTT CA-3'	
Glut-4	Forward	5'-ATG TTG CGG AGG CTA TGG G-3'	Adipogenesis
	Reverse	5'-AAA GAG AGG GTG TCC GGT GG-3'	
PPAR-γ	Forward	5'-TGT GAA GCC CAT TGA AGA CA-3'	Adipogenesis
	Reverse	5'CTG CAG TAG CTG CAC GTG TT-3'	
B3-Tubulin	Forward	5'-CAG ATG TTC GAT GCC AAG AA-3'	Neurogenesis
	Reverse	5'-GGG ATC CAC TCC ACG AAG TA-3'	
Nestin	Forward	5'-GTG GGA AGA TAC GGT GGA GA-3'	Neurogenesis
	Reverse	5'-ACC TGT TGT GAT TGC CCT TC-3'	
Sox9	Forward	5'-AGA CAG CCC CCT ATC GAC TT-3'	Chondrogenic
	Reverse	5'-CGG CAG GTA CTG GTC AAA CT-3'	
OCN	Forward	5'-CAG CGA GGT AGT GAA GAG ACC-3'	Osteogenesis
	Reverse	5'-TCTGGAGTTTATTTGGGAGCAG-3'	
OPN	Forward	5'-AGC TGG ATG ACC AGA GTG CT-3'	Osteogenesis
	Reverse	5'-TGA AAT TCA TGG CTG TGG AA-3'	

Table 2.1 Primer sequence

2.4 Discussion

Cell culture is an important tool for studying MSC behaviour *in vitro*. However, this method cannot reproduce the complex environment of the native bone marrow niche which comprises of extensive biochemical and topographical cues. Despite this, *in vitro* cell culture has provided us with a better understanding of how MSCs behave in response to chemical and topographical stimuli.

The ages of the donors, as well as origin of cell extraction are important factors to consider when studying MSCs *in vitro* as cellular ageing might affect MSC numbers and differentiation potential (Stolzing *et al.*, 2008). Only a small percentage of cells obtained from the bone marrow tissue meet the MSC criteria, while others are more committed such as osteoblast cells or osteoprogenitors which are known to proliferate in culture before becoming mature osteoblasts through a number of maturation stages (Lv *et al.*, 2014). The frequency of which bone marrow MSCs can be found has been investigated and it is believed that approximately 1 in every 100,000 nucleated cells is a stem cell (Friedenstein *et al.*, 1970 and Montjovent *et al.*, 2004) and therefore a selection process such as $CD271^+$ positive selection can be used to obtain a pure cell population. The CD271 cell surface marker was chosen as it has been repeatedly shown as a reliable method for isolating MSCs with multipotency potential (Watson *et al.*, 2013 and Flores-Torales *et al.*, 2010). As donor age increases, MSCs undergo a number of changes such as telomere shortening, impairment of function as well as a gradual decrease in proliferation potential (Bonab *et al.*, 2006). However, as the bone marrow samples from collaboration through the Southern General hospital were routinely obtained from patients undergoing hip and knee replacement surgery, the age of the donors was generally greater than 50 years of age. The MSCs obtained therefore did not have the proliferative capacity of those obtained from a younger patient and proved more difficult to culture on some occasions. There is a degree of controversy in the literature regarding age related osteoprogenitor populations, and this is complicated more by sex-dependent differences (Muscher *et al.*, 2001). However, obtaining cells from older patients and incorporating these with materials and scaffolds for regenerative applications may be beneficial, as it would generally be this aging population that would require the need for tissue replacement surgeries.

Therefore, this thesis provides an introduction for the study of MSCs obtained from older donors and how substrates affect their behaviour.

The use of pericyte cells is of interest in this thesis as it has been suggested that MSCs may originate from this cell population and therefore they are also believed to have multipotent potential (Crisan *et al.*, 2008). The use of these cells is of interest as they can be isolated from the vascular system during aspiration of adipose tissue, from young and older patients. By isolating these cells from this abundant tissue source, the cells can be excised from the body easier than performing bone marrow aspirations from the patients' hip joint.

Chapter 3

Peptide based hydrogel Protocol and Development

3. General Introduction

3.1. Hydrogels

Essentially, hydrogels are a class of material that are highly hydrated and are becoming increasingly popular because they are similar structurally to the ECM of a number of tissues types (Drury & Mooney, 2003). Hydrogels are an emerging biomaterial class that have successfully provided biologists with a new culture condition to control MSC fate that may be fundamental in the future for tissue engineering and regenerative medicine (Midha *et al.*, 2003; Phelps *et al.*, 2013). Hydrogels can be composed of a number of components such as collagen and arginate and also synthesized by various means such as crosslinking copolymerization, pH derived self-assembly and two-photon chemistry mechanisms, each producing a substrate favourable and fundamental to the desired application (Bosnakovski *et al.*, 2006; Maia *et al.*, 2014; Kuru *et al.*, 2007; He *et al.*, 2011 and Wylie *et al.*, 2011). The resulting hydrogel material essentially acts as a synthetic substrate, with the intention of incorporating particular aspects of the native ECM for culture of various cell types *in vitro*.

Peptides with a large aromatic 9-fluorenylmethoxycarbonyl (Fmoc) protective group at the N-terminus have been shown to form hydrogels with a fibrous structure with networks of peptide fibrils (Cheng *et al.*, 2010). A number of motifs have been incorporated into Fmoc hydrogels such as the integrin receptor Arginine-Glycine-Aspartate acid (RGD) that is commonly used to enhance cell growth and survival of cells (Guler *et al.*, 2006, and Castalletto *et al.*, 2012) due to the presence of this motif in the native ECM. As well as motifs such as RGD, singular peptides have been capped with the Fmoc moiety that can alter the properties of the resulting hydrogel as these peptides can interact in defined ways (as reviewed by Ulijn & Smith., 2008). Non-covalent, hydrophobic and hydrogen bonding as well as π-π stacking can result in a number of hydrogel formations. By fabricating hydrogels with two Fmoc peptides with different properties, essentially one peptide acts as a gelator and the other a surfactant which essentially coats the gelator molecules forming fibres within the hydrogel which have the ability to self-assemble on demand in response to different enzyme concentrations as described by Abul-Haija (Abul-Haija *et al.*, 2013).

3.1.1 The Fmoc Peptide Substrate

Di-phenylalanine (F_2) and Serine (S) (Figure 3.1) have been incorporated with the Fmoc moiety at the N terminus and results in hydrogels which can be used in culture due to the stiffness properties of these gels. They are favourable as the elastic properties can be tuned to alter the tension felt by the cells (Jayawarna, *et al.*, 2011). These properties are ideal as they can affect gene expression, differentiation commitment or self-renewal. These peptides self-assemble and are becoming increasingly popular due to their inexpensive and relatively easily production in comparison to the manufacturing of patterned or chemically defined surfaces. Fmoc-F2/S hydrogels have proved to be a biocompatible substrate for cell culture as shown by Jayawarna where bovine chondrocytes were successfully cultured and cell proliferation was supported (Jayawarna *et al*, 2007). Fmoc hydrogels have also been altered to incorporate biological ligands such as RGD which promoted human dermal fibroblast cell attachment and spreading due to adhesions through Fmoc RGD-integrin binding in a 3D environment (Zhou *et al*, 2009).

With regards to cell culture, the surface or the 3D environments in which cells are grown are vital in controlling many cellular functions such as survival, proliferation and differentiation (Frith *et al.*, 2010; Peterson *et al.*, 1992 and Pek *et al.*, 2010). Thus, through utilising tuneable peptide hydrogels with hydration levels similar to many human tissues and incorporating biological ligands such RGD, it may be possible to manipulate the environment to mimic that of the natural niche. Properties such as tuning peptides to form fibres of varying diameter, density, length and crosslinking patterns can be controlled (Lutolf 2008 and Jayawarna, 2011/ unpublished data).

The hydrogels used in this thesis are composed of Fmoc-F_2 and Fmoc-S (Figure 3.1) and will be referred to as Fmoc-F2/S from here on. The mechanism by which these hydrogels self-assemble occurs by two bonding interactions. The aromatic rings of the Fmoc moiety interact via π stacking interactions, and the peptide components interact via hydrogen bonding. Once assembled, these gels have some similarities to the ECM due to their high levels of hydration and their nanofibrous architecture. The hydrogels are formed by physical crosslinking of the COOH functionalised group through divalent cations (Ca^{2+}) when subjected to

cell culture media. The nanofibres formed are of importance as they have an effect on the stiffness properties of the resulting hydrogel. By combining Fmoc-F_2 and Fmoc-S in solution, Fmoc-S acts as a surfactant and is hypothesized to be present around the fibrous chains of Fmoc-F_2 as illustrated by Figure 3.1b.

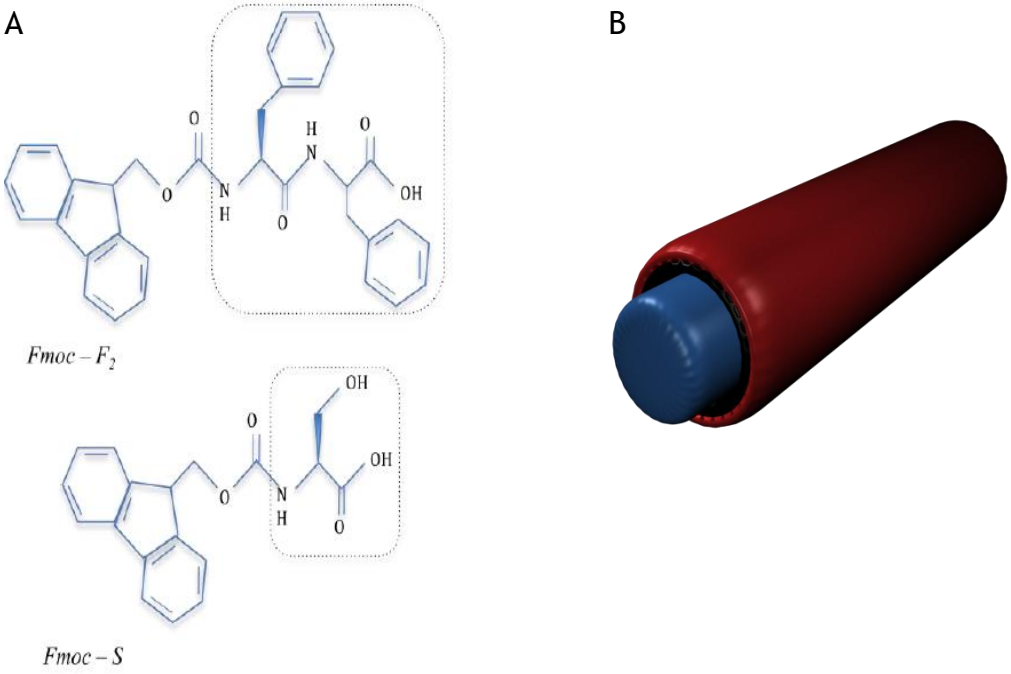

Figure 3.1 Fmoc-F_2 and Fmoc-S peptide residues and hydrogel self-assembly. (A) Presents the chemical structures of the Fmoc peptide, Fmoc diphenylalanine (Fmoc-F_2) and Fmoc amino acid, Fmoc –Serine (Fmoc-S). The peptide and amino moieties of these structures are present within the dashed section, with the unmarked section referring to the Fmoc moiety. Section (B) illustrates each structure colour coded to represent the location within the self-assembling nanofibres. The Fmoc-F_2 peptides self assembles and form rod like nanofibres through π stacking of the aromatic rings as well as the hydrogel bonding between the diphenylalanine proteins. The Fmoc-S amino acid is not involved in the nanofibre formation and instead bonds to these fibres, acting as a surfactant around the Fmoc-F_2 fibres.

3.2 Objectives

This chapter aims to create a potential pool of hydrogels, composed of Fmoc-F_2 and Fmoc-S in a 1:1 ratio, following on from the work of Jayawarna *et al.*, 2007. This will produce hydrogels with elastic modulus values that could be used for cell culture purposes with further study to develop a range of potential hydrogels which will mimic the elasticity of a number of human tissues as described by Engler *et al.*, 2006. Secondly, the characteristics of the peptide solutions and resulting hydrogels will be studied with regards to stiffness and how culture conditions alter this over time, using scanning electron microscopy

(SEM) and transmission electron microscopy (TEM) to visualise the self-assembling fibres and high performance liquid chromatography (HPLC) to determine the actual concentrations of each Fmoc peptide after self-assembly has occurred.

3.3 Materials and Methodology

3.3.1 Materials

Materials / Reagents	Supplier
Fmoc - F_2 (original)	Bachem, UK
Fmoc- F_2 (new)	Made in-house at Biogelx, Glasgow, UK
Fmoc –S	Bachem, UK
Sodium Hydroxide	Fischer chemicals, UK
Hydrochloric acid	Sigma Aldrich, UK
Distilled water	Invitrogen, UK
DMEM cell culture media	Sigma Aldrich, UK
ThinCert Tissue Culture Inserts	Greiner, BioOne, Germany
Acetronitrile	Sigma Aldrich, UK
Trifluoroacetic acid	Sigma Aldrich, UK

3.3.2 Methodology

3.3.2.1. Preparation of peptide solution - original method

The peptide solutions were prepared from Fmoc- F_2, and Fmoc-S from Bachem, UK. A 10 mM concentration of each peptide powder was weighed out in turn in a glass vial so that a range of rigidities would be obtained upon self-assembly to hydrogels according to published results (Jayawarna *et al.*, 2007). Peptide solutions were prepared by suspending the Fmoc-F_2 and Fmoc-S peptide powder in 4ml of distilled water (dH_20) and a volume of 0.5M NaOH to allow powder to dissolve and modify the pH of the peptide solution, which ultimately had an effect on hydrogel stiffness. By doing so, an overall 20 mM peptide solution was

produced. Solutions were then subjected to 30-second cycles of vortexing and sonication in an ice water bath until the powder had fully dissolved and a clear peptide solution was made. Solutions were subjected to ultraviolet (UV) light for 60 minutes for sterilisation and then kept at 4°C until required to make hydrogels. Table 3.1 refers to the volume of 0.5 M NaOH added that dissolved the Fmoc powders and altered the pH of the solution, which ultimately formed three distinct Fmoc-F2/S hydrogels, with stiffness values of 1.7, 6.36 and 38.3 kPa referred to as "soft", "stiff" and "rigid" hydrogels respectively. With reference to Figure 4.3, these three hydrogels relate to neural, muscular and pre-osteoid bone range of human tissue respectively.

Concentration of Fmoc-F_2/S Peptide solution	Volume of 0.5 NaOH (μl)	Name of which hydrogel is referred to within text	pH of peptide solution	Stiffness of Hydrogel (kPa)
20 mM	130	"soft"	7.2	1.7 ± 0.45
	145	"stiff"	7.9	6.36 ± 1.02
	155	"rigid"	8.1	38.3 ± 0.86

Table 3.1 Composition of original peptide solution recipe.
This table presents the properties that result in three distinct hydrogels substrates, with uniform chemical composition but with different elastic modulus properties as a result of the crosslinking produced by the alteration of pH.

3.3.2.2 Further peptide solution development

The purification protocol process by which Bachem commercially produced the Fmoc- F_2 powder was modified during this thesis, which gave rise to different polymorphs of the Fmoc-F_2 material with different aqueous solubilities. As a result, this had substantial impact on the gelation protocol and altered the properties of the three 20 mM hydrogels described in Table 3.1. Therefore, these hydrogels could not be reproduced as elastic modulus properties were modified. As the stiffness of the gels was altered, Fmoc- F_2 powder synthesis was moved in-house at the University of Strathclyde, UK. Due to this new method of Fmoc-F_2 peptide synthesis, the hydrogel protocol required further optimisation, and the opportunity arose to create a new set of hydrogels by increasing the concentration of the two peptides, still in a 1:1 Fmoc-F_2/Fmoc-S ratio. Table 3.2

describes the components of this new potential pool of hydrogels created from the new in-house synthesized Fmoc-F_2 and the original Bachem Fmoc-Serine. Once each powder was weighed out, 4 ml dH_20 was added as described in section 3.2.2.1, but after sonication and vortexing cycles, pH was measured and 0.5 M HCl was added to lower pH to within physiological range, e.g between pH 7.2 and 7.8. This new method did not rely on alteration of pH to alter the hydrogel stiffness; instead the volume of NaOH was added to simply dissolve the powder. Addition of 0.5 M HCl was to lower the pH of the solutions for later use with cell culture. Solutions did not appear as clear in appearance as the original peptide solutions described in section 3.3.2.1, therefore they were subjected to a 0.8 µm filter to remove impurities. Therefore, this new method relies solely on the concentration of the peptides, and is not pH dependent as the method described previously in section 3.3.2.1.

Concentration of Fmoc-F_2/S peptide solution (mM)	Weight of Fmoc-F_2 (g)	Weight of Fmoc-S (g)	Volume NaOH (µl)	Sonication/ vortex (mins)	Volume HCl (µl)	Stiffness of Hydrogel (kPa)
5	0.0053	0.0034	40	5	7	n/a
10	0.0107	0.0069	83	5	15	0.64 ± 0.046
20	0.0214	0.0138	170	10	16	2.58 ± 0.102
30	0.0321	0.0207	255	11	16	5.66 ± 0.421
40	0.0428	0.0276	335	11	19	12.02 ± 0.288

Table 3.2 Composition of new Fmoc-F_2/S hydrogel pool
This table describes the composition of the peptide solutions and resulting hydrogels which were created from the new in-house synthesised Fmoc -F_2 peptide and the original Bachem Fmoc-S powder.

3.3.2.3 Hydrogel Formation from peptide solutions

Once peptide solutions were created, as shown in tables 3.1 and 3.2, they were stored at 4°C until ready for use. To form hydrogels from the solutions, the

peptide mixtures were warmed in cell culture incubator for approximately 30 minutes to reach 37 °C. A 300 µl volume was transferred into tissue culture inserts (Thincerts™) with a 1.0 µm diameter pore size transparent membrane located within a 12 well cell culture plate. A 1400 µl volume of pre-warmed complete DMEM cell culture media was added to the surrounding well plate to ensure the permeable membrane of the ThinCert tissue culture insert was in contact with the cell culture media. The multiwall plate was placed in a 37 °C cell culture incubator with 5 % CO_2 concentration for 90 minutes. After this time, the 1400 µl volume of complete DMEM media was replaced with new DMEM media as per original volume. An additional 300 µl of media was added to the upper surface of the newly formed hydrogel and the multiwall plate was returned to the cell culture incubator to equilibrate pH and remained there until experiments commenced. Figure 3.2 illustrates the process of hydrogel formation from peptide solution.

Figure 3.2 Process of hydrogel formation from peptide solution.
This illustrates the process by which peptide solution is added to ThinCert tissue culture inserts and how gelation is initiated by addition of cell culture media, locking the Fmoc -F_2-S nanofibres in place. This method applies with solutions consisting of Bachem and in-house produced Fmoc-F_2 solution formations into hydrogel substrates.

3.3.2.4 Rheology

To address the mechanical properties of the hydrogels, dynamic strain sweep experiments were carried out on a strain- controlled rheometer (rotational rheometer from Malvern) using parallel plate geometry of 20 mm diameter with a gap of 0.5 mm. The temperature of the sample stage was controlled at 25 °C (approximately room temperature) throughout by an integrated temperature controller and a solvent trap was used to keep the hydrogel sample hydrated and

a water solvent trap was used to prevent evaporation. To ensure the measurements were made in the linear viscoelastic regime, an amplitude sweep was performed and the value of which the results presented no differences in the elastic modulus (G') and viscous modulus (G") up to a strain of 1 % was taken forward as the strain used for the frequency measurements. The dynamic modulus of the hydrogel was measured as a frequency function, where frequency was carried out between 1 and 100 Hz. Overall, measurements were repeated in triplicate to ensure hydrogel stiffness reproducibility. Rheology analysis to determine hydrogel stiffness was performed on Excel, where the uniform G' values of the frequency sweep were averaged, omitting the outliers as frequency approached 100 Hz. Figure 3.3 presents an example of the data obtained when performing an amplitude sweep and frequency sweep to determine hydrogel stiffness.

3.3.2.5 Atomic force microscopy (AFM)

In order to observe the self-assembling structures present within the peptide solutions studied, samples were prepared prior to measurement on AFM microscopy. A 50 μl volume of peptide solution was placed onto a trimmed, freshly cleaved micra sheet attached to an AFM support stub and allowed to air dry for 60 seconds. Excess solution removed by capillary action and a 100 μl volume of distilled water was dropped onto the slide and excess removed as before after 60 seconds. This cleaning step with dH_20 was repeated to ensure all excess peptide solution was removed and the slides were left for 48 hours to air dry prior to AFM imaging. Images obtained by scanning the mica surface in air under ambient conditions using a Veeco Multimode with NanoScope IID Controller Scanning Probe Microscope (Digital Instruments, Santa Barbara, CA, USA; Veeco software Version 6.14 r1) operated in tapping mode. The AFM measurements were obtained using a sharp probe (TESP; normal length (l_{nom}) = 125 μm, width (W_{nom}) = 40 μm, tip radius (R_{nom}) = 8 nm, resonant frequency (U_{nom}) = 320 kHz, spring constant (k_{nom}) = 42 N m^{-1}; Veeco Instruments SAS, Dourdan, France), and AFM scans were taken at 512 x 512 pixel resolution. Typical scanning parameters were as follows: tapping frequency 308 kHz, integral and proportional gains 0.3 and 0.5, respectively, set point 0.5- 0.8 V and scanning speed 1.0 Hz. AFM images were analysed using Veeco Image Analysis software Version 6.14r1.

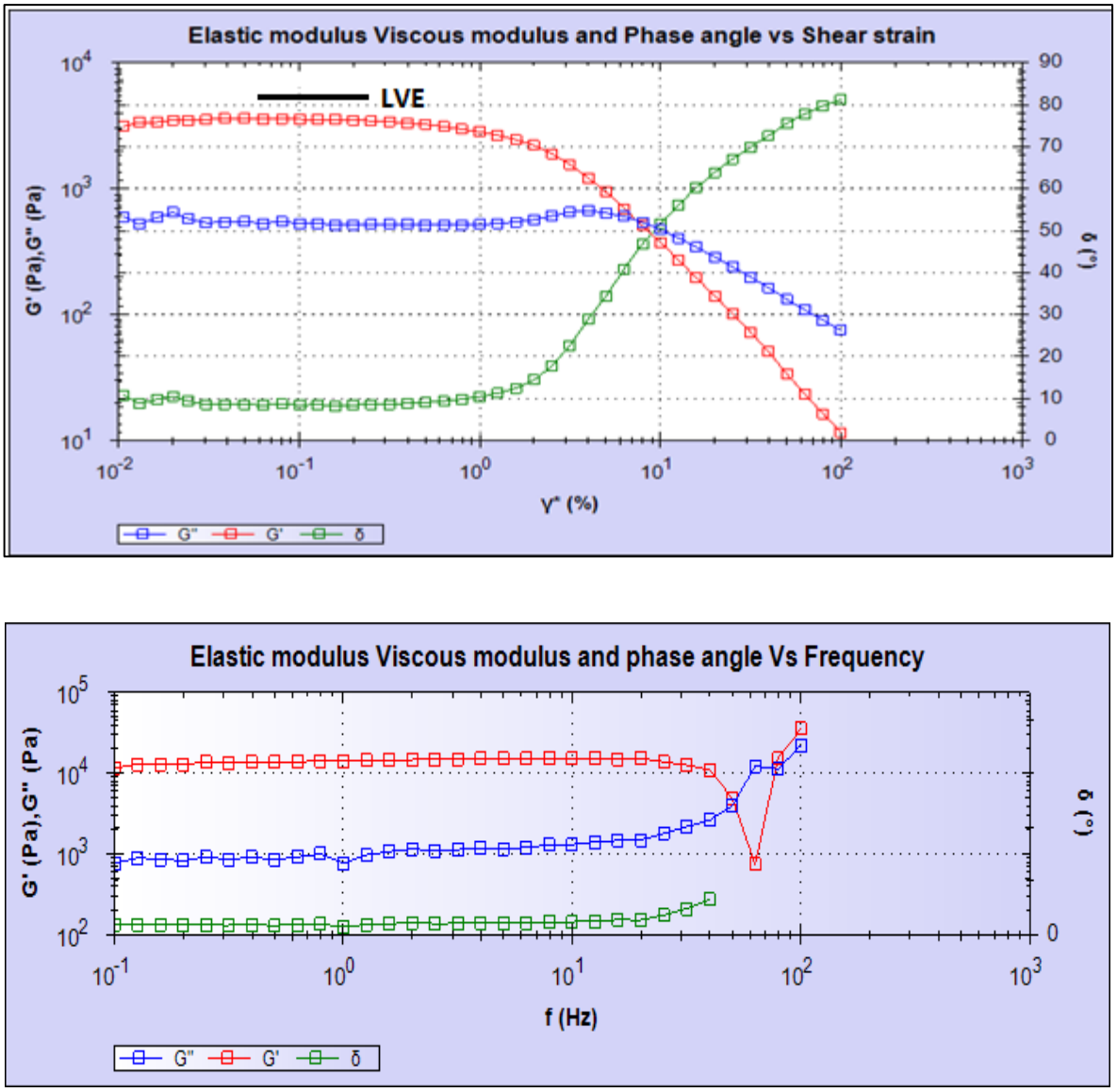

Figure 3.3. Amplitude and Frequency sweep observations.

In order to obtain stiffness values of hydrogel, sample is subjected to an amplitude sweep (A) whereby the gel is subjected to an increasing shear stress. The stress by which the G' and G" values are unchanged is referred to as the LVE region and this stress value is taken forward for frequency sweep tests. In Frequency sweep rheology (B), the hydrogel stiffness is calculated over a defined frequency region, omitting the final few outlier values as the hydrogel dinintegrates at high frequency.

3.3.2.6 Transmission electron microscopy (TEM)

300 mesh carbon-coated grids were glow discharged for 5 seconds and placed shiny surface down onto the hydrogels and peptide solutions for approximately 5 seconds. The grids was blotted with filter paper to remove excess sample and then 10 µl of negative stain (Nanovan: 1% aqueous methylamine vanadate, from

Nanoprobes) was placed onto sample on the carbon coated grid and allowed to dry for 10 minutes. Samples were then imaged using LEO 912 energy filtering electron microscope operating at 120 kV fitted with a 14-bit/2 K Proscan CCD camera. Fibre diameters measured using ImageJ software version v1. 43u.

3.3.2.7 Scanning electron microscopy (SEM)

Peptide solution samples were prepared for SEM by Margaret Mullin of the University of Glasgow Electron Microscope Facility and visualised using a JEOL6400 SEM microscope.

3.3.2.8 Image J analysis of fibre width

Image J software version 1.45s was then used to open desired image and the scale was set with this image so that the nanofibre widths were in proportion to the original scale bar set on the image. For each image, 50 width measurements were taken, and the average was used as the result for that particular sample. The standard deviation was also calculated.

3.3.2.9 High performance liquid chromatograpy (HPLC)

The HPLC analysis began with creating a range of Fmoc-F_2 concentrations that were dissolved in a HPLC solvent of acetrontrile in water (1000 μl, 50:50 ratio) containing 0.1% trifluoroacetic acid, to create a standard curve from which the percentage of Fmoc-F_2 peptides in the samples could be calculated. This was repeated in turn with only Fmoc-S peptides, using the same concentration standards. A 30 μl volume of each peptide solution sample to be tested was mixed with the HPLC solvent and the leaching of each powder was determined by UV light detection at 280 nm. HPLC was performed on a Dionex P680 HPLC pump.

3.4 Results & Discussion

3.4.1 Preliminary Results with original hydrogel method

Initial results in this section arise from peptide solutions and hydrogels that are formed from Bachem Fmoc-F_2 and Fmoc-S peptide powder.

3.4.1.1 Rheology results

The original 20 mM soft, stiff and rigid hydrogels described in section 3.3.2.1, underwent rheological testing to determine the elastic modulus values. Rheological data illustrates that the “soft” hydrogel is 1.7 kPa, “stiff” is 6.36 kPa and the “rigid” hydrogel is 38.3 kPa in stiffness. Figure 3.4 presents the rheological data for each of these hydrogels in turn demonstrating that the G’ values exceed that of G” concluding that the hydrogels are a solid substrate rather than a viscous solution. G’ is defined as the elastic modulus and G” is defined as the viscoelastic modulus. A product which does not form a hydrogel substrate has G” values exceeding that of G’,

3.4.1.2 AFM of peptide solutions and hydrogels

AFM imaging was performed on the peptide solution and resulting hydrogel as described in section 3.3.2.5. The aim was to observe the self-assembling nanofibres of Fmoc- F_2 with Fmoc- S coating these structures. Figure 3.5 illustrates the nanofibres present within the three 20 mM peptides, and of the structures present within the resulting hydrogel.

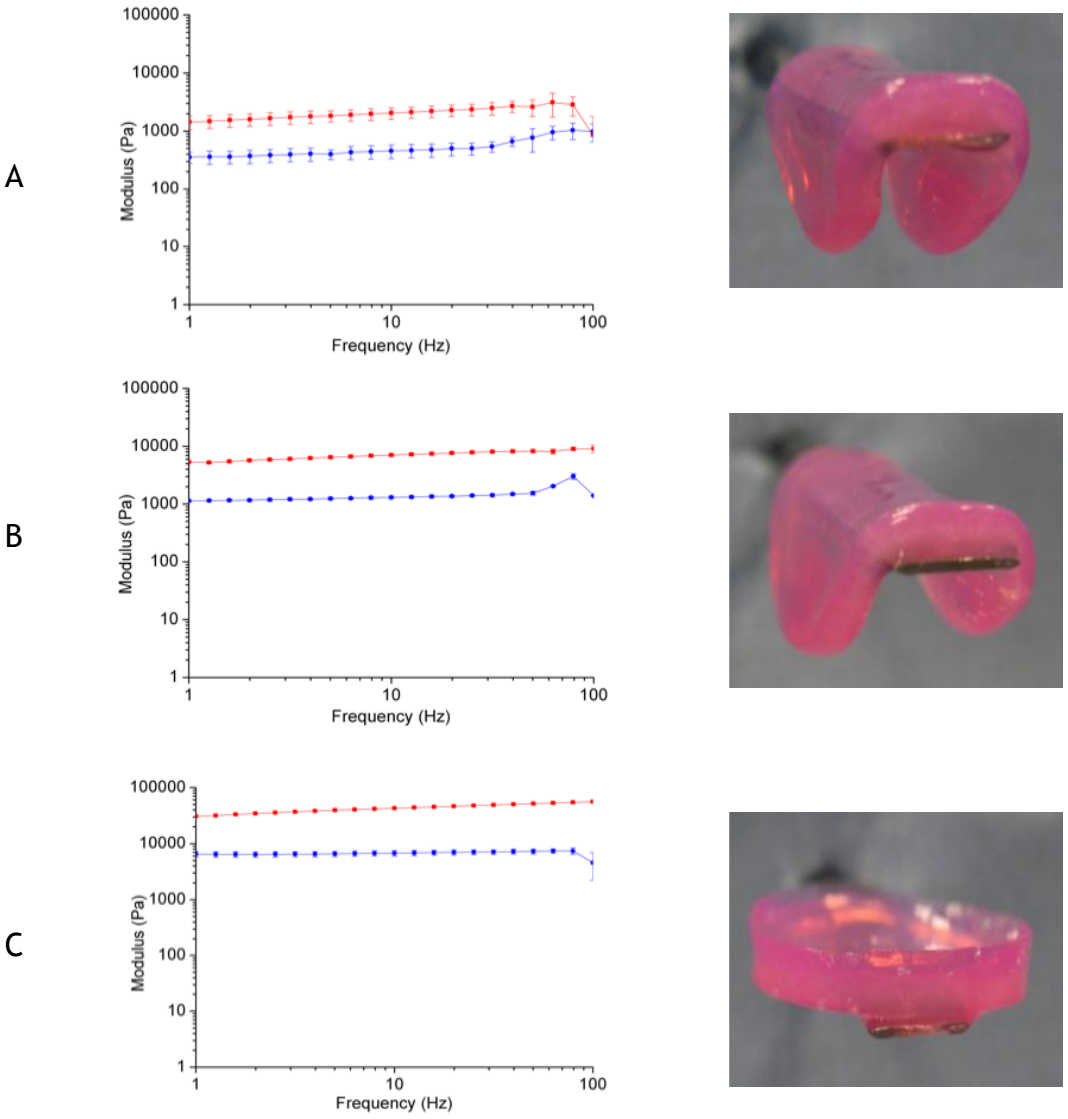

Figure 3.4 Rheological results of the soft (A), stiff (B) and rigid (C) hydrogels.
In each of the graphs, G' elastic modulus values (red) exceed G" viscous modulus values (blue) which indicates that each of the hydrogels is elastic in nature and thus are not viscous materials. The images on the right hand side correspond to the soft, stiff and rigid hydrogel in A-C respectively.

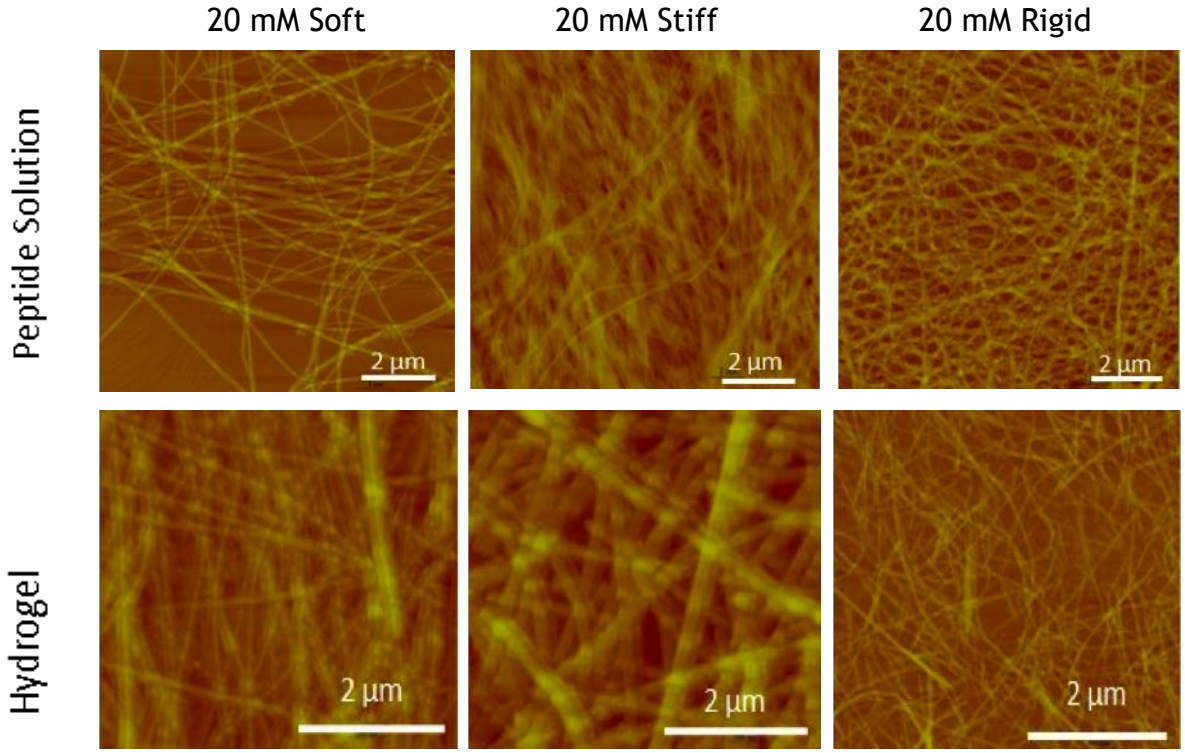

Figure 3.5 AFM Images of 20 mM peptide solutions and hydrogel self-assembling nanofibres Figure illustrates the self-assembling nanofibres present within each peptide solution and hydrogel corresponding to "soft", "stiff" and "rigid" samples as described in section 3.3.2. Scale bar illustrates 2 µm. The nanofibres in the soft samples are thick and less crosslinking is present, in the stiff samples the fibres are thinner and more crosslinking present. In the rigid samples, the nanofibres are extremely thin and the most crosslinking is present. This crosslinking observed is due to the alteration of pH when creating the peptide solutions.

AFM imaging has illustrated the nanofibres present within the soft, stiff and rigid peptide solutions and hydrogel samples. The alteration of pH results in different fibre profiles, as can be observed within the peptide solution images. The concentration of the Fmoc-F_2 and Fmoc-S peptides are uniform in each sample condition, but by altering the pH the fibres appear to be present in different arrangements. By altering the peptide solution pH to 7.2 (soft hydrogel), the fibres are thicker and less crosslinking occurs between them resulting in larger open spaces between the fibres. A solution of pH 7.9 (stiff hydrogel), allows more crosslinking to occur, and by increasing the pH to 8.1 (rigid hydrogel) results in a sample with thinner nanofibres and a high degree of crosslinking resulting in smaller spaces between the fibres. The presence of a highly nanofibrous network, as shown in the rigid hydrogel solution, increases stiffness of the hydrogelas as expected, and the hydrogel with fewer fibres results in a soft material due to the lack of fibre support. The pH of the peptide solution

therefore affects the extent of self-assembly which impacts the stiffness properties of the resulting hydrogel substrate.

3.4.1.3 TEM Imaging of peptide solutions & hydrogels

In preparation for TEM imaging, samples were treated as described in section 3.3.2.6. TEM was used to determine the characteristics of the nanofibres of both the peptide solutions and hydrogels of the soft, stiff and rigid samples due to TEM providing higher resolution images than AFM imaging due to the delivery of electrons to the sample. TEM relies on the delivery of transmitted electrons, which allows the visualisation of the internal structures of the samples due to the use of negative staining to present contrast within the samples as shown by Figure 3.6. TEM images show a 2D representation of the nanofibres, and differences in the fibre pattern and network can be observed in the samples below. Fibre width was analysed as described in section 3.3.2.8, with results presented in Table 3.3.

Again, as with the AFM images we can see that there are three distinct nanofibrous profiles occurring as previously shown with Figure 3.5. Particularly with the hydrogel images, can observe thicker fibres in the soft hydrogel image, and thinner more crosslinked fibres with the rigid hydrogel material. The fibre widths were analysed and it was shown that the fibre diameter increases slightly as the peptide solution forms a hydrogel from the peptide solution. However, as the samples are dehydrated under imaging conditions, the fibre widths are not due to fibre swelling when the hydrogel is formed. Also, the fibre width decreases as the hydrogel material becomes stiffer in rigidity. These findings are due to the extent of the nanofibre formation and crosslinking which occurs due to the alteration in pH within the samples.

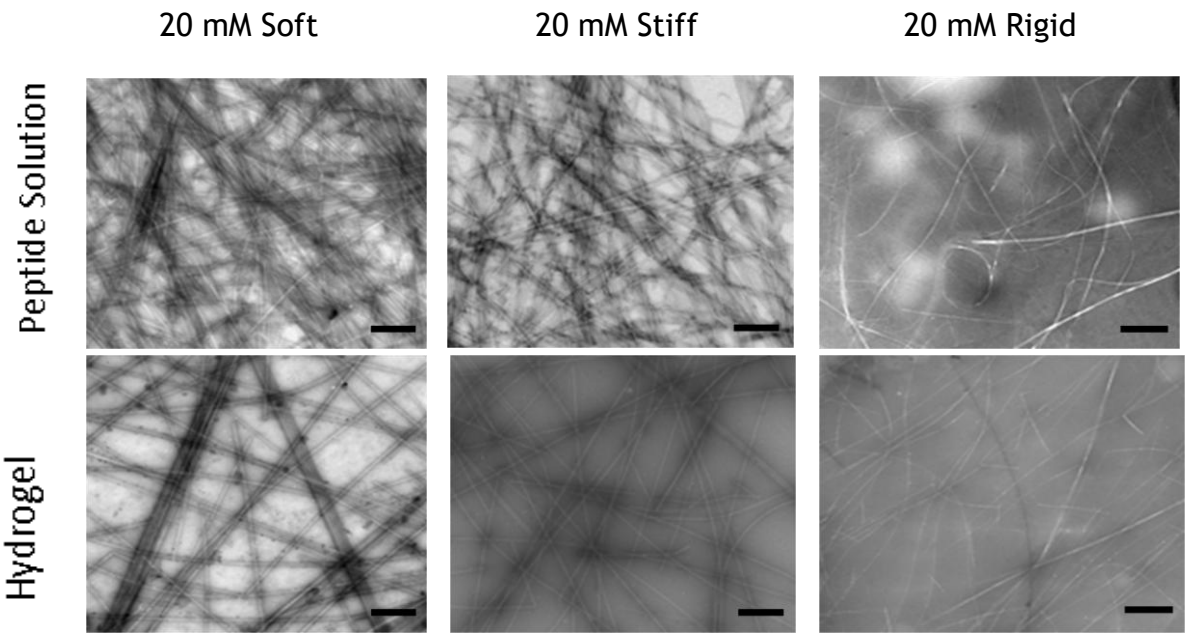

Figure 3.6 TEM images of the 20 mM peptide solutions and hydrogels. Figure illustrates the nanofibres present by TEM imaging of the soft, stiff and rigid peptide solutions and hydrogel samples. Again, the width of the fibres is due to the pH of the sample, with the soft samples presenting thicker fibres, and the rigid samples presenting thinner fibres due to a more crosslinking of the nanofibres. Scale bar represents 500 nm

Sample	Fibre width (nm)
"soft" peptide solution	29 ± 8
"soft" Hydrogel	34 ± 9
"stiff" peptide solution	27 ± 8
"stiff" hydrogel	31 ± 7
"rigid" peptide solution	6 ± 9
"rigid" hydrogel	15 ± 4

Table 3.3 Nanofibre widths of original soft, stiff and rigid peptide solutions and hydrogels. Values obtained by Image J analysis of TEM images as described by section 3.3.9.

3.4.1.4 Fluorescence Spectrometry

Fluorescence spectrometry is a method used to measure the fluorescence emitted from a sample by utilizing UV light. The peak around 320 nm indicates emission of the Fmoc group in the peptide solution. Decrease in intensity between solution and hydrogel formation indicates Fmoc quenching upon assembly. The presence of a peak at 450 nm relates to formation of extended linear aggregates of the Fmoc groups present in the fibres, referred to as J-aggregates. Fmoc- F_2-S peptide solutions were analysed by fluorescence spectroscopy and all 20 mM samples illustrated a peak at 325 nm indicating the monomeric peak for the Fmoc group. Observing a peak at this wavelength can

confirm that π-π stacking formation is present between the Fmoc-F_2 and Fmoc-S components in the peptide solution (Figure 3.7).

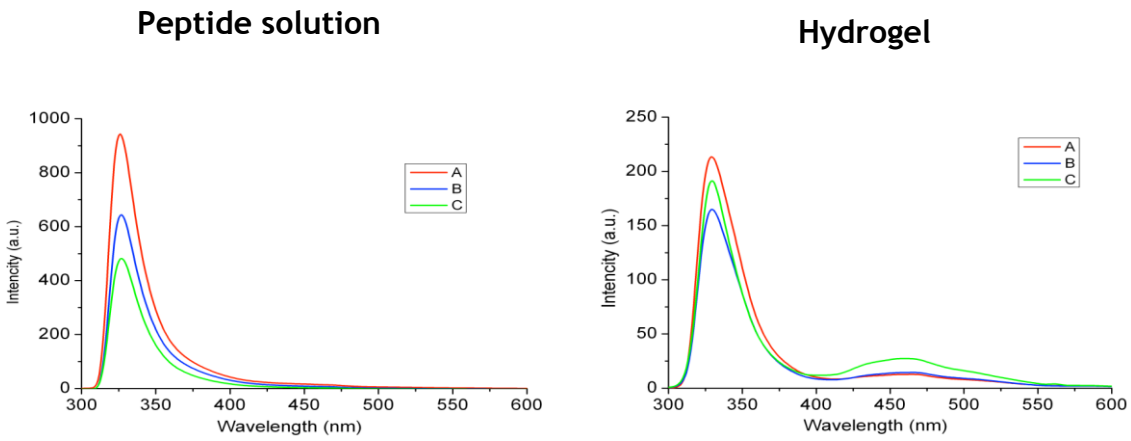

Figure 3.7 Fluorescence spectrometry of soft, stiff and rigid Fmoc-F_2 /S peptide solutions and hydrogels. The inset represents within each graphs represents (A) Soft, (B) Stiff and (C) Rigid samples. The fluorescence spectra of both the 20 mM peptide solutions and hydrogels showed a peak at 325 nm wavelength illustrating that π-π stacking is present in all of the samples and when a hydrogel is formed from the corresponding peptide solution, the intensity of the 325 nm peak decreases indicating quenching and locking of the Fmoc groups forming the nanofibres.

The Fmoc π-π stacking at 325 nm was observed in all three 20 mM samples. However, the intensity of this peak decreases when the resulting hydrogel is formed, which determines that there is Fmoc quenching which is consistent with extensive π stacking. Therefore, the Fmoc groups are locked in conformation by the addition of cell culture media and there are more Fmoc interactions within the gel. The next section will describe the hydrogels created with the in-house synthesised Fmoc-F_2 peptide powder. This concludes the results from the original method whereby stiffness of hydrogel was pH dependent. The results described from here on are from hydrogels that are dependent on peptide concentration to change the properties such as elasticity.

3.4.2 New Fmoc-F_2/S hydrogel development

As a result of changes in Bachem purity effecting gelation properties, the Ulijn group at the University of Strathclyde, Glasgow, begun in-house synthesis of the Fmoc-F_2 peptide which resulted in modification of the 20 mM protocol as described in section 3.3.2.1. This led to developing a new potential pool of

hydrogel substrates, which began by increasing the molar concentration of the two Fmoc protected peptides, shown in section 3.3.2.2.

3.4.2.1 Rheology testing to determine hydrogel stiffness

Hydrogels were made as described in section 3.3.2.2 and underwent rheological testing at days 1 and 7 to determine the initial stiffness of the substrate, and how it changes in response over time in culture. Figure 3.8 illustrates that the G' value exceeds the G" value at day 1, for hydrogels 10- 40 mM in concentration, confirming that the solution has formed into a hydrogel material rather than remained a viscous solution.

Figure 3.8 illustrates that all the hydrogels tested remain as a solid substrate over 7 days in culture. The stiffness of the hydrogels was also tested at day 1 and 7 time points to determine if the stiffness changes over time as these substrates have the potential to be used for cell culture purposes. As the G' value is used to calculate the stiffness of the hydrogels, Figure 3.9 compares the stiffness of the hydrogels at days 1 and 7 for 10 – 40 mM concentrations by only presenting the G' values. Table 3.4 presents the stiffness values corresponding to the values obtained from rheological testing at these time points from the data in Figure 3.7. The 5 mM hydrogel failed to form a hydrogel substrate and instead remained a viscous solution. At this stage the 5 mM solution can be eliminated from the potential pool as it is not possible to culture on a viscous material. Further study and characterisation will continue with 10- 40 mM hydrogels.

Concentration (mM)	Stiffness Day 1 (kPa)	Stiffness Day 7 (kPa)	Fibre diameter (nm)
5	n/a	n/a	19.71 ± 2.9
10	0.64 ± 0.046	0.43 ± 0.02	21.87 ± 3.2
20	2.58 ±0.102	2.51 ± 0.2	16.06 ± 3.9
30	5.66 ± 0.421	5.01 ± 0.44	17.16 ± 3.7
40	12.02 ± 0.288	12.2 ± 0.55	22.05 ± 3.5

Table 3.4 Stiffness values of hydrogels with in house synthesis of Fmoc-F_2. Table illustrates the differences in stiffness of the hydrogels as a result of 7 days in culture. Results were measured in triplicate, with standard error presented alongside stiffness measurement. Fibre width diameter is also presented, which was calculated using TEM images and Image J analysis as described in section 3.3.9

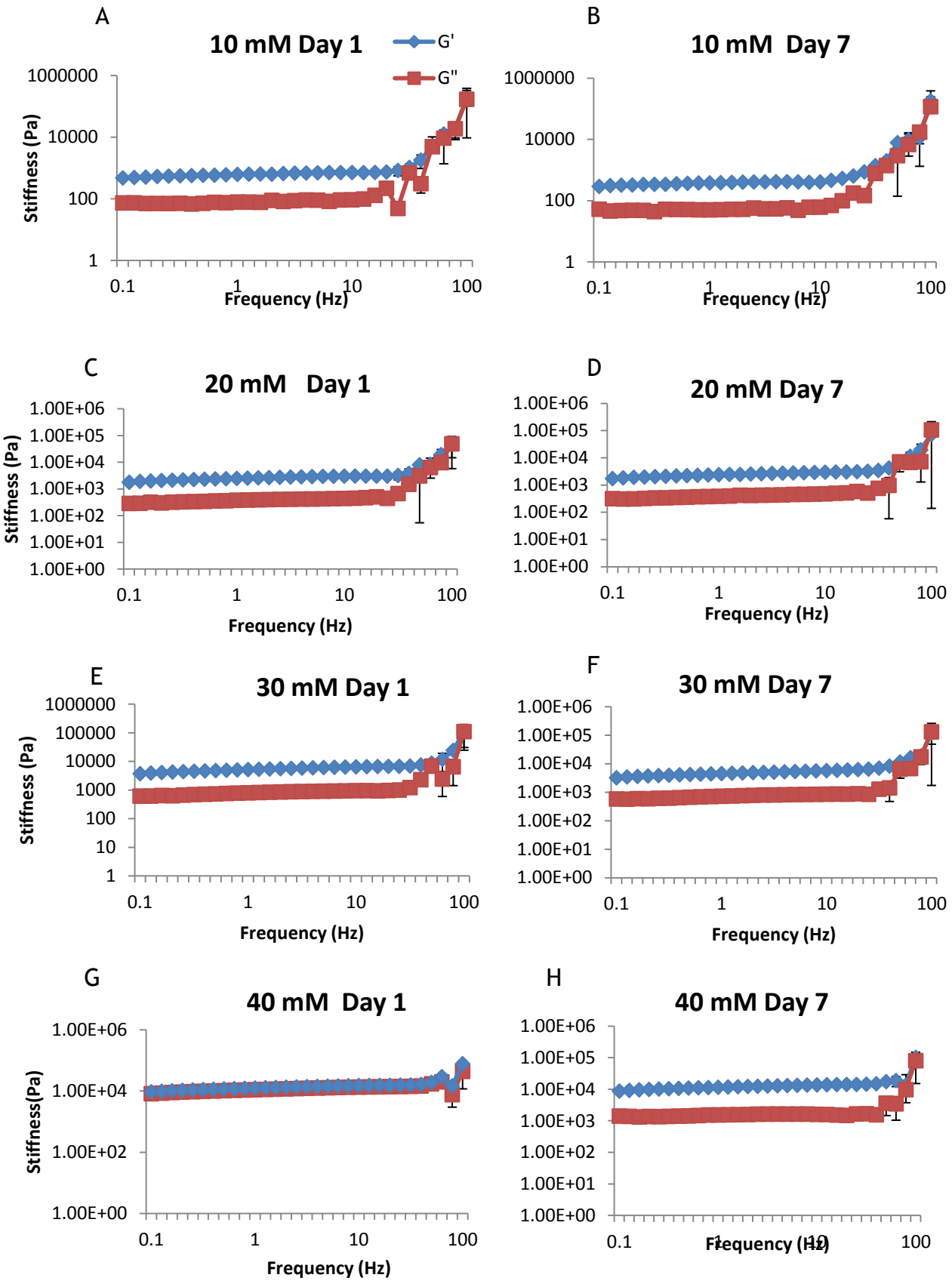

Figure 3.8 Rheological data for in house synthesised hydrogels. Data illustrates that G'(storage modulus) illustrated by blue ,exceeds that of G" (viscous modulus) shown in red, in A-H confirming that the hydrogels have formed and maintained this conformation up to 7 days in culture. The stiffness is presented on the Y axis, which is where the overall elasticity values are

taken from as substrate stiffness is calculated based on the average G' values over the frequency range of 1 to 100 Hz.

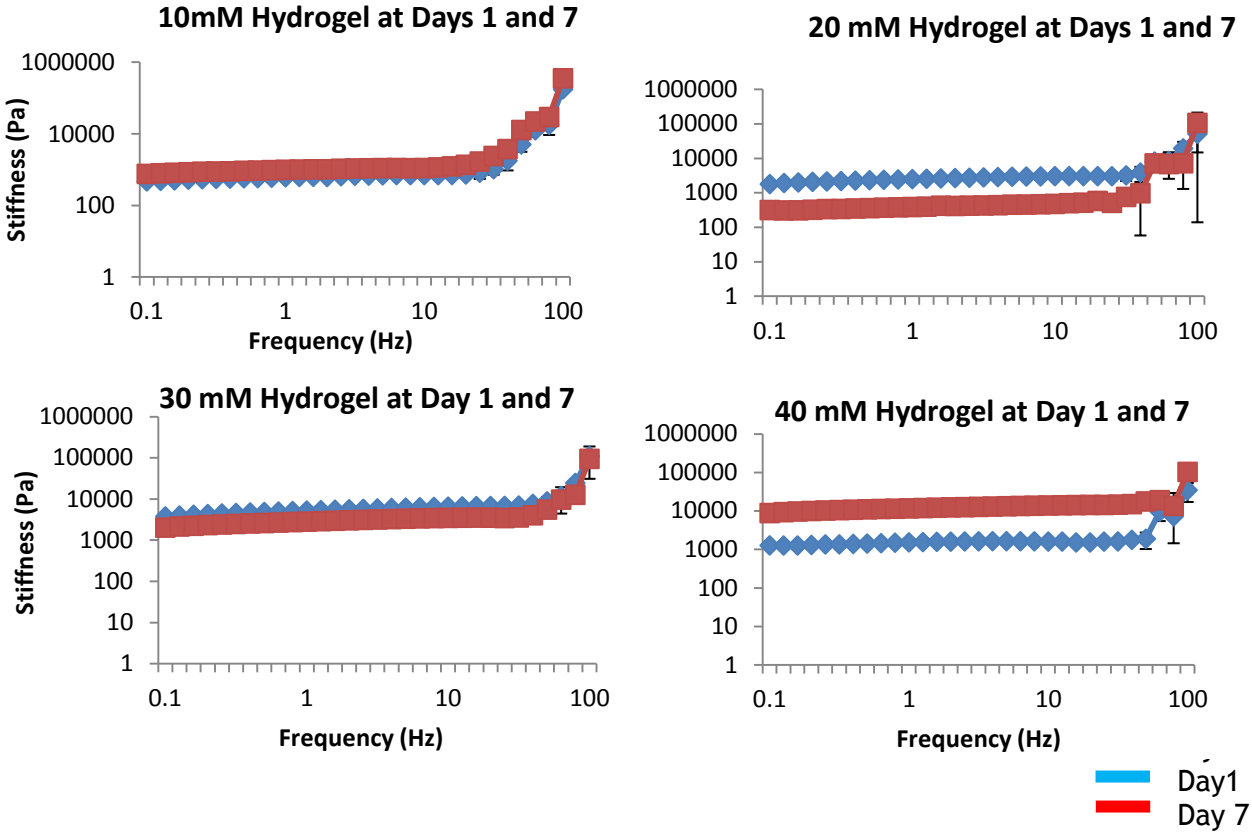

Figure 3.9 Comparing hydrogel stiffness at days 1 and 7.
Of the hydrogels that maintained their elastic properties, the stiffness values were compared at days 1 and 7 to determine if elasticity is lost. Figure illustrates that hydrogel stiffness is lost slightly over time in the 10, 20 and 30 mM hydrogel substrates, but the 40 mM hydrogel increases in rigidity slightly.

Overall, a total of five peptide solutions of increasing concentration were created. The 5 mM peptide solution failed to form a hydrogel, and instead remained as a viscous peptide solution. By rheological testing, it was determined that four of these solutions resulted in hydrogel formation by the addition of cell culture media. With regards to the 10 – 40 mM hydrogels studied, the storage modulus value G', exceeded that of the viscous modulus value, G". This illustrates that the hydrogels are an elastic material rather than a viscous liquid, as illustrated in Figure 3.8. Hydrogels ranging from 10 mM to 40mM were again rheologically tested at day 7 to compare the stiffness of each gel in comparison to day 1 as cells will be cultured upon these hydrogels in latter chapters for prolonged culture periods. Again, all the hydrogels remained elastic in character but there was a slight decrease in stiffness values, as shown in Table 3.4. The 40 mM Hydrogel increased in stiffness between time points suggesting that due to the concentration of the Fmoc-F2/S peptides, the nanofibres became associated

with the ions and proteins present within the DMEM cell culture media and continued to increase in stiffness. This suggests that it may take longer for hydrogel formation to occur with the more concentrated peptide solutions. The reasoning for determining the stiffness after seven days is to gauge how the material withstands culture conditions. A suitable biomaterial for cell culture purposes should remain stable over a set period of time and stiffness should not fluctuate as there is no external stimulus such as cells at this stage to cause changes in the elastic modulus properties.

3.4.2.2 TEM imaging of peptide solutions

Transmission electron microscopy was used to visualise the nanofibres present within the new Fmoc- F_2 -S peptide solutions (Figure 3.10). The samples were prepared as described in section 3.3.2.6. All five solutions were tested, even though it was discovered that the 5 mM solution failed to form a hydrogel substrate. Image J software was used to measure the average nanofibre width and results are presented in Table 3.4.

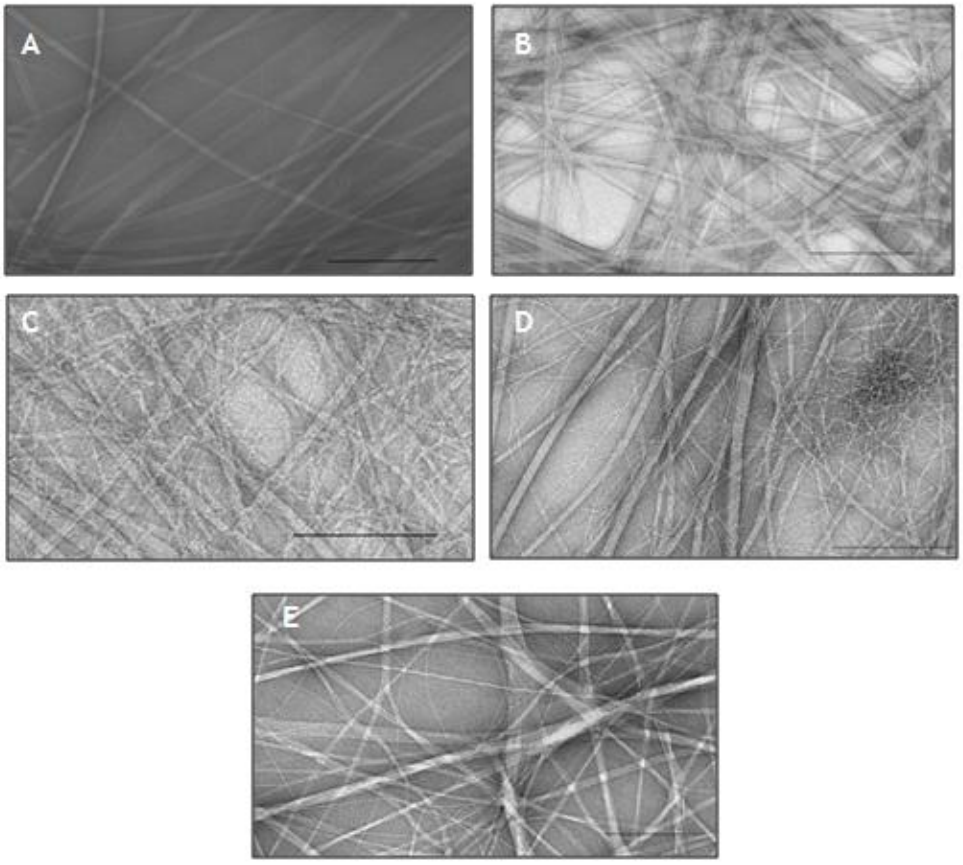

Figure 3.10 TEM peptide solution images. Images A – E illustrates 5mM, 10mM, 20mM, 30mM and 40mM peptide solutions respectively. Scale bar represents 200nm in all images and images were taken under 20,000 x magnification. Nanofibres were used to measure the fibre width, results of which are shown in Table 3.4.

As the concentration of the peptides increases, the overall networking of these nanofibers also follows this trend, with a noticeable difference in profile between 5 mM and 30 mM samples. With this new set of substrates, the fibre width should be uniform in every sample, as the concentration of the Fmoc-F_2 peptides will only affect the stiffness properties of the resulting hydrogel as there is more peptides available to form the cylindrical fibres which ultimately made up the hydrogel substrate. Sample preparation may be accountable for the small differences in fibre widths presented in Table 3.4. As the Fmoc-F_2 synthesis method was changed, the new method of creating hydrogels is not pH dependent, and therefore the fibre widths are not following the same trend as what was observed in figures 3.5 and 3.6. Before, the stiffest hydrogel of 36.8 kPa presented thin narrow cross-linked fibres, whereas with the new concentration based hydrogels, fibre width properties should be uniform throughout. When using the pH method, the individual fibres change in width, which influences the network properties, while with the concentration method the base fibre morphology remains the same, with the density of the fibres now controlling the gel properties.

3.4.2.3 SEM Imaging of peptide solutions

Samples were prepared for scanning electron microscopy by Mrs Margaret Mullen at the University of Glasgow. SEM was used to provide information on the surface characterisation of the overall nano-structure within the five peptide solutions as shown in Figure 3.11.

SEM images demonstrate that as the molar concentration increases, the overall networking becomes increasingly web-like and the pore-like structures become less apparent. This demonstrates that the Fmoc fibres form a continuous interconnecting mesh-like pattern rather than forming single isolated fibres within the solution. This will impact on the stiffness values as those solutions with fewer fibres will ultimately produce a hydrogel with very soft properties. SEM imaging illustrated that the complexity of the solutions increases in line with the rigidity of the hydrogels. Analysis of the spaces residing within the peptide solutions were not undertaken as the process of sample preparation of freeze drying by plunging into liquid nitrogen at -180°C may result in artificial gaps between the fibres. Therefore SEM is presented as an illustration of the

complex patterning observed as the molar concentration increases. This resulting framework affects the rigidity of the resulting hydrogel and resembles the morphology of the native ECM that these substrates are mimicking.

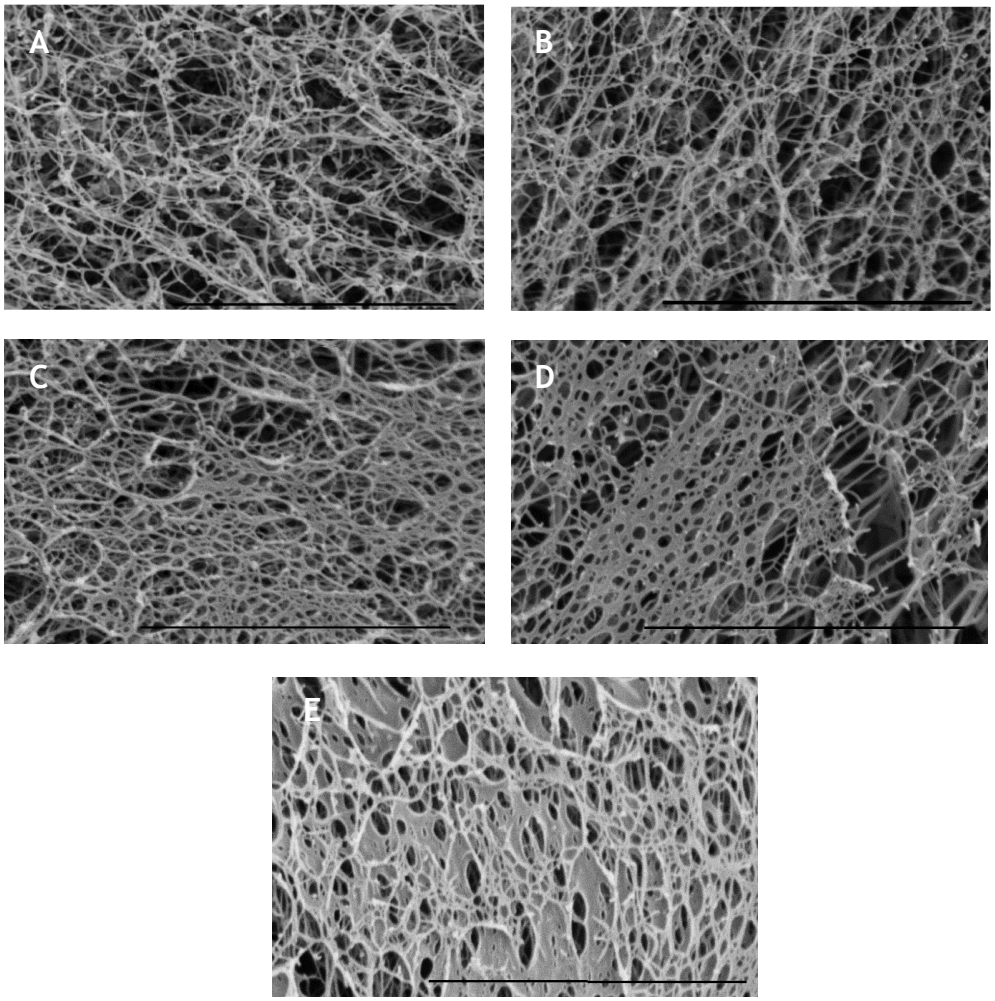

Figure 3.11 SEM images of peptide solutions under 5000x magnification
Images A-E illustrates 5mM, 10mM, 20mM, 30mM and 40mM peptide solutions respectively. Scale bar represents 5µm. SEM imaging is presenting the pores within the peptide solution. As concentration increases from A-E, the space between the fibres decreases due to the increase in Fmoc-F_2 and Fmoc-S peptides present within the solutions.

3.4.2.4 HPLC

HPLC analysis was performed to determine the ratio of the Fmoc- F_2 and Fmoc-S peptides in the solution after sample filtration, as it is believed that some undissolved peptides may be lost in this process. Table 3.5 presents the percentage of each peptide in the solution, with Figure 3.12 illustrating that after filtration the ratio of Fmoc- F_2 and Fmoc-S is not 1:1 as originally expected. However, in all samples Fmoc- F_2 is present in a higher concentration than Fmoc-S, and hydrogels do form from these 10 to 40 mM solutions when the 1:1 ratio of prepared peptides is modified slightly. Figure 3.12 illustrates the HPLC graphs.

Concentration of peptide solution (mM)	Percentage of Fmoc- F_2 peptides	Percentage of Fmoc-S peptides
10	60.33	39.67
20	55.14	44.86
30	51.82	48.12
40	53	47

Table 3.5 Fmoc peptides as analysed by HPLC.

The 10 mM solution presents a higher percentage of Fmoc-F_2 in comparison to the 20, 30 and 40 mM solutions (Table 3.5). This result may have an effect on hydrogel stability as ideally the hydrogels should have Fmoc-F_2 and Fmoc-S peptides in an approximate 1:1 ratio. Hydrogels are formed from all peptide solutions discussed, however, the 10 mM substrate has a higher Fmoc-F_2 concentration and this may affect the substrates stability for long-term culture experiments. However, the peptide ratios observed for the 20, 30 and 40 mM samples are still within the accepted allowances, as experimental errors may account for the small differences in peptide ratios due to measuring minute peptide weights. As well as this, a further error may arise as only a 30 μl volume of each sample was used to measure the percentages of each peptide present in the solutions. As the hydrogels form self-assembling nanofibres, and it is the Fmoc-F_2 peptide which form the basis of these structure as shown by Figure 3.1, it can be hypothesised that a higher Fmoc-F_2 percentage does not affect hydrogels formation by addition of complete cell culture media, and the altered

ratios do not impact the stability of the hydrogel samples when cultured up to 7 days.

A

B

C

D

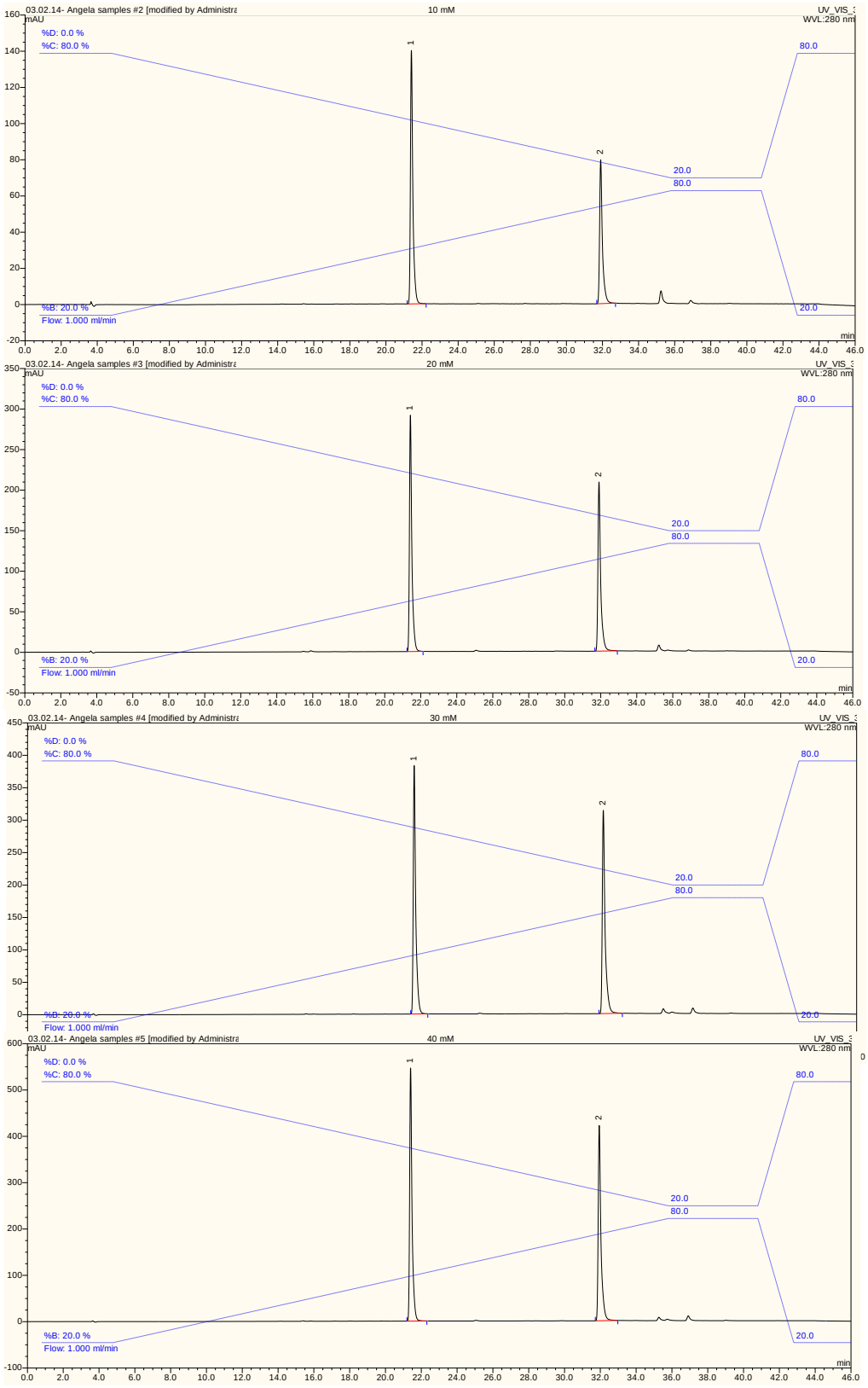

Figure 3.12 HPLC graphs for Fmoc-F2/S peptide solutions
(A) corresponds to 10 mM (B) 20 mM (C) 30 mM and (D) 40 mM solutions. The first peak observed at approximately 22 minutes refers to the Fmoc-F_2 peptide component, with Fmoc-S detected at approximately 32 minutes. Observation of two different heights signifies that the peptides are not present in a 1:1 ratio of one another.

3.5 Conclusion

The initial method of hydrogel production with the Bachem Fmoc-F_2 peptides was reliant on creating a substrate where the stiffness property could be tailored depending on the pH of the peptide solution. When creating a suitable biomaterial, it would be beneficial to create a standard solution and then alter the pH properties depending on the desired application. For example, the original 20 mM hydrogels discussed had elastic modulus values of 1.7, 6.36 and 38.3 kPa for soft, stiff and rigid hydrogels respectively. The hydrogel stiffness occurs as a result of altering the pH and shift in the pK_a which causes the Fmoc-F_2 nanofibres to crosslink. Self-assembly of the nanofibres within the peptide solution occurs when the pH is lowered, the pK_a shift occurs between pH 10.2 and 9.5, and results in the Fmoc-F_2 peptides forming fibrils consisting of ß-sheets. By lowering the pH again to between 9.5 and 6.2 decreases the surface charge of the fibres, allowing them to cross-link laterally as discussed by Tang *et al.*, 2009. By addition of various volumes of 0.5 M NaOH when creating the peptide solution, the pH is altered to incorporate the formation of ß-sheets and degree of cross-linking in one continual step. The differences in the cross linking due to pH of peptide samples can be visualised in Figures 3.5 and 3.6.

Following on from original modification of 20 mM hydrogels and as described by Jayawarna *et al.*, 2007, new protocols were developed with the aim of developing a pool of hydrogels that would range in stiffness properties. In this chapter, the concentration of the Fmoc-F_2 and Fmoc-S peptides increased and the pH kept in the range of 7-7.8, therefore ideal for cell culture purposes. As a result, a range of hydrogels from 10 mM to 40 mM created substrates of 0.64 to 12 kPa in stiffness and are potential substrates for cell culture. This method of hydrogel synthesis does not rely on pH to promote cross-linkage of the Fmoc nanofibres, and instead concentration of Fmoc peptides was the constituent part of altering the elastic modulus of the hydrogel substrate. The reasoning behind the development of concentration dependent hydrogel elasticity was reliant on the synthesis method that Bachem, UK used to create the original Fmoc-F_2 peptides. The synthesis method was changed during initial hydrogel studies and this resulted in hydrogels with different properties to that described in Table 3.1. However, as this is a commercial product, the manufacturer would not disclose the original method used to synthesise the Fmoc-F_2 peptides, and as a

result, in-house synthesis began at the University of Strathclyde. This enabled us to control the synthesis and to develop highly reproducible protocols based on density. By having a pool of hydrogels with varying stiffness as a result of increasing peptide concentration, the aim will be to mimic the stiffness of the bone marrow MSC niche and therefore maintain cell multipotency, as well as culturing MSCs on gels that mimic the stiffness of other tissues in the human body and therefore promote substrate driven differentiation, as discussed by Engler *et al.*, 2006. This would allow a targeted application, as ideally in tissue engineering the aim is to find a substrate which promotes MSC maintenance, and also use substrates which promote the differentiation of these cells when they are required, ie in response to injury or disease. When needed, these cells could be differentiated towards the osteogenic lineage when patient requires osteopedic repair or towards the neurogenic lineage for treatment for alzheimers disease.

The nanofibrous structures present within the peptide solutions were investigated and it can be concluded that as concentration of the Fmoc-F_2 and Fmoc-S increases, so does that of the overall fibre networking as there is more available Fmoc-F_2 present to self-assemble into nanofibres. Fibre width should not increase in line with increase in peptide concentration, but rather the networking patterning and degree of fibre overlap is the defining factor in the stiffness range observed between the samples, as shown in Table 3.4. It is therefore possible to tune the stiffness properties of the self-assembled gels by altering the molar concentration of the peptides with this new in-house synthesis method. HPLC confirmed that after peptide solution was filtered during preparation, the ratio of the Fmoc-F_2 and Fmoc-S peptides were not present in a 1:1 ratio as expected, but the peptides were present in a ratio that still promoted the 10- 40 mM peptide solutions to gelate in culture. Fmoc-F_2 was present in a higher concentration and as this forms the basis of the nanofibres within the substrate it was hypothesised that the HPLC ratios presented in Table 3.4 are suitable for hydrogel formation and culture as they can be maintained for more than 7 days in culture. This chapter demonstrates the protocol development and characterisation of these hydrogels, and the following chapters will discuss their use as substrate materials for 2D and 3D study of MSCs.

Chapter 4

Introduction to Fmoc-F_2/S Hydrogels for use in cell culture

4.1 Introduction

4.1.1 Identifying the stem cell population

MSCs are a multipotent population that reside in locations such as the bone marrow niche. In this niche there are believed to be a range of other cell types present, which includes pre-osteoblasts, red blood cells and hematopoietic stem cells (HSCs) that facilitate the maintenance of a balanced MSC population (Shiozawa *et al*., 2008). Bone marrow tissue contains the cells of interest for the purposes of regenerative medicine. However, typically less than 1 in 10,000 cells extracted from the marrow is classed as a stem cell (Williams *et al*., 2013) and therefore selection processes are necessary in order to obtain a multipotent MSC population.

Bone marrow cell populations can initially be separated based on adherence properties, as stem cells, as well as pre-committed cells, can be identified as they are able to adhere to tissue culture plastic and form colony forming fibroblastic units (CFU-F) *in vitro*. However, HSCs and other blood cells do not attach and can be easily separated from the adherent population by removal of supernatant after the adherent population have been observed in culture (Wan *et al*., 2005*)*.In the current literature, MSCs have been defined by the presence or absence of cell surface markers. STRO-1 is one such marker, and is a cell membrane single pass type I protein that has shown to differentiate in accordance to the classical MSC lineages (McMurray *et al*, 2011). CD146 is another classical MSC marker, and is defined as a cell adhesion molecule (CAM) involved in cell activity and angiogenesis. Presence of CAMs allows cells to bind to other cells in the niche and with the ECM for cell adhesion (Wang and Yan., 2013). The CD271 marker, commonly referred to as low-affinity nerve growth factor receptor (LNGFR), has been addressed as a MSC marker in bone marrow mononuclear cells. Cells selected for this receptor have been found to be proliferative and also contain progenitors for the osteo and adipogenic lineages and could be engaged in the process of chondrogenic differentiation (Flores-Torales *et al*., 2010). As there are a number of identified MSC cell surface markers, there is a great deal of interest with regards to determining if there

are distinct MSC populations based on these markers, or if co-expression occurs and if so what is the mechanism for this.

MSCs have been known to differentiate in culture due to chemical, mechanical and nanotopography cues as previously discussed. It is known, that insulin as well as dexamethasone and 1-methyl-3-isobutylxanthine in culture media induces MSCs towards the adipogenic lineage (Pittenger et al., 1999). In adipocyte differentiation, a number of transcription factors such as CCAAT/enhancer binding protein (C/EBP) ß, δ and α, PPARγ are all induced in a unique sequence. Adipogenic culture media promotes these transcription factors resulting in adipogenic induction *in vitro* (Klemm *et al.*, 2001) that can be confirmed by observation of fat globules in culture.

Dexamethasone is a glucocorticoid which in alternate concentrations can be used for the differentiation of osteoblast cells therefore inducing osteogenic lineage commitment (Beloti *et al.*, 2005). Treatment with 10^{-7} M dexamethasone has been found to modulate procollagen type 1 carboxy-terminal peptide production, alkaline phosphatase activity (ALP) and osteocalcin secretion all of which are associated with human osteoblast cultures (Yamenouchi *et al.*, 1997). The mechanism by which dexamethasone induces osteogenesis was defined by Hamidouche and contemporaries in 2008. They discovered that dexamethasone up-regulates the Four and Half Lim Protein 2 (FHL2). FHL2 is a LIM domain protein and acts in tissue specific gene expression. It has been reported that FHL2 interacts with integrins to promote differentiation towards the osteoblast lineage (Lai *et al.*, 2006). Expression of FHL2 promotes the transcription of RUNX2 as well as alkaline phosphatase (ALP), type 1 collagen resulting in increased mineralisation in both human and murine MSCs (Hamidouche *et al.*, 2008). Figure 4.1 illustrates how dexamethasone promotes osteogenic differentiation by the transcription of FHL2 in response to chemical induction for example.

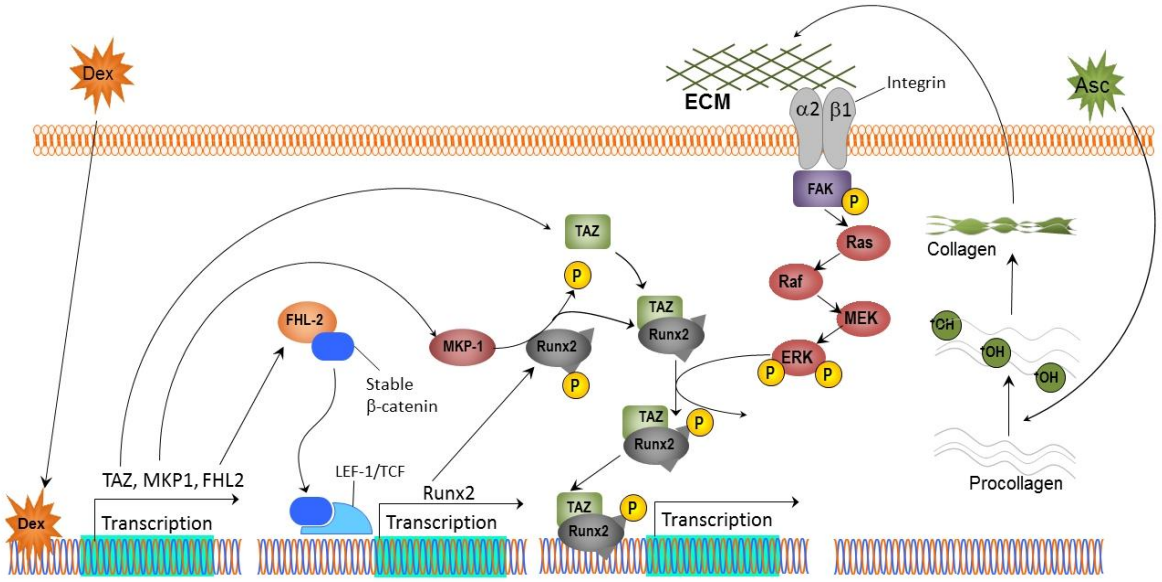

Figure 4.1 Osteogenic differentiation promotion by the increased transcription of the FHL2 protein due to dexamethasone. Presence of Dexamethasone induces the transcription of a number of factors including FHL2. The binding of this protein to ß-catenin initiates transport to the cell nucleus, where binding to T Cell factor/ lymphoid enhancer protein (LEF-1/TCP) occurs. This in turn induces the osteogenic transcription of RunX2 co-activator, TAZ. As well as Dex activating FHL2, MKP1 (a member of the MAPK signalling pathway) is also transcribed which dephosphorylates and activates Runx2 by the Extracellular related kinase (ERK) pathway. Ascorbic acid (Asc) which is commonly present in osteogenic differentiation media, increases procollagen type 1 production. Figure adapted from Langenbach & Handschel., 2013.

4.1.2 Mechanical response to culture substrate

Cells can alter the force applied to the substrate in response to 2D or 3D environments. Cells initially respond to the elasticity of the microenvironment and exert contractile force at a magnitude that scales with this stiffness resulting in a feedback loop until equilibrium is reached as shown in Figure 4.2a. The contractile force generated by the cell when cultured on a given substrate is not uniform, and depends on the elasticity or stiffness of the material (McBeath *et al.*, 2004). Softer materials deform as cells contract thus dispersing cell traction forces into the substrates and resulting in less cytoskeletal contraction (Provenzano & Keely., 2011). However, MSCs on stiffer substrates can generate much greater contractile forces through the cytoskeleton. This is a linear relationship between matrix elasticity and the forces the cell utilises to deform the matrix as shown in Figure 4.2b. However, there will become a point where the cell contraction force will plateau in response to a stiff substrate material.

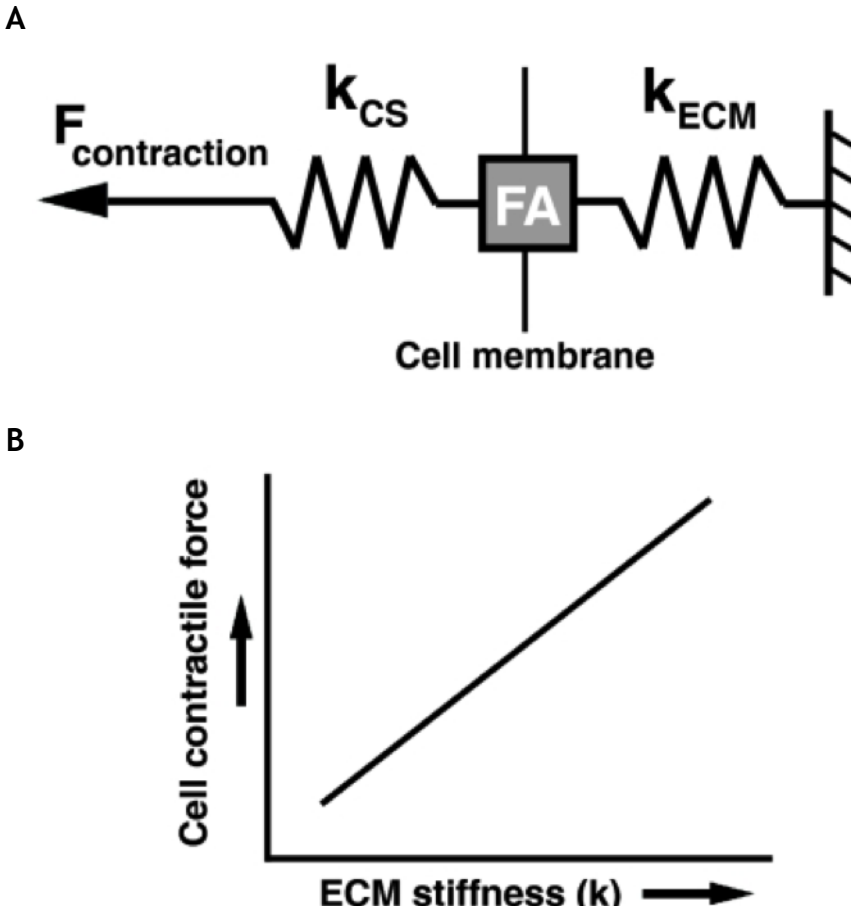

Figure 4.2 Cell contraction and ECM stiffness.
(A) The stiffness of the ECM (kECM) is felt by the Focal adhesions of the MSC which in turn leads to cell signalling to create a contractile force to deform the matrix. This loop is repeated until the correct contractile force is generated in response to the kECM. (B) Illustrates the increased contractile forces required by the cell to deform the ECM in response to the varying stiffness felt. Soft substrates require a low contractile force to deform the matrix, whereas stiffer materials require greater force to illicit the same response. Adapted from Provenzano & Keely, 2011.

Elastic properties of the substrate material have also demonstrated the ability to tune differentiation of MSCs in accordance with the stiffness of the material in question. Materials mimicking the physical properties of a number of tissue types have been shown to induce differentiation down the corresponding lineage; a process referred to as modulus driven differentiation (Perekh *et al.*, 2010). It is also hypothesised that if the substrate mimics the elastic nature of the native niche, then stem cell multipotency can be maintained. For example, a hydrogel material mimicking the elasticity of muscle which is approximately 12 kPa has demonstrated maintenance of mouse muscle multipotency in culture, and such

cells can be transplanted back into the animal model and contribute to cellular muscular repair (Gilbert *et al.*, 2010). In the human body, there are a range of tissues which differ in stiffness, as shown in Figure 4.3, that can be take advantage of in tissue engineering.

Figure 4.3 Tissue elasticity
Predictions of Tissue microenvironments are shown above, demonstrating the range of stiffness's present within the human body. The resistance felt by the cells when they are cultured upon given substrate and try to deform the matrix is illustrated by E, the elasticity of the microenvironment. Figure adapted from Engler *et al.*, 2006.

In 2006, Engler (Engler *et al.*, 2006) described how cells initially pull on their substrate to sense the stiffness, and how a mechantransducer is required to generate signals based on the matrix stiffness. The stiffness of the culture substrate will have a downstream effect on the cell morphology, as a soft matrix will prevent spreading and may result in rounded cells, whereas stiffer substrates allow contraction and the cell morphology becomes more polygonal in appearance. Focal adhesion related signalling and force transmission through the cytoskeleton are relayed to the cell nucleus which effects transcription and hence lineage commitment. Adipogenic and neurogenic commitment typically results following an observed rounded cell morphology, whereas highly spread MSCs on a stiff substrate generally commit to the osteogenic lineage. In fact, MSCs have illustrated neurogenic, adipogenic, as well as chondrogenic lineage commitment on hydrogel biomaterials. However, many research groups have incorporated the use of induction media to promote this differentiation to occur rather than use the stiffness of the gels to induce modulus driven differentiation (Xie *et al.*, 2011; Gruene *et al.*, 2011 and Dickhut *et al.*, 2008).

4.1.3 Metabolomics

Metabolomics is a relatively new field, which is described as the systemic study of the unique chemical fingerprints that cellular process leave behind (Daviss, 2005). This technique can be used to analyse the MSC metabolome, described as the cells full complement of small molecule metabolites and may be used to indicate phenotype diversity or how the cell responds to its environmental factors such as material stiffness or chemical induction (Zenobi, 2013). Figure 4.4 illustrates the link between DNA and metabolites, with this process being a continuous feedback loop and not a stationary process within the organism or cell population.

Although this technique is still in its infancy, it has had a profound effect in a range of research fields. As metabolites form the building blocks of genes, ribonucleic acids and proteins, this technique is now routinely being used and developed further for diagnostic applications. For example, it has effectively been used to detect Down's syndrome metabolic markers from maternal blood in the first trimester of pregnancies (Bahado-Singh *et al,* 2012). Other groups have used metabolomics as a means of testing toxicity as well as detecting biomarkers of disease, and detecting specific metabolite changes associated with various cancer types such as breast cancer. Cancerous cells possess a unique phenotype and biomarkers related to glycolysis, TCA cycle, choline and fatty acid metabolism (Serkova *et al.*, 2006 and Serkova & Glunde., 2009). Modern day testing for diabetes mellitus also utilises the detection of glucose metabolites in the urine illustrating that this technique has great potential and will be further developed for improving diagnostic techniques for a range of diseases in modern medicine.

An untargeted or targeted approach can be taken when carrying out a metabolomics study. The former relies on the global unbiased analysis of small mass molecules that can be detected by the chosen method of sample preparation and detection (Naz *et al.*, 2014), whereas targeted analysis focuses on a particular subset or single metabolite of interest (Lu *et al.*, 2008). The latter is the primary focus of drug toxicity and pharmaceutical drug trials as the aim is to detect small changes in response to the therapeutic agent in question.

Metabolite fingerprinting or footprinting can both be coupled with an untargeted or targeted approach for detection of more specific metabolites. Fingerprinting focuses on the general analysis of intracellular metabolites within a particular sample, commonly referred to as the cell endometabolome. The metabolites the cells expel or exhaust are detailed through metabolite footprinting, (Monton & Soga., 2007) and are commonly found in cell culture media if focussing on adherent cell populations. The exometabolome is the term coined which describes this particular subset of emitted metabolites.

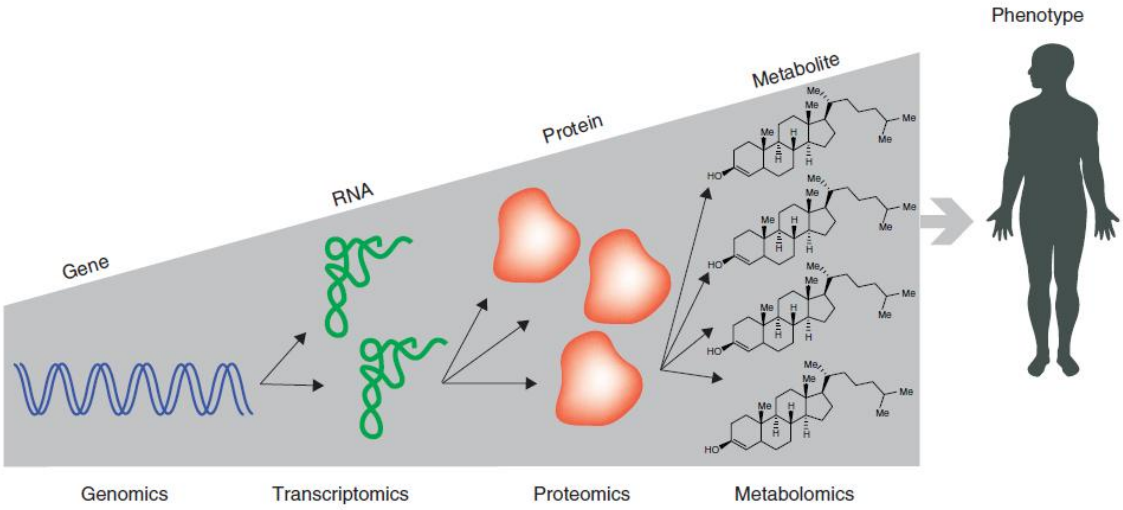

Figure 4.4 The link between the genome and the metabolome.
An organisms phenotype originates with the genome, with the study of the DNA and genes referred to as genomics. From here, particular genes are transcribed into RNA, and translated into proteins. Transcriptomics and proteomics are the terms used to describe the subsequent study of RNA and proteins respectively. Proteins can be post -translationally modified resulting in a diverse metabolite profile. This figure presents a continual feedback loop where specific RNA is transcribed in response to external stimuli and will result in a different metabolite profile. These factors described all have an impact of the phenotype of the organism or cell population in the case of MSCs. Figure adapted from Wilcoxen *et al.*, 2010.

As well as being able to detect changes in response to drugs or disease, metabolomics has also been utilised to detect stem cell phenotype changes such as proliferation and commitment phases as shown by Figure 4.5 (McNamara *et al.*, 2012 and Yanes *et al.*, 2010). Through the use of an untargeted metabolomics approach, it was discovered that iPSCs share a distinct profile with ESCs, particularly with those metabolites involved in the process of cellular respiration and these are distinct from the profile of their original parent cell

before they were transformed into iPSCs (Panopoulos *et al.*, 2011). This provides further confirmation that iPSCs share common properties with ESCs.

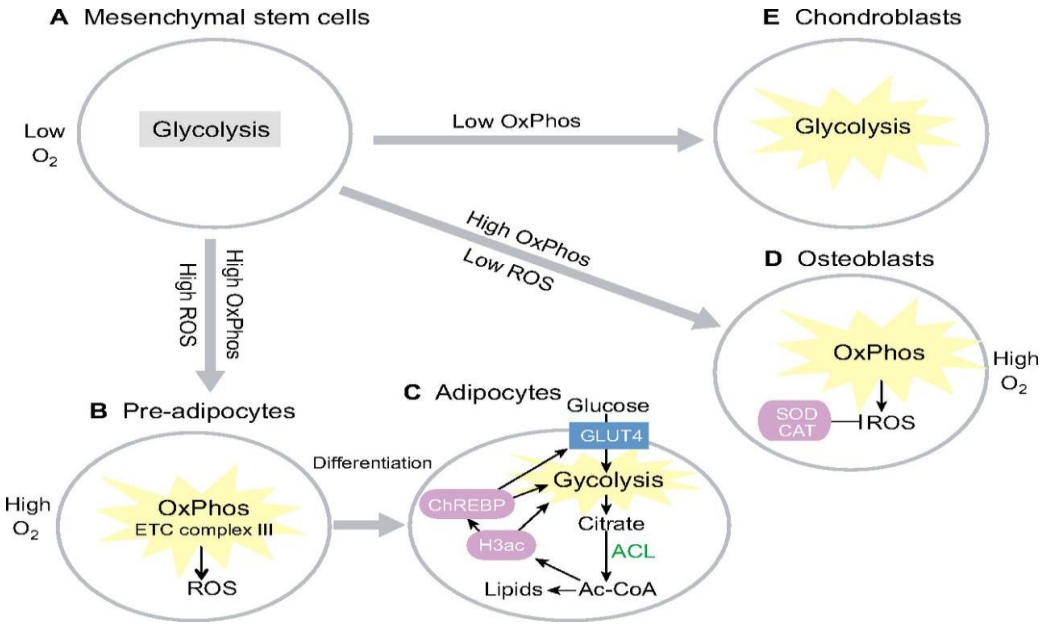

Figure 4.5 Metabolism in MSCs.
Mesenchymal stem cells in the niche (A) are metabolically quiet, quiescent and undergo glycoslysis metabolism. Commitment to the adipogenic lineage is a two-step process as shown by (B) and (C). Initially the MSCs upregulated Oxidative Phosphorylation (OxPhos) and reactive oxygen Species (ROS) from the electron transfer chain (ETC) III to become pre-adipocytes. Full commitment to the adipogenic lineage is characterised by increased glycolysis metabolism and ATP citrate lyase (ACL), which results in high levels of cytosolic acetyl CoA (Ac-CoA) and an increased in Histone H3 acetylation (H3ac). This activates the transcription factor, carbohydrate responsive element binding protein (ChREBP) promotes Glucose uptake mediated by Glut-4 and glycolysis to generate more acetyl CoA. Osteogenic differentiation (D) occurs from a quiescent state to an OxPhos rich high oxygen consumption state, however ROS is inhibited by means of superoxide dismutase (SOD) and catalase (CAT). Finally, Chondrogenic differentiation (E) is promoted by upregulation of the glycolic pathway. Adapted from Shyh-Chang *et al.*, 2013)

4.2 Objective

The first part of this chapter set out to use immunocytochemistry and histology to report the expression of phenotypical proteins associated with multipotency of MSCs isolated from human bone marrow.

The second part of this chapter aims to investigate the effect of the hydrogel substrate mechanics on various cell types. A soft hydrogel material will be studied with the aim of mimicking the elasticity and stiffness of the bone marrow niche, where the MSCs and OPGs are situated in the human body. By conducting studies in two and three dimensions, the most niche-like environment will be evaluated and methods such as metabolomics, qRT-PCR and

rheological studies will be used to detect changes in cells and their environment due to differentiation or maintenance of the stem cell state.

Next, to investigate conflicting cues in the gels, pericytes will also be cultured in a 2D and 3D study along with the osteogenic metabolite cholesterol sulphate (Alakpa, data being prepared for publication). This metabolite is classed as a glucorticoid, a group which are known to play an integral role in osteogenic differentiation (Mirmalek-Sani *et al.*, 2006). However, it is noted that over exposure can cause the adverse effect and induce adipogenic differentiation (Justesen *et al.*, 2004 and Bujalska *et al.*, 2008). Cholesterol sulphate will be used to induce differentiation of cells down the osteogenic lineage whilst culture within a soft hydrogel material. This will provide valuable results for further studies with regards to creating a suitable model for regenerative medicine in the following chapter.

4.3 Materials & Methodology

4.3.1 Materials

Reagent	***Supplier***
Cell culture reagents	
Human Bone marrow cells	Southern General Hospital, Glasgow
Human pericytes	University of Edinburgh
DMEM culture media	Sigma Aldrich
Antibiotic Mix	In-house
L-glutamine (200 mM)	Sigma
Penicillin Strepomycin	Sigma
Ampotericin B (250 µg/ml)	Invitrogen
Sodium Pyruvate	Sigma Aldrich
Non Essential Amino Acids	Sigma Aldrich
Foetal Bovine Serum	Sigma
Trypsin	Sigma
Cholesterol Sulphate	Sigma Aldrich
Versine	In-house
PBS/FBS	In-house
EasySep™ Human $CD271^+$ Cell Selection kit	Stem Cell Technologies
Differentiating Media reagents	
Dexamethasone	Sigma Aldrich
Ascorbate-2-phosphate	Sigma Aldrich
Insulin	Sigma Aldrich
Indomethacin	Sigma Aldrich

Indobutylmethylxanthine	Sigma Aldrich
Immunocytochemistry Reagents	
1 x Phosphate buffer saline	Sigma-Aldrich
PBS/BSA	In-house
Formaldehyde	Sigma-Aldrich
Permeabilisation buffer (PBST)	In-house
Sucrose	Sigma-Aldrich
Triton® x 100	Sigma-Aldrich
Magnesium chloride hexahydrate	Sigma-Aldrich
Bovine serum Albumin	Sigma-Aldrich
Tween 20®	Sigma-Aldrich
Rhodamine Phalloidin	Vector Laboratories
Fluorescin streptavidin	Vector Laboratories
Vectorshield mounting media with DAPI	Vector Laboratories
RNA Extraction & PCR Reagents	
TRIzol Reagent	Life Technologies
Glycoblue	Sigma Aldrich
Chloroform	Sigma Aldrich
Isoporopanol	Sigma ALdrich
QuantiTect Reverse Transcription Kit	Qiagen
Syber Green MasterMix	Qiagen
TaqMan Master Mix	Life Technologies
Syber Green Primers	Eurofins
TaqMan Probes	Applied Biosystems
Hydrogel reagents	
Fmoc-FF	BioGelx, UK
Fmoc-S	Bachem
0.5 M Sodium Chloride	Fisher chemicals
Distilled water	Invitrogen
0.5 M Hydrochloric Acid	Sigma Aldrich
Other Reagents	
Guanidine Hydrochloride	Sigma Aldrich
Ethanol	VWR Chemicals
Sodium dodecyl sulphate (SDS)	Sigma Aldrich
Methanol	Sigma Aldrich
Chloroform	Sigma Aldrich

4.3.2 Methodology

4.3.2.1 Immunocytochemistry

Cells were cultured on glass coverslips and hydrogels preparation for immunostaining, were washed with 1 x PBS and fixed with 10% v/v formaldehyde/PBS for 15 minutes at 37°C. Cells were permeabilised at 4°C for 5 minutes and subjected to 1% w/v BSA/PBS for 15 minutes at 37°C to prevent non-specific binding. Primary antibodies were diluted (1:50) in BSA/PBS with

rhodamine –phalloidin (1:500). Samples were incubated for 1 hour at 37°C and rinsed with 0.5% v/v PBST (agitated for 3x 5 minute cycles) to minimise background binding. Secondary biotinylated antibody was added in BSA/PBS Samples then proceeded to be incubated at 1 hour at 37°C then washed again with PBST. After agitated washing, samples were incubated for 30 minutes with fluorescein isothyiocyanate streptavidin (FITC) (1:50) in BSA/PBS at 4°C and then washed a final time. Coverslips were mounted onto glass slides in DAPI mountant solution and cells were imaged with Zeiss Axiovert fluorescence microscope at 20 x magnification (0.40 NA). Images were taken with an Evolution QEi digital monochromatic CCD camera (Media Cybernetics, USA) with ImagePro software. In summary, details of the primary secondary and tertiary antibodies for this chapter are given in Table 4.1.

Differentiation Lineage	Biomarker	Primary Antibody	Secondary Antibody	Fluorphore
Adipogenesis	PPARγ	Goat Monoclonal IgG	Biotinylated anti goat	Streptavidin conjugated to FITC
Neurogenesis	Nestin	Mouse Monoclonal IgG	Biotinylated anti mouse	
	B3 Tubulin			
Multipotency	CD63			
Osteogenesis	OPN			
Multipotency	ALCAM	Rabbit Monocolonal IgG	Biotinylated anti rabbit	
	CD271			
Cytoskeleton	F-actin			Phalloidin conjugated to rhodamine
Nucleus				DAPI

Table 4.1 Biomarkers used for detection of MSC differentiation & multipotency

4.3.2.2 Preparing cell differentiation media

Differentiation of MSCs was accomplished by supplementing DMEM cell culture media with a specific mixture of inducing agents. These were used to illustrate that the MSCs in question had the capacity to differentiate down the adipo and osteo lineages. Osteogenic media was created using DMEM media containing 10% FBS, 350 μM ascorbate-2- phosphate and 100 nM dexamethasone. For adipogenic inducing media, DMEM media with 10% FBS was supplemented with 1.7 nM

insulin, 200 µM Indomethacin, 50 µM Isobutylmethylxanthine and 0.1 µM Dexamthasone. Cells were removed from cell culture flasks, seeded onto glass and maintained overnight at 37 °C with DMEM cell culture media, and then subjected to differentiation media for the remainder of the experiment.

4.3.2.2.1 Cholesterol Sulphate Cell Culture Media

A 5 mg weight of cholesterol sulphate was dissolved in 0.25 ml DMSO to give a stock solution of 20 mg/ml. A 29.4 µl volume of stock solution was added to 12 ml DMEM culture media to create a 100 µM stock, of which 0.1 µl was added to 99.9 µl DMEM media to create a working solution of 0.1 µM used throughout within this chapter. This supplemented media was used with pericyte cells in 3D studies, and media was added to upper surface of hydrogel substrate, as well as the surrounding well. Cholesterol sulphate was used at 0.1 µl throughout as previous work by Dr Enateri Alakpa illustrated that this concentration was non toxic to cells

4.3.2.3 Histology staining

4.3.2.3.1 Oil Red O staining for fat globlets

Oil red O stock solution was made by dissolving 0.3 g of oil red O powder in isopropanol overnight resulting in a solution of 3mg/ml. This was passed through a 0.2µm filter and kept at 4°C. A working solution was made by adding three parts of the stock solution to two parts distilled water, resulting in a solution of 1.8mg/ml. This solution was allowed to come to room temperature before passing through a 0.2 µm filter.

Cells cultured in adipogenic induction media had their culture solution aspirated to waste and washed with 1 x PBS solution. After washing, a 500µl volume 10% formaldehyde was added to fix the samples and incubated at room temperature for 10 minutes. This was decanted to waste and samples washed three times with 1 x PBS. A 500 µl volume of oil red O working solution was added to the samples and incubated at room temperature for 30 minutes. Cells were then washed with sterile water until the liquid became clear. A small volume of water between 250- 300 µl was added to the cells prior to microscopy.

4.3.2.3.2 Alzarin red staining for calcium deposits

Cells cultured with osteogenic differentiation media were washed with 1 x PBS and fixed with 10% formaldehyde for 10 minutes at room temperature and then washed twice with 1 x PBS. A 1 ml volume of 2% alizarin red solution at pH 4.3 was added to the cells and incubated at room temperature for 15 minutes. Solution was aspirated to waste and cells washed with sterile water until solution became clear. Samples were then viewed under microscope.

4.3.2.4 Extraction of RNA

4.3.2.4.1.RNA extraction, reverse transcription and qRT-PCR

At each desired timepoint, TRIzol reagent was added to cells cultured on hydrogel substrate and on glass, which acted as our controls and to the hydrogel samples. The solution was left at ten minutes at room temperature to effectively lyse all cells and release RNA as described in section 2.1.5. RNA concentration was measured using Nanodrop, and was reverse transcribed to uniform concentration of cDNA by use of QuantiTect Reverse Transcriptase according to manufacturer's instructions. cDNA samples were stored at -20°C until qRT-PCR was performed. Primers to detect markers of multipotency and differentiation are described in Table 2.1 and cycling conditions are presented in section 2.2.9. Primers were previously designed and tested by previous lab member.

4.3.2.4.2 DNA Extraction and protein measurements

DNA was isolated during the TRIzol RNA isolation procedure. The DNA was present within the interphase and phenol-chloroform layer and extracted as described in section 2.1.6. The DNA was measured using nanodrop.

4.3.2.4.3 Protein extraction and measurements

Isolating the protein within the samples was also possible during the TRIzol procedure and it described in section 2.1.7. Again, measurements of protein concentration were performed on nanodrop.

4.3.2.5 Metabolomics

4.3.2.5.1 Extraction of Metabolites

Metabolites were extracted from samples using an extraction solvent composed of chloroform, methanol and water in a 1:3:1 ratio (v/v). The quenching extraction solvent used in this study is a general quenching agent used to extract a relatively broad range of metabolites. Prior to extraction, samples were washed with warm PBS solution and then placed in a new tissue culture plate before addition of ice-cold extraction solvent. Due to the sensitivity of the metabolic approach, hydrogels without MSCs also underwent metabolite extraction and acted as a blank internal sample to which all hydrogels containing cells were subtracted from. The culture plate was sealed with parafilm and kept on ice and agitated for 60 minutes in cold room. Working at low temperatures prevents evaporation of the extraction fluid and subsequent loss of metabolites. After this time, samples were transferred to clean eppendorf tubes and centrifuged at 13,000 g for 5 minutes at 4°C to pellet any cell debris. The supernatant was transferred to clean tube and stored at -80°C until ready to be run on the Liquid chromatography-Mass Spectrometry (LC-MS).

4.3.2.5.2 Liquid chromatography- mass spectrometry (LC-MS)

The liquid chromatography separation of the metabolite samples was performed on a zwitterionic hydrophilic interaction liquid chromatography (ZIC-HILIC) 150 x 4.6 mm, 100A column as the stationary phase with acetonitrile with 0.08% formic acid as the organic mobile phase and water with 0.1% formic acid as the aqueous mobile phase. The mobile phase was run over a gradient of 46 minutes, details of which are described in Table 4.2. Of the metabolites extracted from samples, a 10 μl volume was injected into the LC-MS. A pooled aliquot comprising of 5 μl of every sample to be run was injected into the LC-MS several times over the duration of the sample batch. The purpose of this was to monitor metabolite quality and stability. All samples were run alongside three internal standards, which contain known metabolites and LC retention times.

Time (mins)	Aqueous (%)	Organic (%)	Flow rate (ml/min)
0	20	80	0.3
30	20	80	0.3
32	80	20	0.3
40	95	5	0.3
42	95	5	0.3
46	20	80	0.3

Table 4.2 Gradient elution conditions used in chromatographic separation.

After separation, Mass Spectrometry was performed using an Exactive orbitrap mass spectrometer. Scans were performed at 50,000 resolutions at 100 m/z in both positive and negative modes within the range of 70-1400 m/z for mass for the entire time of the LC gradient.

4.3.2.5.3 Data processing

Raw data files were obtained after LC-MS batch was complete, and these were converted using IDEOM/MzMatch Excel Interface, which measured chromatographic peak intensities and could normalise against blank samples and controls (Creek, 2012 and Scheltema, 2011). Identification of metabolites was possible due to the presence of internal standards from which masses and retention times were known. After processing, putative metabolites in hydrogel and control samples were identified on the basis of these predicted retention times.

4.3.2.5.4 Data analysis

Data analysis was performed using Metaboanalyst 2.0 (Xia, 2009.,and 2012). This software was used to distinguish up and down regulation of metabolites of interest by creating heat-maps and principle component analysis illustrations.

4.4 Results and discussion

4.4.1 MSCs and differentiation commitment

Bone marrow adherent cells were prepared as described in section 2.3.1 and were positively selected for the CD271 cell surface marker using a tetrimeric

antibody complex coupled with magnetic nanoparticles. Following selection, those cells positively selected were immuno-labelled to detect the presence of this CD271 cell surface marker as well a STRO-1 and ALCAM (Figure 4.6) which are also associated with a MSC multipotent population.

The non-selected cells from the CD271 selection process, as described in section 2.3.2, are referred to as OPGs were cultured on glass coverslips and allowed to adhere for approximately 2 hours. Cells were fixed with formaldehyde and stained for MSC cell surface markers and those associated with the osteogenic lineage due to the location of cell extraction from the bone marrow of the femoral canal. Figure 4.7 illustrates the presence of such markers and confirms that the OPG population is highly diverse and contains MSC markers such as STRO-1 and ALCAM and is therefore a suitable cell source for further study in this thesis.

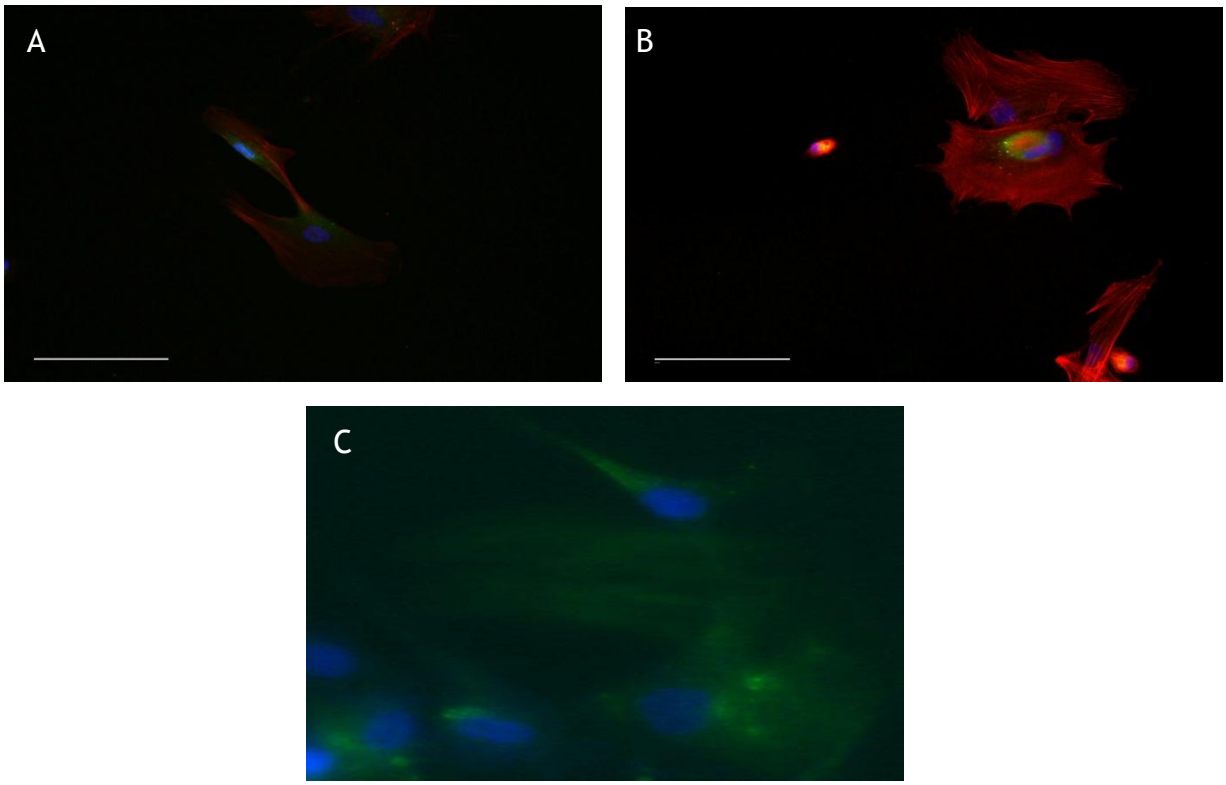

Figure 4.6 Immuno-fluorescence images of CD271$^+$ MSCs. Cells were immuno-labelled for (A)STRO-1, (B) ALCAM, and (C) CD271. Colours are red (actin), blue (nuclei) and green (marker). Scale bar denotes 100 μm.

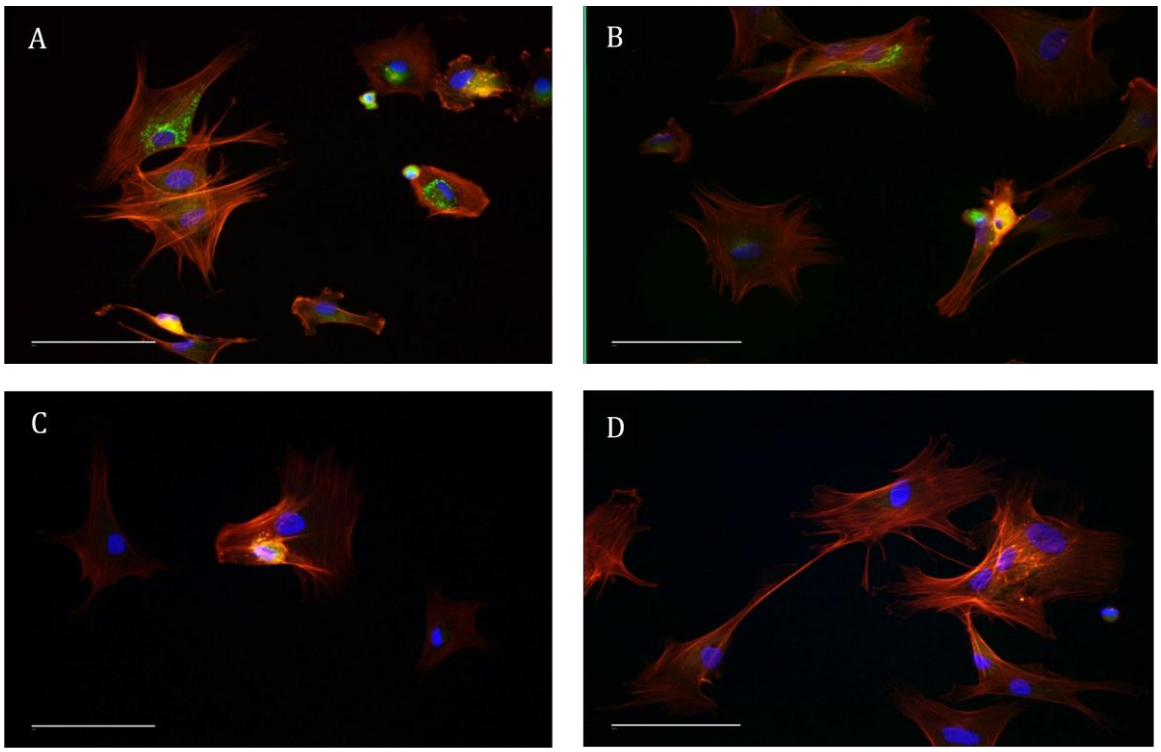

Figure 4.7 Immuno-fluorescence images of the OPG cell population. Cells were immune labelled for (A) Osteopontin (B) Nestin (C) STRO-1 and (D) ALCAM. Colours are red (actin), blue (nuclei) and green (marker). Scale bar denotes 100 μm.

$CD271^+$ MSCs have illustrated that as well as displaying the CD271 cell surface marker, further MSC markers ALCAM and STRO-1 are also present (Figure 4.6). This signifies that this population are positive for a number of MSC markers even though this selection process was based purely on the CD271 cell surface marker. However, to confirm this fully, more stringent testing such as FACS would be needed. The OPG immune staining (Figure 4.7) illustrated presence of osteopontin (OPN), as well as markers associated with multipotency such as STRO-1 and ALCAM potentially indicating an osteogenic preference of the unselected cells. The detection of nestin, which is commonly referred to as a neurogenic marker but more recently has illustrated to be involved in illustrating multipotency, signifies that these cells play a role in maintaining the hematopoietic stem cell (HSC) niche as it has been found that HSCs are attracted to MSCs expressing the nestin marker (Mendez-Ferrer, 2010). This is expected in this population as the cells were obtained from the bone marrow present within the femoral head, which is where HSCs reside in the red bone marrow tissue.

$CD271^+$ MSCs and the OPG cell population have both illustrated expression of MSC cell surface markers associated with multipotency such as ALCAM and STRO-1. To confirm such cells possess the ability to differentiate prior to culture upon Fmoc hydrogel substrates, MSCs and OPGs were cultured in cell culture media supplemented with chemical cues as described in section 4.3.2.2 to drive lineage commitment down the adipogenic and osteogenic pathways. Cells were cultured in this supplemented media for 14 days, after which cells underwent histological staining as described in section 4.3.2.3, for detection of fat globlets and calcium deposits associated with adipogenic and osteogenic differentiation respectively (Figure 4.8).

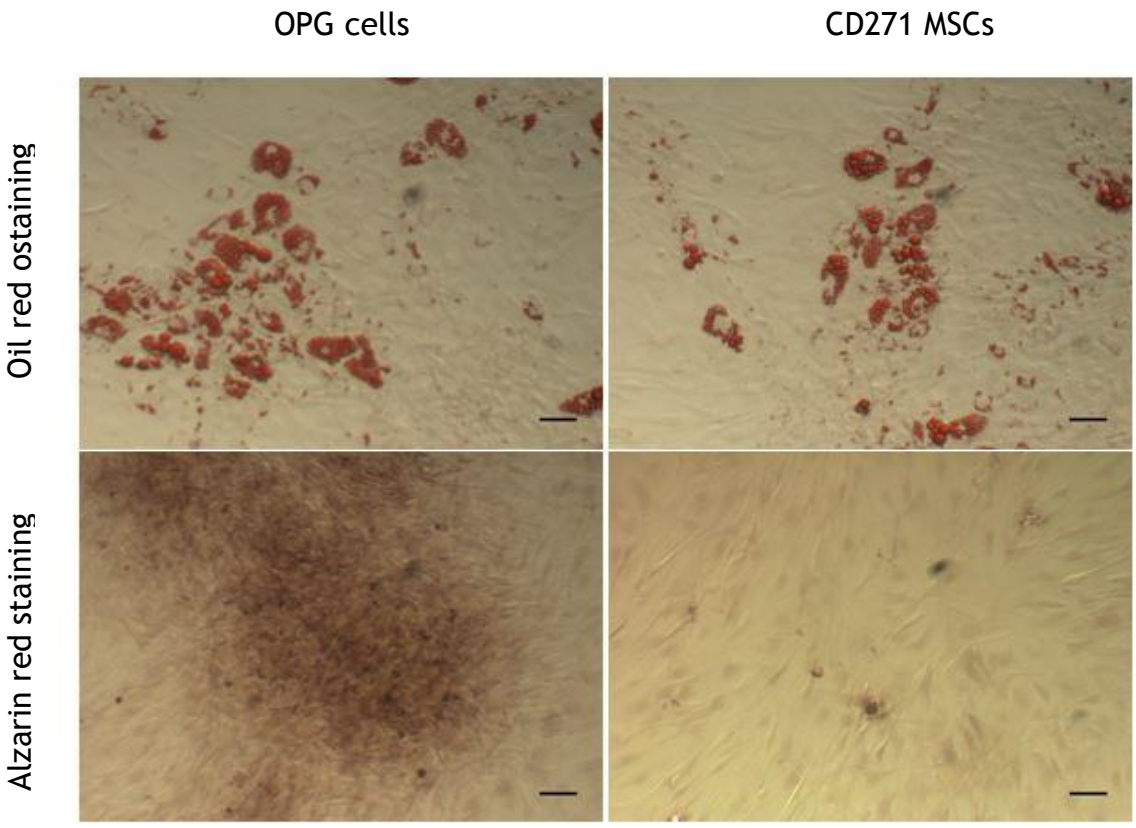

Figure 4.8 OPG and CD271 MSCs stained for oil red o and alizarin red
Cells were cultured for 28 days and then stained with oil red o stain to detect fat globules as a result of adipogenic differentiation, and alizarin red stain to detect the presence of calcium deposition due to osteogenic differentiation. Scale bar denotes 50 μm

The $CD271^+$ MSC and OPG cell population both differentiated down the adipogenic and osteogenic lineages as shown by the presence of fat globules and calcium deposits due to *in vitro* chemical induction on glass coverslips. Presence

of cells expressing OPN in the OPG cell population as shown in Figure 4.7, do not hinder the ability to differentiate and form fat globules when cultured with adipogenic induction media.

qRT-PCR was further used to detect transcription factors and markers such as Glut4 and OPN associated with adipogenesis and osteogenesis respectively (Figure 4.9) to further confirm that the OPG and $CD271^+$ MSC cell populations had committed and differentiated towards the adipopgenic and osteogenic cell lineages.

qRT-PCR analysis also illustrated expression of transcripts Glut4 and OPN, associated with adipogenic and osteogenic lineages upon induction. This confirms that the $CD271^+$ MSCs and the OPG cell population can undergo differentiation. Detection of Glut 4 by qRT-PCR as well as positive oil red o histology of fat globules confirm that adipogensic differentiation has occurred in both cell populations. Also, OPN detection and alizarin red histology present that these cells can also commit to the ostegenic lineage. It is important to use a multipotent population for the study of biomaterials for the purposes of regenerative medicine to determine the effect the properties of the substrate modulus has on adherence. With regards to this thesis, the hydrogel substrate elasticity will play a vital role in manipulation MSC behaviour, so it is vital to start cell culture studies with a multipotent cell population.

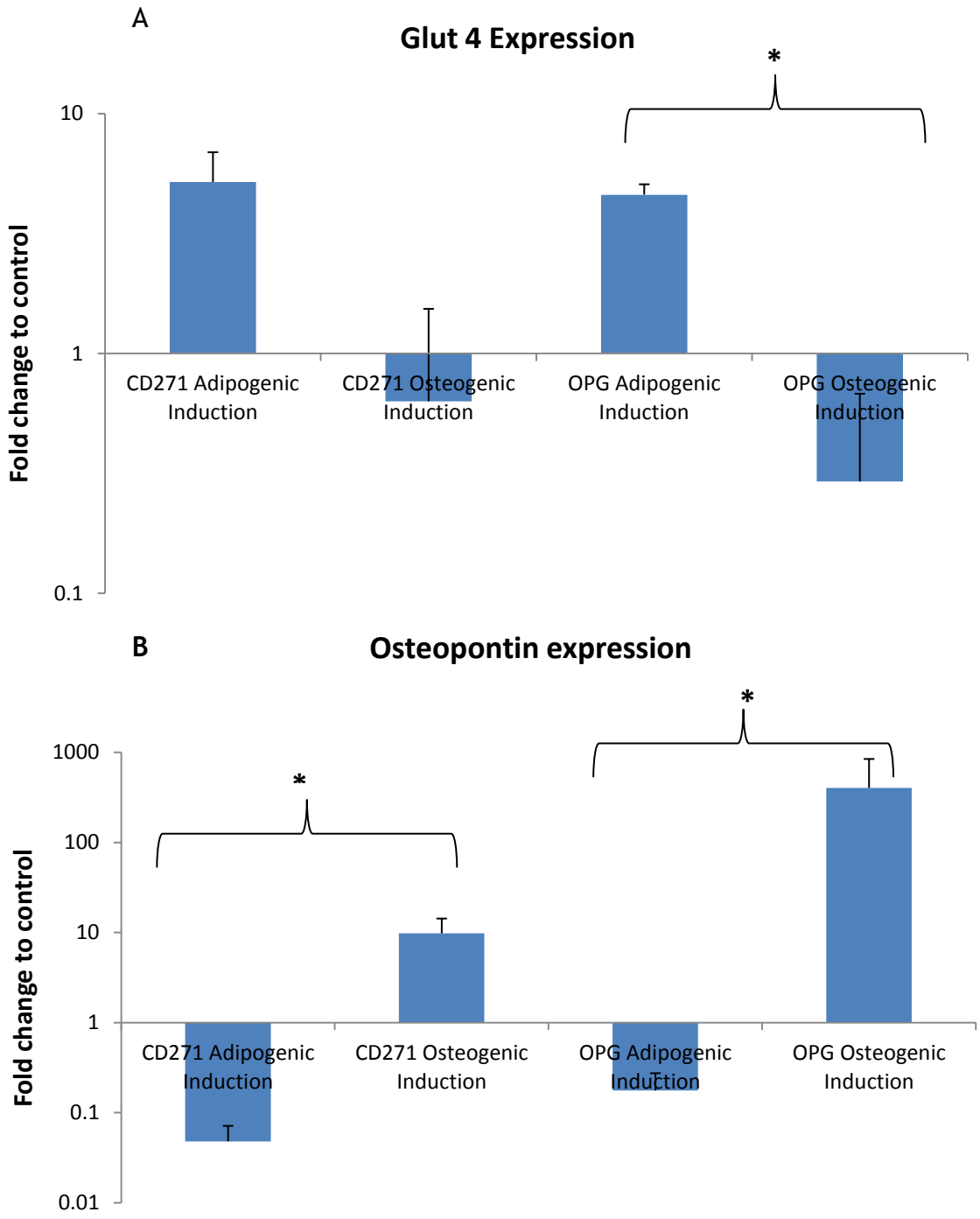

Figure 4.9 Gene expression of MSCs and OPGs with induction media
(A) Illustrates the detection of Glut4 an insulin regulated glucose transporter found in adipose cells. Cells cultured in the presence of adipogenic induction media present up regulation of this protein in comparison to those cells cultured in osteogenic media, demonstrating that adipogenic differentiation is occurring. (B) Illustrates expression of OPN, a sialoprotein which is found in the ECM of bone and teeth. By culturing $CD271^+$ and OPGs with osteogenic induction media, can see up regulation of this protein, however can also see a small degree of expression in those cells cultured in adipogenic media. Gene expression measured as fold change to control which was either $CD271^+$ MSCs or OPGs cultured on glass coverslips in presence of complete cell culture media. Stars indicate significant differences between groups using one-way ANOVA with Dunn's post hoc test, where *P<0.05. Error bars signify standard error of the mean (n=3) for all samples.

4.4.2 $CD271^+$ cell culture with 10 mM hydrogel

Chapter three presented a pool of hydrogel substrates that have been characterised and have the potential to be used as culture substrates for the study of $CD271^+$ MSCs and the OPG cell population. In the present study, $CD271^+$ MSCs were cultured in a 2D study with the 10 mM hydrogel substrate due to its low elasticity of 0.64 kPa to determine if the stiffness will maintain the MSC phenotype, or if the hydrogel promotes modulus driven differentiation.

4.4.2.1 Quantitiative polymerase chain reaction

MSCs positively selected for the CD271 cell surface marker were cultured on the upper surface of the softest hydrogel substrate in a 2D study. RNA was extracted and reverse transcribed prior to qRT-PCR as described in sections 2.3.5 and 2.3.8-2.3.9. In line with the relevant literature, Taqman probes were used to detect gene expression associated with soft tissue type markers (Banerjee *et al.*, 2009) and results were presented as fold change to control (cells on glass substrates). Figure 4.10 presents fold change of gene expression to control, with the table alongside presenting the detection of the markers at each time point.

Gene expression studies indicate potential loss of multipotency as time course progresses due to failure to detect the CD271 marker after three days in culture. Detection of ß3tubulin was apparent throughout the study, with levels increasing over time. The adipogenic marker PPAR-γ was also detected; however fold change was negligible in comparison to control. This study illustrates that the CD271 MSCs are losing their multipotency potential over time when cultured upon this 10 mM substrate and suggests commitment to the neurogenic lineage. One-way ANOVA was performed with Dunn's post host test; however, no statistical significance was observed using this test. Due to large sample variation, students T test was performed with Welch's correction to determine if markers were significantly upregulated in comparison to glass control. It was found that B3 Tubulin was significantly higher at day 7, and that CD271 was statistically significant in comparison to control after 1 day in culture. These results suggest that neurogenesis is occurring on the 10 mM hydrogel due to steady incline of B3 tubulin, however, and that initially the MSC appears to be maintained on the hydrogel substrate due to detection of CD271. However, loss

of the CD271 marker as the time course progresses implies that multipotency is lost on this hydrogel substrate of 0.64 kPa.

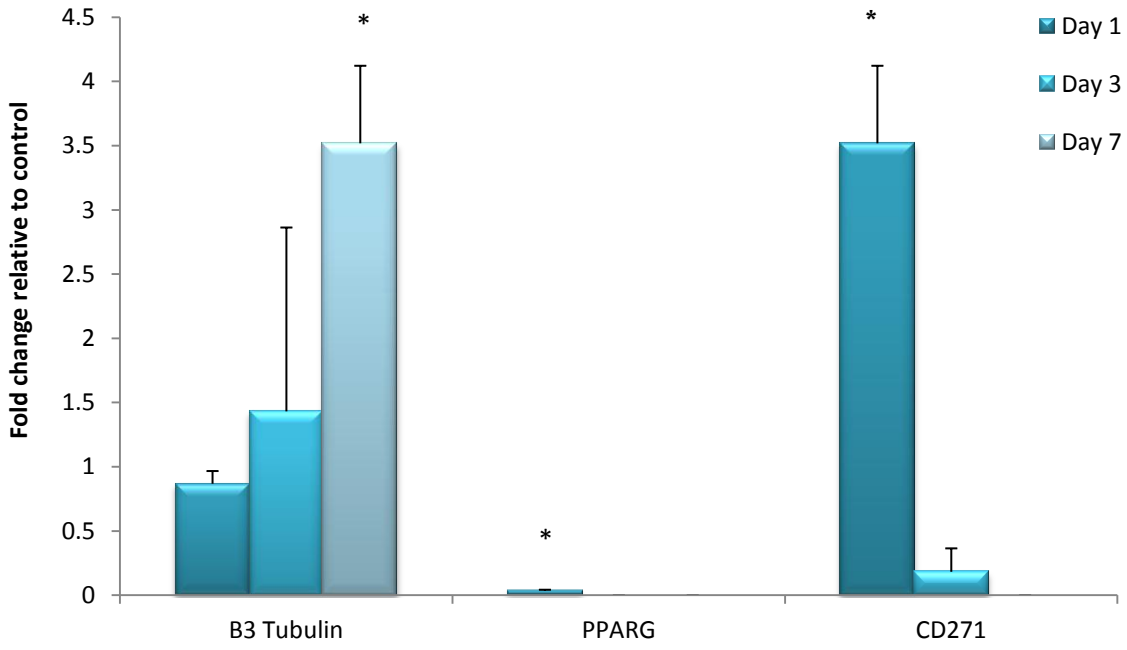

Taqman Probe	Marker for	Day 1	Day 3	Day 7
GapDH	House-keeping gene	+	+	+
CD271	MSC multipotency	+	+	-
PPAR-γ	Adipogenesis	+	-	-
B3 Tubulin	Neurogenesis	+	+	+

Figure 4.10 Gene expression of CD271$^+$ MSCs cultured on 10 mM hydrogel.
CD271 positive MSCs were cultured and RNA was extracted at said time points. Cells were analysed for soft tissue type markers including CD271 for MSC multipotency, PPAR-γ for adipogenesis, and B3-Tubulin for neurogenesis. Gene expression measured as fold change relative to cells cultured on glass surfaces. No significance was determined using one-way ANOVA and Dunn's post hoc test. Statistical significance was calculated using an unpaired TTest paired with Welch's correction in comparison to control and noted as *P<0.05. Error bars represent standard error (n=4 for all substrates).The table which follows presents the markers which were used to detect gene expression in the MSC population.

4.4.2.2 Cell morphology on 10 mM Hydrogel

Cells were seeded on surface of 10 mM hydrogel and glass controls to illustrate the differences in cell morphology. Cell shape has been known to affect gene expression and in turn promote differentiation of such cells due to the transfer of signals from the focal adhesions to the actin cytoskeleton. MSCs morphology was visualised after 1, 3 and 7 days in culture, in line with the qRT-PCR time points as shown in Figure 4.10.

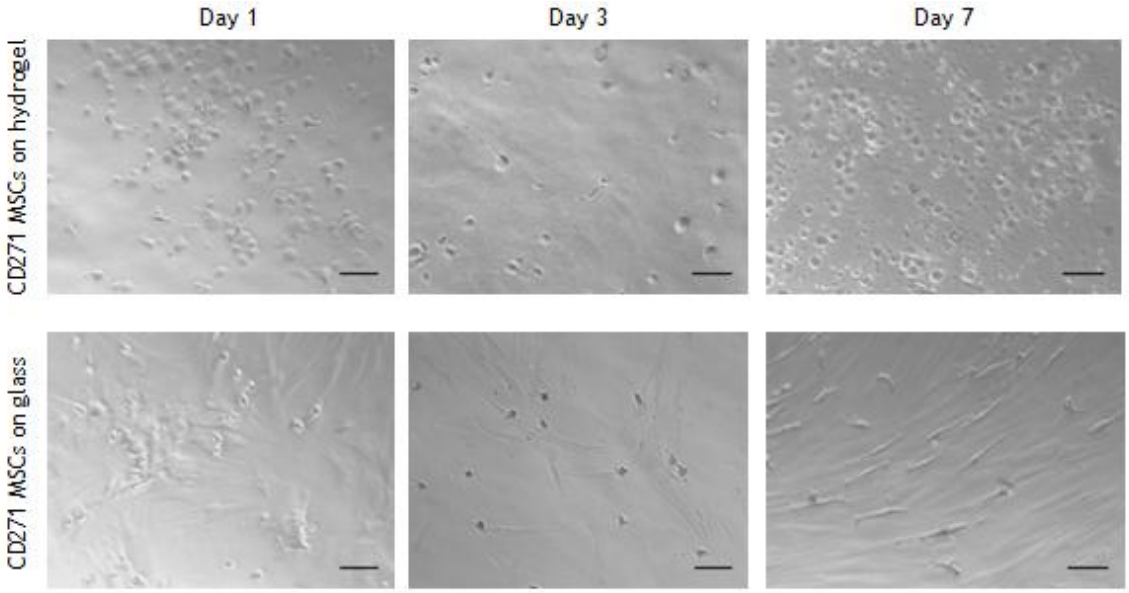

Figure 4.11 Brightfield image of CD271$^+$ MSC morphology.
Cells were cultured on upper surface of 10 mM hydrogel and imaged after 1, 3 and 7 days in culture. Cells present a rounded morphology on this hydrogel substrate due to the low intracellular tension within the cell relating to the modulus of the hydrogel. CD271$^+$ MSCs were also cultured on glass and imaged at these time points to demonstrate the difference between cell morphology on a stiff and soft substrates. Scale bar denotes 50 μm.

MSCs cultured on this 10 mM soft hydrogel of 0.64 kPa in stiffness, maintained a rounded morphology resulting in lower cytoskeletal tension than those cells cultured on glass control. This cytoskeletal tension with the MSC ultimately leads to changes in cell morphology and gene expression in line with differentiation (Lee *et al.*, 2013). The stiffness of this 10 mM hydrogel is similar to that of brain tissue, which ranges from approximately 0.1 to 1 kPa in stiffness (*Flanagan et al.*, 2012), as shown in Figure 4.3. In the literature, MSCs cultured upon a collagen gel of this elasticity, exhibit a branched morphology (Engler *et al.*, 2006) in comparison to the rounded MSCs observed in row one of Figure 4.11. The elasticity properties of the gel may not be the sole contributor to the results shown in Figure 4.10 and 4.11. The adhesion ligands on the collagen gel discussed by Engler may allow cells to spread on the surface more readily and develop a spindle, branched or polygonal morphology, more so than MSCs cultured upon a Fmoc F_2/S hydrogel composed of nanofibres which lack ECM adhesions. This may be the reasoning as to why the elasticity of collagen and the 10 mM Fmoc hydrogel appear to be uniform in elasticity but produce entirely different cell morphologies when MSCs are cultured in a 2D study.

4.4.2.3 Metabolite Profiles of CD271+ MSCs

Metabolites were extracted as described in section 4.3.2.5 and the metabolite profile for each hydrogel time point was measured by averaging the peak intensity of all detected putative metabolites and shown in Figure 4.12. This was presented to highlight the differences in MSC activity in response to the cell culture substrate. Samples were normalised to hydrogels cultured in the absence of MSCs, which due to the components of this substrate material does highlight metabolites due to the Fmoc protected peptides present. The intensity of each metabolite was subtracted from the blank hydrogel substrate and represented as a fold change in comparison to metabolite profile of isolated $CD271^+$ MSCs from the adherent bone marrow population, referred to as the experimental control. Freshly isolated $CD271^+$ MSCs were used as the experimental control as ideally, to maintain the MSC phenotype, the metabolite profile of cells cultured on the 10 mM hydrogel should be uniform to that of this cell population as differentiation has not occurred. The aim of this investigation was to determine how the MSC metabolic profile differs from the control profile due to the elastic properties of the 10 mM hydrogel culture substrate, thus providing insight into the activity level of the MSCs.

It is believed that MSCs which are cultured upon a culture substrate mimicking that of their native niche will remain metabolically quiet, and therefore if this substrate mimics the conditions of the niche, the profiles observed will be similar to the experimental control (CD271 isolated MSCs) at every time point. However, if multipotency is not supported by this 10 mM hydrogel, there will be a hypothesised increase of activity and metabolites will be up-regulated in comparison to the naïve CD271 population. However, as qRT-PCR studies presented loss of the CD271 marker and up-regulation of the neurogenic marker β3 tubulin, theoretically there should be a distinct difference in metabolite profiles between the control cell population and those cells cultured upon the hydrogel substrate as the metabolome is directly related to the proteome, which in turn coupled to the MSC transcriptome which is what qRT-PCR detects (Bustin & Nolan., 2004), as shown in Figure 4.4.

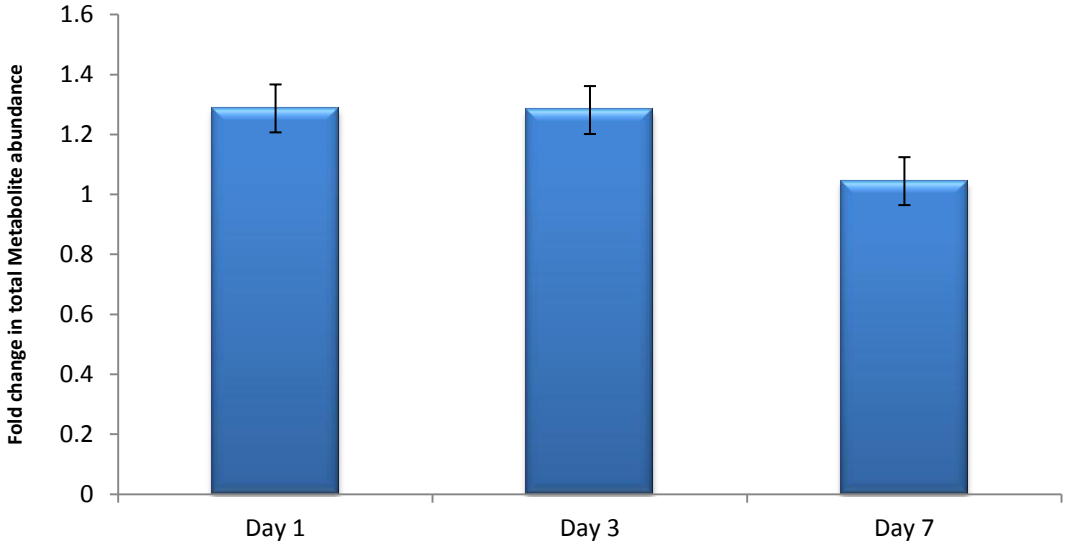

Figure 4.12 Average metabolite abundance.
Figure presents the difference in metabolite abundance between cells cultured on hydrogels at each time point in comparison to the CD271 multipotent population. There appears to be similar levels of metabolites after 1 day in culture in comparison to control, and this level is unchanged after 3 days; however the metabolite abundance decreases slightly after 7 days in culture. Metabolite abundance was calculated from the average peak values of all putatively identified metabolites and presented as fold change to $CD271^+$ population. Error bars illustrate standard error from the mean and n=3 for all samples.

The overall metabolite intensity profiles shown in Figure 4.12 are relatively unchanged at days 1 and 3, and are slightly higher than that of the $CD271^+$ MSC control population; however results were not statistically significant. This suggests that when cultured on this hydrogel substrate, the cells even after 1 day in culture are becoming metabolically active as a result of potential differentiation in response to this culture material. After 7 days in culture, the MSCs are still metabolically active in comparison, but the overall identified metabolite intensity has decreased somewhat, as the initial intracellular changes have occurred and the cells have initiated their lineage commitment to that of the neurogenic lineage suggested by Figure 4.10. This method of measuring the metabolite abundance per time point is simply highlighting the differences in the samples, as it does not present which metabolites are present in one sample in comparison to another.

All identified putative metabolites identified from $CD271^+$ MSC experimental control and 10 mM hydrogels at each time point underwent hierarchical cluster analysis. This measures differences in samples and presents them in colour in

response to up regulation of intensity (red) or down regulation (green). The nature of this analysis allows the observation of contrasting metabolites between each population; however, it does not take into account subtle changes between metabolite abundance. Figure 4.13 Illustrates a heat map distribution of all identified putative metabolites as identified by IDEOM, and compares each population prior to further analysis of specific pathway.

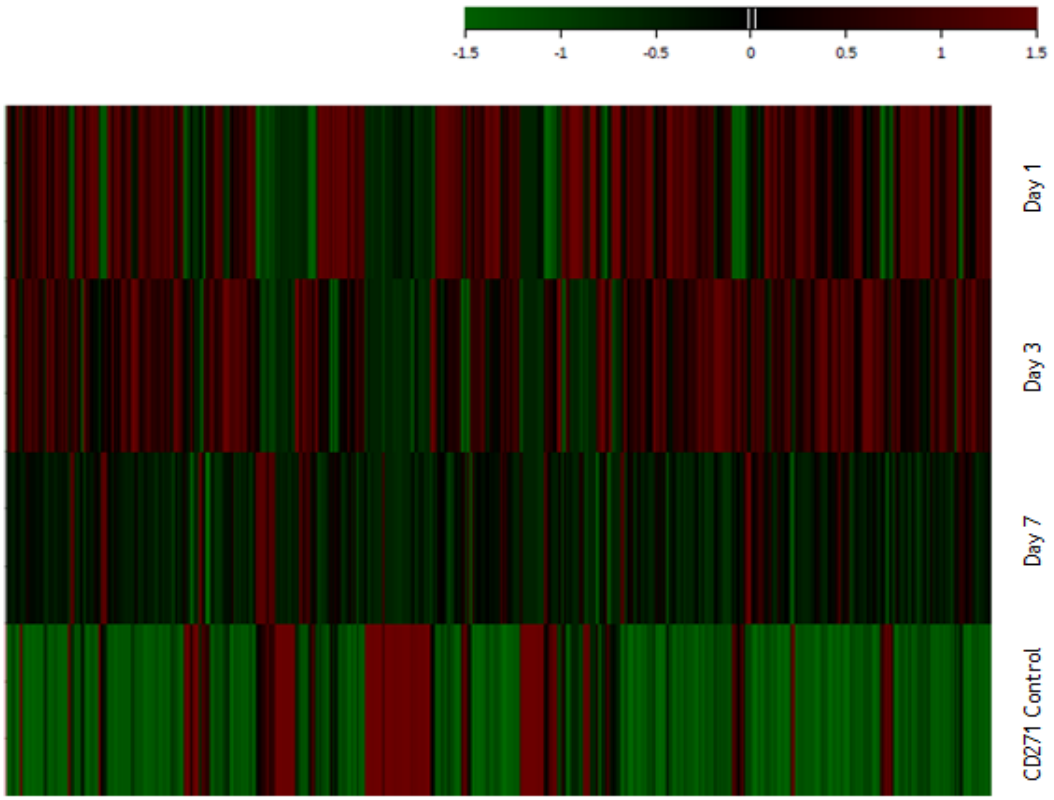

Figure 4.13 Global metabolite profile.
This figure compares CD271 MSCs to cells cultured on hydrogel at days 1,3 and 7. Heatmap analysis presents up and down regulation of metabolites identified by Ideom software. Overall, it appears that the metabolites detected in the CD271 control population have a lower intensity and said to be "down-regulated" in comparison to when MSCs are cultured on the 10 mM hydrogel material. Therefore, the control MSCs are less metabolically active in comparison to those cells subjected to the 10 mM hydrogel substrate. The highest intensity of metabolites is illustrated at days 1 and 3, with this heat map suggesting MSCs undergoing a change of activity at these time points. Key presents upregulation of metabolites and is shown in red, whereas down regulation is presented in green.

The heatmap presented in Figure 4.13 illustrates the differences between the cells at each time point in comparison to the CD271 control population. In comparison to cells cultured upon a 10 mM hydrogel, the CD271 control population is relatively metabolically quiet with lower identified intensities of the majority of metabolites. This representation does not signify that the cells

are not metabolically active however, as metabolites were detected in this control, but it does present that the overall intensity of these metabolites were lower than those detected on the hydrogels. This suggests that the CD271 control population were not extensively partaking in metabolic pathways which are involved in driving the energy requirements of the proliferating cell (Mason & Rathmell., 2011 and Heiden *et al.*, 2009). MSCs in the native niche are said to be metabolically quiet, and qRT-PCR analysis revealed (Figure 4.10) that after 24 hours in culture with the 10 mM hydrogel, the expression of the CD271 marker was still present. Detection of this marker at day 1, lower expression at day 3 and failure to detect after 7 days in culture would suggest that the metabolite profile of day 1 MSCs would be the similar to the control population, however the metabolite profile is highly diverse and open to drastic changes and modifications. When comparing the profiles obtained from cells on the control and at day 1 (Figure 4.13) we can see that there is a significant difference in metabolites and that even though qRT-PCR suggests similarities by detection of the MSC cell surface marker, metabolite changes will be detected before changes are detected at the transcriptome level.

4.4.4.3.1 Nucleotide Metabolism

The global metabolite profile is illustrating the degree of variation between the time points and the control freshly isolated CD271 population which are described as being metabolically quiet, and this can be explained by the down regulation of metabolites as shown by the heat map representation in Figure 4.13. The masses of the putative metabolites as described previously were analysed using Pathos which is a web based facility which allows the detected masses to be mapped to the metabolic pathway they belong to using the Kyoto Encyclopedia for Genes and Genomes (KEGG), (Leader *et al.*, 2011). It must be noted however; a single metabolite within a pathway cannot be attributed to a particular function, and by looking at the global metabolites and what pathways they are associated with, can only provide insight alongside correlating gene expression analysis with metabolic pathways which may be associated with differentiation and multipotency. However, as this technique is still considered to be in its infancy, the identified metabolite list generated is limited, and there

will be a great number of metabolites not identified in the hydrogel and control populations due to database identification and available information.

Nucleotide metabolism is an umbrella term which takes purine and pyrimidine metabolism into account, both of which are DNA constituents. DNA synthesis is required for cell division and an increase in cell number and therefore up-regulation of metabolites associated with this pathway would suggest cell differentiation and division as the cells are actively partaking in symmetric commitment. A hydrogel promoting multipotency would have a general uniform heat map between time points as the process of DNA synthesis would be arrested due to a lower requirement of cellular division due to MSCs being in a quiescent state. Metabolites extracted from MSCs on the 10 mM hydrogel at each time point are compared to the $CD271^+$ experimental control population. Figure 4.14 illustrates that after 24 hours in culture, a number of nucleotide metabolites are up regulated, and as the time course continues these are down regulated and metabolite intensities are far lower than previously observed.

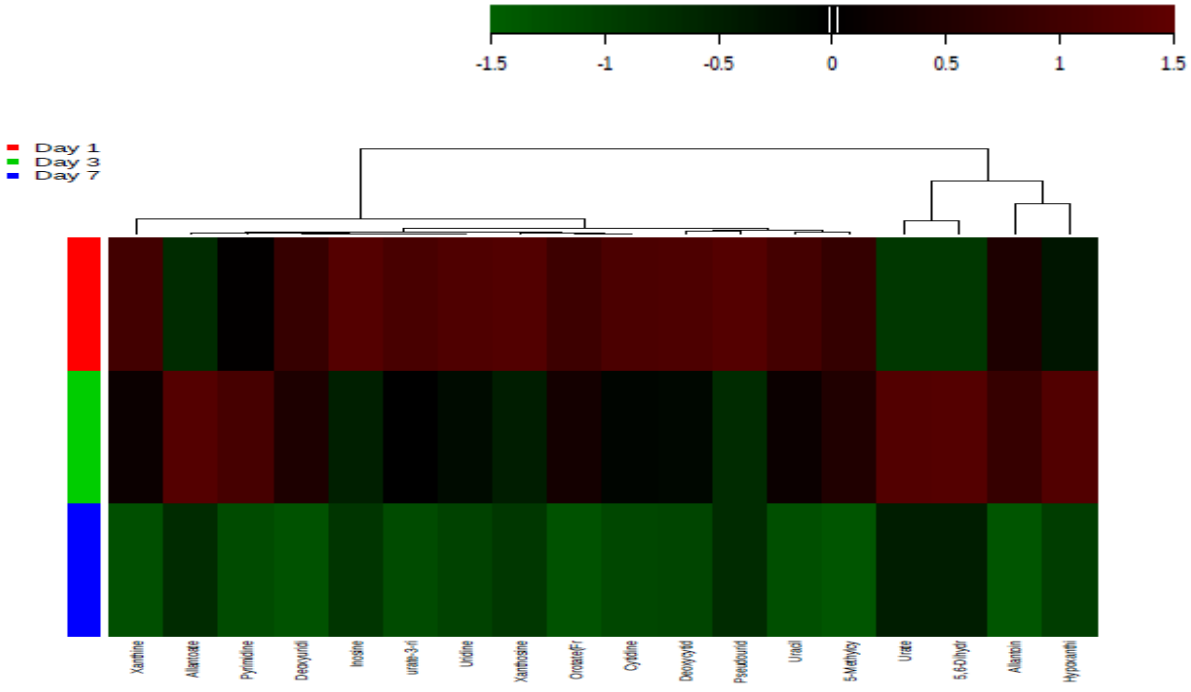

Figure 4.14 Nucleotide metabolism heat map analysis.
Data sets were obtained from putative metabolites that were present at each time point as shown by key. The image shows the heat maps generated from average of the samples (n=3) cultured at each time point. Blank hydrogel metabolite values were subtracted from the results to obtain the true cell profile as a result of culturing upon a hydrogel of 0.64 kPa in elasticity. The most contrasting change where metabolites were most up regulated on hydrogels in comparison to controls was at day 1, where a change of activity is shown by up-regulation of metabolites associated with nucleotide metabolism.

In summary, the metabolic results show a preliminary study where MSCs were cultured upon a soft hydrogel substrate for 7 days. Metabolic analysis can provide important data to define key molecules that may be involved in MSC differentiation and maintenance of the multipotent state or to illustrate differentiation. These findings present that MSCs were metabolically active at day 1 in culture, in comparison to freshly isolated $CD271^+$ MSCs. By day 7 however, the metabolites identified were exceedingly low in comparison, and in some cases metabolites failed to be detected. The durability of the soft hydrogel substrate may have affected this study somewhat, as the gel was observed to partially dissolve in the cell culture media as the study progressed, providing a potentially inaccurate portrayal. However, protein concentration was used to normalise results also to take into account this variation.

With reference to figures 4.13 and 4.14, it would appear that at days 1 and 3 there is a change of great deal of metabolic activity and now at day 7 the MSCs are observing a quieter metabolic response in comparison. This data as well as gene expression in Figure 4.10, demonstrate that MSC multipotency is lost, and that the metabolome highlights intracellular changes in response to the substrate faster than gene expression by qRT-PCR detection. This is true as by day 1, we can observe changes in the metabolome in comparison to the experimental control, whereas with qRT-PCR, the results are still demonstrating multipotency due to detection of the CD271 MSC cell surface marker.

As the results take into account normalisation to a hydrogel without MSCs and are used to compare the differences in metabolites from the CD271 control cell population, this alongside Figure 4.10 demonstrates loss of $CD271^+$ and increase of ß3tubulin, therefore a loss of the multipotent state. However, early neurogenic differentiation may be complex as there was no distinct pathways up regulated which can be used for further study of this lineage commitment. Further in depth analysis is required if metabolites involved in neurogeneic differentiation commitment are to be classified, and overall this study with the 10 mM hydrogel presents loss of the MSC multipotent state and differentiation towards the neurogenic lineage.

4.4.3 Further development with 20 mM hydrogel

As the 10 mM hydrogel failed to maintain itself as an elastic substrate after 7 days in culture, a different Fmoc F_2/S hydrogel substrate was taken forward for further study from the pool created in chapter 3. A 20 mM hydrogel was chosen to study MSC behaviour in 2D and 3D studies, as it was the next softest hydrogel substrate, and to illustrate the differentiation potential in response to the substrate elasticity, which may be useful for further studies in the field of regenerative medicine. The MSCs and OPGs were cultured in 2D (where cells are cultured upon the upper surface after hydrogel has formed) and 3D (where cells are incorporated with the peptide solution and a hydrogel was formed with the cells present throughout the hydrogel).The effects of this will be discussed.

4.4.3.1 DNA and Protein Expression Assays for cell viability

The phenol phase from samples that underwent TRIzol extraction to obtain RNA as described in section 2.3.5 was used to determine the total amount of protein and DNA present within each culture condition. The increase in DNA and protein was monitored over time as a means to initially illustrate cell survival and cell growth in the 2D and 3D hydrogel studies as shown by Figures 4.15 and 4.16. The final protein and DNA concentration was compared to those cells cultured on glass substrate and expressed as fold change. Protein expression was measured as a means to detect activity within the cell, in response to culture upon the hydrogel substrate, as the process of RNA translation into proteins signifies the viability of cells when cultured with this hydrogel substrate.

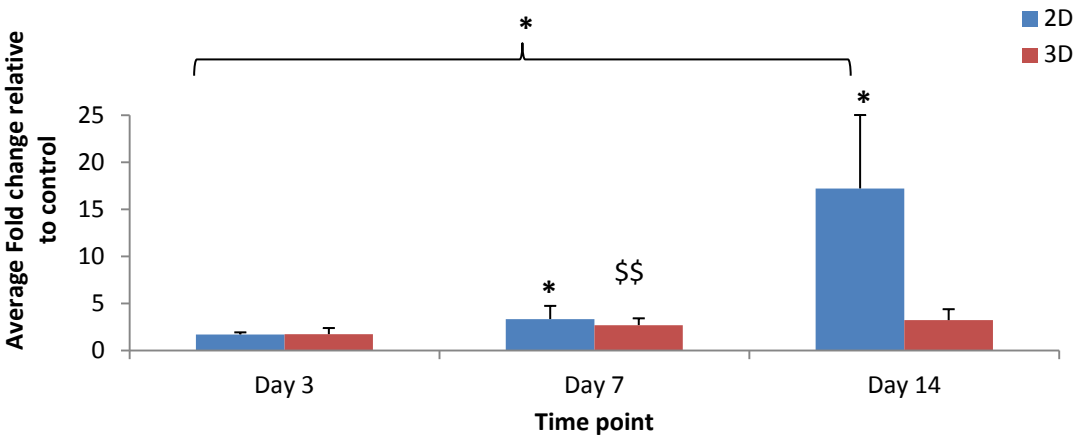

Figure 4.15 DNA content of OPGs cultured with 20 mM hydrogel.
Fold change was normalised to cells on glass control at designated time point. Stars indicate significant differences between groups as described by one-way ANOVA and Dunn's post hoc test, where *P<0.05. Students TTest paired with Welch's correction was performed to compare samples to controls and noted as $$ for P<0.01. Error bars represent standard error (n=4 for all substrates). At each timepoint, DNA content underwent statistical testing using one-way ANOVA and with *P<0.05. DNA content was generally higher on the 2D hydrogel substrate with a steady increase between each time point.

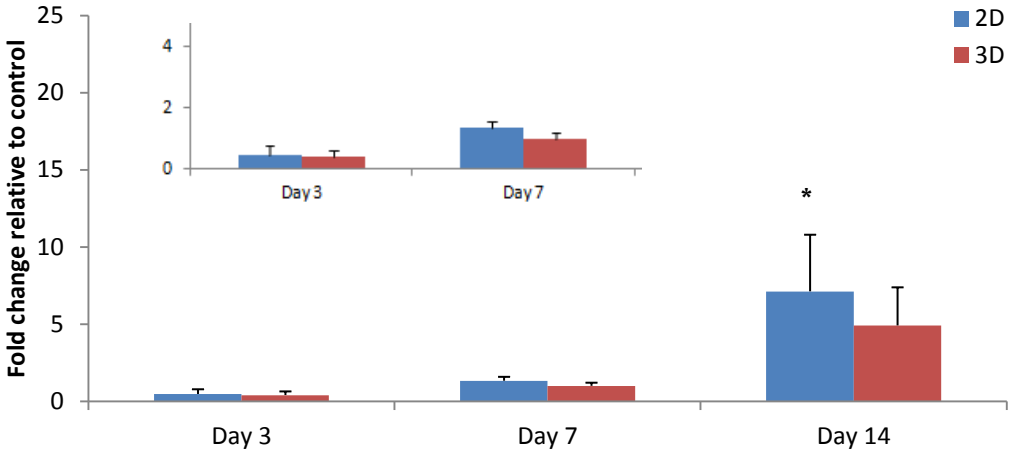

Figure 4.16 Protein concentration of OPGs cultured with 20 mM hydrogel.
Fold change was normalised to cells on glass control at designated time point. Protein levels were generally higher in the 2D substrate than the 3D, but both illustrating increased protein levels than glass control at each time point. Stars indicate significance differences between groups as described by one-way ANOVA and Dunn's post hoc test, where *P<0.05. Error bars signify standard deviation and n= minimum of 3

DNA fold change was higher with those cells cultured in the 2D conformation when compared to cells cultured on glass at the same time point. When cultured in 3D, the cells also illustrated a steady increase in their concentration of DNA. This increase in DNA fold change over the course of 14 days, suggests that in comparison to control, cells were viable and were able to undergo cell division

on and within this 20 mM hydrogel. Using one-way ANOVA, the DNA content of cells cultured in 2D were significantly higher than on glass and in 3D at days 7 and 14 indicating that cell proliferation is supported on this 2D substrate.

The same pattern emerged with protein fold change as shown by Figure 4.16. The 2D hydrogel gave greater protein levels than the glass control, with the 3D substrate still presenting increased levels, but not as high as the 2D substrate. By 14 days in culture, the protein concentration had increased again, with the 2D substrate presenting significantly higher levels of protein in comparison to 3D and glass culture of OPG MSCs.

Measuring cell viability and protein concentration was a means to present that cells are steadily increasing in DNA and protein content over the period of the time course experiments in comparison to cells cultured on a glass substrate. This signifies cell viability on and within (2D and 3D) the 20 mM hydrogel and further gene expression studies can commence with this material. There are other methods of confirming cell viability such as use of the classical MTT assay, and these were trialled. However due to the nature of the peptide substrate, it was not possible to use these and reasons will be discussed in experimental limitations discussed in section 4.5 of this chapter. Overall, it appears that the 2D culture of OPGs supports greater cell proliferation and viability in comparison to 3D culture. However, both culture conditions present higher levels of DNA and protein than culture upon glass. Now viability has been established, qRT-PCR studies will provide insight with regards to the substrate maintaining the MSC phenotype or promoting cell differentiation in response to the stiffness of the gel.

4.4.4 2D cell culture studies with 20 mM hydrogel

4.4.4.1 Gene expression profiles with CD271+ MSCs and OPGs

Cell viability with the 20 mM hydrogel was confirmed and the cells cultured in 2D to determine if the substrate represented a niche-like environment, or promoted the process of modulus driven differentiation. The presence of a number of biomarkers associated with differentiation and multipotency were quantified by

means of qRT-PCR. Expressions of markers are shown as fold change in relation to cells cultured on glass controls with CD271 MSCs (Figure 4.17) and OPGs (Figure 4.18). Cells were cultured for a total of 14 days to provide an initial study in the investigation of MSC behaviour in response to this hydrogel substrate.

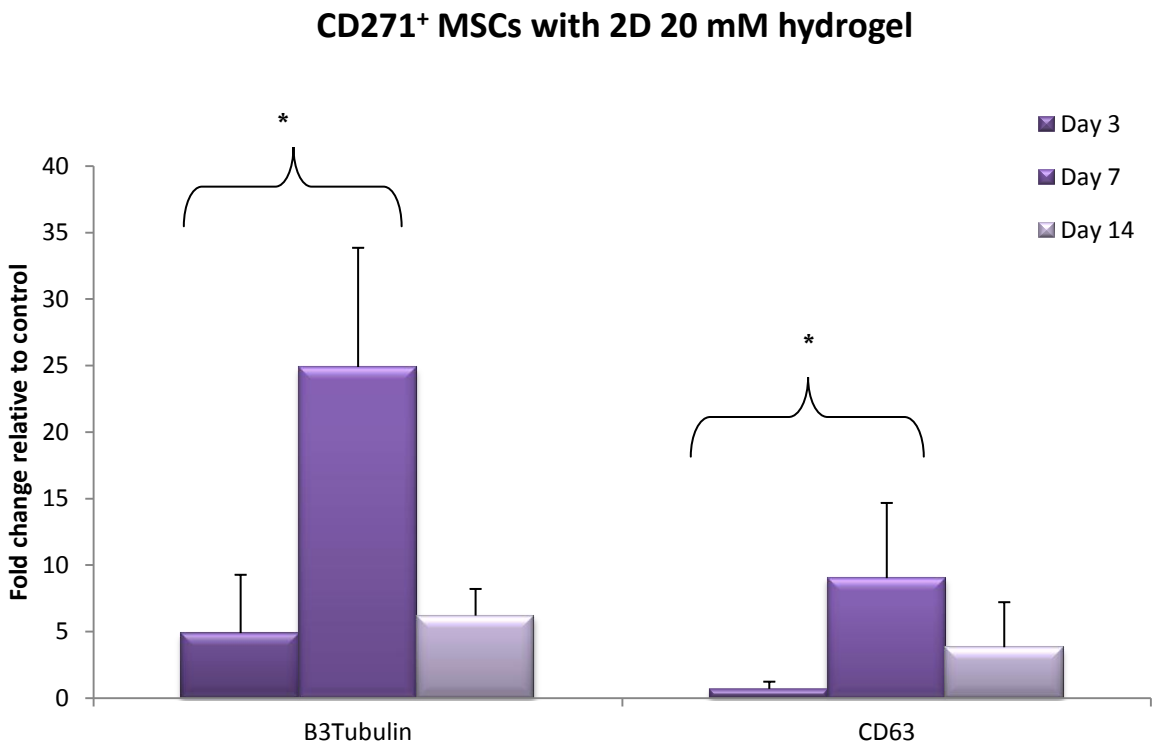

	Primers used									
	GapDH	CD271	ALCAM	CD63	Glut4	PPAR-γ	B3Tub	Nestin	SOX9	OCN
Day 3	+	-	-	+	-	-	+	-	-	-
Day 7	+	-	-	+	-	-	+	-	-	-
Day 14	+	-	-	+	-	-	+	-	-	-

Figure 4.17 CD271+ MSC profile with 2D 20 mM hydrogel
MSCs were cultured, and RNA extracted at said time points, from which gene expression was analysed. Cells were analysed for CD271, ALCAM and CD63 for MSC multipotency, Glut-4 & PPAR-γ for adipogenesis, ß3-Tubulin and Nestin for neurogenesis, SOX-9 for chondrogenesis and OCN for osteogenesis. Gene expression measured as fold change relative to cells cultured on glass surfaces. Stars indicate significance differences between groups as described by one-way ANOVA and Dunn's post hoc test, where *P<0.05. Error bars signify standard error from the mean; (n=4).

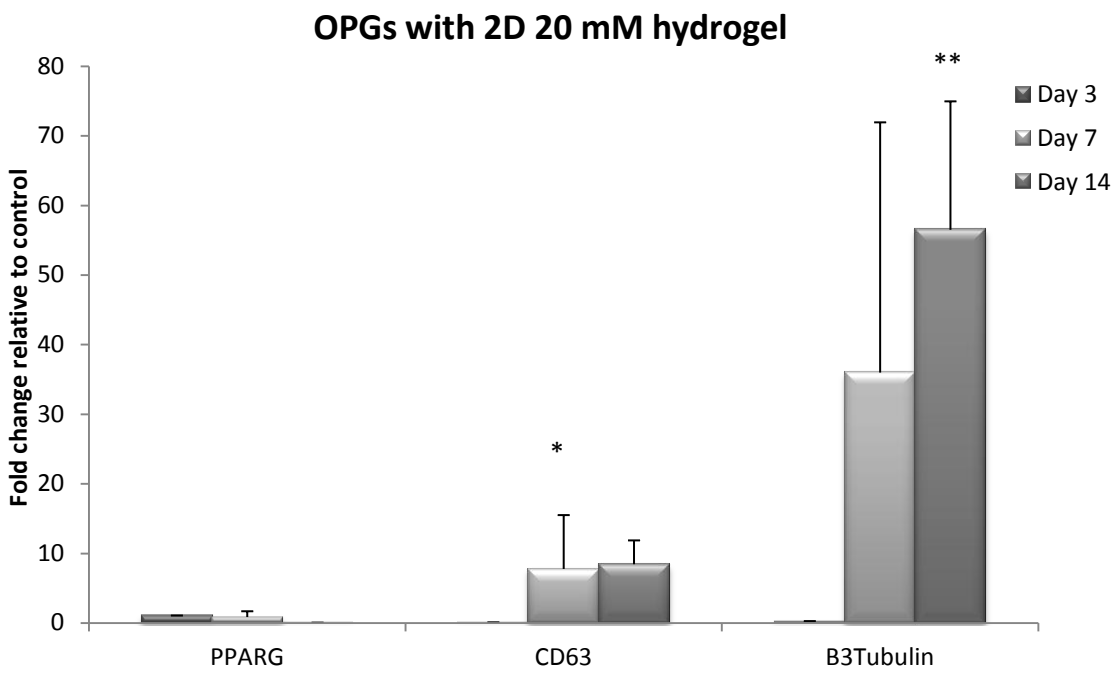

	Primers used								
	CD271	ALCAM	CD63	Glut4	PPAR-γ	B3Tub	Nestin	SOX9	OCN
Day 3	-	-	+	-	+	+	-	-	-
Day 7	-	-	+	-	+	+	-	-	-
Day 14	-	-	+	-	+	+	-	-	-

Figure 4.18 OPG profile with 2D 20 mM hydrogel.
MSCs were cultured, and RNA extracted at said time points, from which gene expression was analysed. Cells were analysed for CD271, ALCAM and CD63 for MSC multipotency, Glut-4 & PPAR-γ for adipogenesis, ß3-Tubulin and Nestin for neurogenesis, SOX-9 for chondrogenesis and OCN for osteogenesis. Gene expression measured as fold change relative to cells cultured on glass surfaces. Stars indicate significance differences between groups as described by one-way ANOVA and Dunn's post hoc test, where *P<0.05 and **P<0.01. Error bars signify standard error from the mean; (n=4) for hydrogel samples.

$CD271^+$ MSCs cultured on a 2D hydrogel substrate shown in Figure 4.17 presented expression of ß3-Tubulin and CD63 markers which are associated with neurogenesis and multipotency respectively. A significant increase in transcripts was observed between days 3 and 7 with both of these markers. Although these transcripts were detected, a number of other transcripts associated with differentiation were not identified such as SOX9 and OCN associated commonly with chondrogenic and osteogenic differentiation. 2D culture with OPGs (Figure 4.18) presents similar differentiation markers to that of the $CD271^+$ cell population. Presence of CD63 is indicative of MSC multipotency, and there is a significant increase of this marker at day 7 as detected by one-way ANOVA with Dunn's post hoc test. The adipogenic marker PPAR-γ is also detected in the OPG

cell population, however, levels are extremely low and not significant in comparison to controls. Again, ß3tubulin is detected suggesting neurogenic differentiation, however there was large variations within samples and hence why there was no significance with this marker. Instead, it presents a general trend that this 2D hydrogel promotes increasing levels of this neurogenic marker.

This 2D culture initially suggests that there is a heterogeneous cell population arising in response to this culture substrate due to detection of stem cell markers and the neurogenic marker B3tubulin. This may be due to the morphology the cells take on the substrate and the elasticity properties of the hydrogel, both of which will be investigated. With $CD271^+$ MSCs, the levels of CD63 and ß3tubulin increase up to day 7 then transcript levels fall by day 14. This may be due to cells detaching from the hydrogel surface when media is replaced every 2-3 days due to poor attachment to surface of this soft hydrogel. Levels of transcripts with the OPG cell population are steadily increasing as time study progresses, which is what is to be expected as differentiation progresses. . Independent of cell type, the markers observed are typically associated with soft tissue types such as fat and neural tissue.

4.4.4.2 Cell Morphology on 2D Hydrogel substrate

$CD271^+$ MSCs and OPGs were cultured on the 20 mM hydrogel and cell morphology imaged at time points corresponding to gene expression studies. Glass cover slips were used as control to observe the variation in morphology, and as bright field microscopy was used, protein assemblies such as focal adhesions could not be observed. However, cell morphology can provide information on the intracellular tension of the cell cytoskeleton, as low tension results in rounded cells, and stiff substrates produce the typical polygonal stretched phenotype. Figures 4.19 and 4.20 illustrate the cell profiles on this 2D hydrogel in comparison to glass control.

Cell morphology between cells cultured upon 2D hydrogel and glass were distinctly different from the initial time point after 3 days in culture. Those cells cultured upon the hydrogel remained rounded in morphology. The tension within the cells is changed as less force is required to deform their substrate matrix, resulting in altered MSC morphology which potentially effects gene expression in

line with differentiation (Lee *et al.*, 2013). Low intracellular tension within the cells is typically observed in adipocytes and cells associated with soft tissue types. MSCs in their native niche are hypothesised to be rounded in morphology due to the low elasticity of the tissue and also because they have not undergone differentiation commitment, therefore the shape the cells are presenting in Figures 4.19 and 4.20 is sensible considering the gene expressions observed in Figures 4.17 and 4.18 as soft tissue markers are detected. Therefore, the 20 mM hydrogel can be implied to illicit low levels of intracellular tension due to their rounded morphology of MSCs and OPGs when cultured in 2D prientation

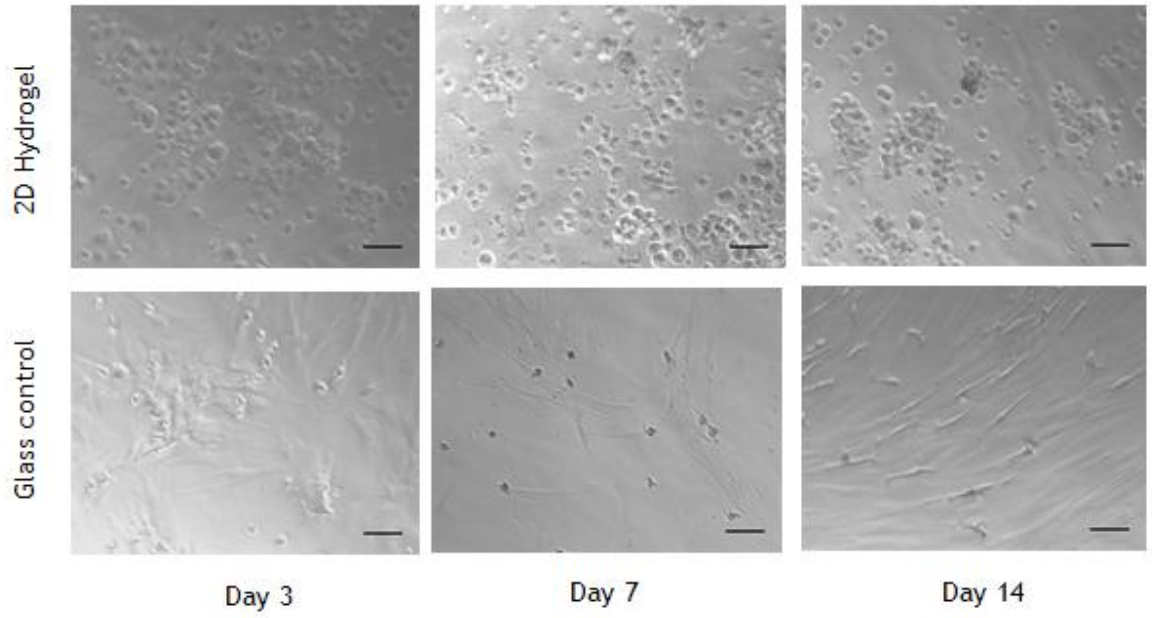

Figure 4.19 CD271 MSC cell morphology with 2D culture.
MSCs were seeded on 20 mM hydrogel 2D substrate and images were taken at days 3, 7 and 14 correlating to gene expression time line. Cell morphology is drastically altered upon the hydrogel, as cells appear rounded rather than spread and polygonal as observed with MSCs cultured upon glass cover slips. Scale bar denotes 100 μm.

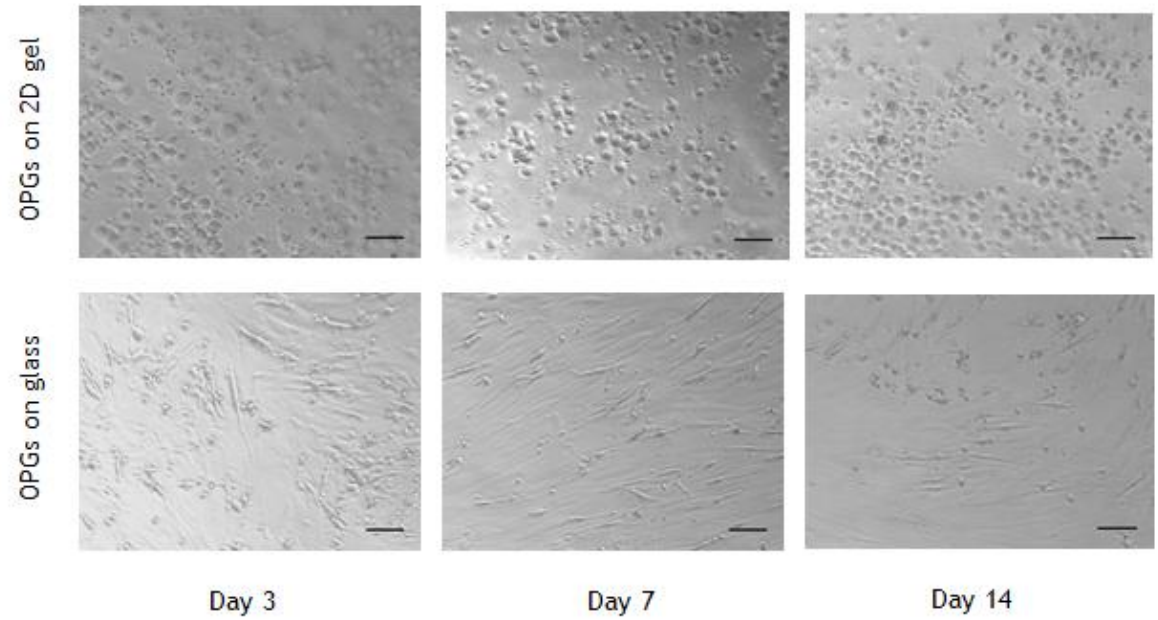

Figure 4.20 OPG cell morphology with 2D culture.
OPGs were seeded on 20 mM hydrogel 2D substrate and images were taken at days 3, 7 and 14 correlating to gene expression time line. Cell morphology is drastically altered upon the hydrogel, as cells appear rounded rather than spread and polygonal as observed with OPGs cultured upon glass cover slips. Scale bar denotes 100 μm.

4.4.4.3 Hydrogel stiffness in response to 2D culture

When cultured in 2D, MSCs and OPGs present similar transcription profiles to one another as illustrated by presence of CD63 and B3 Tubulin. A rheological study was conducted, as shown by Figure 4.21 in the presence of these two cell populations to determine if cell activity affects stiffness properties of the hydrogel over time. It was hypothesised that elasticity of the culture substrates should be similar in the presence of these two cell types over the course of the experiment due to comparable gene expression profiles and cell morphologies as discussed previously.

Rheological studies in the presence of these two cell populations illustrates that stiffness is not uniform over the course of 14 days in culture. Particularly with the CD271 MSC population after 3 days in culture, there is a large degree of variation within each sample group as demonstrated by standard deviation values presented in table below figure 4.21. There are however no significant differences in hydrogel stiffness values over time. Taking into account the deviations, the general trend is that the stiffness values increase over time and

then decrease in response to MSC culture, demonstrating that cells may be altering their substrate environment and differentiating in accordance to the stiffness of the hydrogel material. Large variations in elasticity between samples, particularly at day 3 can be due to the cells initially remodelling their environment. However, both gels are still mimicking that of soft tissue types hence why observations of neurogenic and multipotent markers are presented by qRT-PCR. Although there is a large variation at day 3, it is not believed to be a real change in hydrogel stiffness, and would need to be repeated to give confidence in these rheological results, as an outlier is causing the extreme error bar results. If this was still the outcome after repetition of experiment, then SEM imaging could be used to detect any ECM deposits produced by the cells in response to the hydrogel culture substrate.

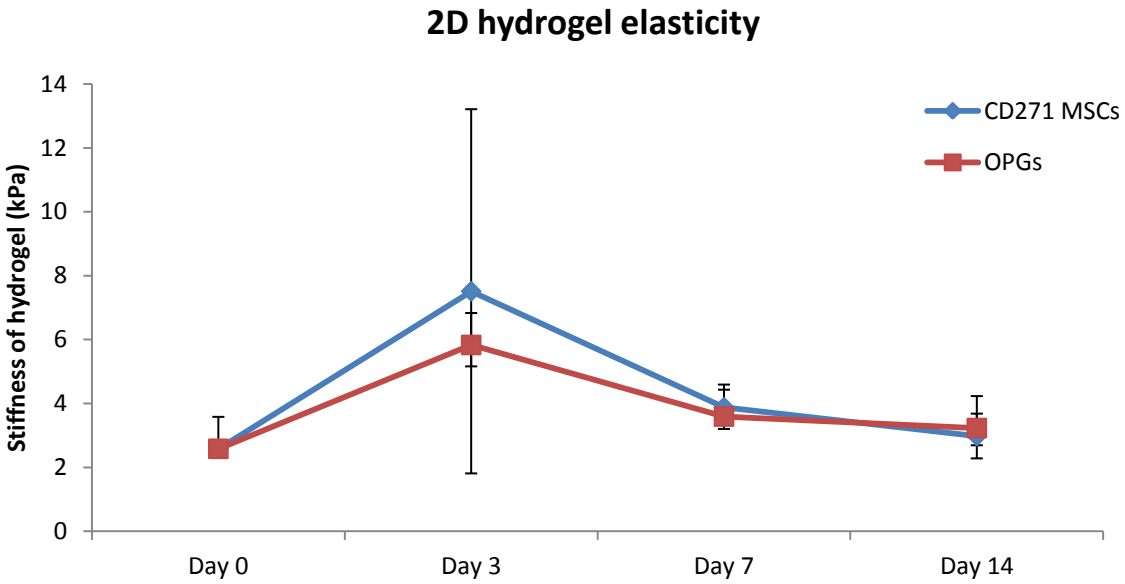

Cell type	Day 0	Day 3	Day 7	Day 14
CD271	2.58 ± 0.1	7.51 ± 5.7	3.88 ± 0.55	2.98 ± 0.7
OPG	2.58 ±0.1	5.83 ± 0.67	3.59 ± 0.39	3.23 ± 0.54

Figure 4.21 Elasticity of 2D hydrogel due to cell culture.
Cells were cultured upon or within the 20 mM hydrogel and stiffness measured at days 3, 7 and 14. Day 0 measurement portrays the stiffness of the blank hydrogel in the absence of MSCs to illustrate how culturing with cells can affect the elastic properties of the gel over time. Table below illustrates the actual stiffness values alongside standard deviation. N=4 for all hydrogel samples, and ANOVA statistical tests were performed to determine if hydrogel stiffness was significantly changed over time. Changes in the hydrogel elasticity are not statistically significant.

4.4.5 3D cell culture studies with 20 mM hydrogel substrate

4.4.5.1 Gene Expression studies with CD271$^+$ MSCs and OPGs

Culture in a 3D environment enables the cells to be surrounded by their substrate which may provide a more niche like environment than the previous 2D culture method. CD271$^+$ MSCs and OPGs were cultured within the hydrogel and qRT-PCR performed as a means to detect cell differentiation or maintenance of the MSC phenotype.

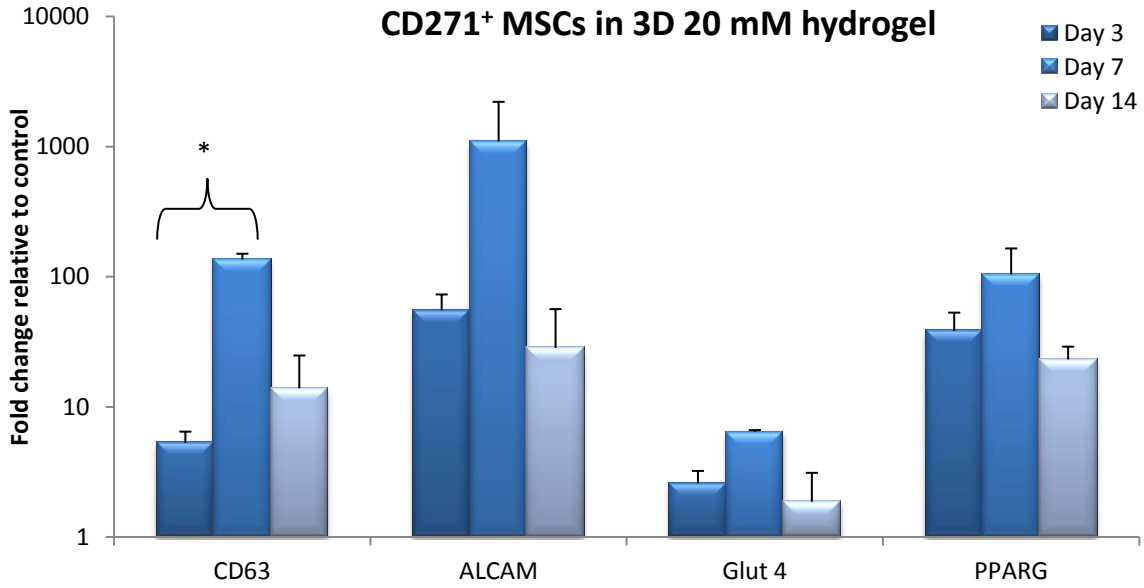

	Primers used									
	GapDH	CD271	ALCAM	CD63	Glut4	PPAR-γ	B3Tub	Nestin	SOX9	OCN
Day 3	+	-	+	+	+	+	-	-	-	-
Day 7	+	-	+	+	+	+	-	-	-	-
Day 14	+	-	+	+	+	+	-	-	-	-

Figure 4.22 CD271$^+$ MSC profile with 3D 20 mM hydrogel.
MSCs were cultured, and RNA extracted at said time points, from which gene expression was analysed. Cells were analysed for CD271, ALCAM and CD63 for MSC multipotency, Glut-4 & PPAR-γ for adipogenesis, β3-Tubulin and Nestin for neurogenesis, SOX-9 for chondrogenesis and OCN for osteogenesis. Gene expression measured as fold change relative to cells cultured on glass surfaces. Stars indicate significance differences between groups as described by one-way ANOVA and Dunn's post hoc test, where *P<0.05. Error bars signify standard error from the mean; (n=4).

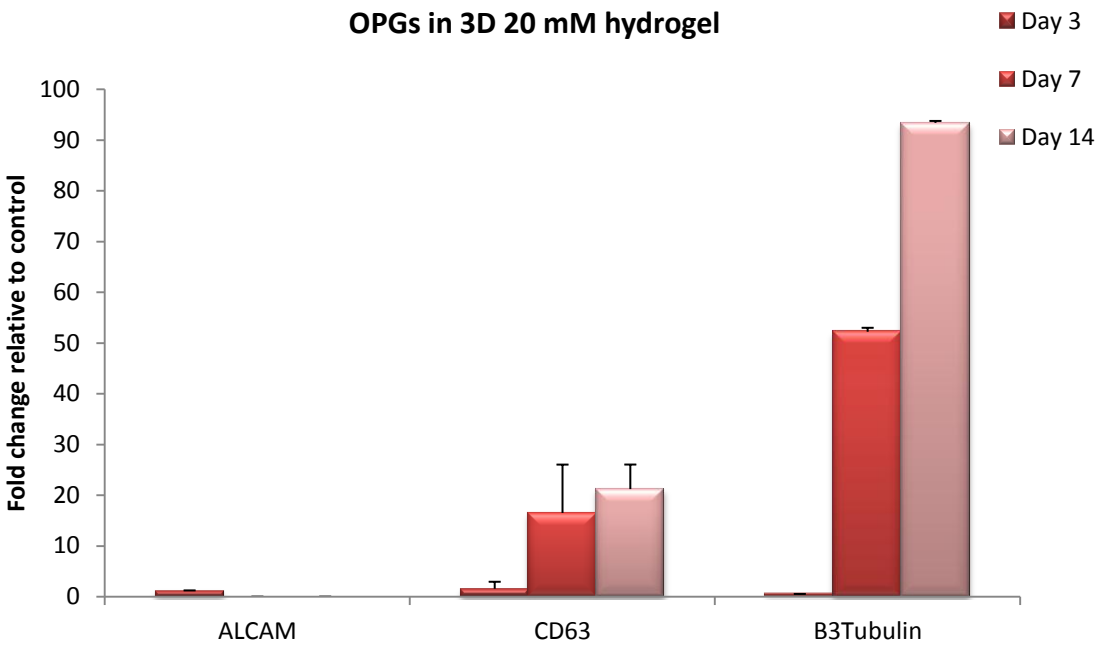

	Primers used									
	GapDH	CD271	ALCAM	CD63	Glut4	PPAR-γ	B3Tub	Nestin	SOX9	OCN
Day 3	+	-	+	+	-	-	-	-	+	-
Day 7	+	-	+	+	-	-	-	-	+	-
Day 14	+	-	+	+	-	-	-	-	+	-

Figure 4.23 OPG profile with 3D 20 mM hydrogel.
MSCs were cultured, and RNA extracted at said time points, from which gene expression was analysed. Cells were analysed for CD271, ALCAM and CD63 for MSC multipotency, Glut-4 & PPAR-γ for adipogenesis, ß3-Tubulin and Nestin for neurogenesis, SOX-9 for chondrogenesis and OCN for osteogenesis. Gene expression measured as fold change relative to cells cultured on glass surfaces. Error bars signify standard error from the mean; n=3 for controls and n=4 for hydrogel samples. Statistical significance was performed using ANOVA.

When MSCs were cultured in 3D as shown in Figure 4.22, detection of the multipotency associated markers CD63 and ALCAM were observed, as well as adipogenic associated markers Glut-4 and PPAR-γ which were also found to be elevated in comparison to control. Identification of two distinct populations expressing multipotent and adipogenic markers implies that there is a heterogeneous population present in this 3D substrate. Detection of Glut-4 and PPAR-γ markers in this culture condition may be associated with the cells lack of

spreading, constrained within the hydrogel nanofibres and therefore promoting adipogenic lineage commitment as described by Kilian *et al.*, 2009.

The expression of markers from OPGs cultured in 3D with this 20 mM hydrogel illustrates a different pattern to that observed with the CD271 positive population as shown in Figure 4.23. This population of cells is considered to be more diverse than $CD271^+$ MSCs, as it contains a mixture of MSCs and pre committed cells. Detecting increasing levels of ß3 tubulin, a neurogenic marker, is suggesting neurogenic differentiation between time points in 3D studies. It is also thought that neural markers are expressed by niche MSCs as a response to their close connection with adipogenic nerve fibres giving the niche circadian regulation. A number of other transcripts are being detected such as ALCAM and CD63 however their expression levels are predominantly lower. The expression of CD63 which is associated with multipotency, is approximately expressed 20 fold higher than in OPGs cultured upon glass cover slips, indicative that there is still a multipotent cell population present when cultured within this 20 mM hydrogel substrate. OCN primers were used to detect expression of osteogenic transcripts, but failure to detect proposes that the stiffness of the substrate is not promoting pre-committed cells to continue in their lineage commitment towards the osteogenic lineage.

The very nature of incorporating MSCs into this 3D hydrogel environment can introduce an uneven distribution of cells, therefore introducing microenvironments within this one substrate. For example cell clustering may be the contributing factor to the expression of ALCAM and CD63 in figures 4.22 and 4.23, as it is believed that cell-cell contact of MSCs can maintain the multipotent phenotype in the native niche whereas the modulus properties of the hydrogel may also be mimicking that of soft tissue, and hence why expression of Glut4, PPAR- γ and B3tulbulin markers are up-regulated by this hydrogel when cultured with $CD271^+$ MSCs.

The 3D environment is promoting two distinct cell populations, and the expression of MSC markers may portray that the stiffness properties may be mimicking that of the bone marrow niche, but cell clustering within the hydrogel

may be the deciding factor for the switch between multipotency and differentiation in this 20 mM hydrogel substrate.

4.4.5.3 Hydrogel stiffness in response to 3D cell culture

The stiffness of the hydrogel in the presence of $CD271^+$ MSCs and OPGs was measured to provide insight into how cells alter their substrate environment over time in culture and how this would relate to the gene expression profiles observed in Figure 4.22 and 4.23. Figure 4.24 presents the rheological results which provide insight into the changes made to the substrate in response to cell differentiation.

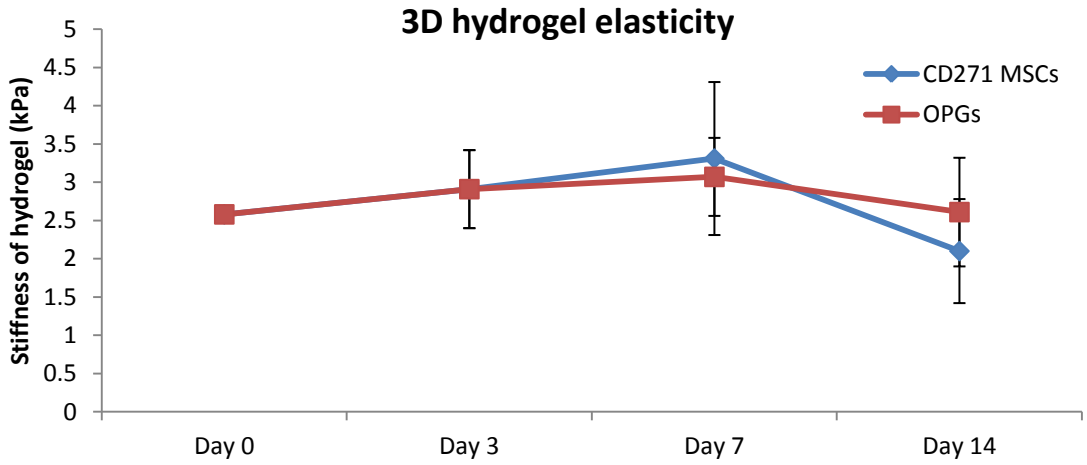

	Day 0	Day 3	Day 7	Day 14
CD271 MSCs	2.58 ± 0.1	2.91 ±0.51	3.31 ± 1.00	2.1 0.68
OPGs	2.58 ± 0.1	2.91 ± 0.54	3.07 ± 0.51	2.61 ± 0.71

Figure 4.24 Elasticity of 3D hydrogels due to cell culture.
MSCs and OPGs were cultured within the 20 mM hydrogel, and stiffness measured at days 3, 7 and 14. The hydrogel stiffness measurement was measured as gel only in the absence of cells to illustrate how culture can affect the elastic properties of the gel over time. Table below presents the actual stiffness values alongside standard deviation. Table which follows present the modulus values at each time point. ANOVA statistical tests were performed on 3D Hydrogel stiffness values over time course experiment, however changes in elasticity were not statistically significant.

Generally, the rheology study does not present significant changes in hydrogel stiffness over time in response to 3D culture with MSCs or OPGs cells. By culturing in 3D, the cells are present within the gel rather than simply on the upper surface, and ECM remodelling may not be able to occur as readily, if this

is indeed what the cells are doing on this culture substrate. In comparison, the 2D hydrogels remain stiffer than 3D gels as shown by Figure 4.21, which may be caused by the cells remodelling the upper surface only rather than the entire hydrogel substrate and may explain the large increase in stiffness at day 3. The elasticity of the 3D hydrogels remains low and therefore is mimicking the stiffness of soft tissue types such as neural and adipose tissue hence why markers associated with these lineages are detected by qRT-PCR with CD271 and OPG MSCs.

4.4.6. Pericyte cell study

4.4.6.1 Gene Expression Profiles in 2D and 3D studies

Pericytes cells are perivascular and it is believed that MSCs may originate from this cell population and therefore they are also believed to have multipotent potential (Crisan *et al.*, 2008). By introducing these cells and, again, culturing them in a soft hydrogel material in 2D and 3D I hope to provide insight into their resulting gene expression profile and relate this to that observed with MSCs and OPGs. This cell population is of interest as they may have potential in regenerative medicine as they are easily isolated from patient adipose tissue. A pool of primers was used to detect transcripts associated with differentiation, as this was the behaviour which was of interest with this cell type. Pericytes are not believed to express multipotent markers such as ALCAM, CD271 or CD63 hence why these were not included in this experimentation. Pericytes are however selected from adipose tissue by $CD146^+/CD34^-$ selection. Figures 4.25 and 4.26 present gene expression of pericytes when cultured in 2D and 3D with the 20 mM hydrogel which was previously studied with $CD271^+$ MSCs and OPGs. Markers were chosen due to previous results in 2D and 3D studies, and location of pericyte isolation.

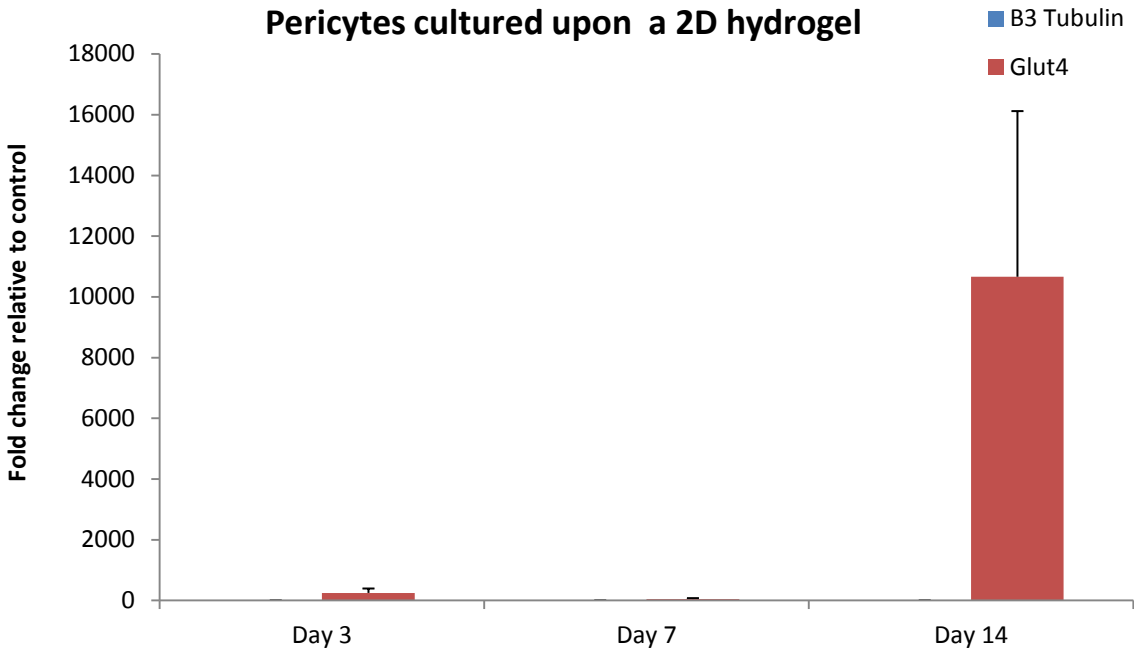

Primers to detect					
	PPAR-γ	Glut-4	B3 Tubulin	Nestin	SOX-9
Day 3	-	+	+	-	-
Day 7	-	+	+	-	-
Day 14	-	+	+	-	-

Figure 4.25 Pericyte profile with 2D 20 mM hydrogel.
Pericytes were cultured, and RNA extracted at said time points, from which gene expression was analysed. Cells were analysed for Glut-4 & PPAR-γ for adipogenesis, ß3-Tubulin and Nestin for neurogenesis, and SOX-9 for chondrogenesis. Gene expression measured as fold change relative to cells cultured on glass surfaces. Error bars signify standard error from the mean; n=3. ANOVA statistical tests were performed, however they were not significant.

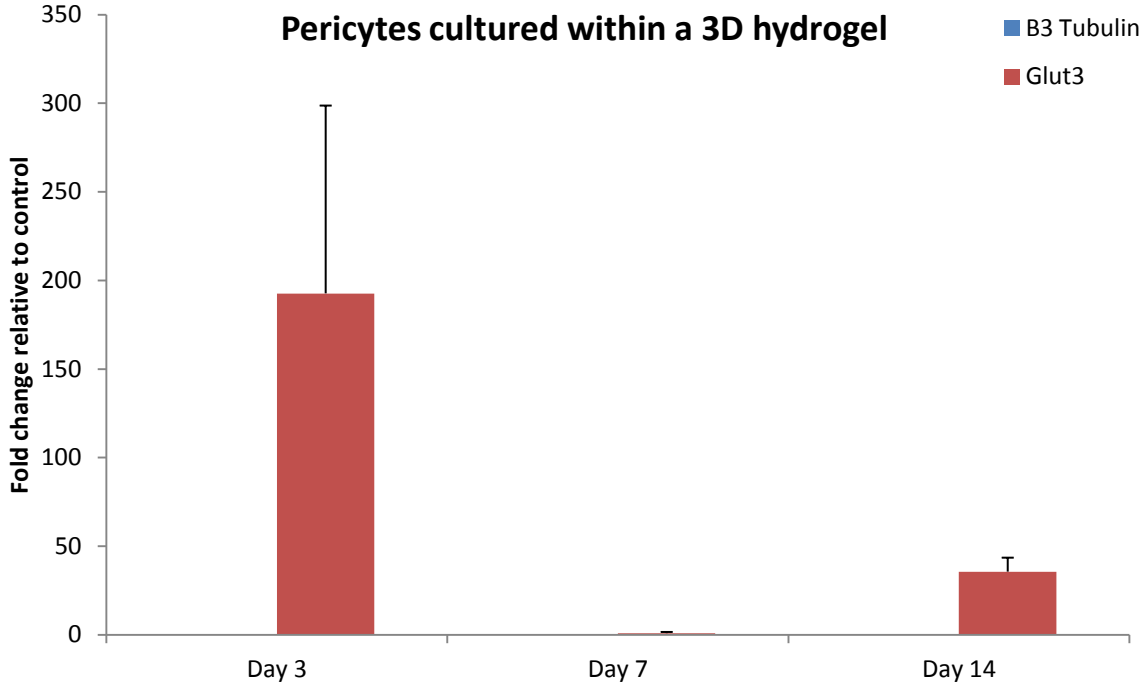

Primers to detect					
	PPAR-γ	Glut-4	B3 Tubulin	Nestin	SOX-9
Day 3	-	+	+	-	-
Day 7	-	+	+	-	-
Day 14	-	+	+	-	-

Figure 4.26 Pericyte profile with 3D 20 mM hydrogel.
Pericytess were cultured, and RNA extracted at said time points, from which gene expression was analysed. Cells were analysed for Glut-4 & PPAR-γ for adipogenesis, ß3-Tubulin and Nestin for neurogenesis,and SOX-9 for chondrogenesis. Gene expression measured as fold change relative to cells cultured on glass surfaces. Error bars signify standard error from the mean; n=3. ANOVA statistical tests performed to determine significance of data, however results not significant.

Pericytes are cultured in 2D and 3D with this 20 mM hydrogel, two markers are detected by qRT-PCR analysis. Glut4 is a plasma membrane protein and also an adipogenic marker, believed to occur after expression of PPARγ. Expression of Glut4 is assumed to be involved after differentiation has occurred and while the cells are acquiring fat deposits (Fernyhough *et al.*, 2007), however PPARγ was not detected in this qRT-PCR experiment. The neurogenic marker, ß3 tubulin is also detected; however, expression is not as high as that of Glut 4 in both culture conditions. It would suggest that on this 20 mM hydrogel substrate, the pericytes cells are predominantly committing to the adipogenic lineage perhaps reflecting their adipose origin or the stiffness of the hydrogel substrate as adipogeneic markers had previously been detected with $CD271^+$ MSCs in 3D and

OPGs in 2D culture. This hypothesis is only speculative, as PPARγ was not detected. It may the case however, the the time frame for detecting PPARγ was missed and in fact the substrate may possess adipogenic potential.

4.4.6.2.2 Hydrogel stiffness in response to Pericyte cell culture

Rheological studies were performed on 20 mM hydrogels cultured with pericytes in the 2D and 3D state as previously described. This was performed as an indicator of how this cell source alters the culture environment in comparison to $CD271^+$ MSCs as well as the OPG population. Figure 4.27 presents the stiffness obtained by culturing pericytes with the 20 mM hydrogel over period of 7 days in culture

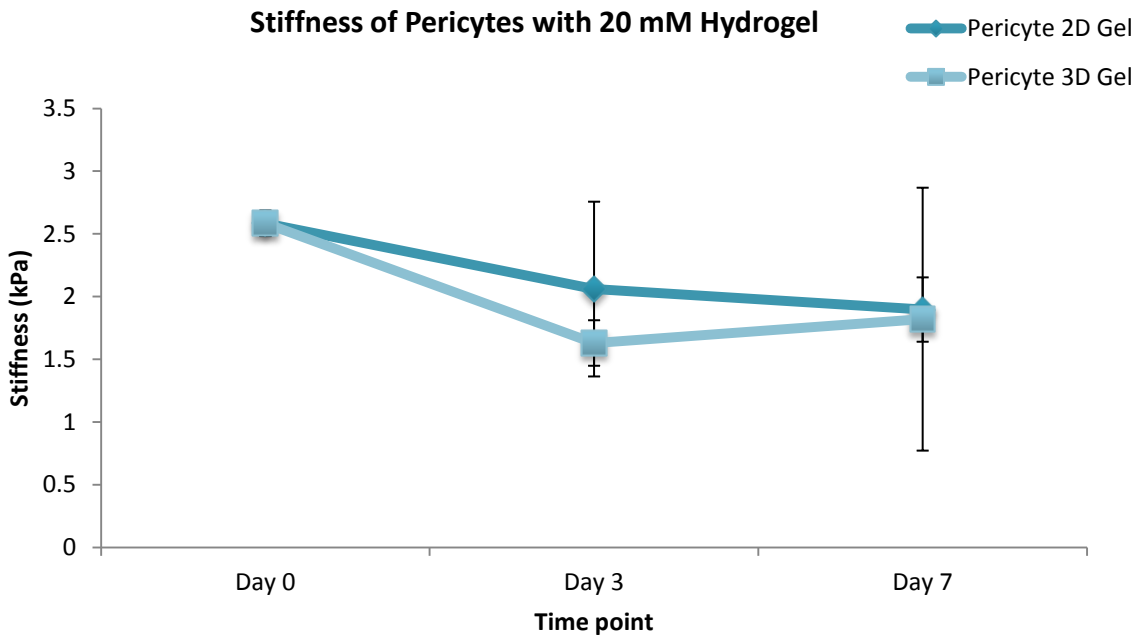

	Day 0	Day 3	Day 7
2D	2.58 ± 0.1	2.06 ± 0.69	1.89 ± 0.25
3D	2.58 ± 0.1	1.63 ± 0.18	2.32 ± 0.718

Figure 4.27 Elasticity of hydrogel with 2D and 3D pericyte culture.
Pericytes were cultured on the upper surface of the 20 mM hydrogel (2D) or suspended within the peptide solution resulting in the cells present throughout the gel (3D). Figure presents that the 2D gel is slightly stiffer at day 3 in culture, and then modulus decreases, whereas with regards to he 3D hydrogel, stiffness decreases at day 3 and then increases again slightly. The table that follows presents the values obtained from rheological studies at each time points. ANOVA statistical tests were performed over time to determine if stiffness changed significantly. Changes in hydrogel elasticity were not statistically significant.

The stiffness of the hydrogels when pericytes are cultured in 2D and 3D as shown in Figure 4.27 decreases over time, however, there was no significant change in hydrogel stiffness over the course of the experiment. The modulus of the hydrogel substrate is stiffer than that of neural tissue as shown in Figure 4.3, which may suggest that the cells are modulating the 2D substrate surface and undergoing adipogenic differentiation, confirming the results of the qRT-PCR study where adipogenic markers were detected.

4.4.7 Pericytes with cholesterol sulphate

Pericytes were cultured within a 3D 20 mM hydrogel of 2.58 kPa. Cholesterol sulphate is a metabolite which has a role in cartilage production and osteogenesis as stated previously in section 4.2. The metabolite is a glucorticoid which are known to play a key role in the differentiation of MSCs along the osteogenic lineage (Hong *et al.*, 2008 and Cooper *et al.*, 1999). By introducing Cholesterol sulphate into the cell culture media, the aim is to initiate a differentiation response, different to that observed when cultured with the hydrogel substrate. This will determine if cells respond to gel stiffness versus chemical induction. It also provides an initial study for further investigation with cholesterol sulphate which will follow in chapter 5 of this thesis.

4.4.7.1 3D Pericyte culture with Cholesterol Sulphate

4.4.7.1.1 Cholesterol sulphate induced gene expression

Pericytes were cultured within the hydrogel and RNA extracted after 7 and 14 days in culture. Cells were analysed for a number of markers associated with the neuorgenic to osteogenic lineages in the aim of picking up the effects of cholesterol sulphate driven differentiation.

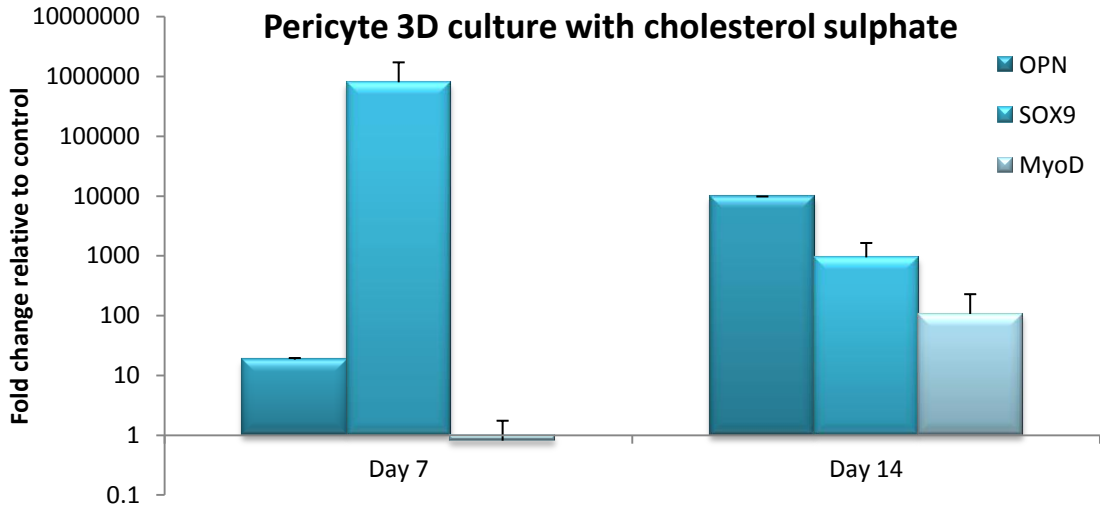

Primers to detect							
	B3 Tubulin	Glut 4	Myo D	Sox-9	Coll 2A	OCN	OPN
Day 7	-	-	+	+	-	-	+
Day 14	-	-	+	+	-	-	+

Figure 4.28 Pericyte profile in response to 20 mM 3D culture with cholesterol sulphate. Pericytes were cultured, and RNA extracted at said time points, from which gene expression was analysed. Cells were analysed for Glut-4 for adipogenesis, ß3-Tubulin, MyoD for myogenesis, Sox-9 for chondrogenesis and OCN and OPN for osteogenesis. Gene expression measured as fold change relative to cells cultured on glass surfaces. Error bars signify standard error from the mean; n=3.

Pericytes cultured in a 3D environment with the addition of cholesterol sulphate induces a different phenotypic profile than that observed in Figure 4.26, where response to hydrogel elasticity alone was shown. The pericytes 3D phenotype profile when cultured with cholesterol sulphate is again, heterogeneous in nature, with the expression of markers associated with myogenesis, chondrogenesis and osteogenesis. Sox-9 associated with chondrogenesis was expressed highest at day 7; however, as the time course continues expression was down regulated. Interestingly, MyoD which is expressed during muscle differentiation was present at day 7 and increased at day 14. Expression of this marker would be expected on a stiffer hydrogel substrate rather than one at 2.58 kPa as muscle differentiation has previously been described to be approximately 12 kPa (Gilbert *et al.*, 2009). It would imply that two populations are arising, one population differentiating in response to cholesterol sulphate and another population with a mixed phenotype due to competition between the cholesterol sulphate induction and the elastic properties of the 20 mM hydrogel substrate. OPN is also upregulated as the time course progresses, and is the predominant marker after 14 days in culture. OPN is associated with osteogenic

differentiation and is suggesting that a sub population are committing to this lineage due to the cells in the presence of the glucorticoid cholesterol sulphate. This provides interesting results which will be further investigated in chapter 5. Culture with this molecule has shifted the gene expression profile away from soft tissue markers such as Glut4 and ß3tubulin and towards markers associated with stiffer tissues such as cartilage and bone.

4.4.7.1.2 3D Cholesterol sulphate rheology study

The results in this chapter have shown that when pericytes are cultured in a 3D environment in the presence of 0.1 µM cholesterol sulphate supplemented media, they express markers associated with stiffer tissue types such as OPN, Sox9 and MyoD associated with osteogenisis, chondrogenesis and myogenesis respectively. A rheological study was next performed to determine if the cholesterol sulphate is inducing the cells to differentiate and has an effect on increasing the stiffness of the hydrogel in line with what would be expected due to the detection of OPN and MyoD, therefore somewhere in the range of 12-100 kPa as shown in Figure 4.3. Figure 4.29 presents the results of the rheology study and results are compared to the stiffness obtained with pericytes in 3D study cultured with complete cell culture media.

Figure 4.29 presents the findings of the 3D cholesterol sulphate linked rheology study alongside the results obtained from 3D culture of pericytes with complete cell culture media. It was found that the stiffness after 7 days in culture was similar in both hydrogels, and that the presence of cholesterol sulphate does not impact the stiffness of the hydrogel at this time point. It may be possible that this compound may affect the stiffness measured over time, but long term culture to determine if this was the case was not possible due to lack of sterile cell culture facilities at the University of Strathclyde where rheological experimentation took place. The action of cholesterol sulphate may up-regulate pathways which leads to bone marker expression at this early time point such as that shown in Figure 4.1, however, increase in hydrogel stiffness may occur downstream as differentiation is occurring and cells are laying down their own

ECM and mineralisation is initiated. Overall, it presents that stiffness is not the sole driving mechanism for cell differentiation.

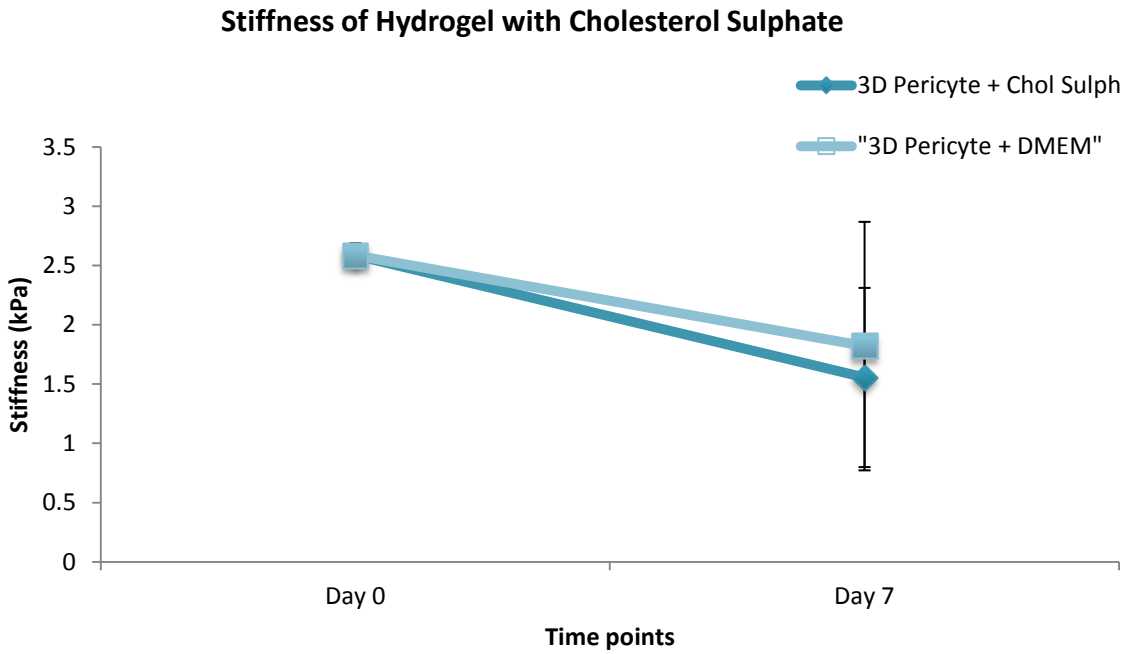

Timepoint	Pericytes + DMEM	Pericytes + Cholesterol Sulphate
Day 0	2.58 ± 0.1	2.58 ± 0.1
Day 7	1.82 ± 0.718	1.55 ± 0.52

Figure 4.29 Elasticity of 3D pericyte hydrogels.
Figure presents the elastic modulus values of a 3D pericyte hydrogel cultured with complete cell culture media, and a further hydrogel cultured in the presence of cholesterol sulphate supplemented media. This was performed to determine the effect this molecule had on the pericytes and to determine if the compound was inducing the cells to lay down a more complex osteogenic ECM due to detection of OPN by means of qRT-PCR.

4.5 Limitations

In order to confirm MSCs were differentiating down the lineage corresponding to the markers detected through qRT-PCR, further studies would be required to verify the true commitment of the cells in response to the hydrogel substrate. Detecting proteins by means of immuno histochemistry coupled 3D images obtained by use of the confocal microscope would be ideal as the cells are hypothesised to move within the hydrogel substrate. All cell types discussed in this chapter, cultured in both 2D and 3D studies underwent immunostaining to

detect proteins and cell surface markers to confirm qRT-PCR results. The standard method as described in section 4.3.2.1 was modified to allow the solutions to penetrate the substrate and come into contact with the cells in the 3D cultures. The washing steps with PBST were extended to ensure all reagents were removed to prevent unspecific binding. Unfortunately, the hydrogel substrates failed to maintain their elastic structure and dissolved in the presence of repeated washes after being subjected to fixative solution. The hydrogel substrate is too delicate at this stiffness to be subjected to altering temperatures and washes therefore detection of specific proteins in 2D and 3D studies was not successful. Other methods such as Western blotting or enzyme linked immunosorbent assay (ELISA) could be used to detect presence of specific proteins associated with cell differentiation, however the extraction methods would need to be modified as the hydrogel samples are sensitive to chemical extraction solvents.

Colourimetric assays are widely used in the field of cell biology as they are used as a measurement of cell viability, proliferation and cytotoxity. The 3-[4,5-dimethylthiazol-2-yl]-2,5 diphenyl tetrazolium bromide (MTT) assay can be used to assess living cells as MTT can be reduced by dehydrogenases cells in culture resulting in the formation of a violet formazan from a yellow aqueous solution. This reaction determines the mitochondrial activity of living cells and a linear relationship was found between the viable number of living cells the MTT formazan produced, as it can be measured using optical density (OD) (Gerlier & Thomasset., 1986 and Van Meerloo *et al.*, 2011). There are alternative methods to measuring cell viability, one such assay in the CellTiter-Glo® Luminescent assay that measures cell viability based on the quantity of Adenosine Triphosphate (ATP) in cells. These methods were utilized in determining the viability of cells cultured in 2D and 3D with the 20 mM hydrogel substrate. However, results did not provide insight into cell viability as hydrogel controls cultured in the absence of cells provided an OD reading that was similar to the results obtained in the presence of cells. This was repeated over time course as cell number was expected to increase as study continued, but due to negligible results it was hypothesized that due to the presence of Fmoc protected peptides in the hydrogel substrate that the reagents could not penetrate the gel to reach the cells, or that the colour change due to cell viability was masked or absorbed

by the hydrogel substrate. Due to the downfalls of these colourimetric assays with this Fmoc F_2/S hydrogel substrates, cell viability was measured by extracting DNA and protein from the cells as it is believed that an increase in DNA content over time would imply that cells are undergo cell division, (Shuter *et al.*, 1983) a result which would imply that the hydrogel was supporting cell growth and viability. Other assays for cell viability such as Lactate Dehydrogenase (LDH) and CyQuant could also be trialed with these hydrogels in future studies, as ideally, a commercially available assay would be beneficial for future studies with these hydrogels as it would obtain a quick and reliable result. Currently, extracting DNA and protein from these substrates is a time consuming method, and many variables can be introduced as there are numerous steps involved and use of a number of chemicals.

4.6 Summary

Bone marrow adherent cells positively selected for the CD271 cell surface marker can successfully differentiate down the adipogenic and osteogenic lineages (Figures 4.8 and 4.9). These lineages were chosen as it is takes into account two diverse cell types from a soft and extremely rigid tissue. The OPG cell population is believed to contain a number of cell types such as MSCs, cells pre-committed to the osteogenic lineage as well as osteoblasts. Through immunostaining, it was determined that these cells express a number of cell surface markers associated with multipotency such as nestin, STRO-1 and ALCAM (Figure 4.7) and also could be differentiated down fat and bone lineages (Figure 4.8). Due to both cell populations displaying multipotent properties, it was decided that both cell populations could be used to study modulus driven differentiation or maintenance of the multipotent state by mimicking the bone marrow niche environment on the hydrogels described in the previous chapter.

To begin with, a 10 mM hydrogel of 0.64 kPa was used to study the effect the stiffness had on maintenance of the multipotent state, or if modulus driven differentiation was occurring. Through use of qRT-PCR, it was discovered that the 10 mM hydrogel promoted expression of ß3 Tubulin, a neurogenic marker, and this was paired with metabolomics to detect metabolite changes in response to MSC differentiation. Metabolomic data presented that a number of metabolic

pathways were active at early time points and then metabolites were down regulated by day 7. It was suggested that MSC differentiation occurs early in response to the 10 mM hydrogel substrate due to upregulation of metabolites at days 1 and 3, and by day 7 cells have committed and intensity has decreased as cells settle within their environment. Although this 10 mM presented interesting data, unfortunately this substrate failed to remain in hydrogel form past 7 days in culture. This material was discarded for future work as the very nature of a MSC supporting material is for long-term culture, ideally for stem cell proliferation or full lineage commitment.

A further hydrogel of 20 mM was taken forward as the next most suitable substrate for use with MSCs as it was able to withstand longer time in culture conditions and promoted cell growth. Culturing $CD271^+$ MSCs, OPGs and pericytes in a 2D and 3D study presented diverse transcription profiles by means of qRT-PCR. $CD271^+$ MSCs displayed neurogenic and multipotent markers when cultured upon the surface of the hydrogel, whereas when mixed with the peptide solution and grown within the hydrogel substrate, they presented expression of MSC and adipogenic markers. OPGs in 2D also expressed neurogenic markers, alongside those associated with the adipogenic lineage and multipotentcy. When grown in 3D, markers detected were similar to that of the 2D study, except the adipogenic marker Glut4 failed to be detected. Pericytes were the last cell type to be studied with this hydrogel substrate, and in both culture conditions two markers were detected, of which they were associated with nerogenesis and adipogenesis. Overall, it can be concluded that a varied cell population arises due to culture with this substrate and it neither promotes complete differentiation or maintenance of the multipotent state due to a range of markers detected by qRT-PCR, which may be promoted by small clusters of cells or presence of microenvironments within the gel itself. Ultimately cell morphology on these substrates remained rounded in comparison to cells cultured upon glass, demonstrating low cytoskeletal tension within the cells and explains why sot tissue markers were detected.

Pericytes were taken forward for further investigation by culturing them in the presence of cholesterol sulphate, a metabolite believed to be involved in chondrogenesis, as well as osteogenesis. When cultured with this molecule, it

was discovered that markers associated with myogenesis, chondrogenesis and osteogenesis were all detected by qRT-PCR, and the markers previously detected in the 3D study were not expressed by the cells. This molecule has shown promise with this cell type at inducing an osteogenic effect (through personal communication with Enateri Alakpa). Pericytes were the initial population to be trialled with cholesterol sulphate as they had been selected by FACS for particular cell markers and therefore believed to be a purer cell population than previously studied $CD271^+$ MSCs and OPGS. As pericytes showed a clear shift in their gene expression profile, studies with cholesterol sulphate was taken forward for a prospective use in oral and maxillofacial reconstruction studies, and here this molecule will be studied with $CD271^+$ MSCS.

Overall, cell viability is promoted on these hydrogel substrates and can be used to support MSC growth. These hydrogels could have a potential role in regenerative medicine as the substrate alone has shown to effect gene expression rather than by chemical means by use of induction media. The effects of cholesterol sulphate will be further investigated as a hydrogel is taken developed for the prospective use in the case of inducing osteogenic differentiation of cells for repairing maxillofacial defects. Overall, this chapter presents that these hydrogels maintain cell viability and can be a valuable tool for studying cell behaviour before focussing on a particular application which will be discussed in chapter 5.

Chapter 5

Hydrogels as a model for Maxillofacial Reconstruction

5.1 Introduction

5.1.1 Introduction to mandibular reconstruction methods

Surgery to remove cancerous bone tissue of the oral and maxillofacial (OMF) region can result in large defect areas that are proving troublesome for repairing or filling by use of scaffolds and corrective surgery (George and Krishmanurthy, 2013). A mandibular resection procedure is required when cancerous tissue has spread to the jawbone and an area of tissue is removed such as that shown by Figure 5.1. Surgeries such as this can leave a considerable area to be filled, depending on the amount of cancerous or diseased tissue removed. Corrective surgery to repair these defects is troublesome as it is proving difficult to restore the functional aspect of the native bone as well as to consider the aesthetic appearance of bone tissue (Tatara *et al.*, 1994).

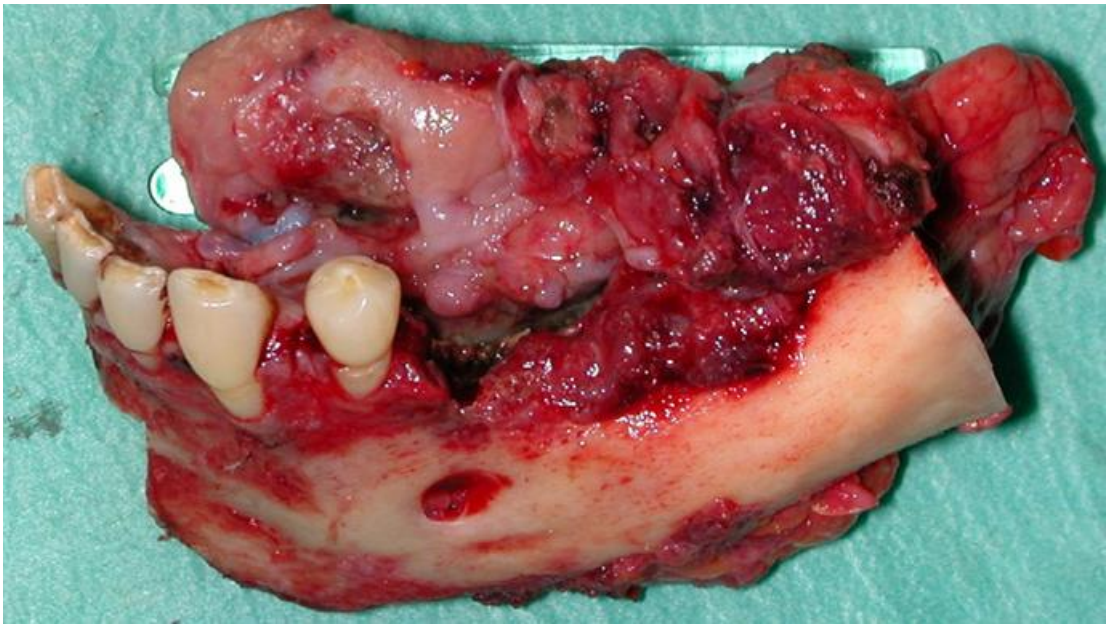

Figure 5.1 Resected section of mandibular bone tissue as a result of squamous cell carcinoma of the gum . Adapted from Pieptu *et al.*, 2005.

A number of surgical techniques have been approached in order to replace the excised diseased tissue. One such method is the use of the free fibula flap, where surgeons remove part of the fibula bone from the patients' leg, and transfer a section of the bony tissue to the defect area (Hidalgo, 2005). Tseng (Tseng *et al.*, 2013) describe how the use of a device such as that shown in

Figure 5.2 could be beneficial as it could still allow the free fibula flap method to continue being used, ensuring the fibula bone is able to fit the mandibular defect effectively, as the excised piece of bone will not match that of the defect site exactly. This device also eliminates the difficulty of sawing exact sizes of fibular bone. The method has benefits as it incorporates homogeneous vascularised tissue and does not require the dispensing of immunosuppressive drugs. There are, however, limitations to the method, as the patient may experience leg weakness and ankle instability depending on the size of the excised bone fragment.

Figure 5.2 Device design for use in repairing mandibular defects.
Illustration displays how fibula bone blocks are assembled and fit into the defect of the mandibular tissue. Figure adapted from Tseng *et al.*, 2013

Bone cements such as poly (propylene fumarate) and poly(methyl-methacrylate) have been studied with regards to filling the craniofacial defects, with the latter being used since the mid 1990's (Henslee, 2012). The nature of these polymers requires high curing temperatures (up to 100°C) that have negative effects on local tissue damage and cellnecrosis when delivered to the bone wound site (DiMaio, 2002). In order to repair the defect area, the incision site must be filled with a combination of cement and cells to induce osteogenic differentiation for correct tissue formation and incorporation.

There has also been research on potential space maintainers in reconstruction. This is where an allosteric material in inserted into the excised bone space and functions to prevent wound contraction, maintaining the bony space and ultimately delaying bone tissue regeneration until a suitable wound bed has been created. The porous properties of this material also aid in drug release to the damaged site aiding in wound healing (Spicer, 2011).

Distraction osteogenesis is a method whereby new bone can be generated in the absence of a graft, but relies on applying tensile strength leading to tissue growth and regeneration (Lucchese, 2014). This method began in the 1950's and this approach ultimately relies on the process of mechanotransduction to generate this new bone formation (Ilakarov, 1989). In doing so, the facial bone is fractured and a device is inserted which will allow separation of the two bone segments at a rate of 1 mm per day. This procedure however, tends to be applied more in the case of craniofacial skeleton abnormalities (Natu, 2014), but the principle may be applied after removing cancerous tissue, depending on the severity of the bone abnormality.

These methods have numerous drawbacks and may involve subsequent surgeries. Alternative methods are being investigated to use stem cells incorporated with a material able to set or gelate at body temperature, but still are able to induce or stimulate new bone formation at the required site (Alfotawi *et al.*, 2013).

5.1.2 Alternative methods for maxillofacial reconstruction

Instead of removing homogeneous bone tissue which has limitations in itself, a suitable biomaterial for maxillofacial reconstruction is required to possess a number of desirable properties such as biocompatibility, mechanical stability in the body and can be easily shaped to the patients' defective site (Cho, 2004). Recently, there has been interest in using a biomimetic scaffold for induction of osteogeneic differentiation that could potentially be injected into the patient's facial muscular tissue prior to corrective surgery to create a large area of potential tissue that could be excised and placed into the defective bone site once diseased tissue has been removed (Alfotawi *et al.*, 2013). Skeletal muscle has the ability to form bone tissue, as in the case of fibrodysplasia ossificans

progressive, a genetic disease in which the patients muscle tissue can ossify resulting in extra skeletal bone formation and restriction in mobility (Shore & Kaplan., 2008 and Kaplan *et al.*, 2012). As well as this, muscle tissue is also a promising site for osteoinduction as it has also been found to contain osteogenic progenitor cells (Bosch *et al.*, 2000). These findings present muscle as a suitable tissue for the aim of inducing an osteogenic response within, for the use in corrective maxillofacial surgery.

The use of muscular tissue to promote new bone formation has been applied in an animal model. In 2012, an animal study was performed on rabbits which had a section of their mandibular bone removed creating a critical sized defect. A pre-fabricated beta-tricalcium phosphate (β-TCP) scaffold loaded with recombinant human bone morphogenic protein 7 (rhBMP-7) was added to the incision site over time and illustrated continuation with the adjacent bone and remodeled to a comparable size of the defect site. However, the presence of the scaffold alone in the absence of rhBMP-7 failed to promote adequate osteogeneic induction to repair the bone defect in the rabbit model (Naudi *et al.*, 2012). This is just one example of how a scaffold alone has been designed to induce osteogenic differentiation of a mandibular defect.

In 2014, Alfotawi injected the masseter muscle flap of rabbits with 60% calcium, 40% hydroxyapatite (Cerament™/ Spine Support) with a liquid phase composed of water and pacifier with BMP-7 incorporated. Rabbit MSCs (rMSCs) were then injected around the cement once the solution had set and through a 3D radiology investigation, it was determined that this method produced a thin layer of hard tissue to form between the muscle fibres. The method utilised the use of rMSCs coupled with an osteogenic scaffold to promote bone formation *in vivo* within three months of injection inside the muscle flap. The muscle flap, within which the cement and cells were injected, provided an adequate blood supply for bone formation and essentially acted as a bioreactor, a property which would aim to be mimicked in the case of human trials with a suitable injectable scaffold for osteostimulation. Ideally, the scaffold, or delivery medium, would be biocompatible and would ultimately degrade once fully incorporated allowing tissue regeneration to complete integration.

For a scaffold or biomaterial to be functional for the prospective use in maxillofacial reconstruction, the MSCs must differentiate down the osteogenic lineage to become mature osteoblasts in order to begin the process of bone mineralisation, which is described as the process by which hydroxyapatite is deposited in the ECM (Orimo., 2010). MSC differentiation towards the osteogenic lineage is characterised by the decline in proliferation and the induction of matrix maturation and minerlisation. Bone matrix markers (Figure 5.3) such as OPN and OCN are commonly used as indicators of the onset of osteogenesis (Kim *et al*., 2005). By using this model proposed by Lian & Stein, the progress of MSCs to osteoblasts can be followed by detection of proteins associated with the osteogenic phenotype. Osteopontin is a highly phosphorylated major cell and hydroxyapatite binding protein synthesized by osteoblasts, and found in the ECM of mineralised tissues (Reinholt *et al*., 1990 and Denhardt and Noda., 1998). Osteocalcin is a calcium binding protein in bone and is expressed post-proliferatively in osteoblasts, preosteocytes and mature osteocytes (Lian *et al*., 1998). Alkaline phosphatase is a metalloenzyme is involved in producing free phosphate for use in bone minerlisation (Yang *et al*., 2014) and collagen type I provides a mechanical function, providing elasticity for the tissue (Viguet-Carrin *et al*., 2006). The detection of these markers would signify that osteogenic differentiation is occurring within a suitable scaffold used in OMF reconstruction therapies.

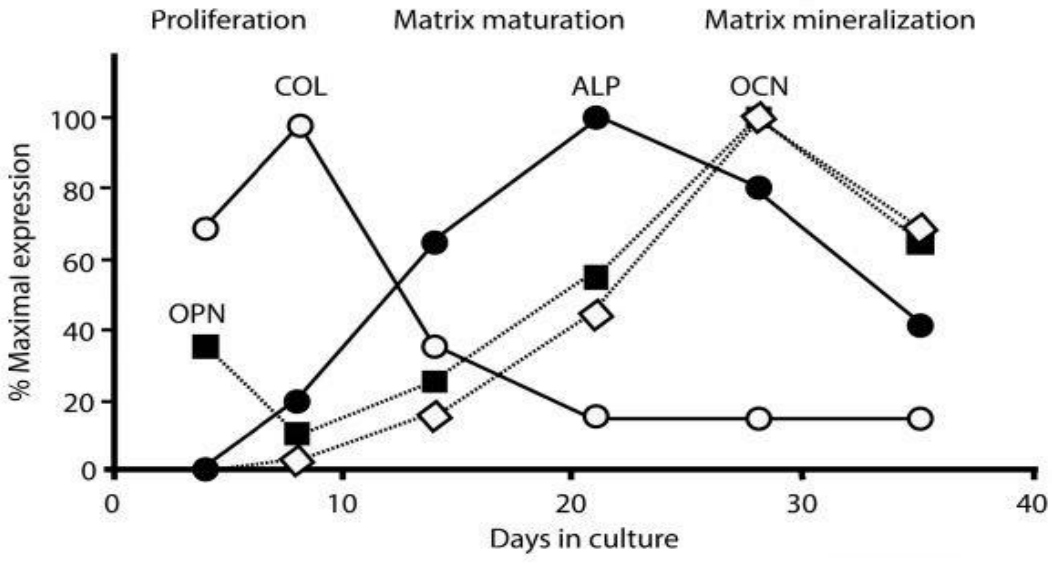

Figure 5.3 Osteoblast development.
The figure presents markers expressed during osteoblast differentiation at each time point and during each phase of cell commitment from cell proliferation, to matrix maturation and matrix minerlisation. Collagen is expressed highest in the early stages of proliferation and tails off as differentiation progresses towards the osteoblast phenotype. Osteopontin is also expressed in this early proliferation stage, with levels falling by 8 days in culture and progressively increases again through matrix maturation and reaches highest expression approximately 28 days during the matrix mineralization phase. Alkaline phosphatase levels begin to rise during early cell proliferation, peaking at approximately 21 days in culture during matrix maturation and tails off during matrix mineralisation. Finally, osteocalcin follows a similar trend to alkaline phosphatase, however expression is detected later at approximately 8 days in culture, and peaks at during the process of matrix mineralisation after 28 days in culture. OPN signifies osteopontin, ALP= alkaline phosphatase, COL= collagen an OCN = osteocalcin. Adapted from Loan and Stein, 1995.

5.2 Objectives

This chapter aims to develop a suitable 3D model, which has bioactive elastic modulus properties, is mechanically stable in culture and can be an appropriate medium for encapsulating cells for promoting osteogeneic differentiation *in vitro*. Such a substrate will be cultured in the presence of MSCs and pericytes and mineralization and bone markers will be quantified by means of von kossa and qRT-PCR. This model will also examine the outcome of cholesterol sulphate induction on the effects of markers associated with bone formation as previous studies indicate it to promote expression of OPN when cells were cultured upon a soft hydrogel substrate (Alakpa, unpublished data, and section 4.4.7.1). Figure 5.4 illustrates this proposed model for inducing osteogenic stimulation with the aim of creating a suitable system that can be up-scaled for regenerative medical properties for those undergoing maxillofacial reconstruction surgery involving

critical sized defects. The objective of this model is to create a biomaterial that could be mixed with a suitable cell source, which could be injected into the patient's own muscle tissue to promote osteogenic differentiation in this tissue. Essentially, the diseased tissue would be removed prior, and a section of muscle excised and rotated into the defect site. The aim is to initiate osteogenic differentiation in the muscle tissue so that in theory it could integrate with the healthy bone tissue, retaining function and aesthetic appearance.

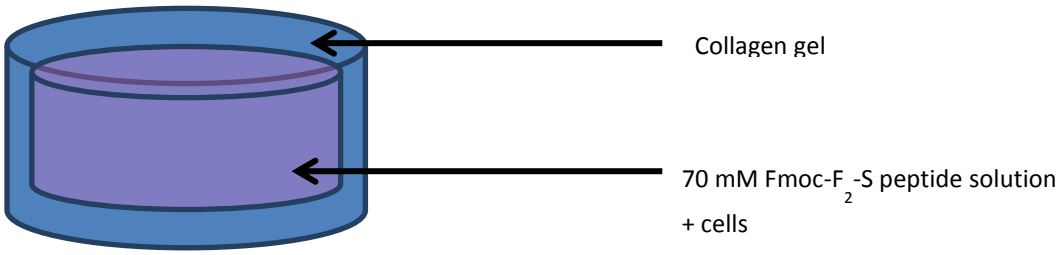

Figure 5.4 3D collagen-Fmoc model for Maxillofacial osteostimulation.
This model illustrates the collagen component of the gel in blue, with the 70 mM Fmoc F_2/S hydrogel in pink. The Fmoc gel will be injected to the centre of the collagen, which will, in this model, mimic native muscular tissue. Cells will be cultured within the Fmoc gel with the aim of differentiating down the osteogenic lineage due to the stiffness of this 3D substrate.

5.3 Materials & Methodology

5.3.1 Materials

Material	Supplier
Rat Tail Collagen	First Link
10 x Modified Eagles Media (10 x DMEM)	First Link
Foetal bovine serum (FBS)	Sigma Aldrich, UK
0.1 M NaOH	Fluka
Fmoc- F_2	BioGel
Fmoc-S	Bachem, UK
0.5 M NaOH	Fisher Chemical
0.5 M HCl	Fisher Chemical
ThinCert Tissue Culture Insert	Greiner Bio-One
1 x Phosphate Buffer Solution	In-house
Silver Nitrate	Sigma Aldrich, UK
Sodium Thiosulphate	Sigma Aldrich, UK
Nuclear fast red	Sigma Aldrich, UK
Aluminium Sulphate	Sigma Aldrich, UK

5.3.2 Methodology

5.3.2.1 Collagen Gels

All solutions were pre-chilled and kept on ice during preparation of collagen gels. A volume of 1 ml 10x DMEM was added to 1 ml of FBS and 1 ml of cell culture media in one universal tube. A 5 ml volume of Collagen was added to 2 ml 0.1 M NaOH solution in another tube and one was poured slowly into the other, continuously vortexing to ensure even distribution. To this, 0.1 M NaOH was added to the solution until it became uniform in colour to that of complete cell culture media. A 1ml volume of the collagen mix was added to ThinCert Tissue Culture Inserts within a 12 well cell culture plate and 1.4 ml cell complete culture media was added to the surrounding well and placed in 37 °C incubator for 90 minutes.

5.3.2.2 Preperation of 70 mM Hydrogel

Chapter three of this thesis discusses the process of peptide solution to hydrogel formation with 10- 40 mM peptide concentrations. The stiffest gel described was the 40 mM substrate that was 12 kPa in rigidity that we hypothesised would fail to induce osteogenic as this stiffness is similar to that of muscle tissue. A 70 mM peptide solution was created with 0.0718g Fmoc-F_2 and 0.04g Fmoc-S with the addition of 4 ml dH_20 and 585 µl 0.5 M NaOH. The solution underwent cycles of sonication and vortexing for 20 minutes, after which the pH was measured and reduced to between 7.2 and 7.8 by addition of 0.5 HCl. The solution was not filtered as described previously, but was subject to UV light sterilisation for approximately 45 minutes. After this, solution was warmed in cell culture incubator and 500 µl was injected into the middle of the pre-formed collagen gel as described in section 5.2.2.1. For biological studies, cells were added to the 70 mM Fmoc- F_2-S peptide solution prior to injection into collagen gel. The collagen-Fmoc hydrogels were returned to the cell culture incubator for 90 minutes and all media replaced, with the addition of complete media to the upper surface of the newly formed gel.

5.3.2.3 Injecting 70 mM solution into muscle model

A piece of pork muscle was obtained and washed twice with sterile 1 x PBS and placed in cell culture incubator for 1 hour whilst peptide solution was warmed to 37°C. A small area of tissue was removed from the tissue to mimic the potential sight for injection and a volume of approximately 500 μl 70 mM Fmoc-F_2-S peptide solution was injected into the wound site and returned to incubator for 1 hour with the addition of complete cell culture media. After this time the muscle was removed and photographed to illustrate hydrogel formation and complete media replaced. The tissue was returned to cell culture incubator and photographed again one day post injection.

5.3.2.4 Introduction of Cholesterol Sulphate

In section 4.4.7, cholesterol sulphate has shown to induce pericyte differentiation towards the osteogenic lineage when cultured in a 3D hydrogel of 2.58 kPa which had previously illustrated markers predominantly associated with soft tissue types. Cholesterol sulphate was added to cell culture media to create an overall concentration of 0.1 μM, as previously described in section 4.3.2.2.1, and added to the surrounding insert and on top of the hydrogel once gelation was complete at approximately 90 minutes after injection of the 70 mM Fmoc F_2-S peptide solution into the centre of the collagen gel.

5.3.2.5 Rheology

Rheology experiments were performed on hydrogels composed solely of 70 mM Fmoc-F_2/S as described in section 3.3.2.4 Collagen hydrogels also underwent rheological testing as this section describes, however the tests were performed at 37 °C as collagen forms a gel and is cultured at this temperature. When the 70 mM peptide solution was injected into pre-formed collagen, rheological studies were performed at 37 °C with a 20 mm diameter geometric plate with a working gap 0.75 mm.

5.3.2.6 qRT-PCR analysis

Gene expression in hydrogels was compared to that of glass controls and presented as fold change. This was carried out as described in sections 2.3.5,

2.3.8 and 2.3.9 and primers chosen were associated with detection of stiffer tissue markers such as Sox-9 and OCN. These were chosen to investigate the effect of the stiffer 70 mM Fmoc F_2/S on osteogenic differentiation.

5.3.2.7 Von Kossa Staining

Von Kossa staining was performed on 3D collagen-Fmoc hydrogels after 14 and 28 days in culture to identify mineralization of the MSCs as osteostimulation can be initiated due to the stiffness properties of the culture material. Hydrogels were subjected to a 5% silver nitrate solution and each side of the hydrogel was exposed to UV light for 30 minutes. The solution was removed and gels washed with deionised water before addition of 5% sodium thiosulphate for 30 minutes, and solution discarded and samples washed under running tepid water for 10 minutes. Hydrogels were counterstained with nuclear fast red for 10 minutes, and again solution aspirated to waste and rinsed with deionised water. Samples were rinsed in 70% ethanol for 10 minutes and then maintained in 1 x PBS solution until ready to be imaged. Hydrogels were sliced and imaged using scanning facilities, and image analysis performed on Image J. Of each sliced gel, a uniform area was highlighted, and the intensity reading was measured. The hydrogels were normalized to a blank hydrogel that had been either cultured with cholesterol sulphate on media or standard DMEM media, but in the absence of cells. Figure 5.5 illustrates an example of the images of the hydrogel with and without cells, when cultured in DMEM cell culture media. These images were used to detect the intensity of mineralisation using Image J software.

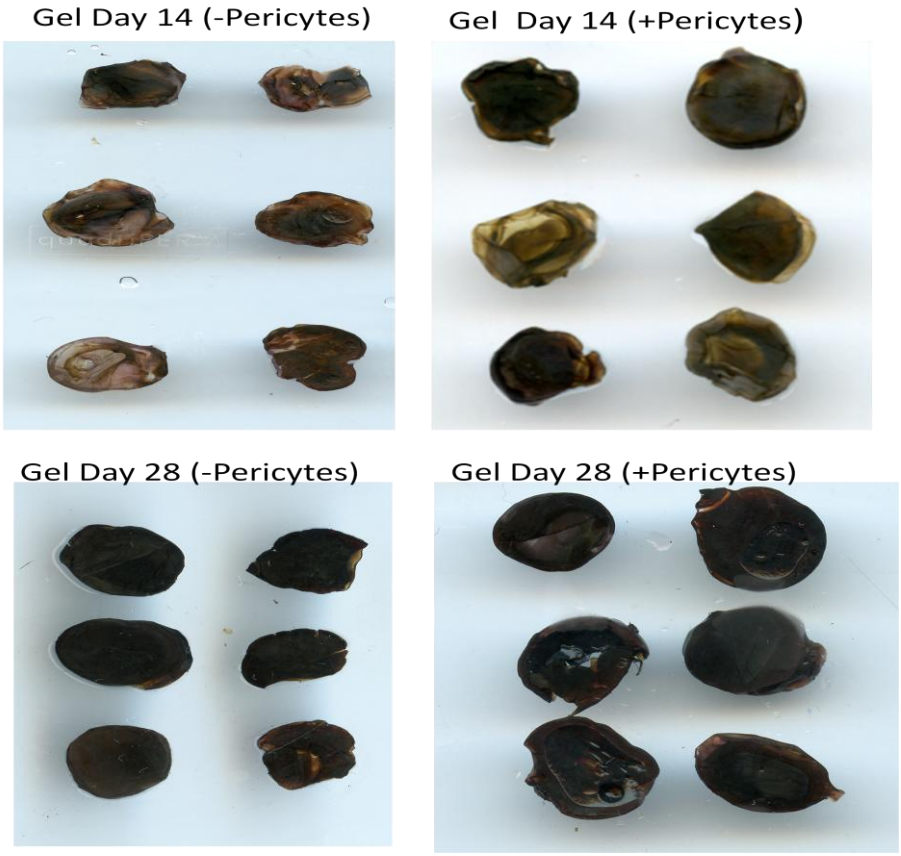

Figure 5.5 Von Kossa Mineralisation of Hydrogels

Figure illustrates imaging of the hydrogels which had underwent von kossa minerlisation staining. These hydrogels were sliced and imaged as shown. These images were then subject to image J software analysis to detect intensity of staining in the samples.

5.4 Results

5.4.1 Creating 70 mM Fmoc F2/S Hydrogel

5.4.1.1 Rheological studies

Following on from chapter three, where a pool of hydrogels were created ranging from 10-40 mM concentrations of the Fmoc-F_2/S peptides, further substrates were created ranging from 50 to 70 mM. These hydrogels underwent rheological testing as described in section 3.3.2.4 and Table 5.1 illustrates the composition as well as the stiffness properties of these materials. It was decided that the 70 mM hydrogel would be taken forward as the substrate produced a hydrogel of 38.8 kPa, which is believed to be in the stiffness range of pre-osteoid bone tissue (Engler *et al.*, 2006). Therefore it was hypothesized that this material may be a suitable choice for culture of cells to promote osteogenic

differentiation. $CD271^+$ MSCs and pericytes will be cultured within a 70 mM gel with the aim of detecting osteogenic differentiation. OPGS were not studied in this chapter as ideally, using a pure population would be beneficial as ideally the outcome would be a homogeneous differentiated cell population. OPGs were shown to express markers associated with osteogenic and stem cells markers as shown in Figure 4.7.

Hydrogel Concentration (mM)	Fmoc-F_2 (g)	Fmoc –S (g)	Volume 0.5 M NaOH (μl)	Sonication/Vortex (minutes)	Stiffness (kPa)
50	0.0534	0.03454	415	15	28.6 ± 14.8
60	0.06415	0.04144	495	17	32.4 ± 3.7
70	0.07484	0.04835	575	20	38.8 ± 1.09

Table 5.1 High concentration hydrogels.
Continuation from chapter three, hydrogels with increased peptide concentration were created and rheologically tested to create a suitable substrate for the use of culturing cells within and to promote an osteogenic response due to the elastic properties of the material.

The chosen 70 mM hydrogel underwent rheological testing again at day 7 to determine the stability of the substrate as a culture medium over time. Figure 5.6 illustrates the rheological values of the 70 mM Fmoc-F_2-S hydrogel at days 1 and 7 by presentation of the G' and G" values signifying the substrate is elastic in nature.

5.3.1.2 HPLC analysis

HPLC was performed on the 70 mM pre –gelation peptide solution as described in section 3.3.2.9 to confirm that the 70 mM pre-gelation peptide solution contained an approximate 50:50 ratio of Fmoc F_2-S peptides as previously examined with the 10- 40 mM peptide solution hydrogels discussed in section 3.4.2.4. As the pre-gelation peptide solution was extremely viscous, SEM and TEM would be troublesome to perform, so HPLC was used to present if this 70

mM solution had similar properties to previous results presented in section 3.4.2.4. Figure 5.7 illustrates the HPLC results obtained from the 70 mM peptide solution.

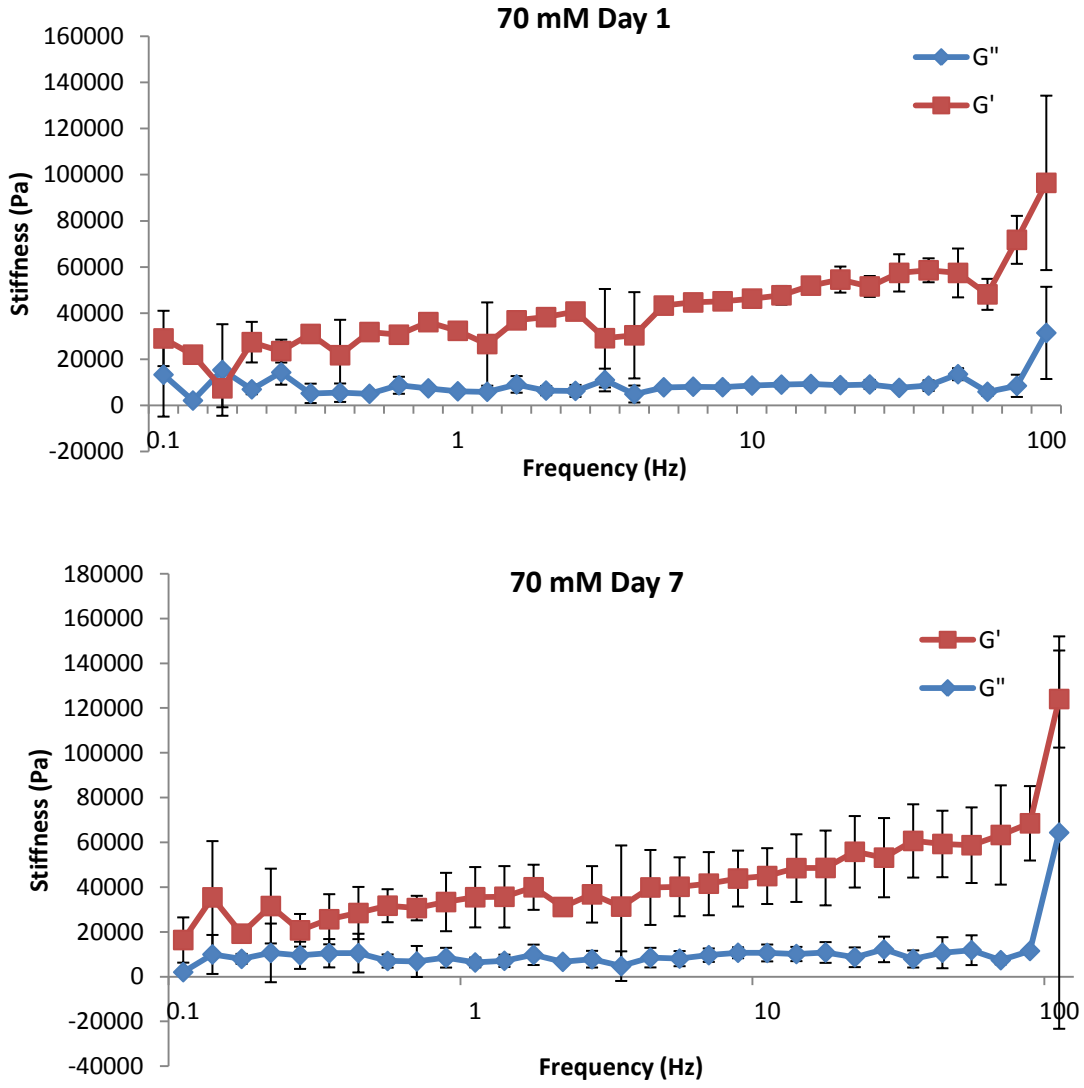

Time point	Stiffness of 70 mM Fmoc-F_2/S Hydrogel
Day 1	38.8 ±1.09
Day 7	43.1 ±11.6

Figure 5.6 70 mM Fmoc F_2/S Hydrogel rheology.
The 70 mM hydrogel underwent rheological study at days 1 and 7 to illustrate the elasticity of the substrate due to time in culture. The elastic modulus shown by G' in red illustrates that the substrate is elastic in nature, forming a hydrogel as this value exceed the G" values in blue which signify the viscous modulus. The stiffness of the hydrogel is measured by averaging the G' values over a frequency of 0.1 to 100 Hertz (Hz). The table which follows presents that the stiffness of the hydrogel increases over time.

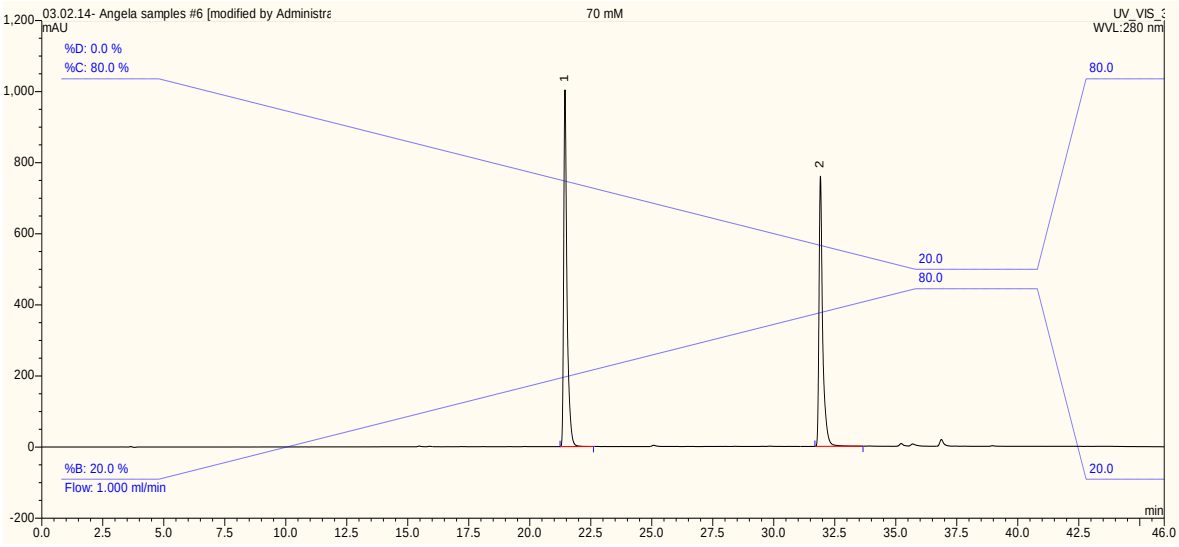

Concentration of Peptide Solution	Percentage of Fmoc-F_2 Peptides	Percentage of Fmoc-S peptides
70 mM	54.37	45.63

Figure 5.7 HPLC data for 70 mM peptide solution.
The first peak observed illustrates the Fmoc-F_2 peptides, with the second smaller peak representing Fmoc-S. The table which follows presents the concentration of each peptide in the 70 mM pepide solution.

The 70 mM Fmoc F_2-S peptide solution confirms that the ratio of Fmoc F_2 to Fmoc S peptides is similar to that observed with the previous pool of hydrogels as discussed in section 3.4.2.4, and that the discrepancies in failure to detect a 1:1 ration may be due to experimental error.

5.4.2 Creation of the Fmoc 3D model

A suitable 3D material to which the stiff 70 mM gel would be injected into was investigated, as ideally it would mimic that of human muscular tissue. Initially a softer Fmoc F_2/S gel was trailed, but the difference between the two gels could not be distinguished in culture and realistically a biological tissue replicate would be used. Hence, type 1 collagen gel was trialled as it is present within connective tissue and the ECM, which plays an important role in force transmission in muscle and ligaments (Kjaer, 2004). Collagen also mimics the

native muscle ECM very closely; however, the native environment contains more than one type of collagen (Macfelda *et al.*, 2007).

5.4.2.1 Measuring stiffness of Collagen gel

Collagen gel was prepared according to section 5.3.2.1 and underwent rheological testing (Figure 5.8) to confirm that this material is stable in cell culture conditions over a period of 7 days as ideally the substrate should withstand long culture studies for regenerative medical studies. Ideally, rheological studies would continue for longer than 7 days, however, the University of Strathclyde do not possess sterile cell culture conditions and hydrogel samples were becoming contaminated after 7 days in culture at this facility.

As the collagen elastic characteristics remain uniform when maintained in cell culture conditions, this material was hypothesised to be a suitable material for creating the 3D gel, which would encapsulate the 70 mM Fmoc hydrogel could be injected. The Fmoc F_2/S hydrogel was then injected into the centre of this collagen gel for further investigation.

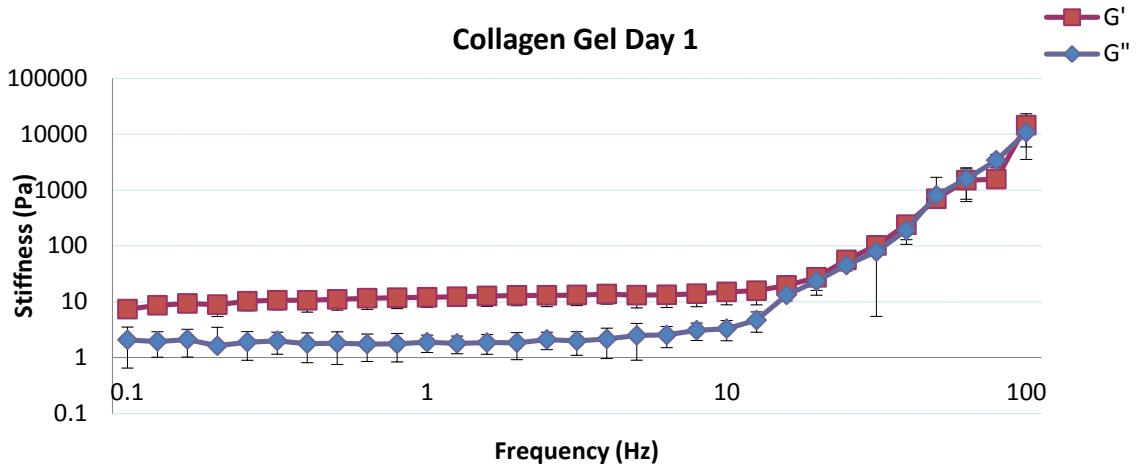

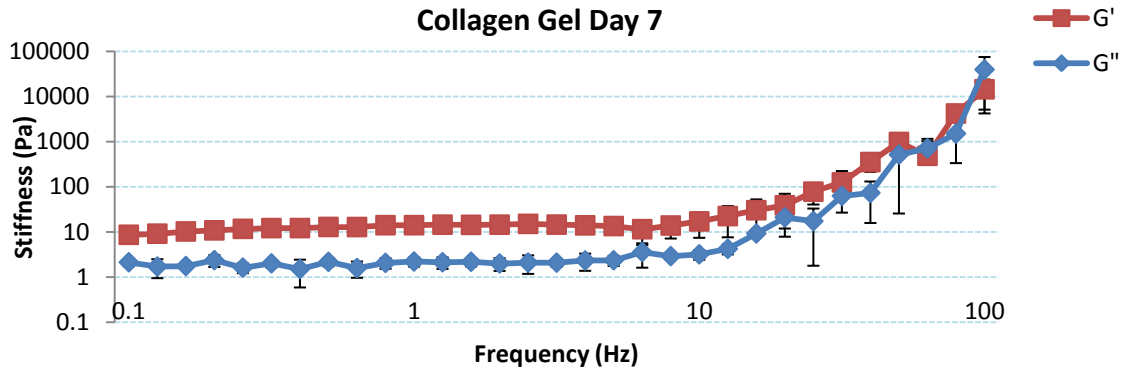

Timepoint	Stiffness of Collagen (kPa)
Day 1	13.08 ± 5.61
Day 7	13.21 ± 2.64

Figure 5.8 Elastic modulus values for collagen substrate at days 1 and 7.
Collagen underwent rheological study to determine if the stiffness of this material changed over a period of 7 days in culture. G' represent the elastic modulus of the hydrogels, with G" signifying the viscous modulus. As G' values shown in red over frequency of 1-100 Hz exceed that of G" shown in blue, the substrate is confirmed to be a hydrogel material rather than a viscous solution.

5.4.2.2 The Collagen-Fmoc 3D Model

In order to create the collagen-Fmoc 3D model, collagen gels were created in ThinCert tissue culture inserts with the addition of 70 mM peptide solution injected into the middle the gel. This created a preliminary model for maxillofacial reconstruction. The collagen was used as a mimic for the mandibular muscle and therefore it needed to be of substantial strength to hold and maintain the hydrogel forming within it. The semi-permeable membrane on the underside of the tissue culture insert was removed and this determined

whether the structure was self-supportive and produced a 3D incorporating material. Figure 5.9 illustrates the collagen-Fmoc-F_2/S complex within the insert, once the insert had been removed.

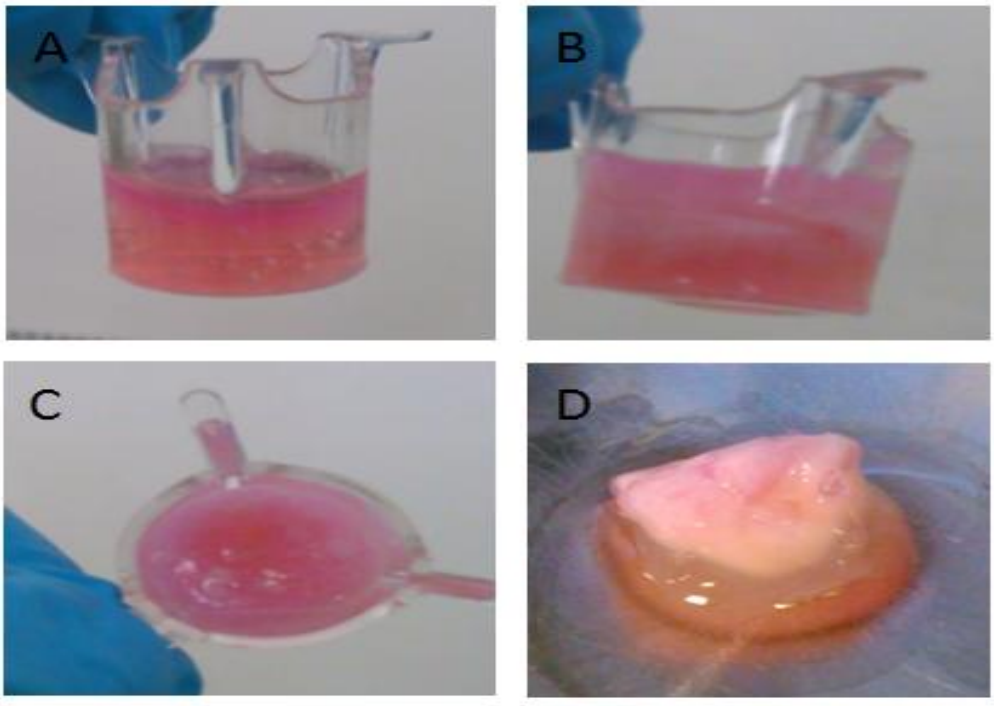

Figure 5.9 Illustrating the Collagen-Fmoc-F_2/ S Hydrogel model
(A) Illustrates collagen only (B) presents gel after injection of 70 mM peptide solution. (C) collagen-Fmoc-F_2- S model taken looking down at the upper surface and (D) the self-supporting 3D collagen –Fmoc hydrogel.

Figure 5.8d presents that when the scaffold is removed from the ThinCert tissue culture inserts, the collagen component does not remain supportive of the injected Fmoc hydrogel. However, as collagen is a natural component of muscle and can be easily used in cell culture, the encapsulating collagen model was retained for use as an *in vitro* for studying differentiation. Further tests were performed with the 70 mM hydrogel, by injecting it into muscle tissue to determine if this material could support the hydrogel.

5.4.2.3 Injecting into muscle model

For regenerative medical purposes for use in maxillofacial reconstruction this gel containing MSCs would be injected into muscle tissue to promote osteogenic differentiation. The proposed scenario is that the section of diseased bone tissue would be removed; a section of muscle excised and rotated into place where the

bone defect was removed. Then, the proposed peptide solution containing desired cell type would be injected this muscle tissue and the material should promote osteogenesis, the cells should commit to this lineage within the hydrogel and ideally, should integrate with the healthy bone tissue retaining the function of the removed diseased bone tissue.

A small incision was made into a piece of muscle material to represent how the peptide solution could be delivered to the patient, and how 37°C culture conditions would affect the setting properties of the 70 mM gel in a tissue mimicking that of the native human muscle. A 500 μl volume of solution without cells was injected into the wound sight, and placed into cell culture incubator for 1 hour. After this time the muscle- gel interaction was monitored and imaged as shown in Figure 5.10. After 1 day in culture, there appears to be some shrinkage of the peptide solution but it did appear fully set and stiff to touch. This supports the initial hypothesis that the gel can form within a defined muscle defect and will set at 37 °C. Further studies will confirm if cell viability is maintained within this high molar concentration Fmoc-F_2/S hydrogel as this would be ideal for the proposed model for use in maxillofacial reconstruction. Overall, this was a successful short-term study to illustrate that the peptide solution could be injected within the tissue and form a hydrogel that was completely set all the way through in the wound site without exiting the muscle tissue.

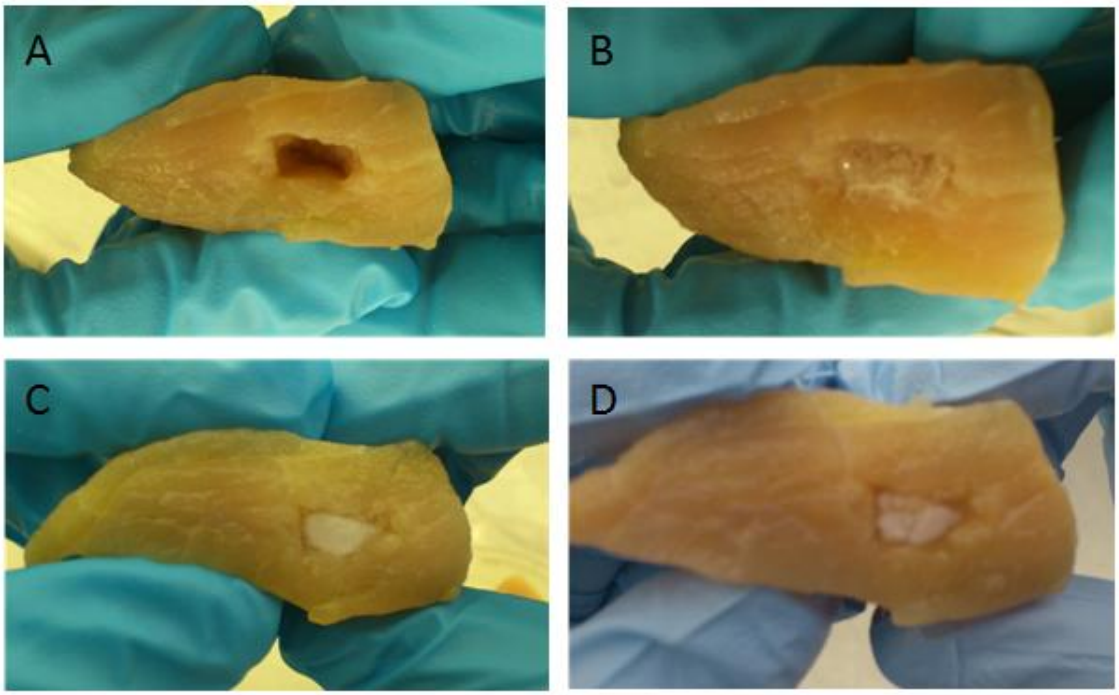

Figure 5.10 Illustration of muscle injection process with 70 mM Peptide solution.
(A) Represents the muscle incision, (B) shows the 70 mM solution filling the incision sit,(C) illustrates the solidified hydrogel after 1 hour in culture and (D) shows the material in the wound site 1 day after injection.

5.4.2.4 Rheological studies

Collagen gels were made as discussed in section 5.3.2.1 and the 70 mM Fmoc F_2-S peptide solution was mixed with MSCs and injected into the pre-formed collagen as described in section 5.3.2.2. Hydrogels cultured were subjected to complete cell culture media or cholesterol sulphate induction media to determine the effect this had on the elastic properties of the 3D model over time.

Rheological studies of the 3D collagen-Fmoc hydrogel model cultured in the presence of complete DMEM media or cholesterol sulphate supplemented media presented that over time in culture, the stiffness of the materials reduces and that the 3D model cultured with complete cell culture media is stiffer after 7 days in culture. However, by 14 days in culture conditions the elasticity of the two hydrogels in question were approximately the same, at 21 kPa.

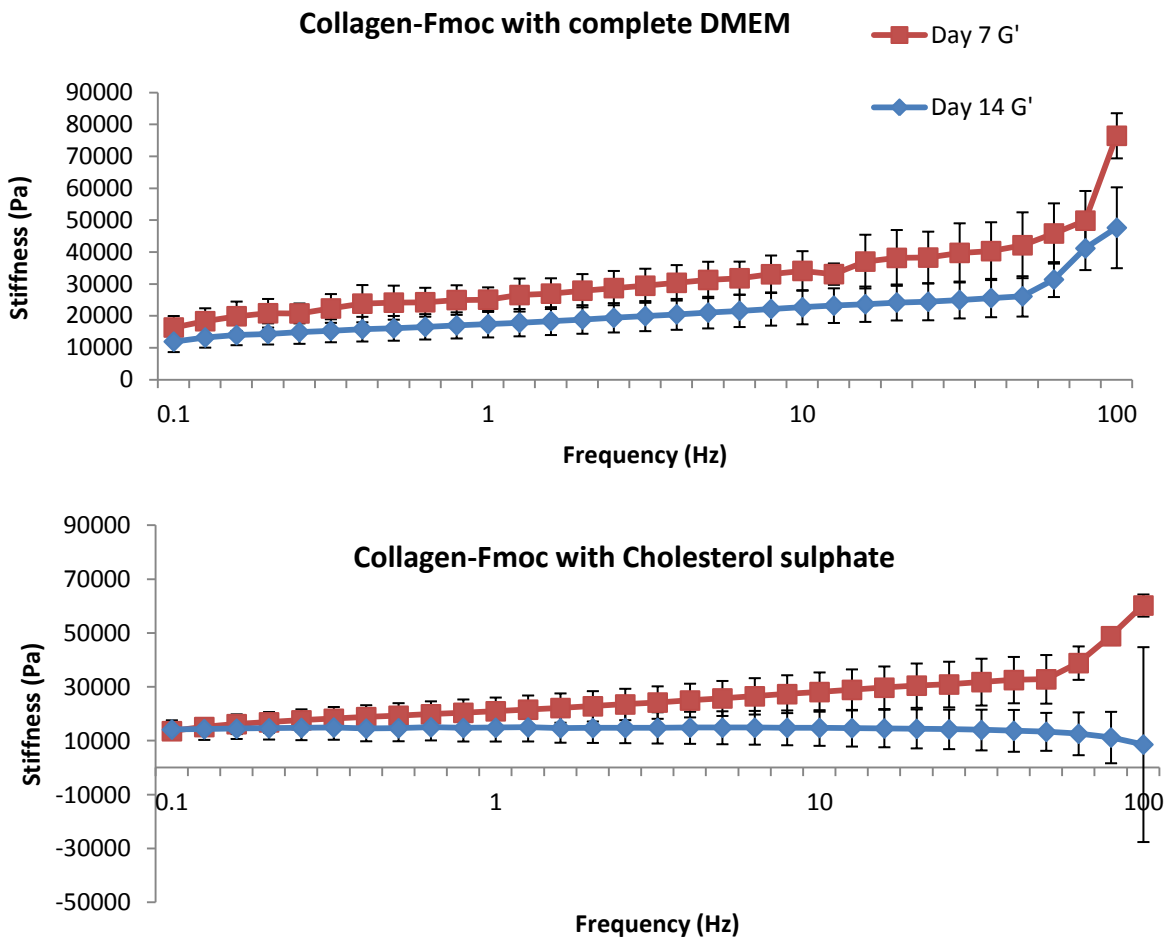

	Stiffness Day 7 (kPa)	Stiffness Day 14 (kPa)
Coll-Fmoc + Cell culture media	31.7 ± 5.9	21.3 ± 4.8
Coll- Fmoc + Cholesterold sulphate media	26.1 ± 5.5	21.7 ± 6.8

Figure 5.11 Hydrogel stiffness with cholesterol sulphate and complete media.
The collagen- Fmoc hydrogels cultured in the absence of cells, in the presence of either complete cell culture media or cholesterol sulphate supplemented media. The elastic modulus as shown by G', is shown for day 7 and day 14 in culture. G' exceeded G" in all studies confirming that the substrate was a gel material rather than a viscous solution.

With reference to the results presented in Figure 5.6, the stiffness of the 70 mM hydrogel after 7 days in culture was 43.1 kPa, whereas when cells were introduced into the Fmoc peptide solution and injected into a collagen hydrogel, after 7 days in culture the stiffness is 31.7 kPa (Figure 5.11). The difference in stiffness between these two substrates is believed to be due to the presence of the collagen surrounding the stiffer 70 mM, therefore resulting in a

heterogeneous sample that may not be illustrating the correct elasticity to which the cells are responding to within the 70 mM hydrogels. Alternative methods of measuring stiffness of specific parts of the hydrogel could be addressed such as nanoindentation. However, this was not performed and would be an aspect to look into in the future.

5.4.3. 3D study with CD271+ MSCs

Gel characterization was complete, and $CD271^+$ MSCs were seeded within the 70 mM peptide solution and injected into the collagen model to determine the effect of the hydrogel stiffness and cholesterol sulphate on the osteogenic potential of this model.

5.4.3.1 Cell Viability

Cell viability of cells within the 3D collagen-70 mM Fmoc hydrogel was measured by extracting DNA from the samples and measuring this to assess cell growth. As discussed previously (section 2.3.6) DNA extraction was possible by precipitating DNA from the organic phase during TRIzol extraction. Cell viability assays were proving troublesome with the Fmoc-F_2/S hydrogels, and due to the stiffer nature of this 70 mM material it was considered that the MTT assay would not be suitable with this substrate. Figure 5.12 illustrates the DNA concentration as a measure of fold change against MSCs cultured upon glass cover slip.

$CD271^+$ MSCs cultured within a 70 mM Fmoc-F_2/S hydrogel, residing within a collagen gel present increased DNA concentrations in comparison to cells cultured on glass cover slips are presented in Figure 5.12. After 14 days in culture, the fold change is greatest between cells cultured with cholesterol sulphate supplemented media, with approximately 198-fold increase in DNA, and cells cultured with complete DMEM media in hydrogel presented 118-fold increase in DNA concentration in comparison to control. DNA content of cells cultured with cholesterol sulphate after 14 days present a significant increase in DNA content at this time point. By 28 days in culture the trend is similar. However, the fold change differences between gels and controls is much lower, with hydrogels cultured with cholesterol sulphate supplemented media and standard DMEM media presenting 7 fold change increase in comparison to glass

control. This data suggests that cells are proliferating within this substrate and that the increase in cell numbers occurs in the first 14 days due to cell proliferation as cells were originally seeded at the same concentration in all samples. As the greatest increase in DNA concentration is observed at 14 days, qRT-PCR was performed in order to link the increase in cell proliferation to differentiation down the osteogenic lineage due to the stiffness of the hydrogel.

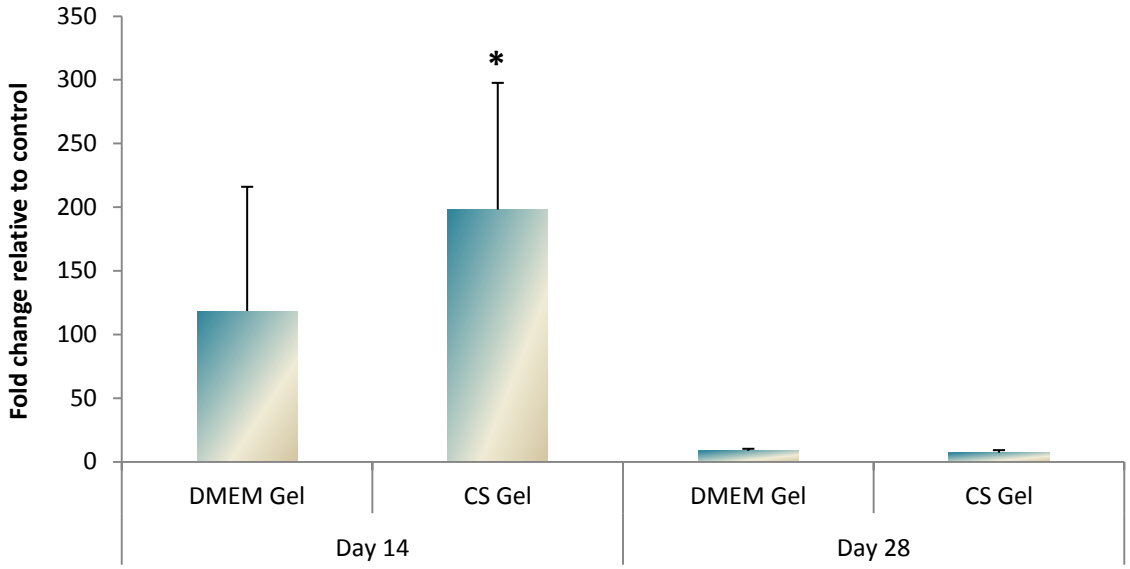

Figure 5.12 DNA Content of MSCs within 3D collagen-Fmoc model.
DNA content of MSCs cultured on hydrogel was normalised to blank hydrogel without presence of cells, and presented as fold change in comparison to glass control. Stars indicate significant difference between groups as determined by one-way ANOVA and Dunn's post hoc test where *P<0.05. Error bars are standard deviation of the mean and n=4 per sample type.

5.4.3.2 qRT-PCR analysis

MSCs positively selected for the CD271 cell surface marker were suspended in the 70 mM Fmoc F_2/S peptide solution and injected into the pre-formed collagen gel. These were then cultured in the presence of DMEM cell culture media or a 0.1 μM cholesterol sulphate supplemented DMEM media. qRT-RNA was extracted at day 14 and 28 as described in section 2.3.5 then, underwent reverse transcription, section 2.3.8, and was subjected to qRT-PCR as presented in section 2.3.9. Figure 5.13 illustrates an accelerated up-regulation of OPN, an osteogenic marker in comparison to glass control by day 14.

OPN is a major cell (contains the RGD motif) and hydroxyapatite binding protein that is synthesised by osteoblast cells, the cell type responsible for bone formation (Reinholt *et al.*, 1990 and Caetano-Lopes *et al.*, 2007). This protein was detected in CD271$^+$ MSCs which were cultured within the 70 mM hydrogel and in the presence of cholesterol sulphate or standard cell culture media. At day 14, the cells cultured in the presence of cholesterol sulphate illustrated a greater fold change of OPN in comparison to those cells cultured with cell culture media. During osteoblast development, the cells initially expresses a moderate level of OPN which falls until 8 days in culture, before increasing up until 28 days as shown in Figure 5.3. Initially, OPN expression appears accelerated with cholesterol sulphate supplemented media and then, by day 28 cells cultured in standard DMEM media catch up. However, both cultures present higher OPN expression than glass control. The levels of OPN are not significantly higher than that of glass control due to large variations within samples, however it is presenting a trend that the 70 mM hydrogel is promoting expression of OPN.

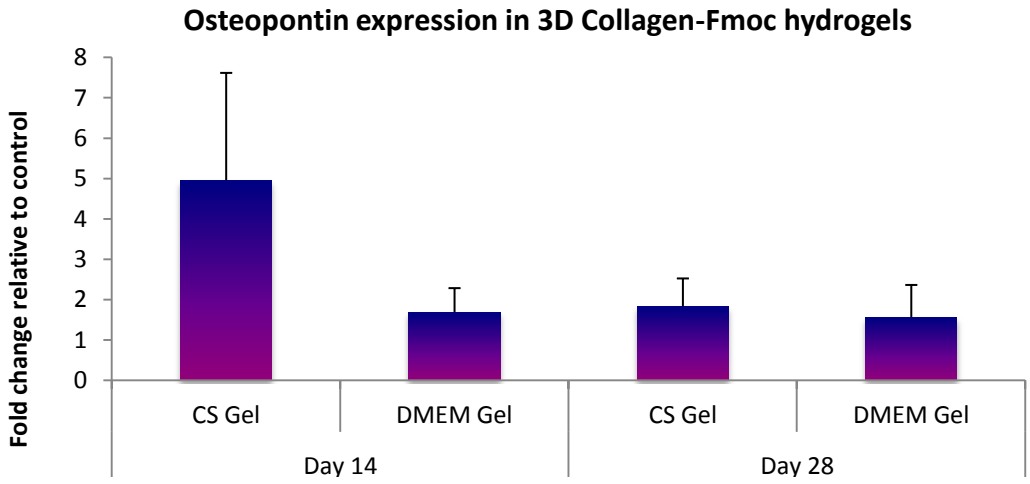

Figure 5.13 Osteopontin Expression of Collagen-Fmoc hydrogels
Osteopontin was detected by means of qRT-PCR within each sample and normalised to CD271$^+$ MSCs cultured on glass coverslips. Statistical significance performed by one-way ANOVA and Dunn's post hoc test; however no significance in samples was noted. Error bars present standard error of the mean and n=4 for all sample types.

5.4.3.3. Von Kossa stain for mineralisation

Von Kossa staining was performed as described in section 5.3.2.7 on hydrogels cultured with complete cell culture media, or cholesterol sulphate supplemented media. As the hydrogel material had previously illustrated the

uptake of immunostaining reagents, the mineralisation detected was compared to a hydrogel substrate in the absence of MSCs, which acted as a blank control.

With CD271$^+$ MSCs, mineralisation was greater than that observed in hydrogels cultured in the absence of cells. With both culture media types, mineralisation increased between 14 and 28 days in culture which is expected due to the detection of OPN by qRT-PCR which is typically synthesized by osteoblast cells, the cell type involved in bone minerlisation (Karsenty *et al.*, 2009). Use of cholesterol sulphate did not present significant results, however, use of this metabolite did give a trend of increased von Kossa stain compared to use of standard DMEM media.

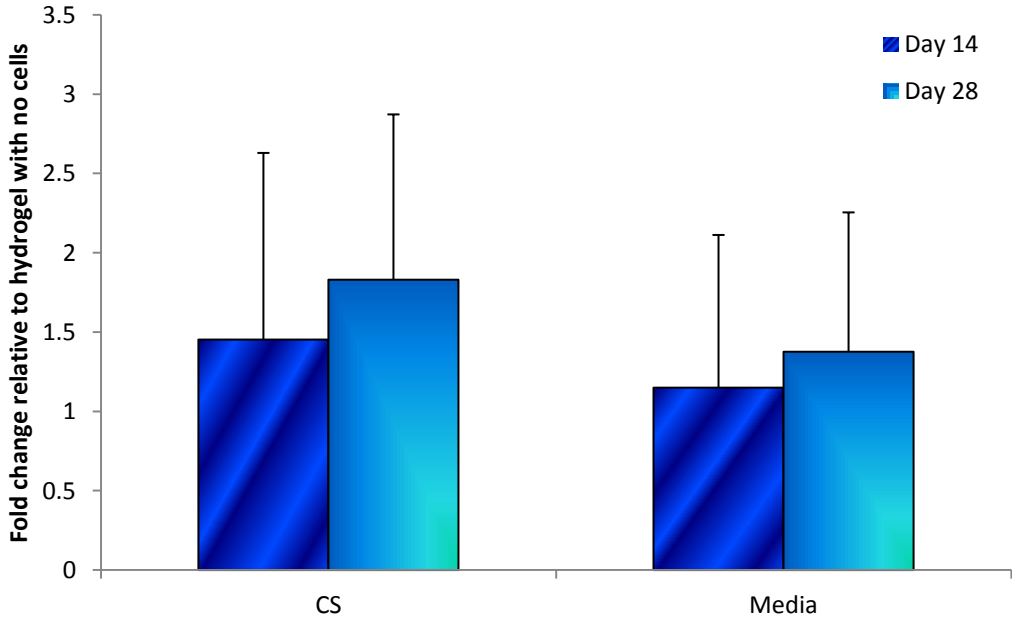

Figure 5.14 Intensity of mineralisation by Von Kossa staining.
Hydrogels were stained, sliced and scanned to view sections of the hydrogel containing the CD271$^+$ MSCs. The intensity of minerlisation due to culture with either cholesterol sulphate (CS) supplemented media or complete cell culture media (Media) was determined by comparing intensity of gels containing cells as fold change to hydrogels cultured under uniform conditions but did not contain CD271$^+$ cells. One-way ANOVA and Dunn's post hoc test was performed, however no significance was noted. Error bars are standard deviation of the mean and n=4 per sample type.

5.4.4 Collagen Fmoc model with Pericyte cell culture

Pericyte cells were incorporated within the 70 mM Fmoc peptide solution to be injected into the 3D collagen model as this cell source represents an autologous multipotent cell source that can give rise to osteoblasts (Crisan *et al.*, 2008).

5.4.4.1 qRT-PCR analysis

As previously described, RNA from within the 70 mM hydrogel was removed by TRIzol extraction, which was reverse transcribed and underwent qRT-PCR analysis to detect expression of markers associated with osteogenic differentiation. Due to the difficulty of extracting RNA from this dense substrate, only three markers associated with bone formation, OPN, OCN and RunX2 were chosen to exemplify if differentiation was occurring within this 3D model. The markers chosen were in line with those associated with the osteogenic lineage.

By means of qRT-PCR a number of markers associated with osteogenic differentiation were detected in pericytes that were cultured within the collagen-Fmoc 3D model either in the presence of complete cell culture or cholesterol sulphate supplemented media. The results presented in figure 5.15 are not statistically significant due to the variation present within the sample population, however a trend can be observed. Generally, the osteogenic markers are up regulated between 14 and 28 days in culture suggesting that osteogenic lineage commitment is progressing, and after 28 days in culture can detect higher OCN levels in pericytes cultures with cholesterol sulphate indicative of matrix mineralisation as presented by Figure 5.3. Overall, the osteogenic markers are up regulated more so in pericytes cultured with cholesterol sulphate supplemented media, than cells cultured in standard cell culture media in the 3D 70 mM culture environment.

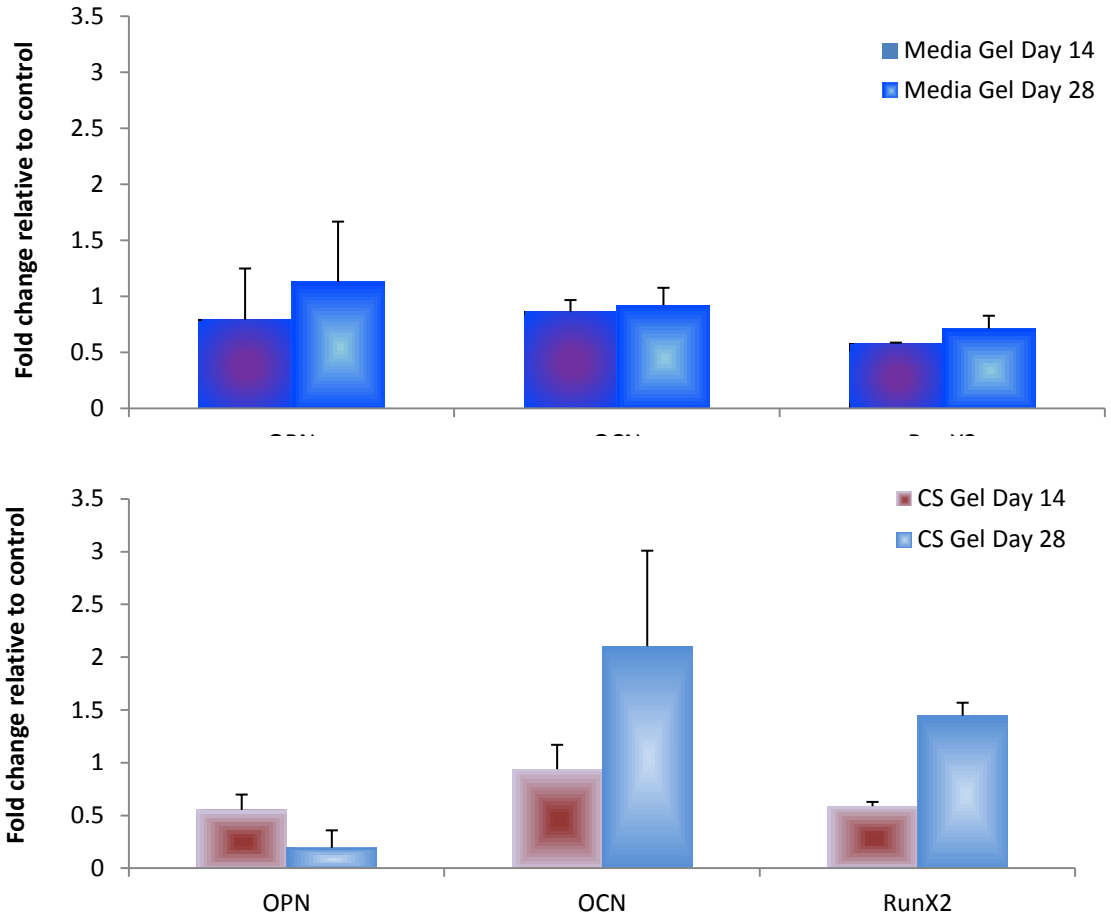

Figure 5.15 Up regulation of markers from pericytes cultured within the Collagen-Fmoc hydrogel. Osteogenic markers were used to detect pericyte differentiation towards the osteogenic lineage. One-way ANOVA and Dunn's post hoc tests were performed; however no statistical significance was noted. Error bars are standard deviation of the mean and n=4 per sample type.

5.4.4.2 Von Kossa mineralisation

Von Kossa staining was performed as described in section 5.3.2.7, and gels were sliced, scanned and analysed using Image J software. The average density measurement was used to detect the amount of mineralization present within each section of sliced hydrogel. All samples were normalized to the intensity observed in hydrogels that were cultured without cells, either cholesterol sulphate or DMEM cell culture media and presented in Figure 5.16.

Von Kossa staining is commonly used to represent phosphate mineralisation due to presence of bone formation. Pericytes within the hydrogels illustrated increased mineralization between days 14 and 28, but the presence of

cholesterol sulphate did not present greater staining intensity than cell culture media alone. In comparison to control hydrogels, culture with cholesterol sulphate resulted in a significant increase in mineralisation at days 14 and 28, with culture media only inducing a significant increase in mineralisation at day 28 time point.

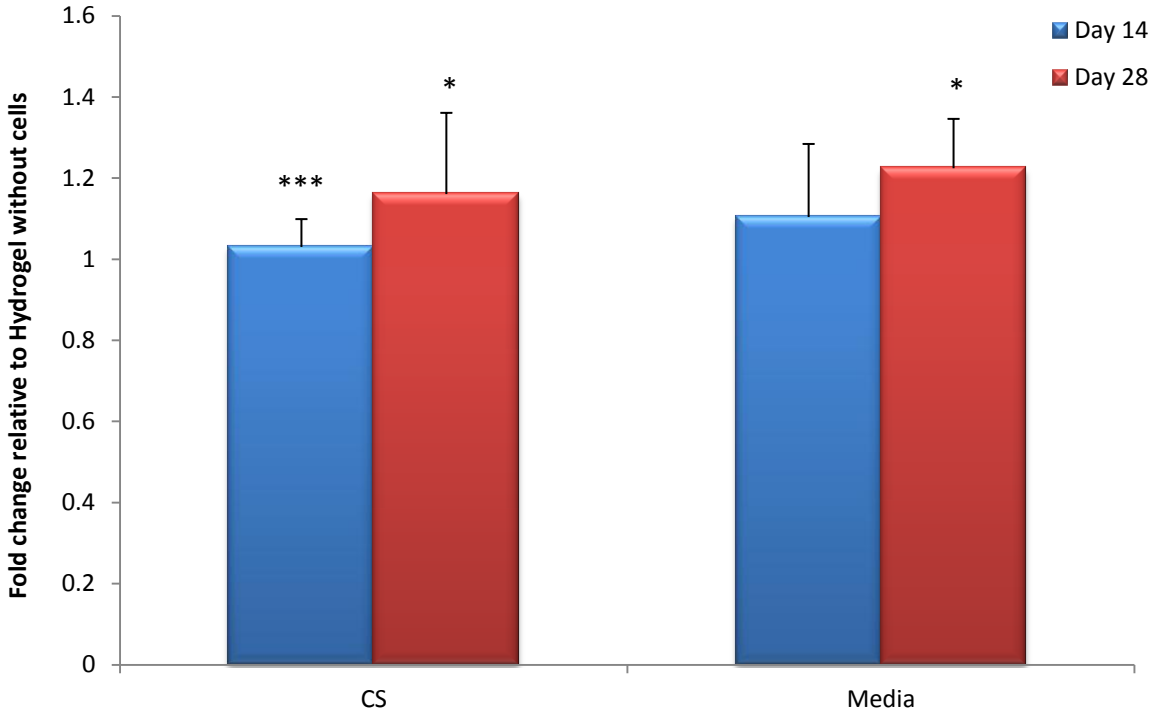

Figure 5.16 Intensity of mineralisation by Von Kossa Staining.
Hydrogels were stained, sliced and scanned to view sections of the hydrogel containing the pericyte cells. The intensity of mineralisation due to culture with either cholesterol sulphate supplemented media or complete cell culture media was determined by comparing intensity of gels containing cells as fold change to hydrogels cultured under uniform conditions but did not contain pericyte cells. One-way ANOVA and Dunn's post hoc test statistical tests were performed, however no significance was noted. An unpaired TTest with Welch's correction was performed to determine if mineralisation intensity differed between cells in gel and blank hydrogel. For this test, *P<0.05 and *** of P<0.001. Error bars are standard deviation of the mean and n=4 per sample type.

5.5 Limitations

The dense 70 mM Fmoc hydrogel proved troublesome in some aspects of this study for creating a suitable 3D model for the purposes of maxillofacial reconstruction. This was because the method for extracting RNA was not 100% effective at dissolving the gels as it had previously been when used with the

softer 20 mM hydrogels. As a result very little RNA was extracted from the hydrogels and this was the reasoning as to why only OPN was tested with $CD271^+$ MSCs in section 5.4.3.2. Alternative methods of isolating RNA would be beneficial as the hydrogel formed is a strong complex structure and appears to not be as dissolvable in TRIzol reagent as previously studied hydrogels has been.

5.6 Conclusion

Overall, this chapter presents the creation of a high concentration Fmoc-F_2/S hydrogel which was coupled with collagen as a prospective model for the use in maxillofacial reconstruction surgeries. By creating a collagen gel, and injecting a 70 mM Fmoc hydrogel mixed with cells into this material, the aim was to induce osteogenic differentiation and detect mineralisation and markers associated with bone lineage commitment. The culture of hydrogels in the presence of cholesterol sulphate was also investigated to observe the effects on bone formation this biological compound had. Fmoc hydrogels were cultured with $CD271^+$ MSCs as well as pericytes to identify the most favourable cell source for further use.

With $CD271^+$ MSCs, DNA content was used to measure cell viability over time, at 14 and 28 days in culture. It was discovered that after 14 days, DNA content in comparison to glass control was higher than controls when cultured in presence of cholesterol sulphate and standard cell culture media. By 28 days, culture with both media types promoted an increase in DNA content, as shown by Figure 5.12. The large fall in DNA measurements between time points can be put down to experimental error or contamination with RNA which would tie in with the reasoning behind the low RNA extracted from the hydrogels before performing qRT-PCR. The results may also suggest cell proliferation has ceased in the hydrogels and that now the cells are undergoing matrix mineralization as what would be expected as shown by Figure 5.3. qRT-PCR detected expression of OPN, a marker associated with osteoblasts which is found in the ECM of mineralised bone and suggests bone differentiation has occurred. This finding alongside Von Kossa staining for matrix mineralisation also confirmed this as cells cultured with cholesterol sulphate presented higher intensity in comparison to cells cultured with complete cell culture media only.

Pericytes were also mixed with the 70 mM peptide solution and injected within a collagen gel. qRT-PCR analysis was used to detect a number of osteogenic markers and it was discovered that cells cultured with cholesterol sulphate supplemented media up regulated the chosen osteogenic marker more so than pericytes cultured with standard DMEM cell culture media. These findings suggest that this metabolite is promoting osteogenic differentiation, however due to the variation within the sample population the results were not statistically significant. Von kossa mineralisation steadily increased as time course study progressed in the presence of both media types, however, culture with cholesterol sulphate resulted in significantly higher levels particularly at day 14 which would indicate that cells were differentiating and mineralising the culture substrate.

Overall, this chapter concludes a preliminary study where a high concentration peptide solution mixed with $CD271^+$ MSCs or pericytes was injected into a collagen tissue mimic, to induce osteogenic differentiation to determine if this was a suitable candidate scaffold for use in maxillofacial reconstruction. Osteogenic markers were detected with both cell population, and it was suggested that cholesterol sulphate did induce a higher osteogeneic response in $CD271^+$ MSCs as shown by increased OPN expression (Figure 5.13). With regards to culture with pericyte cells, cholesterol sulphate induced increased expression of OCN and RunX2 (Figure 5.15). With both cell types, mineralisation was not greatly increased by the presence of cells with cholesterol sulphate supplemented media, or complete DMEM media. This may be because mineralisation was not fully established as the cells had not begun to lay down new ECM as osteogenic differentiation was not fully established. It could be proposed that as the 40 kPa stiffness range is osteogenic itself (Engler *et al.*, 2006), the use of cholesterol sulphate only augments bone response. In order to validate the qRT-PCR results, further investigation into protein or matrix production would be required to validate what is observed.

Chapter 6

Discussion

6.1 General Introduction

This thesis investigated the elastic modulus properties of Fmoc F_2/S hydrogel materials on the guidance and maintenance of MSC differentiation. A potential pool of hydrogels was developed following on from the research by Jayawarna *et al.*, 2007 whereby elastic modulus was modified by increasing short chain peptide concentration rather than employing a pH approach to modify the stiffness properties of this culture substrate.

By employing techniques such as qRT-PCR and immunocytochemistry, two cell populations were initially defined from bone marrow tissue, the $CD271^+$ MSCs and the OPG MSCs, both of which were multipotent as confirmed by differentiation down the adipogenic and osteogenic lineages, however the cell populations were overall, heterogeneous in nature. These cells were used throughout this research project and were cultured with the hydrogel substrate in two and three dimensions with the aim of mimicking the MSC niche environment, with the 2D environment aiming to resemble that of the endosteal niche, and by culturing in 3D recreating the sinusoidal niche, both of which are described by Ehninger & Trump., 2011. It was believed that the stiffness properties of the hydrogels were the sole effecter in influencing the MSC phenotype, however, it is now understood that other factors play a role in cell differentiation with this culture substrate. After initial investigation with 10 mM and 20 mM hydrogels, further investigation was performed into the development of a 3D model for use in the regenerative medical field, more specifically for maxillofacial reconstruction surgeries. Again, qRT-PCR was utilised, alongside mineralisation studies to provide an introduction for the further development this material requires if it is to be taken forward for human trials. Studies into ECM matrix production as well as utilising Western blotting could be used to confirm the results by qRT-PCR and Von Kossa staining.

This chapter goes on to scrutinise the outcomes of the obtained results and also explores a number of ideas that may go towards resolving some of the questions raised.

6.2 Differentiation due to hydrogel elasticity

Self-assembled Fmoc-F_2/S hydrogels have a surface topography as observed by SEM and TEM imaging (Figures 3.9 and 3.10), but this feature was not optimised in this thesis, as the main focus was on creating a hydrogel pool with a range of elastic modulus properties to mimic human tissue. It would have been beneficial to obtain more information regarding the hydrogel topography as this thesis suggests that the cells are differentiating due to the nanotopography of the fibres as well as well as the overall hydrogel elasticity. MSC differentiation studies with stiffness alone could be performed with a hydrogel substrate that does not form fibres and therefore the cells would be responding to the elasticity rather than individual fibres. Cell morphology of cells cultured upon the 10 and 20 mM hydrogels appeared rounded in morphology (Figures 4.11, 4.19 and 4.20) suggesting cells are constricted in a pseudo 3D environment which effect how the cells are spreading on the upper surface of the gels. Cell morphology in the 2D low stiffness hydrogels of 10 and 20 mM concentrations resembles that of cells that have been encapsulated and imaged in a 3D culture (Parekh *et al.*, 2011). The morphology of such cells differs again in comparison to cells cultured upon glass, pits and grooves and previously described nanopatterns (Dalby *et al.*, 2006a, b; McMurray *et al.*, 2011; Biggs *et al.*, 2010), which are also 2D substrates. Cell morphology can therefore be modified due to the 2D culture substrate that MSCs are cultured upon. The presence of Fmoc-F_2 nanofibres may constrain the cells and therefore has an effect on the adopted morphology, and lowering substrate elasticity may further reduce intracellular tension and hence modulate phenotype markers observed on the hydrogels in chapters 4.

It is noted that while it is stiffness that is described to tune MSC fate as illustrated by sections 1.9.2.2, 4.1.2 and Kilian *et al.*, 2009, changes of topography from fibre density may also have effect. Topography and elastic modulus both play an important role in cell differentiation (Discher *et al.*, 2005; Yim *et al.*, 2010) and this may explain why a heterogeneous cell population arises due to culture with these hydrogel substrates, which was observed in chapters 4 and 5. The Fmoc hydrogels in this thesis are not formed with 100% uniformity unlike a fabricated substrate like that used by McMurray *et al.*, 2012.

Therefore, variation can arise throughout the hydrogel preparation process and the fibres self assemble uniformly, however the pattern they take within the gel cannot be pre-defined.

6.3 2D and 3D culture environments

$CD271^+$ MSCs, OPGs and pericytes were cultured upon Fmoc-F_2/S hydrogels in 2D and 3D studies to mimic the endosteal and sinusoidal aspects of the bone marrow niche respectively (Huurne., 2010 and Di maggio *et al*., 2011). In 1972, Elsdale and Bard described a 3D model culture system of fibroblast cells in a collagen gel to induce changes in fibroblasts that would mimic the connective tissue cells in vitro (Elsdale & Bard., 1972). This was one of the first 3D experiments performed to determine how 2D and 3D studies affect cellular behaviour. MSCs are commonly cultured in 2D such as in a monolayer, but this method has difficulty in maintaining the self-renewal properties in vitro (Gerecht-Nir *et al*., 2004). In human tissues, cells are embedded in a 3D environment that promotes a cell morphology that differs from monolayer cell cultures. However, relatively little is known about the cell-matrix adhesive structures formed in 3D living tissues (Cukierman *et al*., 2001).

6.4 Mesenchymal and pericyte stem cells

MSCs are a multipotent stem cell population and are of great interest in the field of tissue engineering due to their regenerative properties, manipulability and relative ease of isolation (Rosenbaum *et al*., 2008). However, a number of problems have arisen such as the inability to obtain large population numbers when extracted from the body and inability to expand this population *in vitro*. These problems are due to the removal of the MSCs from their native environment which may alter their naïve characteristics, with *ex vivo* manipulation causing loss of MSC markers and acquisition of new ones due to the new culture environment (Jones *et al*., 2008). Due to these limitations, there is great interest in obtaining stem cells from sources other than that of the human bone marrow. Thus, in order to meet demands for enhancing research in the regenerative medical field, stem cells have been identified from a number of different tissues such as adipose, muscle and pancreas tissue (Wilson *et al*., 2011; Wu *et al*., 2010 and Smukler *et al*., 2011).

Pericytes are perivascular cells and are associated with the vasculature system therefore providing a cell source that is easily accessible and can be collected from adipose tissue, in a less traumatic manner than that of MSCs derived from the bone marrow (Lee *et al.*, 2004). The exact MSC phenotype is ill defined by physical, phenotype and functional properties (Ho *et al.*, 2008) with a number of cell markers associated with multipotency such as CD271, Stro-1, CD166 and CD63, and stem cells derived from various tissues may not possess uniform surface markers and as a result may behave differently in response to culture substrates and biomaterials.

This thesis began with the use of $CD271^+$ and OPG MSCs, both of which were derived from human bone marrow; however, pericytes were then incorporated with 2D and 3D studies to determine if the hydrogels promoted a heterogeneous cell population arising as this was observed with the former cell populations (as described in chapter 4). There is much debate with regards to classifying pericytes as MSCs, but as they are isolated based on the cell surface marker profile $CD146^+$ and $CD46^-$ they possess multilineage differentiation capacity (Covas *et al.*, 2008; Blocki *et al.*, 2013) and have shown to commit to a lineage in response to the Fmoc-F_2/S hydrogels. High levels of expression of CD146 from cells derived from bone marrow has indicated that these cells can commit to the vascular smooth muscle lineage (Espagnolle *et al.*, 2014) suggesting that there is a possible link between pericytes and sub populations of MSCs. Crisan *et al.*, 2008 describe the connection between MSCs and pericytes, and suggest that MSCs are derived from a subset of perivascular cells. Pericytes cultured in 2D and 3D in this thesis displayed mixed phenotypes as presented by expression of a number of lineage markers, but this may be caused by the incomplete dispersion of cells within the gels as well as cells undergoing hydrogel remodelling and potentially differentiating in this culture substrate. However, this remodelling theory has yet to be confirmed. Pericytes as well as $CD271^+$ MSCs were taken forward in chapter 5 to study the extent of osteogenic differentiation in response to a 70 mM hydrogel and to examine the most effective cell population for further potential studies into this 3D model.

6.5 Biomimetic materials for tissue engineering

The field of biomimetics involves the development of new technology through the transfer of function from biological systems, and is an expanding field illustrated by the increase in number of publications relating to this research area since 1995 (Lepora *et al.*, 2013). A biomimetic construct for use in the tissue engineering field would ideally mimic the multidimensional hierarchical structure of the native tissue (as reviewed by Porter *et al.*, 2009 and Stevens & George., 2005) whether that is an environment to maintain MSCs in their multipotent, self-renewal state, or one that mimics that of a particular tissue such as bone and which will promote MSC differentiation towards the osteogenic lineage. Niches are believed to control stem cell proliferation, quiescence and mobility out of the niche environment in response to cues from the external environment, as discussed in section 1.6, and such niches are predicted to be present in most adult tissues (Doorn *et al.*, 2012). It would be beneficial to identify aspects of the niche that contribute to self-renewal and to use these for *in vitro* studies for MSC proliferation so that a large population of stem cells can be produced from a relatively small patient sample. These could theoretically be stored and used when a patient requires them due to injury or disease.

In response to external signals such as chemokines and cytokines, MSCs can exit the niche and locate to an injury site, a process referred to as MSC homing. During this process, cells leave the niche, migrate and engraft in the tissue that is damaged, and can differentiate and incorporate within this new environment (Yagi *et al.*, 2010). This new location will have properties different to that of the niche and therefore will have an effect on the behaviour of these cells and promote MSC differentiation to occur, as was observed in the study by Gilbert *et al.*, 2010 when muscle stem cells were transplanted into damaged muscle tissue and contributed to repair after culture upon a hydrogel maintaining the stem cell phenotype. While the niche may maintain the MSC phenotype, biomimetic materials will need to incorporate a number of factors for mimicking native niche properties (Dellatore *et al.*, 2008), as well as that of a desired tissue type such as that of bone.

A number of aspects whereby the ECM can be mimicked to maintain the MSC phenotype were discussed in 1.9.1. Specifically, nanotopography such as nanogrooves and pits on a substrate material has been shown to affect the phenotype and behaviour of a cell such as its morphology and ability to spread on the substrate surface. Research by the Cell Engineering research group at the University of Glasgow has demonstrated that nanotopography in a square nanopit pattern promotes long-term multipotency by retention of the MSC markers Stro-1 and ALCAM. However, a similar nanopattern with a nanopit offset of ± 50nm elicited a different response where MSCs differentiated into osteoblasts with the detection of OPN and OCN and the loss of Stro-1 and ALCAM over time (McMurray *et al.*, 2011). Therefore, this presents the use of two desirable nanotopographies for use in biomimetic materials which is beneficial as cells can be removed from the substrate maintaining the MSC phenotype and cultured upon the square topography to induce differentiation.

Mechanical properties of the culture substrate have also been investigated to promote self-renewal or cell commitment to a specific cell lineage. In current research, a culture substrate composed of polyacrylamide gel was altered to produce a material of different degrees of stiffness which influenced cell differentiation. In this study, cells cultured upon a stiff gel resulted in an osteogenic phenotype (Engler *et al.*, 2006). However, stem cells such as muscle stem cells and MSCs can respond to mechanical properties and maintain their self-renewal phenotype as discussed by Gilbert *et al.*, 2010 and Winer *et al.*, 2009 with the latter presenting that MSCs cultured upon polyacrylamide of 250 Pa, a modulus similar to that of marrow, remained in a quiescent state but still are able to differentiate in response to appropriate cues. Ideally, a biomimetic material would mimic the elasticity of the niche or desired tissue to induce the desired cellular response.

A biomimetic material for self-renewal or differentiation promotion should possess a suitable environment such as the correct density of ligands to which cells will adhere to via integrin receptors. The Spatz research group have patterned substrates with 8 nm adhesion islands to promote single cell binding as the integrin diameter is between 8-12 nm in size. It was found that ligand spacing exceeding 70 nm prevents effective integrin clustering, resulting in

inability to form stable focal adhesions and actin fibre networks therefore preventing full cell spreading. However, adhesion islands 28 to 58 nm apart allow cells to attach and spread on the substrate (Huang *et al.*, 2009 and Arnold *et al.*, 2004).

Nanotopography, substrate elasticity and ligand receptors, all of which have been used to mimic cellular behaviour and aspects of the ECM environment, are sensed by integrin receptors. These integrin receptors support the cell in anchorage and support to the ECM as well as transmitting forces through intracellular cascades that are translated into biochemical signals (Janostiak *et al.*, 2014). With regards to integrins and sensing the mechanical properties of the substrate material, there is a feedback mechanism between the actomyosin complex and the forces at the focal adhesion site (Gardel *et al.*, 2010). As a result, cells on a stiff substrate have high intracellular tension, whereas on a softer material the forces are lower. Therefore, by the MSC remodelling their actin cytoskeleton, the cells adapt their internal stiffness to match the compliance of their substrate material (Solon *et al.*, 2007 and Assosian *et al.*, 2008).

In the native niche, integrins are believed to anchor the cells to the basement membrane (Taddei *et al.*, 2008 and O'Reilly *et al.*, 2008). Integrins control the progression through the cell cycle by tension mediated mechanisms and may be involved in maintaining MSCs in their quiescent state in the niche and when cultured with substrates mimicking niche elasticity such as that described by Winer *et al.*, 2009. The cell cycle consists of four stages, growth phase 1 (G_1), synthesis phase (S), growth phase 2 (G_2) and mitosis (M). MSCs that are quiescent are able to exit the cell cycle, and enter the G_0 phase which is a resting phase where the cells are quiescent and do not divide. ESCs and iPSCs have shown to have a short G_1 phase (Savatier *et al.*, 1994 and Ghule *et al.*, 2011), and HSCs have been found to switch between stages of quiescence and self-renewal by entering and leaving the cell cycle, but in the case of hematopoietic demand these cells can rapidly enter the cell cycle progression once again (Passegue *et al.*, 2005).

As well as controlling adhesion, biomimetics could be used to also promote differentiation to occur in order to influence stem cell commitment. However, in an ideal scenario, one cell culture substrate would be able to promote two cell fates, self-renewal and cell commitment. Stimuli responsive materials (SRMs) have been studied by a number of research groups where light, temperature and enzymes have been utilised to modify the culture substrate to aid in controlling cell behaviour on a substrate (Wirkner *et al.*, 2011; Ebara *et al.*, 2014 and Todd *et al.*, 2007). For example, cells can be cultured, and to promote a desired response such as the process of cell attachment and spreading, SRMs can become activated by removal of a blocking group, and can present a functional group such as the integrin binding peptide RGD to the cells, allowing cellular behaviour to be influenced.

To summarise, biomimetic materials are being designed to incorporate aspects of the niche *in vivo*, in order to be used *in vitro*. In this thesis, current studies in the field with nanotopography, ligands and elastic modulus have been discussed as each has been used to mimic an aspect of the MSC niche. Each study requires the use of integrins, and it is becoming apparent that in order to understand the exact mechanisms involved to stimulate the desired MSC phenotype requires further investigation. However, in this thesis, the culture substrate used focussed on stiffness, although there was underlying nanotopography which may have also played a role in how the MSCs differentiated.

6.6 Translation of biomaterials into a clinical application

The progression from developing a suitable biomaterial to it being used in a clinical application, such as that of the 70 mM Fmoc-F_2/S hydrogel proposed in chapter 5 as a model for maxillofacial reconstruction, requires *in vitro* biocompatibility assays prior to animal studies for biomaterial testing. In some situations, there may not be an adequate non-clinical target for the human clinical application (Hart *et al.*, 2012). However, for maxillofacial reconstruction, animal modelling has been successful using a rabbit model (Naudi *et al.*, 2012 and Alfotawi *et al.*, 2014). A scaffold or biomaterial for use in bone tissue engineering must possess a number of essential requirements such as those highlighted below (Porter *et al.*, 2009):

1. To provide temporary mechanical support to the affected area.
2. Act as a substrate for osteoid deposition.
3. Contain a porous architecture to allow for vascularisation and bone in-growth.
4. Encourage bone cell migration into the scaffold.
5. Supports and promotes osteogenic differentiation in the non-osseous, synthetic, scaffold. A process referred to as osteoinduction.
6. To enhance cellular activity towards scaffold-host tissue integration (osseointegration).
7. To degrade in a controlled manner to facilitate load transfer to developing bone.
8. Must produce non-toxic degradation products.
9. Not induce an active chronic inflammatory response.
10. Must be capable of sterilization without loss of bioactivity.
11. To deliver bioactive molecules or drugs in a controlled manner to accelerate healing and prevent pathology.

Bone tissue engineering in maxillofacial reconstruction has developed from the initial surgeries which involved using the free fibula flap method, to the use of scaffolds, and now development of fillers and cements to induce osteostimulation by incorporation of homogeneous stem cells with a scaffold and bone promoting agents such as BMPs (Schmidaier *et al*., 2007). It is also possible to use native vascularised tissue for OMF surgery. The use of the masseter muscle of rabbits has been described, and this tissue was ossified by injection of calcium sulphate/hydroxyapatite, BMP-7 and MSCs (Al-Fotawei *et al*., 2014). However, the approach taken in OMF surgeries should comply with most of the criteria set out by Porter *et al*., 2009, particularly providing mechanical support to the affected area as this would provide aesthetically the appearance of bone in the facial region and promote osteogenesis.

The use of a 3D model in this thesis is used to study a possible biomaterial that could be used to deliver a patient's own stem cells and bioactive differentiation cues simultaneously to the patient's own vascularised muscle tissue, which could aid in the development of methods to treat OMF defects.

6.7 Conclusion

The demands placed on the field of tissue engineering and regenerative medicine for the repair of damaged or diseased tissues is on the rise, with the proportion of the population over the age of 65 set to rise further in the future. The need for surgeries such as hip and knee replacements will be placed under increasing demand. However, it is not just the elderly population susceptible, as those who are younger are also open to require such surgeries from sports injury or early onset arthritis. However, with regards to these replacement surgeries, extensive research has been undertaken to improve the scaffolds and biomaterials used to ensure the devices implant are retain tissue function and do not fail resulting in subsequent surgeries.

Maxillofacial reconstruction is practised as a result of trauma, cancer, congenital or anatomical reasons (Kretlow *et al.*, 2009 and Petrovic *et al.*, 2012) and recently there have been currently a number of proposed methods for treating such conditionsusing swine animal models as they exhibit similar physical and biological characteristics to that of humans (Mardas *et al.*, 2014). Bone grafts and biomaterials have been utilised in these studies (Flemming *et al.*, 1990 and Copcu *et al.*, 2006). However, many problems involving biocompatiability, regenerative capacity and restoring function and aesthetic appearance have arisen. By harnessing the use of stem cells in such clinical applications, and taking advantage of their differentiation ability, it would be advantageous to obtain a multipotent MSC population from a patient, expand them *in vitro*, and implant them back alongside a suitable scaffold to aid in tissue repair.

This study was investigated in two ways; first MSCs were cultured with soft 10 and 20 mM Fmoc hydrogels hypothesised to mimic the stem cell niche elasticity with the aim of maintaining the MSC phenotype so that a large population of cells could be obtained from one patient sample. Secondly, MSCs were cultured within a higher concentration hydrogel which was in the stiffness range of pre-osteoid bone, with the aim of inducing an osteogenic response and detection of mineralisation which could be used in a clinical setting for maxilofacial repair.
The findings presented within this thesis indicate that the elasticity of the MSC native niche was not completely replicated, and that a heterogeneous cell

population arose by culture in 2D and 3D studies. It is not surprising that various cell markers were detected by qRT-PCR, as it is not possible to distribute the MSC cell population evenly, and cell-cell interactions, separate micro-environments within the hydrogels and substrate remodelling may promote the mixed phenotype profile with $CD271^{+}$, OPGs and pericyte cells. However, it was noted that under certain conditions the CD271 expression could be seen to increase alongside other markers.

Low intracellular tension has been shown to promote MSC differentiation towards lineages associated with soft tissue types such as adipogeneis and neurogenesis. My hypothesis was that an intermediate tension may also promote MSC self-renewal. It is tempting to speculate that the tension felt by cells when cultured upon and within the hydrogel substrates may be promoting interplay between self-renewal and differentiation and hence why a number of MSC and lineage specific markers are observed.
Lastly, the facile nature of creating hydrogel substrates of various concentrations is advantageous for studying MSC differentiation. It is noteworthy that Fmoc hydrogels greater than 20 mM concentrations can withstand culture conditions for long-term experiments as trialed were performed for culture periods exceeding 28 days. This property provides a valuable tool when studying MSCs for regenerative medical applications.

I therefore propose this thesis to be taken as an introductory study into the effects that Fmoc hydrogels have on MSC behaviour, particularly cell differentiation. The work proposes that the hydrogel stiffness is not only affecting cell differentiation, but the nanofibres present which form these gels also play a role. Overall, further studies will need to be carried out in order to address and answer the questions raised in this thesis, such as alternative methods of detecting mineralisation. Many of the problems which arose are related to the hydrogel material as it not able to be stained due to the auto fluorescent protperties of the Fmoc protecting group. The following section will discuss alternative methods and techniques which could be used to develop this hydrogel substrate for further work in regenerative medicine.

6.8 Future work

The data generated throughout this thesis provides scope of further investigation for future work. In particular, the hydrogel substrate requires further development in order to obtain more information with regards to the extent of MSC self-renewal or differentiation in response to substrate elasticity.

6.8.1 Cell culture and characterisation

The multipotent capacity of the MSC population has been described in the literature; however there is currently a number of cell surface markers described which are present on multipotent MSCs, This thesis focussed on the $CD271^+$ cell surface marker as a method by which we could become self-sufficient in isolating multipotent MSCs from a bone marrow aspirate sample. This selection process allowed us to select for a MSC multipotent marker, however, further experiments should have been performed prior to studies with the Fmoc hydrogel culture substrates. The following studies would need to be performed in order to provide answers to the questions into how effective and necessary $CD271^+$ isolation is, as overall results suggest the $CD271^+$ and OPG cell population are heterogeneous and therefore this can explain the mixed populations arising due to culture within and upon these hydrogel substrates.

1. Defining the % of CD271 MSCs in the adherent bone marrow cell population.
2. By use of FACS analysis, is the selection method effective in isolating the CD271 marker only and using FACS to determine other MSC markers on this cell population.
3. How does CD271 expression change over time in culture and on hydrogel substrates? Is the marker lost in culture like other MSCs markers such as STRO-1?

Further work into CD271 characterisation would provide insight into the effectiveness of the isolation technique and may lead to further isolating methods to obtain a “pure multipotent MSC population”. As observed within chapters 4 and 5, the use of an uncharacterised cell population can have downstream effects as a mixed population arises due to culture upon these hydrogel materials. It is therefore unknown at this stage, whether or not the cells or the hydrogels are initiating the mixed cell response. The outcome of this

cell characterisation may point towards using all of the bone marrow adherent population in future hydrogel studies.

Chapter 4 of this thesis examined the effect of substrate stiffness and cell differentiation. Cell morphology on a culture substrate can provide insight into the potential differentiation pathway a cell is committing to. For example, rounded cells are typically associated with the adipogenic lineage, whereas cells commiting to the osteogenic lineage display large focal adhesions and are highly spread. The cells presented in 4.19 and 4.20 are rounded in morphology which suggested they were either committing to the adipogenic or neurogenic lineage, and qRT-PCR supports this. However, future work could look into the possibility of other differentiated cell types such as the MSCs becoming chondrocytes. By means of qRT-PCR, expression of transcription factors such as SOX-9 could be assessed at various time points. This was not performed during the initial experimentation as typically, chondrogenic differentiation requires cell pellet culture conditions and here, cells were cultured upon and within a hydrogel material, hence why chondrogeneic markers were not investigated at this time. Further work would look into a wider range of markers and transcription factors associated with lineages such as myogensis and chondrogenesis. Also, prolonging culture time past 28 days may be beneficial as then, transcripts and cell markers should be established and detectable.

In chapter 4, Figure 4.28 presents the switch in profile of pericytes when cultured in the presence of cholesterol sulphate, a molecule involved in osteogenic differentiation. The presence of cholesterol sulphate in cell culture media has resulted in markers associated with osteogenesis, chondrogenesis and myogenesis expression. These were detected through qRT-PCR, however to provide insight into long term potential of this culture condition, observing matrix production by SEM would be beneficial as could see the time frame required for lineage commitment, and long term culture would determine the over-riding cell population due to substrate stiffness and this metabolite in culture media. Looking into mineral deposits by the cells on these hydrogels would also provide information about the lineage commitment these cells are differentiating towards.

6.8.2 Removal of MSCs from hydrogel substrate

In 2011, McMurray *et al* illustrated how a PCL substrate patterned with 120 nm pits, with a 100 nm depth and 300 nm centre to centre spacing in a square arrangement promoted MSC self-renewal over culture period of 28 days. The cells could be removed from the substrate and then cultured upon glass cover slips and subjected to chemical induction by means of adipogenic and osteogenic media. The MSCs were then shown to differentiate in accordance to the induction media by displaying markers associated with that lineage which were detected by immunocytochemistry. This illustrates that the PCL patterned substrate promoted MSC self-renewal as the differentiation capacity of the cells was maintained. In this thesis, the cells used could not be extracted from the hydrogel substrate due to the intricate self-assembling nanofibres formed between the Fmoc-F_2 and Fmoc-S short peptides. This is a limiting factor with regards to studying the nature of the MSC phenotype which results in response to culture upon and within these hydrogels. Ideally, the hydrogels could be degraded and the cell integrity maintained so that they could be characterised by means of immunocytochemistry and FACS analysis to present the proportion of cells which still present MSC surface markers in comparison to lineage committed cells. Removal of cells from the hydrogel substrate and culture with chemical induction media would confirm that the cells have remained multipotent and still hold the ability to differentiate.

By removing the cells from these hydrogel substrates, the number of techniques that can be used to determine cell behaviour increases. At this moment in time, qRT-PCR is one of anly a few techniques able to be used with these auto fluorescent Fmoc peptide based hydrogels. So far, immunostaining and methods utilising strong reagents is unsuitable with these gels. qRT-PCR was used throughout this thesis as a means to detect changes in expression of transcription factors associated with MSC multipotency and differentiation. However, as this system lacks a suitable comparatible control, the control used throughout was cells cultured on glass coverslips. This has implications as the results observed with qRT-PCR may not be realistic as they are showing up regulation of transcripts in relation to glass. For example, Figure 4.10 illustrates this point, where ß3 tubulin expression may not be increasing as readily on the

hydrogel but in relation to glass, where this marker may be decreasing over time, it would suggest that the 10 mM hydrogel was indeed promoting neurogenic differentiation. Extracting the cells from the gels would be beneficial in order to characterise the cell population arising in response to culture upon and within these hydrogels.

6.8.3 Role of metabolites in self-renewal and differentiation

Yanes *et al.*, 2010 discussed how the metabolite profile of stem cells can be used as an indicator of stem cell fate. MSCs in their undifferentiated state are believed to maintain a quiescent metabolic state, whereas MSCs undergoing differentiation have increased metabolic profiles and signalling as presented in Figure 4.5.

Yanes also identified that ESCs, a pluripotent population, possess a metabolic profile with an increased number of reduced metabolites; however the roles these metabolites play in the continual maintenance of the MSC multipotent state is not fully understood and how differentiation results in a switch off of the self-renewal status. Further investigation would be required by use of an in-depth investigation into the profile of metabolites present on the CD271 MSC population and how the 10 mM hydrogel substrate induces a change in pathways associated with neurogenic differentiation. However, as all niches are associated with nerve fibres, the expression of neurogenic markers such as B3Tubulin may be to do with this matter rather than neural differentiation occurring on the hydrogel substrate. Coupling a metabolic study with a cell study with a further hydrogel substrate would provide insight into the changes in profile over time, and would provide confirmation if the fall in metabolite intensity after 7 days in culture is uniform throughout or confined to the culture with the 0.64 kPa 10 mM hydrogel.

6.8.4 Use of BMPs in bone regeneration studies for OMF Reconstruction model

Following on from the studies described in chapter 5, the incorporation of bone promoting factors such as BMPs could be used to study further osteogenic

differentiation of the cells residing within the 3D collagen-Fmoc-F_2/S construct. BMPs 2-7 are part of the TGF-β superfamily and have been identified in extracts of demineralised bone (Wozney., 2005) and localising in this location aids in the modelling and remodelling of bone by osteoblasts and osteoclast cells (Sykaras & Opperman., 2003). Osteogenin, known as BMP-3, has been shown to stimulate the osteogenic phenotype in a number of cells such as osteoblasts, bone marrow stromal cells and periosteal cells, as well as promoting a chondrogenic phenotype in chondroblastic cells (Vukicevic *et al.*, 1989). From these results, incorporating BMPs with the 70 mM hydrogel may further induce an enhanced osteogenic response with regards to gene expression and mineralisation as shown in figures 5.12-5.15. These proteins may further enhance the osteogenic phenotype of MSCs cultured in the collagen-Fmoc hydrogel model for maxillofacial repair. In the literature, there have been reports that BMPs may be linked to cancer as this family of proteins has a variety of functions. As a small number of patients receiving BMP treatment develop tumours, the overall conclusion appears to be that BMPs may not be directly linked to tumourogenesis or metastasis (Thawani *et al.*, 2010). However, for future studies dealing with OMF reconstruction surgeries due to cancer, use of BMPs may not be ideal and instead further molecules sch as cholesterol sulphate should be studied.

Appendix

Buffers made in house

1. Phosphate buffer saline (PBS)
A single phosphate buffer saline tablet (Sigma Aldrich, UK) was dissolved in 250ml distilled water as per manufacturers instructions and autoclaved prior to use.

2. Antibiotic mix
Antibiotic mix contained 60% v/v L-Glutamine, 35% v/v penicillin streptomysin and 5% v/v Ampotericin B. All reagents obtained from Sigma Aldrich, UK.

3. Trypsin-Versene
Trypsin verse solution contained 0.5% v/v trypsin and versene: 150 mM NaCl, 5 mM KCl, 5 mM Glucose, 10 mM HEPES, 1 mM ethylenediaminetetraacetic acid (EDTA) and 0.5% v/v phenol red indicator adjusted to pH 7.5

4. HEPES saline solution
150 mM NaCl, 5 mM KCl, 5 mM Glucose, 10 mM HEPES and 0.5% v/v phenol red indicator adjusted to pH 7.5

5. Bone marrow transfer media
Transfer media was made with 200 ml PBS, 0.6g EDTA, 10 ml antibiotic mix, 5ml sodium pyruvate and 5 ml non-essential amino acids. Solution was filtered before use.

6. Fixative
A 10 ml volume of formaldehyde (Sigma Aldrich) was added to 90 ml PBS, and kept at 4°C until required.

7. Permeability buffer
10.3 g sucrose, 0.292g sodium chloride, 0.06g magnesium chloride and 0.476g HEPES was dissolved in 100ml PBS. The pH of the solution was adjusted to 7.2 and 0.5ml triton x was added. Solution stored at 4°C until required. All reagents obtained from Sigma Aldrch, UK.

8. 1% BSA in PBS
To 100 ml PBS, 1g of Bovine serum albumin (BSA) was added and solution kept at 4°C for short term use, or frozen at -4°C for long term storage.

9. 0.5% Tween-20
A 0.5ml volume Tween-20 was added to 100 ml PBS solution and kept at 4°C until required.

10. 2% FBS in PBS
A 200 µl volume of foetal bovine serum (FBS) was added to 10 ml PBS solution and stored at -20°C until required.

References

Abul-Haija, Y.M. et al., 2014. Biocatalytically triggered co-assembly of two-component core/shell nanofibers. *Small*, 10(5), pp.973–979.

Agrawal, C.M. & Ray, R.B., 2001. Biodegradable polymeric scaffolds for musculoskeletal tissue engineering. *Journal of Biomedical Materials Research*, 55(2), pp.141–150.

Ahmed, E.M. et al., 2013. An innovative method for preparation of nanometal hydroxide superabsorbent hydrogel. *Carbohydrate Polymers*, 91(2), pp.693–698.

Alexandrova, A.Y. et al., 2008. Comparative dynamics of retrograde actin flow and focal adhesions: Formation of nascent adhesions triggers transition from fast to slow flow. *PLoS ONE*, 3(9).

Alfotawi, R. et al, 2013. Assessment of cellular viability on calcium sulphate/hydroxyapatite injectable scaffolds. *J Tissue Eng*, 4.

Alvarez, K. & Nakajima, H., 2009. Metallic scaffolds for bone regeneration. *Materials*, 2(3), pp.790–832.

Anderson, D.J., Shah, N.M. & Morrison, S.J., 1997. Regulatory Mechanisms in Stem Cell Biology. *Cell*, 88(3), pp.287–298.

Andersson, A.S. et al., 2003. Nanoscale features influence epithelial cell morphology and cytokine production. *Biomaterials*, 24(20), pp.3427–3436.

Ando, W. et al., 2007. Cartilage repair using an in vitro generated scaffold-free tissue-engineered construct derived from porcine synovial mesenchymal stem cells. *Biomaterials*, 28(36), pp.5462–5470.

Anselme, K., 2000. Osteoblast adhesion on biomaterials. *Biomaterials*, 21(7), pp.667–681.

Armulik, A., Abramsson, A. & Betsholtz, C., 2005. Endothelial/pericyte interactions. *Circulation Research*, 97(6), pp.512–523.

Arnold, M. et al., 2004. Activation of integrin function by nanopatterned adhesive interfaces. *ChemPhysChem*, 5(3), pp.383–388.

Assoian, R.K. & Klein, E.A., 2008. Growth control by intracellular tension and extracellular stiffness. *Trends in Cell Biology*, 18(7), pp.347–352.

Atala, A. & Koh, C.J., 2004. Tissue engineering applications of therapeutic cloning. *Annual review of biomedical engineering*, 6, pp.27–40.

Athanasiou, K.A. et al., 1995. In vitro degradation and release characteristics of biodegradable implants containing trypsin inhibitor. *Clinical orthopaedics and related research*, (315), pp.272–281.

Bahado-Singh, R.O. et al., 2013. Metabolomic analysis for first-trimester Down syndrome prediction. *American Journal of Obstetrics and Gynecology*, 208(5).

Baker, M., 2011. Metabolomics: from small molecules to big ideas. *Nature methods*, 8(2), pp.117–121.

Banerjee, A. et al., 2009. The influence of hydrogel modulus on the proliferation and differentiation of encapsulated neural stem cells. *Biomaterials*, 30(27), pp.4695–4699.

Barczyk, M., Carracedo, S. & Gullberg, D., 2010. Integrins. *Cell and Tissue Research*, 339(1), pp.269–280.

Barrera, D. & Zylstra, E., 1993. Synthesis and RGD peptide modification of a new biodegradable copolymer: poly (lactic acid-co-lysine). *Journal of the American Chemical Society*, 115, pp.11010–11011..

Bellis, S.L., Miller, J.T. & Turner, C.E., 1995. Characterization of tyrosine phosphorylation of paxillin in vitro by focal adhesion kinase. *Journal of Biological Chemistry*, 270(29), pp.17437–17441.

Beloti, M.M. & Rosa, A.L., 2005. Osteoblast differentiation of human bone marrow cells under continuous and discontinuous treatment with dexamethasone. *Brazilian Dental Journal*, 16(2), pp.156–161.

Bergers, G. & Song, S., 2005. The role of pericytes in blood-vessel formation and maintenance. *Neuro-oncology*, 7(4), pp.452–464.

Berkes, C.A. & Tapscott, S.J., 2005. MyoD and the transcriptional control of myogenesis. *Seminars in Cell and Developmental Biology*, 16(4-5), pp.585–595.

Bershadsky, A.D., Balaban, N.Q. & Geiger, B., 2003. Adhesion-dependent cell mechanosensitivity. *Annual review of cell and developmental biology*, 19, pp.677–695.

Bianco, P. et al., 2001. Bone marrow stromal stem cells: nature, biology, and potential applications. *Stem cells*, 19(3), pp.180–192.

Biggs, M.J.P. et al., 2009. Interactions with nanoscale topography: Adhesion quantification and signal transduction in cells of osteogenic and multipotent lineage. *Journal of Biomedical Materials Research - Part A*, 91(1), pp.195–208.

Biggs, M.J.P., Richards, R.G. & Dalby, M.J., 2010. Nanotopographical modification: A regulator of cellular function through focal adhesions. *Nanomedicine: Nanotechnology, Biology, and Medicine*, 6(5), pp.619–633.

Blanpain, C., Horsley, V. & Fuchs, E., 2007. Epithelial Stem Cells: Turning over New Leaves. *Cell*, 128(3), pp.445–458.

Blocki, A. et al., 2013. Not All MSCs Can Act as Pericytes: Functional In Vitro Assays to Distinguish Pericytes from Other Mesenchymal Stem Cells in Angiogenesis. *Stem cells and development*, 22(17), pp.2347–55..

Bonab, M.M. et al., 2006. Aging of mesenchymal stem cell in vitro. *BMC cell biology*, 7, p.14.

Booth, C., O'Shea, J.A. & Potten, C.S., 1999. Maintenance of functional stem cells in isolated and cultured adult intestinal epithelium. *Experimental cell research*, 249(2), pp.359–366.

Bosch, P. et al., 2000. Osteoprogenitor cells within skeletal muscle. *Journal of Orthopaedic Research*, 18(6), pp.933–944.

Bosnakovski, D. et al., 2004. Chondrogenic differentiation of bovine bone marrow mesenchymal stem cells in pellet cultural system. *Experimental Hematology*, 32(5), pp.502–509.

Bratt-Leal, A.M. et al., 2011. Incorporation of biomaterials in multicellular aggregates modulates pluripotent stem cell differentiation. *Biomaterials*, 32(1), pp.48–56.

Brighton, C.T. et al., 1992. The pericyte as a possible osteoblast progenitor cell. *Clinical orthopaedics and related research*, (275), pp.287–299.

Bryant, S.J. & Anseth, K.S., 2002. Hydrogel properties influence ECM production by chondrocytes photoencapsulated in poly(ethylene glycol) hydrogels. *Journal of Biomedical Materials Research*, 59(1), pp.63–72.

Bujalska, I.J. et al., 2008. A novel selective 11beta-hydroxysteroid dehydrogenase type 1 inhibitor prevents human adipogenesis. *The Journal of endocrinology*, 197(2), pp.297–307.

Bustin, S.A. & Nolan, T., 2004. Pitfalls of quantitative real-time reverse-transcription polymerase chain reaction. *Journal of biomolecular techniques : JBT*, 15(3), pp.155–166.

Busuttil Naudi, K. et al., 2012. Mandibular reconstruction in the rabbit using beta-tricalcium phosphate (β-TCP) scaffolding and recombinant bone morphogenetic protein 7 (rhBMP-7) - Histological, radiographic and mechanical evaluations. *Journal of Cranio-Maxillofacial Surgery*, 40(8).

Butler. D et al, 2000. Functional Tissue Engineering: The role of Biomechanics. *Journal of Biomechanical Engineering*, 122, pp.570–575.

Caccamese, J.F. & Coletti, D.P., 2008. Deep Neck Infections: Clinical Considerations in Aggressive Disease. *Oral and Maxillofacial Surgery Clinics of North America*, 20(3), pp.367–380.

Caetano-Lopes, J., Canhão, H. & Fonseca, J.E., 2007. Osteoblasts and bone formation. *Acta reumatológica portuguesa*, 32(2), pp.103–110.

Cai, X. et al., 2009. Bone marrow derived pluripotent cells are pericytes which contribute to vascularization. *Stem Cell Reviews and Reports*, 5(4), pp.437–445.

Camacho, D., Fuente, A. & Mendes, P., 2005. The origin of correlations in metabolomics data. *Metabolomics*, 1(1), pp.53–63.

Caplan, A.I. & Correa, D., 2011. PDGF in bone formation and regeneration: New insights into a novel mechanism involving MSCs. *Journal of Orthopaedic Research*, 29(12), pp.1795–1803.

Castelletto, V. et al., 2012. Slow-Release RGD-peptide hydrogel monoliths. *Langmuir*, 28(34), pp.12575–12580.

Cavalcanti-Adam, E.A. et al., 2007. Cell spreading and focal adhesion dynamics are regulated by spacing of integrin ligands. *Biophysical journal*, 92(8), pp.2964–2974.

Chen, C.S. et al., 1997. Geometric control of cell life and death. *Science (New York, N.Y.)*, 276(5317), pp.1425–1428.

Chen, M., Przyborowski, M. & Berthiaume, F., 2009. Stem cells for skin tissue engineering and wound healing. *Critical Reviews in Biomedical Engineering*, 37(4-5), pp.399–421. Available at: http://www.dl.begellhouse.com/journals/4b27cbfc562e21b8,00f1eff12a65576b,097e8bf01f552566.html.

Chen, W. & Tong, Y.W., 2012. PHBV microspheres as neural tissue engineering scaffold support neuronal cell growth and axon-dendrite polarization. *Acta Biomaterialia*, 8(2), pp.540–548.

Cheng, G. et al., 2010. Hydrogelation and self-assembly of Fmoc-tripeptides: Unexpected influence of sequence on self-assembled fibril structure, and hydrogel modulus and anisotropy. *Langmuir*, 26(7), pp.4990–4998.

Cho, Y.R. & Gosain, A.K., 2004. Biomaterials in craniofacial reconstruction. *Clinics in Plastic Surgery*, 31(3), pp.377–385.

Choi, C.K. et al., 2008. Actin and alpha-actinin orchestrate the assembly and maturation of nascent adhesions in a myosin II motor-independent manner. *Nature cell biology*, 10(9), pp.1039–1050.

Choong, P.F.M. et al., 2011. The molecular pathogenesis of osteosarcoma: A review. *Sarcoma*, 2011.

Ciobanasu, C., Faivre, B. & Le Clainche, C., 2012. Actin dynamics associated with focal adhesions. *International Journal of Cell Biology*.

Clarke, B., 2008. Normal bone anatomy and physiology. *Clinical journal of the American Society of Nephrology : CJASN*, 3 Suppl 3.

Clohisy, J.C. et al., 2004. Reasons for revision hip surgery: a retrospective review. *Clin Orthop Relat Res.*, pp.188–92.

Comisar, W.A. et al., 2007. Engineering RGD nanopatterned hydrogels to control preosteoblast behavior: A combined computational and experimental approach. *Biomaterials*, 28(30), pp.4409–4417.

Cooper, L.F. et al., 2001. Incipient analysis of mesenchymal stem-cell-derived osteogenesis. *Journal of dental research*, 80(1), pp.314–320.

Copcu, E. et al, 2006. Long Term Results of the Reconstruction of Maxillofacial Segmental Bone Defects with Bioactive Glass: Presentation of six casese. *Internet journal of Plastic Surgery*, 3(2).

Covas, D.. et al, 2008. Multipotent Mesenchymal Stem Cells obtained from diverse human tissue samples share functional properties and gene expression profile with CD166+ perivascular cells and fibroblasts. *Experimental Hematology*.

Crisan, M., Yap, S., et al., 2008. A perivascular origin for mesenchymal stem cells in multiple human organs. *Cell stem cell*, 3(3), pp.301–313.

Crisan, M., Deasy, B., et al., 2008. Purification and Long-Term Culture of Multipotent Progenitor Cells Affiliated with the Walls of Human Blood Vessels: Myoendothelial Cells and Pericytes. *Methods in Cell Biology*, 86, pp.295–309.

Cukierman, E. et al., 2001. Taking cell-matrix adhesions to the third dimension. *Science (New York, N.Y.)*, 294(5547), pp.1708–1712.

Cukierman, E., Pankov, R. & Yamada, K.M., 2002. Cell interactions with three-dimensional matrices. *Current Opinion in Cell Biology*, 14(5), pp.633–639.

Curran, J.M. et al., 2010. Introducing dip pen nanolithography as a tool for controlling stem cell behaviour: unlocking the potential of the next generation of smart materials in regenerative medicine. *Lab on a chip*, 10(13), pp.1662–1670.

Curran, J.M., Chen, R. & Hunt, J.A., 2005. Controlling the phenotype and function of mesenchymal stem cells in vitro by adhesion to silane-modified clean glass surfaces. *Biomaterials*, 26(34), pp.7057–7067.

Curran, J.M., Chen, R. & Hunt, J.A., 2006. The guidance of human mesenchymal stem cell differentiation in vitro by controlled modifications to the cell substrate. *Biomaterials*, 27(27), pp.4783–4793.

Dalby, M.J., McCloy, D., Robertson, M., Wilkinson, C.D.W., et al., 2006. Osteoprogenitor response to defined topographies with nanoscale depths. *Biomaterials*, 27(8), pp.1306–1315.

Dalby, M.J., McCloy, D., Robertson, M., Agheli, H., et al., 2006. Osteoprogenitor response to semi-ordered and random nanotopographies. *Biomaterials*, 27(15), pp.2980–2987.

Dalby, M.J. et al., 2007. The control of human mesenchymal cell differentiation using nanoscale symmetry and disorder. *Nature materials*, 6(12), pp.997–1003. Available at: http://www.ncbi.nlm.nih.gov/pubmed/17891143.

Dalby, M.J., 2005. Topographically induced direct cell mechanotransduction. *Medical Engineering and Physics*, 27(9), pp.730–742.

Davies, P.F. et al., 1997. Spatial relationships in early signaling events of flow-mediated endothelial mechanotransduction. *Annual review of physiology*, 59, pp.527–549.

Daviss, B., 2005. Growing pains for metabolomics. *The Scientist*, 19(8), pp.25–28.

Dawson, E. et al., 2008. Biomaterials for stem cell differentiation. *Advanced Drug Delivery Reviews*, 60(2), pp.215–228.

Dellatore, S.M., Garcia, A.S. & Miller, W.M., 2008. Mimicking stem cell niches to increase stem cell expansion. *Current Opinion in Biotechnology*, 19(5), pp.534–540.

Denhardt, D.T. & Noda, M., 1998. Osteopontin expression and function: role in bone remodeling. *Journal of cellular biochemistry. Supplement*, 30-31, pp.92–102.

Dickhut, A. et al., 2008. Chondrogenesis of mesenchymal stem cells in gel-like biomaterials in vitro and in vivo. *Frontiers in bioscience : a journal and virtual library*, 13, pp.4517–4528.

Diefenderfer, D.L. & Brighton, C.T., 2000. Microvascular pericytes express aggrecan message which is regulated by BMP-2. *Biochemical and biophysical research communications*, 269(1), pp.172–178.

DiMaio, F.R., 2002. The science of bone cement: a historical review. *Orthopedics*, 25(12), pp.1399–1407; quiz 1408–1409.

Discher, D.E., Janmey, P. & Wang, Y.-L., 2005. Tissue cells feel and respond to the stiffness of their substrate. *Science (New York, N.Y.)*, 310(5751), pp.1139–1143.

Doorn, J. et al., 2012. Therapeutic Applications of Mesenchymal Stromal Cells: Paracrine Effects and Potential Improvements. *Tissue Engineering Part B: Reviews*, 18(2), pp.101–115.

Drury, J.L. & Mooney, D.J., 2003. Hydrogels for tissue engineering: Scaffold design variables and applications. *Biomaterials*, 24(24), pp.4337–4351.

Ebara, M. et al., 2004. Temperature-responsive cell culture surfaces enable "on-off" affinity control between cell integrins and RGDS ligands. *Biomacromolecules*, 5(2), pp.505–510.

Ehninger, A. & Trumpp, A., 2011. The bone marrow stem cell niche grows up: mesenchymal stem cells and macrophages move in. *The Journal of experimental medicine*, 208(3), pp.421–428.

Elsdale, T. & Bard, J., 1972. Collagen substrata for studies on cell behavior. *Journal of Cell Biology*, 54(3), pp.626–637.

Engler, A.J. et al., 2006. Matrix Elasticity Directs Stem Cell Lineage Specification. *Cell*, 126(4), pp.677–689.

Espagnolle, N. et al., 2014. CD146 expression on mesenchymal stem cells is associated with their vascular smooth muscle commitment. *Journal of Cellular and Molecular Medicine*, 18(1), pp.104–114.

Farrington-Rock, C. et al., 2004. Chondrogenic and adipogenic potential of microvascular pericytes. *Circulation*, 110(15), pp.2226–2232.

Fauza, D.O. et al., 1998. Videofetoscopically assisted fetal tissue engineering: Bladder augmentation. *Journal of Pediatric Surgery*, 33(1), pp.7–12.

Fernyhough, M.E. et al., 2007. PPAR?? and GLUT-4 expression as developmental regulators/markers for preadipocyte differentiation into an adipocyte. *Domestic Animal Endocrinology*, 33(4), pp.367–378.

Flemming, A.F. et al., 1990. Mandibular reconstruction using vascularised fibula. *British journal of plastic surgery*, 43(4), pp.403–409.

Flores-Torales, E. et al., 2010. The CD271 expression could be alone for establisher phenotypic marker in Bone Marrow derived mesenchymal stem cells. *Folia Histochemica et Cytobiologica*, 48(4), pp.682–686.

Fraley, S.I. et al., 2010. A distinctive role for focal adhesion proteins in three-dimensional cell motility. *Nature cell biology*, 12(6), pp.598–604.

Fraley, S.I. et al., 2012. Dimensional and temporal controls of three-dimensional cell migration by zyxin and binding partners. *Nature Communications*, 3, p.719.

Franz-Odendaal, T.A., Hall, B.K. & Witten, P.E., 2006. Buried alive: How osteoblasts become osteocytes. *Developmental Dynamics*, 235(1), pp.176–190.

Friedenstein, A.J., Chailakhjan, R.K. & Lalykina, K.S., 1970. The development of fibroblast colonies in monolayer cultures of guinea-pig bone marrow and spleen cells. *Cell and tissue kinetics*, 3(4), pp.393–403.

Friedland, J.C., Lee, M.H. & Boettiger, D., 2009. Mechanically activated integrin switch controls alpha5beta1 function. *Science (New York, N.Y.)*, 323(5914), pp.642–644.

Frith, J.E., Thomson, B. & Genever, P.G., 2010. Dynamic three-dimensional culture methods enhance mesenchymal stem cell properties and increase therapeutic potential. *Tissue engineering. Part C, Methods*, 16(4), pp.735–749.

Fuchs, E. & Chen, T., 2013. A matter of life and death: self-renewal in stem cells. *EMBO reports*, 14(1), pp.39–48.:

Fuchs, E., Tumbar, T. & Guasch, G., 2004. Socializing with the neighbors: Stem cells and their niche. *Cell*, 116(6), pp.769–778.

Gadegaard, N. et al., 2003. Arrays of nano-dots for cellular engineering. In *Microelectronic Engineering*. pp. 162–168.

Gallagher, J.O. et al., 2002. Interaction of animal cells with ordered nanotopography. *IEEE Transactions on Nanobioscience*, 1(1), pp.24–28.

Gardel, M.L. et al., 2010. Mechanical integration of actin and adhesion dynamics in cell migration. *Annual review of cell and developmental biology*, 26, pp.315–333.

Gates, B.D. et al., 2005. New approaches to nanofabrication: Molding, printing, and other techniques. *Chemical Reviews*, 105(4), pp.1171–1196.

Geiger, B. et al., 2001. Transmembrane crosstalk between the extracellular matrix--cytoskeleton crosstalk. *Nature reviews. Molecular cell biology*, 2(11), pp.793–805.

Geiger, B. et al., 2001. Transmembrane extracellular matrix– cytoskeleton crosstalk. *Nature reviews. Molecular cell biology*, 2(November), pp.793–805.

Geiger, B. & Bershadsky, A., 2001. Assembly and mechanosensory function of focal contacts. *Current Opinion in Cell Biology*, 13(5), pp.584–592.

George, R.K. & Krishnamurthy, A., 2013. Microsurgical free flaps: Controversies in maxillofacial reconstruction. *Annals of maxillofacial surgery*, 3(1), pp.72–9.

Gerecht-Nir, S., Cohen, S. & Itskovitz-Eldor, J., 2004. Bioreactor cultivation enhances the efficiency of human embryoid body (hEB) formation and differentiation. *Biotechnology and Bioengineering*, 86(5), pp.493–502.

Gerlier, D. & Thomasset, N., 1986. Use of MTT colorimetric assay to measure cell activation. *Journal of immunological methods*, 94(1-2), pp.57–63.

Ghule, P.N. et al., 2011. Reprogramming the pluripotent cell cycle: Restoration of an abbreviated G1 phase in human induced pluripotent stem (iPS) cells. *Journal of Cellular Physiology*, 226(5), pp.1149–1156.

Gilbert, P.M. et al., 2010. Substrate elasticity regulates skeletal muscle stem cell self-renewal in culture. *Science (New York, N.Y.)*, 329(5995), pp.1078–1081.

Glorieux, F.H. et al., 2002. Osteogenesis imperfecta type VI: a form of brittle bone disease with a mineralization defect. *Journal of bone and mineral research : the official journal of the American Society for Bone and Mineral Research*, 17(1), pp.30–38.

Goodman, S.B. et al., 2013. The future of biologic coatings for orthopaedic implants. *Biomaterials*, 34(13), pp.3174–3183.

Grande, D.A. et al., 1995. Repair of articular cartilage defects using mesenchymal stem cells. *Tissue engineering*, 1(4), pp.345–353.

Grashoff, C. et al., 2010. Measuring mechanical tension across vinculin reveals regulation of focal adhesion dynamics. *Nature*, 466(7303), pp.263–266.

Griffith, L.G. & Naughton, G., 2002. Tissue engineering--current challenges and expanding opportunities. *Science (New York, N.Y.)*, 295(5557), pp.1009–1014.

Griffith, L.G. & Swartz, M.A., 2006. Capturing complex 3D tissue physiology in vitro. *Nature reviews. Molecular cell biology*, 7(3), pp.211–224.

Grimaud, E., Heymann, D. & Rédini, F., 2002. Recent advances in TGF-beta effects on chondrocyte metabolism. Potential therapeutic roles of TGF-beta in cartilage disorders. *Cytokine & growth factor reviews*, 13(3), pp.241–257.

Grinnell, F. & Ho, C.H., 2013. The effect of growth factor environment on fibroblast morphological response to substrate stiffness. *Biomaterials*, 34(4), pp.965–974.

Gruene, M. et al., 2011. Adipogenic differentiation of laser-printed 3D tissue grafts consisting of human adipose-derived stem cells. *Biofabrication*, 3(1), p.015005.

Guilak, F. et al., 2014. Biomechanics and mechanobiology in functional tissue engineering. *Journal of Biomechanics*, 47(9), pp.1933–1940.

Guilak, F. & Baaijens, F.P.T., 2014. Functional tissue engineering: Ten more years of progress. *Journal of Biomechanics*, 47(9), pp.1931–1932.

Guilak, F., Butler, D.L. & Goldstein, S.A., 2001. Functional tissue engineering: the role of biomechanics in articular cartilage repair. *Clinical orthopaedics and related research*, (391 Suppl), pp.S295–S305.

Guler, M.O. et al., 2006. Presentation of RGDS epitopes on self-assembled nanofibers of branched peptide amphiphiles. *Biomacromolecules*, 7(6), pp.1855–1863.

Gurkan, U.A. & Akkus, O., 2008. The mechanical environment of bone marrow: A review. *Annals of Biomedical Engineering*, 36(12), pp.1978–1991.

Hadjidakis, D.J. & Androulakis, I.I., 2006. Bone remodeling. In *Annals of the New York Academy of Sciences*. pp. 385–396.

Hagmann, S. et al., 2013. Different culture media affect growth characteristics, surface marker distribution and chondrogenic differentiation of human bone marrow-derived mesenchymal stromal cells. *BMC Musculoskelet Disord*, 14, p.223.

Haines, L.A. et al., 2005. Light-activated hydrogel formation via the triggered folding and self-assembly of a designed peptide. *Journal of the American Chemical Society*, 127(48), pp.17025–17029.

Hamidouche, Z. et al., 2008. FHL2 mediates dexamethasone-induced mesenchymal cell differentiation into osteoblasts by activating Wnt/beta-catenin signaling-dependent Runx2 expression. *The FASEB journal : official publication of the Federation of American Societies for Experimental Biology*, 22(11), pp.3813–3822.

Hamilton, D.W. & Brunette, D.M., 2007. The effect of substratum topography on osteoblast adhesion mediated signal transduction and phosphorylation. *Biomaterials*, 28(10), pp.1806–1819.

Hardy, R. & Cooper, M.S., 2011. Glucocorticoid-Induced Osteoporosis ? A Disorder of Mesenchymal Stromal Cells? *Frontiers in Endocrinology*, 2.

Harris, W.H., 2001. Wear and periprosthetic osteolysis: the problem. *Clinical orthopaedics and related research*, (393), pp.66–70.

Hart, C.. et al, 2012. *An Introduction to biomaterials* Second. J. . Hollinger, ed., CRC Press.

Hass, R. et al., 2011. Different populations and sources of human mesenchymal stem cells (MSC): A comparison of adult and neonatal tissue-derived MSC. *Cell communication and signaling : CCS*, 9, p.12.

He, L. et al., 2011. pH responsive self-healing hydrogels formed by boronate-catechol complexation. *Chemical communications (Cambridge, England)*, 47(26), pp.7497–7499.

He, S., Nakada, D. & Morrison, S.J., 2009. Mechanisms of stem cell self-renewal. *Annual review of cell and developmental biology*, 25, pp.377–406.

Healy, K.E. & Guldberg, R.E., 1995. Bone tissue engineering. *Journal of musculoskeletal neuronal interactions*, 7(4), pp.328–330. Available at: http://content.wkhealth.com/linkback/openurl?sid=WKPTLP:landingpage&an=00003086-199910001-00008.

Vander Heiden, M.G., Cantley, L.C. & Thompson, C.B., 2009. Understanding the Warburg effect: the metabolic requirements of cell proliferation. *Science (New York, N.Y.)*, 324(5930), pp.1029–1033.

Heimann, R.B., 2013. Structure, properties, and biomedical performance of osteoconductive bioceramic coatings. *Surface and Coatings Technology*, 233, pp.27–38.

Heinmann, , R.B and Lehmann, H.., 2015. *Bioceramic Coatings for Medical Implants: Trends and Techniques*, John Wiley and sons.

Helary, C., Zarka, M. & Giraud-Guille, M.M., 2012. Fibroblasts within concentrated collagen hydrogels favour chronic skin wound healing. *Journal of Tissue Engineering and Regenerative Medicine*, 6(3), pp.225–237.

Henslee, A.M. et al., 2012. Development of a biodegradable bone cement for craniofacial applications. *Journal of Biomedical Materials Research - Part A*, 100 A(9), pp.2252–2259.

Herrmann, H. et al., 2007. Intermediate filaments: from cell architecture to nanomechanics. *Nature reviews. Molecular cell biology*, 8(7), pp.562–573.

Herrmann, H. et al., 2009. Intermediate filaments: Primary determinants of cell architecture and plasticity. *Journal of Clinical Investigation*, 119(7), pp.1772–1783.

Hidalgo, D.A., 1994. Fibula free flap mandible reconstruction. *Microsurgery*, 15(4), pp.238–244.

Hidalgo, D.A., 1989. *Fibula free flap: a new method of mandible reconstruction.*,

Ho, A.D., Wagner, W. & Franke, W., 2008. Heterogeneity of mesenchymal stromal cell preparations. *Cytotherapy*, 10(4), pp.320–330.

Hong, D. et al., 2008. The biological roles of extracellular and intracytoplasmic glucocorticoids in skeletal cells. *Journal of Steroid Biochemistry and Molecular Biology*, 111(3-5), pp.164–170.

Huang, H., Kamm, R.D. & Lee, R.T., 2004. Cell mechanics and mechanotransduction: pathways, probes, and physiology. *American journal of physiology. Cell physiology*, 287(1), pp.C1–C11.

Huang, J. et al., 2009. Impact of order and disorder in RGD nanopatterns on cell adhesion. *Nano Letters*, 9(3), pp.1111–1116.

Humphries, J.D. et al., 2007. Vinculin controls focal adhesion formation by direct interactions with talin and actin. *Journal of Cell Biology*, 179(5), pp.1043–1057.

Humphries, M.J., 2000. Integrin structure. *Biochemical Society transactions*, 28(4), pp.311–339.

Huttenlocher, A. & Horwitz, A.R., 2011. Integrins in cell migration. *Cold Spring Harbor Perspectives in Biology*, 3(9), pp.1–16.

Ter Huurne, M., Figdor, C.G. & Torensma, R., 2010. Hematopoietic stem cells are coordinated by the molecular cues of the endosteal niche. *Stem cells and development*, 19(8), pp.1131–1141.

Hwang, K.-C. et al., 2008. Chemicals that modulate stem cell differentiation. *Proceedings of the National Academy of Sciences of the United States of America*, 105(21), pp.7467–7471.

Idris, A.I., 2010. Cannabinoid receptors as target for treatment of osteoporosis: a tale of two therapies. *Current neuropharmacology*, 8(3), pp.243–253.

Ilizarov, G.A., 1989. The tension-stress effect on the genesis and growth of tissues: Part II. The influence of the rate and frequency of distraction. *Clinical orthopaedics and related research*, (239), pp.263–285.

Ingber, D.E., 2006. Cellular mechanotransduction: putting all the pieces together again. *The FASEB journal : official publication of the Federation of American Societies for Experimental Biology*, 20(7), pp.811–827.

Isern, J. et al., 2013. Self-renewing human bone marrow mesenspheres promote hematopoietic stem cell expansion. *Cell Rep*, 3(5), pp.1714–1724. Isern, J. & Méndez-Ferrer, S., 2011. Stem cell interactions in a bone marrow niche. *Current Osteoporosis Reports*, 9(4), pp.210–218.

Ivaska, J., 2012. Unanchoring integrins in focal adhesions. *Nature Cell Biology*, 14(10), pp.981–983.

Jaiswal, N. et al., 1997. Osteogenic differentiation of purified, culture-expanded human mesenchymal stem cells in vitro. *Journal of cellular biochemistry*, 64(2), pp.295–312.

James, A.W., 2013. Review of Signaling Pathways Governing MSC Osteogenic and Adipogenic Differentiation. *Scientifica*, 2013, p.684736. Available at: http://www.pubmedcentral.nih.gov/articlerender.fcgi?artid=3874981&tool=pmcentrez&rendertype=abstract.

Janoštiak, R. et al., 2014. Mechanosensors in integrin signaling: The emerging role of p130Cas. *European Journal of Cell Biology*.

Jatav, V.S., Singh, H. & Singh, S.K., 2011. Recent Trends on Hydrogel in Human Body. *International Journal of Research in Pharmaceutical and Biomedical Sciences*, 2(2), pp.442–447.

Jayawarna, V. et al., 2007. Three-dimensional cell culture of chondrocytes on modified di-phenylalanine scaffolds. *Biochemical Society transactions*, 35(Pt 3), pp.535–537.

Jones, E. & McGonagle, D., 2008. Human bone marrow mesenchymal stem cells in vivo. *Rheumatology (Oxford, England)*, 47(2), pp.126–131.

Justesen, J. et al., 2004. Mice deficient in 11beta-hydroxysteroid dehydrogenase type 1 lack bone marrow adipocytes, but maintain normal bone formation. *Endocrinology*, 145(4), pp.1916–1925.

Kanchanawong, P. et al., 2010. Nanoscale architecture of integrin-based cell adhesions. *Nature*, 468(7323), pp.580–584.

Kaplan, F.S. et al., 2008. Early diagnosis of fibrodysplasia ossificans progressiva. *Pediatrics*, 121(5), pp.e1295–e1300.

Karsenty, G., Kronenberg, H.M. & Settembre, C., 2009. Genetic control of bone formation. *Annual review of cell and developmental biology*, 25, pp.629–648.

Kennea, N.L. & Mehmet, H., 2002. Neural stem cells. *The Journal of pathology*, 197(4), pp.536–550.

Keselowsky, B.G., Collard, D.M. & García, A.J., 2005. Integrin binding specificity regulates biomaterial surface chemistry effects on cell differentiation. *Proceedings of the National Academy of Sciences of the United States of America*, 102(17), pp.5953–5957.

Keselowsky, B.G., Collard, D.M. & García, A.J., 2004. Surface chemistry modulates focal adhesion composition and signaling through changes in integrin binding. *Biomaterials*, 25(28), pp.5947–5954.

Kilian, K.A. et al., 2010. Geometric cues for directing the differentiation of mesenchymal stem cells. *Proceedings of the National Academy of Sciences of the United States of America*, 107(11), pp.4872–4877.

Kim, D. et al., 2009. Generation of human induced pluripotent stem cells by direct delivery of reprogramming proteins. *Cell stem cell*, 4(6), pp.472–476.

Kim, D.H. et al., 2005. Gene expression profile of cytokine and growth factor during differentiation of bone marrow-derived mesenchymal stem cell. *Cytokine*, 31(2), pp.119–126.

Kim, J.J. & Huoh, K., 2010. Maxillofacial (midface) fractures. *Neuroimaging Clinics of North America*, 20(4), pp.581–596.

Kitajima, H. & Niwa, H., 2010. Clonal expansion of human pluripotent stem cells on gelatin-coated surface. *Biochemical and Biophysical Research Communications*, 396(4), pp.933–938.

Kjaer, M., 2004. Role of extracellular matrix in adaptation of tendon and skeletal muscle to mechanical loading. *Physiological reviews*, 84(2), pp.649–698.

Klemm, D.J. et al., 2001. Insulin-induced adipocyte differentiation: Activation of CREB rescues adipogenesis from the arrest caused by inhibition of prenylation. *Journal of Biological Chemistry*, 276(30), pp.28430–28435.

Koch, U., Lehal, R. & Radtke, F., 2013. Stem cells living with a Notch. *Development (Cambridge, England)*, 140(4), pp.689–704..

Kokabi, M., Sirousazar, M. & Hassan, Z.M., 2007. PVA-clay nanocomposite hydrogels for wound dressing. *European Polymer Journal*, 43(3), pp.773–781.

Kolf, C.M., Cho, E. & Tuan, R.S., 2007. Mesenchymal stromal cells. Biology of adult mesenchymal stem cells: regulation of niche, self-renewal and differentiation. *Arthritis Res Ther*, 9(1), p.204. Available at: http://www.ncbi.nlm.nih.gov/pubmed/17316462.

Kolf, C.M., Cho, E. & Tuan, R.S., 2007. Mesenchymal stromal cells. Biology of adult mesenchymal stem cells: regulation of niche, self-renewal and differentiation. *Arthritis research & therapy*, 9(1), p.204.

Kong, F. et al., 2009. Demonstration of catch bonds between an integrin and its ligand. *Journal of Cell Biology*, 185(7), pp.1275–1284.

Kopeček, J. & Yang, J., 2009. Peptide-directed self-assembly of hydrogels. *Acta Biomaterialia*, 5(3), pp.805–816.

Kraning-Rush, C.M. et al., 2011. The role of the cytoskeleton in cellular force generation in 2D and 3D environments. *Physical biology*, 8(1), p.015009.

Kretlow, J.D. et al., 2009. Injectable biomaterials for regenerating complex craniofacial tissues. *Advanced Materials*, 21(32-33), pp.3368–3393.

Kuru, E.A., Orakdogen, N. & Okay, O., 2007. Preparation of homogeneous polyacrylamide hydrogels by free-radical crosslinking copolymerization. *European Polymer Journal*, 43(7), pp.2913–2921.

Lai, C.-F. et al., 2006. Four and half lim protein 2 (FHL2) stimulates osteoblast differentiation. *Journal of bone and mineral research : the official journal of the American Society for Bone and Mineral Research*, 21(1), pp.17–28.

Langenbach, F. & Handschel, J.R., 2013. Effects of dexamethasone, ascorbic acid and ?-glycerophosphate on the osteogenic differentiation of stem cells in vitro. *Stem cell research & therapy*, 4(5), p.117. Available at: http://www.ncbi.nlm.nih.gov/pubmed/24073831.

Langer, R. & Vacanti, J.P., 1993. Tissue engineering. *Science*, 260(5110), pp.920–926. Available at: http://www.ncbi.nlm.nih.gov/pubmed/8493529.

Lanniel, M. et al., 2011. Substrate induced differentiation of human mesenchymal stem cells on hydrogels with modified surface chemistry and controlled modulus. *Soft Matter*, 7(14), p.6501.

Lavenus, S. et al., 2011. ADHESION AND OSTEOGENIC DIFFERENTIATION OF HUMAN MESENCHYMAL STEM CELLS ON TITANIUM NANOPORES. *European cells & materials*, 22(0), pp.84–96.

Leader, D.P. et al., 2011. Pathos: A web facility that uses metabolic maps to display experimental changes in metabolites identified by mass spectrometry. *Rapid Communications in Mass Spectrometry*, 25(22), pp.3422–3426.

Lee, J. et al., 2013. Directing stem cell fate on hydrogel substrates by controlling cell geometry, matrix mechanics and adhesion ligand composition. *Biomaterials*, 34(33), pp.8140–8148.

Lee, R.H. et al., 2004. Characterization and expression analysis of mesenchymal stem cells from human bone marrow and adipose tissue. *Cellular physiology and biochemistry : international journal of experimental cellular physiology, biochemistry, and pharmacology*, 14(4-6), pp.311–324.

Lepora, N., 2013. The state of the art in biomimetics. *... & biomimetics*, 8(1), p.013001..

Lerner, U.H., 2012. Osteoblasts, Osteoclasts, and Osteocytes: Unveiling Their Intimate-Associated Responses to Applied Orthodontic Forces. *Seminars in Orthodontics*, 18(4), pp.237–248.

Levesque, J.P., 2013. A niche in a dish: Pericytes support HSC. *Blood*, 121(15), pp.2816–2818.

Li, W.-J.W.-J. et al., 2005. A three-dimensional nanofibrous scaffold for cartilage tissue engineering using human mesenchymal stem cells. *Biomaterials*, 26(6), pp.599–609.

Li, Y. et al., 2013. Magnetic hydrogels and their potential biomedical applications. *Advanced Functional Materials*, 23(6), pp.660–672.

Lian, J.B. et al., 1998. Osteocalcin gene promoter: unlocking the secrets for regulation of osteoblast growth and differentiation. *Journal of cellular biochemistry. Supplement*, 30-31, pp.62–72.

Lian, J.B. & Stein, G.S., 1995. Development of the osteoblast phenotype: molecular mechanisms mediating osteoblast growth and differentiation. *The Iowa orthopaedic journal*, 15, pp.118–140.

Liem, R.K.H., 2013. Intermediate filaments: Not just for structure anymore. *Current Biology*, 23(8).

Lindahl, P. et al., 1997. Pericyte loss and microaneurysm formation in PDGF-B-deficient mice. *Science (New York, N.Y.)*, 277(5323), pp.242–245.

Lindvall, O. & Kokaia, Z., 2006. Stem cells for the treatment of neurological disorders. *Nature*, 441(7097), pp.1094–1096.

Little, N., Rogers, B. & Flannery, M., 2011. Bone formation, remodelling and healing. *Surgery*, 29(4), pp.141–145.

Lu, W., Bennett, B.D. & Rabinowitz, J.D., 2008. Analytical strategies for LC-MS-based targeted metabolomics. *Journal of Chromatography B: Analytical Technologies in the Biomedical and Life Sciences*, 871(2), pp.236–242.

Lucchese, A., 2014. The Distraction Osteogenesis in Midfacial Hypoplasia. *Journal of Craniofacial surgery*, 25, pp.831–834.

Lutolf, M.P. & Blau, H.M., 2009. Artificial stem cell niches. *Advanced Materials*, 21(32-33), pp.3255–3268.

Lutolf, M.P., Gilbert, P.M. & Blau, H.M., 2009. Designing materials to direct stem-cell fate. *Nature*, 462(7272), pp.433–441.

Lv, F.-J. et al., 2014. Concise review: the surface markers and identity of human mesenchymal stem cells. *Stem cells (Dayton, Ohio)*, 32(6), pp.1408–19.

Macfelda, K. et al., 2007. Behavior of cardiomyocytes and skeletal muscle cells on different extracellular matrix components--relevance for cardiac tissue engineering. *Artificial organs*, 31(1), pp.4–12.

Di Maggio, N. et al., 2011. Toward modeling the bone marrow niche using scaffold-based 3D culture systems. *Biomaterials*, 32(2), pp.321–329.

Maheshwari, A. V & Cheng, E.Y., 2010. Ewing sarcoma family of tumors. *The Journal of the American Academy of Orthopaedic Surgeons*, 18(2), pp.94–107.

Maia, F.R. et al., 2014. Matrix-driven formation of mesenchymal stem cell-extracellular matrix microtissues on soft alginate hydrogels. *Acta Biomaterialia*, 10(7), pp.3197–3208.

Mardas, N. et al., 2014. Experimental model for bone regeneration in oral and cranio-maxillo-facial surgery. *Journal of investigative surgery : the official journal of the Academy of Surgical Research*, 27(1), pp.32–49.

Marsich, E. et al., 2011. Biological response of hydrogels embedding gold nanoparticles. *Colloids and Surfaces B: Biointerfaces*, 83(2), pp.331–339.

Martins, A.M. et al., 2008. Natural origin scaffolds with in situ pore forming capability for bone tissue engineering applications. *Acta Biomaterialia*, 4(6), pp.1637–1645.

Mason, E.F. & Rathmell, J.C., 2011. Cell metabolism: An essential link between cell growth and apoptosis. *Biochimica et Biophysica Acta - Molecular Cell Research*, 1813(4), pp.645–654.

Massagué, J. & Wotton, D., 2000. Transcriptional control by the TGF-beta/Smad signaling system. *The EMBO journal*, 19(8), pp.1745–1754.

Mathur, A.M., Moorjani, S.K. & Scranton, A.B., 1996. Methods for Synthesis of Hydrogel Networks: A Review. *Journal of Macromolecular Science, Part C: Polymer Reviews*, 36(2), pp.405–430. Available at: http://www.tandfonline.com/doi/abs/10.1080/15321799608015226\nhttp://www.tandfonline.com/doi/pdf/10.1080/15321799608015226.

McBeath, R. et al., 2004. Cell shape, cytoskeletal tension, and RhoA regulate stem cell lineage commitment. *Developmental Cell*, 6(4), pp.483–495.

McMurray, R.J. et al., 2011. Nanoscale surfaces for the long-term maintenance of mesenchymal stem cell phenotype and multipotency. *Nature materials*, 10(8), pp.637–644.

McNamara, L.E. et al., 2011. Skeletal stem cell physiology on functionally distinct titania nanotopographies. *Biomaterials*, 32(30), pp.7403–7410.

Van Meerloo, J., Kaspers, G.J.L. & Cloos, J., 2011. Cell sensitivity assays: The MTT assay. *Methods in Molecular Biology*, 731, pp.237–245.

Mei, Y. et al., 2010. Combinatorial development of biomaterials for clonal growth of human pluripotent stem cells. *Nature materials*, 9(9), pp.768–778.

Merkl, C. et al., 2013. Efficient Generation of Rat Induced Pluripotent Stem Cells Using a Non-Viral Inducible Vector. *PLoS ONE*, 8(1).

Merkle, F.T., Mirzadeh, Z. & Alvarez-Buylla, A., 2007. Mosaic organization of neural stem cells in the adult brain. *Science (New York, N.Y.)*, 317(5836), pp.381–384.

Midha, R. et al., 2003. Growth factor enhancement of peripheral nerve regeneration through a novel synthetic hydrogel tube. *Journal of neurosurgery*, 99(3), pp.555–565.

Mirmalek-Sani, S.-H. et al., 2006. Characterization and multipotentiality of human fetal femur-derived cells: implications for skeletal tissue regeneration. *Stem cells*, 24(4), pp.1042–1053.

Montjovent, M.-O. et al., 2004. Fetal bone cells for tissue engineering. *Bone*, 35(6), pp.1323–1333.

Monton, M.R. & Soga, T., 2007. Metabolome analysis by capillary electrophoresis-mass spectrometry. *J Chromatogr A*, 1168(1-2), pp.237–246. Available at: http://www.hubmed.org/display.cgi?uids=17376458.

Muratone, M. et al, 2012. No Title. *Clin Cases Miner Bone Metab*, 9, pp.50–55.

Muschler, G.F. et al., 2001. Age- and gender-related changes in the cellularity of human bone marrow and the prevalence of osteoblastic progenitors. *Journal of Orthopaedic Research*, 19(1), pp.117–125.

Na, K., Lee, K.H. & Bae, Y.H., 2004. pH-sensitivity and pH-dependent interior structural change of self-assembled hydrogel nanoparticles of pullulan acetate/oligo-sulfonamide conjugate. *Journal of Controlled Release*, 97(3), pp.513–525.

Nakamura, K. et al., 2000. Tyrosine phosphorylation of paxillin α is involved in temporospatial regulation of paxillin-containing focal adhesion formation and F-actin organization in motile cells. *Journal of Biological Chemistry*, 275(35), pp.27155–27164.

Nakamura, Y. et al., 2010. Isolation and characterization of endosteal niche cell populations that regulate hematopoietic stem cells. *Blood*, 116(9), pp.1422–1432.

Nandi, S.. et al, 2015. Converted marine coral hydroxyapatite implants with growth factors. *Material Science & Engineering*, 49, pp.816–823.

Nathan, C. and S.M., 1991. Cytokines in Context. *Journal of Cell Biology*, 113(5), pp.981–986.

Natu, S.S. et al., 2014. The biology of distraction osteogenesis for correction of mandibular and craniomaxillofacial defects: A review. *Dental research journal*, 11(1), pp.16–26..

Naz, S. et al., 2014. Method validation strategies involved in non-targeted metabolomics. *Journal of Chromatography A*, 1353, pp.99–105.

Nerem, R.M. & Sambanis, A., 1995. Tissue engineering: from biology to biological substitutes. *Tissue engineering*, 1(1), pp.3–13.

Niwa, H., 2009. Mechanisms of Stem Cell Self-renewal. In *Essentials of Stem Cell Biology*. Elsevier Inc., pp. 73–80.

Nussbaum, J. et al., 2007. Transplantation of undifferentiated murine embryonic stem cells in the heart: teratoma formation and immune response. *The FASEB journal : official publication of the Federation of American Societies for Experimental Biology*, 21(7), pp.1345–1357.

O'Reilly, A.M., Lee, H.H. & Simon, M.A., 2008. Integrins control the positioning and proliferation of follicle stem cells in the Drosophila ovary. *Journal of Cell Biology*, 182(4), pp.801–815.

Oeztuerk-Winder, F. & Ventura, J.-J., 2012. The many faces of p38 mitogen-activated protein kinase in progenitor/stem cell differentiation. *The Biochemical journal*, 445(1), pp.1–10. Available at: http://www.ncbi.nlm.nih.gov/pubmed/22702973.

Orbach, R. et al., 2012. The rheological and structural properties of Fmoc-peptide-based hydrogels: The effect of aromatic molecular architecture on self-assembly and physical characteristics. *Langmuir*, 28(4), pp.2015–2022.

Orford, K.W. & Scadden, D.T., 2008. Deconstructing stem cell self-renewal: genetic insights into cell-cycle regulation. *Nature reviews. Genetics*, 9(2), pp.115–128.

Orimo, H., 2010. The mechanism of mineralization and the role of alkaline phosphatase in health and disease. *Journal of Nihon Medical School = Nihon Ika Daigaku zasshi*, 77(1), pp.4–12.

Panopoulos, A.D. et al., 2012. The metabolome of induced pluripotent stem cells reveals metabolic changes occurring in somatic cell reprogramming. *Cell Research*, 22(1), pp.168–177.

Parekh, S.H. et al., 2011. Modulus-driven differentiation of marrow stromal cells in 3D scaffolds that is independent of myosin-based cytoskeletal tension. *Biomaterials*, 32(9), pp.2256–2264.

Parikka, V. et al., 2005. Human mesenchymal stem cell derived osteoblasts degrade organic bone matrix in vitro by matrix metalloproteinases. *Matrix Biology*, 24(6), pp.438–447.

Park, J.S. et al., 2011. The effect of matrix stiffness on the differentiation of mesenchymal stem cells in response to TGF-β. *Biomaterials*, 32(16), pp.3921–3930.

Parsons, M. et al., 2008. Quantification of integrin receptor agonism by fluorescence lifetime imaging. *Journal of cell science*, 121(Pt 3), pp.265–271.

Passegué, E. et al., 2005. Global analysis of proliferation and cell cycle gene expression in the regulation of hematopoietic stem and progenitor cell fates. *The Journal of experimental medicine*, 202(11), pp.1599–1611.

Paszek, M.J. et al., 2009. Integrin clustering is driven by mechanical resistance from the glycocalyx and the substrate. *PLoS Computational Biology*, 5(12).

Pearson, O.M. & Lieberman, D.E., 2004. The aging of Wolff's "law": Ontogeny and responses to mechanical loading in cortical bone. *Yearbook of Physical Anthropology*, 47, pp.63–99.

Pek, Y.S., Wan, A.C.A. & Ying, J.Y., 2010. The effect of matrix stiffness on mesenchymal stem cell differentiation in a 3D thixotropic gel. *Biomaterials*, 31(3), pp.385–391.

Pekkarinen, J. et al., 2000. Impaction bone grafting in revision hip surgery. A high incidence of complications. *The Journal of bone and joint surgery. British volume*, 82(1), pp.103–107.

Petersen, O.W. et al., 1992. Interaction with basement membrane serves to rapidly distinguish growth and differentiation pattern of normal and malignant human breast epithelial cells. *Proceedings of the National Academy of Sciences of the United States of America*, 89(19), pp.9064–9068.

Petit, V. et al., 2000. Phosphorylation of tyrosine residues 31 and 118 on paxillin regulates cell migration through an association with CRK in NBT-II cells. *Journal of Cell Biology*, 148(5), pp.957–969.

Petit, V. & Thiery, J.P., 2000. Focal adhesions: structure and dynamics. *Biology of the cell / under the auspices of the European Cell Biology Organization*, 92(7), pp.477–494.

Petrovic, V. et al., 2012. Craniofacial bone tissue engineering. *Oral Surgery, Oral Medicine, Oral Pathology and Oral Radiology*, 114(3).

Phelps, E.A. et al., 2013. Vasculogenic bio-synthetic hydrogel for enhancement of pancreatic islet engraftment and function in type 1 diabetes. *Biomaterials*, 34(19), pp.4602–4611.

Pieptu, D., 2005. Mandible Reconstruction Using the Free Osteocutaneous Fibula Flap. *Timisoara Medical Journal*, 55(1), pp.43–48.

Pieptu, D. et al., 2005. Mandible Reconstruction using the Free Osteocutaneous Fibula Flap. *Timisoara Medical Journal (TMJ)*, 55(1), pp.43–48.

Pittenger, M.F., 1999. Multilineage Potential of Adult Human Mesenchymal Stem Cells. *Science*, 284(5411), pp.143–147.

Plow, E.F. et al., 2000. Ligand binding to integrins. *Journal of Biological Chemistry*, 275(29), pp.21785–21788.

Porter, J.R., T.T., R. & Popat, K.C., 2009. Bone tissue engineering: A review in bone biomimetics and drug delivery strategies. *Biotech. Prog.*, 25(6), pp.1539–1560.

Potten, C.S. & Loeffler, M., 1990. Stem cells: attributes, cycles, spirals, pitfalls and uncertainties. Lessons for and from the crypt. *Development (Cambridge, England)*, 110(4), pp.1001–1020.

Provenzano, P.P. & Keely, P.J., 2011. Mechanical signaling through the cytoskeleton regulates cell proliferation by coordinated focal adhesion and Rho GTPase signaling. *Journal of cell science*, 124(Pt 8), pp.1195–1205.

Purdue, P.E. et al., 2007. The cellular and molecular biology of periprosthetic osteolysis. *Clinical orthopaedics and related research*, 454, pp.251–261.

Purdue, P.E. et al., 2006. The central role of wear debris in periprosthetic osteolysis. *HSS Journal*, 2(2), pp.102–113.

Qiu, Y. & Park, K., 2012. Environment-sensitive hydrogels for drug delivery. *Advanced Drug Delivery Reviews*, 64(SUPPL.), pp.49–60.

Rajnicek, A. & McCaig, C., 1997. Guidance of CNS growth cones by substratum grooves and ridges: effects of inhibitors of the cytoskeleton, calcium channels and signal transduction pathways. *Journal of cell science*, 110 (Pt 2, pp.2915–2924.

Rape, A.D., Guo, W.H. & Wang, Y.L., 2011. The regulation of traction force in relation to cell shape and focal adhesions. *Biomaterials*, 32(8), pp.2043–2051.

Reichert, J.C. & Hutmacher, D.W., 2011. Bone Tissue Engineering. In N. Pallua & C. V. Suscheck, eds. *Tissue Engineering*. Springer, pp. 431–456. Available at: http://www.springerlink.com/content/r171183246271175/.

Reinholt, F.P. et al., 1990. Osteopontin--a possible anchor of osteoclasts to bone. *Proceedings of the National Academy of Sciences of the United States of America*, 87(12), pp.4473–4475.

Rho, J.Y. et al., 1999. Variations in the individual thick lamellar properties within osteons by nanoindentation. *Bone*, 25(3), pp.295–300.

Rho, J.Y., Kuhn-Spearing, L. & Zioupos, P., 1998. Mechanical properties and the hierarchical structure of bone. *Medical Engineering and Physics*, 20(2), pp.92–102.

Riggs, B.L. & Melton, L.J., 1983. Evidence for two distinct syndromes of involutional osteoporosis. *The American journal of medicine*, 75(6), pp.899–901.

Robling, A.G., Castillo, A.B. & Turner, C.H., 2006. Biomechanical and molecular regulation of bone remodeling. *Annual review of biomedical engineering*, 8, pp.455–498.

Rose, F.R.A.J. & Oreffo, R.O.C., 2002. Bone tissue engineering: hope vs hype. *Biochemical and biophysical research communications*, 292(1), pp.1–7.

Rosenbaum, A.J., Grande, D.A. & Dines, J.S., 2008. The use of mesenchymal stem cells in tissue engineering: A global assessment. *Organogenesis*, 4(1), pp.23–27.

Rossier, O. et al., 2012. Integrins β1 and β3 exhibit distinct dynamic nanoscale organizations inside focal adhesions. *Nature Cell Biology*, 14(10), pp.1057–1067.

Rowlands, A.S., George, P.A. & Cooper-White, J.J., 2008. Directing osteogenic and myogenic differentiation of MSCs: interplay of stiffness and adhesive ligand presentation. *American journal of physiology. Cell physiology*, 295(4), pp.C1037–C1044.

Sakamoto, Y., Boëda, B. & Etienne-Manneville, S., 2013. APC binds intermediate filaments and is required for their reorganization during cell migration. *Journal of Cell Biology*, 200(3), pp.249–258.

Salvi, J.D., Yul Lim, J. & Donahue, H.J., 2010. Increased mechanosensitivity of cells cultured on nanotopographies. *Journal of Biomechanics*, 43(15), pp.3058–3062.

Sanz-Herrera, J.A., García-Aznar, J.M. & Doblaré, M., 2009. On scaffold designing for bone regeneration: A computational multiscale approach. *Acta Biomaterialia*, 5(1), pp.219–229.

Savatier, P. et al., 1994. Contrasting patterns of retinoblastoma protein expression in mouse embryonic stem cells and embryonic fibroblasts. *Oncogene*, 9(3), pp.809–818.

Scadden, D.T., 2006. The stem-cell niche as an entity of action. *Nature*, 441(7097), pp.1075–1079.

Schefe, J.H. et al., 2006. Quantitative real-time RT-PCR data analysis: current concepts and the novel "gene expression's CT difference" formula. *Journal of molecular medicine (Berlin, Germany)*, 84(11), pp.901–910.

Schmidmaier, G. et al., 2007. Use of bone morphogenetic proteins for treatment of non-unions and future perspectives. *Injury*, 38(4 SUPPL.).

Schofield, R., 1978. The relationship between the spleen colony-forming cell and the haemopoietic stem cell. *Blood cells*, 4(1-2), pp.7–25.

Schwartz, M.A. & Ginsberg, M.H., 2002. Networks and crosstalk: integrin signalling spreads. *Nature cell biology*, 4(4), pp.E65–E68.

Scott, M.A. et al., 2011. Current Methods of Adipogenic Differentiation of Mesenchymal Stem Cells. *Stem Cells and Development*, 20(10), pp.1793–1804.

Seita, J. & Weissman, I.L., 2010. Hematopoietic stem cell: Self-renewal versus differentiation. *Wiley Interdisciplinary Reviews: Systems Biology and Medicine*, 2(6), pp.640–653.

Serbo, J. V & Gerecht, S., 2013. Vascular tissue engineering: biodegradable scaffold platforms to promote angiogenesis. *Stem cell research & therapy*, 4(1), p.8. .

Serkova, N.J. & Glunde, K., 2009. Metabolomics of cancer. *Methods in Molecular Biology*, 520, pp.273–295.

Serkova, N.J., Spratlin, J.L. & Eckhardt, S.G., 2007. NMR-based metabolomics: translational application and treatment of cancer. *Current opinion in molecular therapeutics*, 9(6), pp.572–585.

Shaer, A. et al., 2014. Differentiation of Human-Induced Pluripotent Stem Cells Into Insulin-Producing Clusters. *Experimental and clinical transplantation : official journal of the Middle East Society for Organ Transplantation*.

Shanbhag, A.S. et al., 1994. Composition and morphology of wear debris in failed uncemented total hip replacement. *The Journal of bone and joint surgery. British volume*, 76(1), pp.60–67.

Shiozawa, Y. et al., 2008. The bone marrow niche: habitat to hematopoietic and mesenchymal stem cells, and unwitting host to molecular parasites. *Leukemia : official journal of the Leukemia Society of America, Leukemia Research Fund, U.K*, 22(5), pp.941–950.

Shore, E.M. & Kaplan, F.S., 2008. Insights from a rare genetic disorder of extra-skeletal bone formation, fibrodysplasia ossificans progressiva (FOP). *Bone*, 43(3), pp.427–433.

Shuter, B.J. et al., 1983. Phenotypic Correlates of Genomic DNA Content in Unicellular Eukaryotes and Other Cells. *The American Naturalist*, 122(1), p.26.

Shyh-Chang, N., Daley, G.Q. & Cantley, L.C., 2013. Stem cell metabolism in tissue development and aging. *Development (Cambridge, England)*, 140(12), pp.2535–47. Available at: http://www.pubmedcentral.nih.gov/articlerender.fcgi?artid=3666381&tool=pmcentrez&rendertype=abstract.

Sieweke, M.H. & Allen, J.E., 2013. Beyond stem cells: self-renewal of differentiated macrophages. *Science (New York, N.Y.)*, 342(6161), p.1242974. Available at: http://www.ncbi.nlm.nih.gov/pubmed/24264994.

Da Silva Meirelles, L., Chagastelles, P.C. & Nardi, N.B., 2006. Mesenchymal stem cells reside in virtually all post-natal organs and tissues. *Journal of cell science*, 119(Pt 11), pp.2204–2213.

Silver, F.H. & Siperko, L.M., 2003. Mechanosensing and mechanochemical transduction: how is mechanical energy sensed and converted into chemical energy in an extracellular matrix? *Critical reviews in biomedical engineering*, 31(4), pp.255–331.

Simons, B.D. & Clevers, H., 2011. Strategies for homeostatic stem cell self-renewal in adult tissues. *Cell*, 145(6), pp.851–862.

Sittinger, M., Hutmacher, D.W. & Risbud, M. V., 2004. Current strategies for cell delivery in cartilage and bone regeneration. *Current Opinion in Biotechnology*, 15(5), pp.411–418.

Smith, C. & Storms, B., 2000. Hematopoietic stem cells. *Clin Orthop Relat Res*, pp.S91–7. Available at: http://www.ncbi.nlm.nih.gov/pubmed/11039756.

Smukler, S.R. et al., 2011. The adult mouse and human pancreas contain rare multipotent stem cells that express insulin. *Cell Stem Cell*, 8(3), pp.281–293.

Solon, J. et al., 2007. Fibroblast adaptation and stiffness matching to soft elastic substrates. *Biophysical journal*, 93(12), pp.4453–4461.

Spicer, P.P. et al., 2012. In situ formation of porous space maintainers in a composite tissue defect. *Journal of Biomedical Materials Research - Part A*, 100 A(4), pp.827–833.

Stella, J.A. et al., 2010. On the biomechanical function of scaffolds for engineering load-bearing soft tissues. *Acta Biomaterialia*, 6(7), pp.2365–2381.

Stevens, M.M. & George, J.H., 2005. Exploring and engineering the cell surface interface. *Science (New York, N.Y.)*, 310(5751), pp.1135–1138.

Stolzing, a et al., 2008. Age-related changes in human bone marrow-derived mesenchymal stem cells: consequences for cell therapies. *Mechanisms of ageing and development*, 129(3), pp.163–73.

Stupack, D.G. & Cheresh, D.A., 2002. Get a ligand, get a life: integrins, signaling and cell survival. *Journal of cell science*, 115(Pt 19), pp.3729–3738.

Sutton, D.N. et al., 2003. The prognostic implications of the surgical margin in oral squamous cell carcinoma. *International journal of oral and maxillofacial surgery*, 32(1), pp.30–34.

Sykaras, N. & Opperman, L., 2003. Bone morphogenetic proteins (BMPs): how do they function and what can they offer the clinician? *Journl of Oral Science*, 45(2), pp.57–73.

Taddei, I. et al., 2008. Beta1 integrin deletion from the basal compartment of the mammary epithelium affects stem cells. *Nature cell biology*, 10(6), pp.716–722.

Taichman, R.S., 2005. Blood and bone: Two tissues whose fates are intertwined to create the hematopoietic stem-cell niche. *Blood*, 105(7), pp.2631–2639.

Thawani, J.P. et al., 2010. Bone morphogenetic proteins and cancer: review of the literature. *Neurosurgery*, 66(2), pp.233–246; discussion 246.

Thomson, J.A., 1998. Embryonic Stem Cell Lines Derived from Human Blastocysts. *Science*, 282(5391), pp.1145–1147.

Todd, S.J. et al., 2007. Enzyme-triggered cell attachment to hydrogel surfaces. *Soft Matter*, 3(5), p.547.

Torgan, C.E. et al., 2000. Differentiation of mammalian skeletal muscle cells cultured on microcarrier beads in a rotating cell culture system. *Medical & biological engineering & computing*, 38(5), pp.583–590.

Tseng, C.., 2013. Mandible Reconstruction Using the Free Osteocutaneous Fibula Flap. *Journal of Medical Devices*, 55(1).

Tsimbouri, P.M. et al., 2012. Using nanotopography and metabolomics to identify biochemical effectors of multipotency. *ACS Nano*, 6(11), pp.10239–10249.

Tuszynski, J.A., Brown, J.A. & Sept, D., 2003. Models of the Collective Behavior of Proteins in Cells: Tubulin, Actin and Motor Proteins. In *Journal of Biological Physics*. pp. 401–428.

Ulijn, R. V & Smith, A.M., 2008. Designing peptide based nanomaterials. *Chemical Society reviews*, 37(4), pp.664–675.

Viguet-Carrin, S., Garnero, P. & Delmas, P.D., 2006. The role of collagen in bone strength. *Osteoporosis International*, 17(3), pp.319–336.

Vogel, V., 2006. Mechanotransduction involving multimodular proteins: converting force into biochemical signals. *Annual review of biophysics and biomolecular structure*, 35, pp.459–488.

Vukicevic, S., Luyten, F.P. & Reddi, A.H., 1989. Stimulation of the expression of osteogenic and chondrogenic phenotypes in vitro by osteogenin. *Proceedings of the National Academy of Sciences of the United States of America*, 86(22), pp.8793–8797.

Wakitani, S. et al., 2003. Embryonic stem cells injected into the mouse knee joint form teratomas and subsequently destroy the joint. *Rheumatology*, 42(1), pp.162–165.

Wakitani, S., Saito, T. & Caplan, A.I., 1995. Myogenic cells derived from rat bone marrow mesenchymal stem cells exposed to 5-azacytidine. *Muscle & nerve*, 18(12), pp.1417–1426.

Wan, C. et al., 2006. Nonadherent cell population of human marrow culture is a complementary source of mesenchymal stem cells (MSCs). *Journal of Orthopaedic Research*, 24(1), pp.21–28.

Wang, Z. & Yan, X., 2013. CD146, a multi-functional molecule beyond adhesion. *Cancer Letters*, 330(2), pp.150–162.

Watson, J.T. et al., 2013. CD271 as a marker for mesenchymal stem cells in bone marrow versus umbilical cord blood. *Cells Tissues Organs*, 197(6), pp.496–504.

Wehrle-Haller, B., 2012. Structure and function of focal adhesions. *Current Opinion in Cell Biology*, 24(1), pp.116–124.

Wesselschmidt, R.L., 2011. The teratoma assay: An in vivo assessment of pluripotency. *Methods in Molecular Biology*, 767, pp.231–241.

Wilcoxen, K.M. et al., 2010. Practical metabolomics in drug discovery. *Expert Opinion on Drug Discovery*, 5(3), pp.249–263.

Wilkinson, A. et al., 2011. Biomimetic microtopography to enhance osteogenesis in vitro. *Acta Biomaterialia*, 7(7), pp.2919–2925.

Willert, H.G. & Semlitsch, M., 1977. Reactions of the articular capsule to wear products of artificial joint prostheses. *Journal of biomedical materials research*, 11(2), pp.157–164.

Willerth, S.M. & Sakiyama-Elbert, S.E., 2007. Approaches to neural tissue engineering using scaffolds for drug delivery. *Advanced Drug Delivery Reviews*, 59(4-5), pp.325–338.

Williams, D.F., 2008. On the mechanisms of biocompatibility. *Biomaterials*, 29(20), pp.2941–2953.

Williams, E.L., White, K. & Oreffo, R.O., 2013. Isolation and enrichment of stro-1 immunoselected mesenchymal stem cells from adult human bone marrow. *Methods Mol Biol*, 1035, pp.67–73..

Wilson, A., Butler, P.E. & Seifalian, A.M., 2011. Adipose-derived stem cells for clinical applications: A review. *Cell Proliferation*, 44(1), pp.86–98.

Winer, J.P. et al., 2009. Bone marrow-derived human mesenchymal stem cells become quiescent on soft substrates but remain responsive to chemical or mechanical stimuli. *Tissue engineering. Part A*, 15(1), pp.147–154.

Wirkner, M. et al., 2011. Photoactivatable caged cyclic RGD peptide for triggering integrin binding and cell adhesion to surfaces. *ChemBioChem*, 12(17), pp.2623–2629.

Wolf, C.B. & Mofrad, M.R.K., 2009. Mechanotransduction and Its Role in Stem Cell Biology. In *Trends in Stem Cell Biology and Technology*. pp. 389–403. Available at: http://www.springerlink.com/index/10.1007/978-1-60327-905-5.

Wozney, J.M., 1992. The bone morphogenetic protein family and osteogenesis. In *Molecular Reproduction and Development*. pp. 160–167.

Wozniak, M.A. et al., 2004. Focal adhesion regulation of cell behavior. *Biochimica et biophysica acta*, 1692(2-3), pp.103–119.

Wozniak, M.A. et al., 2003. ROCK-generated contractility regulates breast epithelial cell differentiation in response to the physical properties of a three-dimensional collagen matrix. *The Journal of cell biology*, 163(3), pp.583–595.

Wu, X. et al., 2010. Muscle-derived stem cells: Isolation, characterization, differentiation, and application in cell and gene therapy. *Cell and Tissue Research*, 340(3), pp.549–567.

Wylie, R.G. et al., 2011. Spatially controlled simultaneous patterning of multiple growth factors in three-dimensional hydrogels. *Nature Materials*, 10(10), pp.799–806.

Xia, J. et al., 2012. MetaboAnalyst 2.0-a comprehensive server for metabolomic data analysis. *Nucleic Acids Research*, 40(W1).

Xia, J. et al., 2009. MetaboAnalyst: A web server for metabolomic data analysis and interpretation. *Nucleic Acids Research*, 37(SUPPL. 2).

Xie, X. et al., 2006. Differentiation of bone marrow mesenchymal stem cells induced by myocardial medium under hypoxic conditions. *Acta pharmacologica Sinica*, 27(9), pp.1153–1158.

Xie, X. et al., 2011. Neurogenesis of adipose-derived stem cells in hydrogel. *Journal of Huazhong University of Science and Technology - Medical Science*, 31(2), pp.174–177.

Yabut, O. & Bernstein, H.S., 2011. The promise of human embryonic stem cells in aging-associated diseases. *Aging*, 3(5), pp.494–508.

Yagi, H. et al., 2010. Mesenchymal stem cells: Mechanisms of immunomodulation and homing. *Cell Transplantation*, 19(6-7), pp.667–679.

Yamaguchi, A. et al., 1991. Recombinant human bone morphogenetic protein-2 stimulates osteoblastic maturation and inhibits myogenic differentiation in vitro. *The Journal of cell biology*, 113(3), pp.681–687.

Yamashita, Y.M. et al., 2010. Polarity in stem cell division: asymmetric stem cell division in tissue homeostasis. *Cold Spring Harbor perspectives in biology*, 2(1).

Yanes, O. et al., 2010. Metabolic oxidation regulates embryonic stem cell differentiation. *Nature chemical biology*, 6(6), pp.411–417.

Yang, S. et al., 2001. The design of scaffolds for use in tissue engineering. Part I. Traditional factors. *Tissue engineering*, 7(6), pp.679–689.

Yim, E.K.F. et al., 2010. Nanotopography-induced changes in focal adhesions, cytoskeletal organization, and mechanical properties of human mesenchymal stem cells. *Biomaterials*, 31(6), pp.1299–1306.

Yoder, M.C. et al., 2007. Redefining endothelial progenitor cells via clonal analysis and hematopoietic stem/progenitor cell principals. In *Blood*. pp. 1801–1809.

Yogurtcu, O.N., Kim, J.S. & Sun, S.X., 2012. A mechanochemical model of actin filaments. *Biophysical Journal*, 103(4), pp.719–727.

Yu, J. et al., 2007. Induced pluripotent stem cell lines derived from human somatic cells. *Science (New York, N.Y.)*, 318(5858), pp.1917–1920.

Zamir, E. & Geiger, B., 2001. Molecular complexity and dynamics of cell-matrix adhesions. *Journal of cell science*, 114(Pt 20), pp.3583–3590.

Zenobi, R., 2013. Single-cell metabolomics: analytical and biological perspectives. *Science (New York, N.Y.)*, 342(6163), p.1243259. Available at: http://www.ncbi.nlm.nih.gov/pubmed/24311695.

Zhang, D. & Kilian, K.A., 2013. The effect of mesenchymal stem cell shape on the maintenance of multipotency. *Biomaterials*, 34(16), pp.3962–3969.

Zhao, P. et al., 2014. Solving the puzzle of Parkinson's disease using induced pluripotent stem cells. *Experimental biology and medicine (Maywood, N.J.)*. Available at: http://www.ncbi.nlm.nih.gov/pubmed/24939824.

Zhou, M. et al., 2009. Self-assembled peptide-based hydrogels as scaffolds for anchorage-dependent cells. *Biomaterials*, 30(13), pp.2523–2530.

Zimmerlin, L. et al., 2010. Stromal vascular progenitors in adult human adipose tissue. *Cytometry Part A*, 77(1), pp.22–30.

Zuk, P.A. et al., 2002. Human Adipose Tissue Is a Source of Multipotent Stem Cells D. M. Raff, ed. *Molecular biology of the cell*, 13(12), pp.4279–4295.

Zuk, P.A. et al., 2001. Multilineage cells from human adipose tissue: implications for cell-based therapies. *Tissue engineering*, 7(2), pp.211–228.